SPATIAL SITE ASSESSMENT OF SOIL MOISTURE AND PLANT STRESS ON GOLF COURSES

by

JOSEPH M. KRUM

(Under the Direction of Robert N. Carrow)

ABSTRACT

A high degree of spatial and temporal variability associated with golf courses creates microclimates with specific input requirements. Three principles of precision agriculture are to apply inputs only where, when, and at the rate required by the plant. To maximize water-use efficiency on irrigated sites with diverse microclimates, or site-specific management units (SSMUs), these principles must be applied to water as the "input". Several SSMUs were identified during dry-downs (days following rain events) by measuring and mapping (via GIS) the volumetric water content (VWC) and normalized difference vegetative index (NDVI) across 'Salam' seashore paspalum (*Paspalum vaginatum* Sw.) golf course fairways at the Old Collier Golf Club in Naples, FL during the summer of 2006. Areas of excessive and inadequate VWC and corresponding plant NDVI stress indices provided the spatial basis for SSMU delineation. Through modification of irrigation system design and scheduling within SSMUs, turfgrass water-use efficiency can be improved.

INDEX WORDS: GIS, GPS, NDVI, VWC, Efficiency, Evapotranspiration, Irrigation, Microclimates, Precision agriculture, Seashore paspalum, Shade, Spatial variability, Stress, Topography, Traffic, Turfgrass, Water

SPATIAL SITE ASSESSMENT OF SOIL MOISTURE AND PLANT STRESS ON GOLF COURSES

by

JOSEPH M. KRUM

B.S., Michigan State University, 2005

A Thesis Submitted to the Graduate Faculty of The University of Georgia in Partial Fulfillment of the Requirements for the Degree

MASTER OF SCIENCE

ATHENS, GEORGIA

2008

SPATIAL SITE ASSESSMENT OF SOIL MOISTURE AND PLANT STRESS

ON GOLF COURSES

by

JOSEPH M. KRUM

Major Professor: Robert N. Carrow

Committee: Keith J. Karnok
Thomas R. Jordan
David E. Kissel

Electronic Version Approved:

Maureen Grasso
Dean of the Graduate School
The University of Georgia
May 2008

ACKNOWLEGEMENTS

First and foremost, I would like to thank my family for their unwavering guidance, encouragement, and support. Though furthering my education has led me away from them geographically, I know they have and will always be by my side every step of the way.

I would like to express my sincere gratitude to Dr. Robert Carrow. His knowledge and enthusiasm has been inspirational and motivating. I would also like to thank my committee members: Dr. Keith Karnok, Dr. Thomas Jordan, and Dr. David Kissel, for their time, guidance, and recommendations that have aided in the completion of this thesis.

I would like to thank the Toro Company for funding this research. Special thanks go to Troy Carson, Kathy Rice, Dr. Van Cline, and Dana Lonn of Toro for their expertise, advice, and insight during data acquisition and analysis.

I would like to thank Tim Hiers, Todd Draffen, Ricardo Uriarte, Gregory Jack, Kevin Ackerman, Mike Koopman, J.W. Stidham, Linda Bradford, and the rest of the staff at the Old Collier Golf Club for providing the study site and other accommodations that facilitated data acquisition. They have all been extremely helpful and friendly throughout the duration of this research.

I would also like to thank Marisa Farmer, James Hudson, Mitch Gilmer, Mary Flynn, Dr. Ian Flitcroft, and Bill Blum of the University of Georgia (Griffin campus), whose training, assistance, and expertise have contributed to this research.

TABLE OF CONTENTS

CHAPTER 1

INTRODUCTION and LITERATURE REVIEW

Background

Practices promoting natural resource sustainability are gaining popularity and acceptance. With the advent of more fuel efficient automobiles, alternative energy sources, the increasing popularity of mass transit, and attempts to decrease the nation's dependency on foreign oil, extensive measures are being taken that have a focus on the future.

Similarly, people are beginning to understand that freshwater supplies cannot continue to be taken for granted. Though over 75% of earth is covered by water, only approximately 0.75% is available for human use (Gleick, 1993). With the U.S. population projected to double within the next century, the demand for water will rise as well. Golf courses are among the primary types of industries that will be looked upon to develop water conservation practices that focus on increasing water-use efficiency.

The effects of water shortages are not just a future concern. There have already been numerous instances where regions experiencing drought, from Arizona to Michigan, have made adjustments to cope with water shortages. Especially during the summer months, there are times when residents are not allowed to water lawns and golf courses are prohibited from running their irrigation systems. In many areas of the country, golf courses are confronted with reducing water-use at the expense of functional and aesthetic playing conditions.

In times of drought, people will look toward the most visible industries that use high amounts of water. The water-use practices of golf courses are among the first magnified

and scrutinized by the pubic during water shortages. Golf course managers will need to take necessary steps to use avoid wasteful use of water. In order to prepare for a seemingly inevitable increase in water restrictions, it is crucial that golf course irrigation systems perform and are managed in the most efficient manner possible.

Using irrigation systems to apply water to golf courses is not a new idea. Since the early 19th century, golf courses have used irrigation to supplement rainfall to prevent desiccation, enhance density, and to improve overall turfgrass health (Kurtz, 2000). One of the main challenges (and potential opportunities) the turf industry faces is water resource management. Though strides have been made regarding efficient irrigation practices, there is still substantial room for improvement.

Golf courses use an estimated 1.8×10^{12} L of water annually in the United States (Zoldoske, 2003). The Irrigation Association reports that of all fresh water used for irrigation in the United States, 79.6% is for agriculture, 2.9% is for landscaping, and 1.5% is for golf courses. The remaining 16% is used by animals, industry, and humans. However, these figures may be misleading. Because many golf courses are in urban areas, highly treated potable water is used for irrigation. Thus, this water is among the most expensive. Increasing irrigation system efficiency could significantly benefit local water providers.

Water conservation on a golf course is no longer a matter of 'if' or 'when' but of 'how' (Carrow et al., 2005a). Golf courses have dealt with sustainability issues in the past, such as concerns with fertilizer and pesticide use (Sudduth et al., 1997). An effective way to address such issues is to implement holistic, science-based methods (i.e., Best Management Practices or BMPs) (Carrow and Duncan, 2008). Best Management Practices for water conservation can be applied at the site-specific level or across water districts (Carrow and Duncan, 2008; Finch,

2008). In a broad sense, BMPs are practical procedures that effectively protect the ecosystem. Practical application of scientific, economic, environmental, aesthetic, and ethical considerations is at the heart of the BMP approach (Carrow et al., 2005b).

At the regulatory level (i.e., federal, state, and/or local), water conservation issues can be addressed by either implementing rigid mandated regulations, or by using the BMP approach (Carrow et al., 2005a). During periods of water shortages, government agencies may initially respond by employing restrictions. Possible restrictions include: only irrigating on specified days of the week, narrow time frames when watering is permissible, or reducing the amount of water a golf course may apply by a certain percentage.

Several problems exist with the rigid regulation approach. Because this approach is politically-based instead of science-based, proven concepts and technology to maximize water-use efficiency would not be applied. Because scientific approaches are not valued or understood, development of science-based technology is not encouraged. At facilities where BMPs are already applied, regulations would hurt these courses most, since water is already being conserved. Regulations may not be holistic approaches that address all factors related to water conservation (e.g., climate, soil, plant, and landscape), but rather concentrate on limiting irrigation duration and frequency, or reducing the irrigated area.

Conversely, the BMP approach combines a number of strategies to reduce water-use. This approach encourages educated decision making and professionalism on the part of the turf manager. It also promotes research and development to establish new or enhance existing water management practices (Carrow et al. 2007). Two BMP strategies include irrigation design and scheduling for efficient water-use. For efficient irrigation scheduling, the turf manager must

address the questions of when, where, and how much irrigation water to apply within various microclimates throughout the landscape.

Precision Agriculture: Addressing Spatial Variability

There would be no need for precision water management if all golf course attributes were uniform (Mulla and Schepers, 1997). Unfortunately, no golf course exhibits uniform conditions; there is normally a significant degree of spatial variability that creates a number of microclimates, or site-specific management units (SSMUs), that differ in irrigation requirements. Site-specific management units are sub-field areas that have similar soil properties and landscape characteristics, resulting in similar plant response, input-use efficiency, and environmental impact (Boydell and McBratney, 1999; Corwin and Lesch, 2005a, 2005b; Corwin et al., 2006; Duffera et al., 2007; Yan et al., 2007).

As the focus on site-specific or precision input application has increased, due in part to rising costs and environmental concerns, spatial variability of soil properties has become a greater topic of interest. Determination of optimal soil sampling schemes has been investigated (Wollenhaupt et al., 1997; Lesch et al., 2000). By evaluating the coefficient of variation (CV), Wollenhaupt et al. (1997) found that soil pH and, to a lesser extent, crop yield exhibit low spatial variation. Conversely, NO_3-N, organic matter content, plant available phosphorus, and plant available potassium exhibited high spatial variability, as indicated by their correspondingly high CV. Since temporal variability was highly dependent upon precipitation and temperature, Wollenhaupt et al. (1997) concluded that proper timing of soil sampling is essential for site-specific management.

Variability exists above and below the ground (Mulla and Schepers, 1997). Climatic factors influencing variability across the landscape include solar radiation (north and south

exposure, duration, and shade), wind speed, humidity, and air temperature. Soil factors include texture, compaction, organic matter content, slope, depth, water holding capacity, infiltration rate, percolation rate, salinity, pH, and fertility. Hydrophobic soil conditions caused by humic and/or fulvic acid coatings on sand particles can cause localized dry spots, resulting in potentially significant spatial variability (Karnok et al., 1993). High pH treatments (0.1 mol L^{-1} NaOH) to sand-based creeping bentgrass golf course putting greens significantly reduced hydrophobicity. Good irrigation system design, zoning, and hardware should incorporate landscape and soil variability; when the system is not designed properly it becomes another source of variability (Irrigation Association, 2005)

The selected turfgrass species and/or cultivar also affect irrigation requirements (Carrow et al., 2005a). Warm-season grasses are generally associated with greater drought tolerances than cool-season grasses. Of the warm-season grasses, bermudagrass (*Cynodon* spp.) is best, while centipedegrass [*Eremochloa ophiuroides* (Munro.) Hack.] is relatively poor at withstanding drought. Seashore paspalum (*Paspalum vaginatum* Sw.) is moderately adapted to dry conditions.

Of the cool-season grasses, tall fescue (*Festuca arundinacea* Schreb.) is best suited to thrive under dry conditions. Annual bluegrass (*Poa annua* L.) requires a relatively high amount of moisture to flourish. Kentucky bluegrass (*Poa pratensis* L.) is moderately adapted to drought. It is important to keep in mind that plant geneticists have developed and continue to breed cultivars of numerous species that are better adapted to drought stress. Using drought resistant grasses is a popular trend among golf courses, but poor irrigation practices (over-irrigating) can result in drought tolerant grasses using more water than necessary.

Key principles of precision agriculture (PA) include: a) applying an input only when and where it is needed, and b) making the application at the rate required for the specific site (Corwin and Lesch, 2005a). To maximize water-use efficiency and conservation on complex irrigation sites, water must be considered the input on the basis of these principles.

Application of PA principles for site-specific irrigation decisions involving an area with complex microclimates will require that spatial variability be quantified in a manner to identify different water-use areas. Evapotranspiration (ET) is the loss of water from soil and plants, respectively, by evaporation and transpiration (Beard, 1973). Since crop-specific ET (ET_c) varies across the landscape in response to factors noted above, one way to integrate factors that affect ET is to measure ET_c within microclimates or by measuring the spatial variation of ET_c. When the soil moisture content is at or near field capacity (i.e., the moisture content after gravity removes excess water), ET_c is primarily affected by climatic and plant conditions (Tucker, 1999).

After a rainfall, when irrigation uniformity is not an issue, determining the volumetric water content (VWC) in the surface 0- to 10-cm zone on each day for a 2- to 4-day period (until the surface zone becomes limiting for water content) allows daily ET_c to be estimated by differences in soil moisture content. A 10-cm zone is used based on extensive soil moisture monitoring in various studies that has demonstrated that a significant portion of ET_c comes from this zone (Young et al., 1997). Once VWC is determined, ET_c spatial variability can be compared to spatial measurements of soil, plant, and climatic factors. These factors will determine potential contributions to spatial ET_c differences and provide a basis for irrigation system adjustments. After a drying period allows soil moisture to decrease, irrigation could be

applied. Evapotranspiration measurements could be taken again, but irrigation system variability would be included in the factors affecting ET_c.

Corwin and Lesch (2005a) suggested protocols based on using apparent soil electrical conductivity (EC_a) survey data that characterized spatial variability for site-specific management. Their detailed protocols consisted of mobile sensor platforms, defining the mapping purposes or field applications, mapping procedures, soil sampling, laboratory analyses of soil samples, spatial statistical analysis, and geographic information system (GIS) presentation of results. However, they did not carry the protocols through to development of a decision support system (DSS) or inclusion into a DSS for the end-user.

Mobile sensor platforms are necessary to obtain site-specific information of soil and plant properties required for site-specific management decisions. While remote sensing can provide valuable information over large areas, field-scale data normally requires mobile sensor platforms (Corwin and Lesch, 2005a). King et al. (2005) stated that two broad approaches for site-specific management have been to identify patterns within a field related to the crop performance (e.g., yield data and plant stress) or soil factors that affect yield (e.g., soil texture, soil moisture, and salinity). The most widely used field approach to estimate soil properties in PA has been with EC_a measurements, especially by electromagnetic devices, while yield mapping provides crop performance information (Rhoades et al., 1999; Corwin and Lesch, 2005a, 2005b). Electromagnetic devices provide non-intrusive estimates of soil salinity in saline soils, but in non-saline soils it estimates soil moisture and bulk density. The normal zone of determination is approximately 30 cm.

Starr (2005) and Duffera et al. (2007) indicated that soil water content maps would be valuable to design efficient irrigation management plans. They also noted that soil water content

at field capacity has a relatively stable pattern of spatial variability and is highly correlated with other stable landscape properties such as particle size classes and topography.

One means of assessing VWC spatial uniformity (i.e., variability) within a SSMU could be the distribution uniformity (DU) approach used for irrigation systems. A common method for irrigation uniformity assessment is the catch-can test, which involves the placement of evenly spaced reservoirs in a specified area and measuring the amount of water collected from sprinklers (Dukes et al., 2006). The lower quartile distribution uniformity (DU_{lq}) can be calculated to determine the variability of an irrigation system:

$$DU_{lq} = V_{lq}/V_{tot} \qquad \text{Eq. [1]}$$

where V_{lq} is the average of the lowest quarter of catch-can measurements (%), and V_{tot} is average of all catch can measurements (%).

The VWC reduction during a dry-down (i.e., a time span following a significant rain event) throughout the root zone of a crop can be used to estimate ET by the soil water balance method (Sharma, 1985). During dry-down periods following an irrigation or rainfall, temporal VWC variability (i.e., changes in VWC over time) are influenced by a mix of relatively stable landscape properties and variable temporal properties (e.g., climatic parameters) that drive ET (Lascano et al., 1999; Starr, 2005). McVicar et al. (2007) reported substantial spatial and temporal ET variability at the watershed scale, while Pauwels and Samson (2006) and Rana et al. (2007) found similar results at the field level.

Topography, Light, and Traffic Effects

Beard (1973) noted that turfgrass ET across landscapes is influenced by factors that drive ET demand (e.g., solar radiation and duration, temperature, humidity, and wind), water

absorption rate, soil moisture potential, soil water content, plant cover, and plant vigor. Solar radiation is a major driving force of ET, especially when soil moisture is not limited.

Topography not only influences initial VWC after irrigation or rainfall through infiltration and runoff, but it also affects the absorption and reflection of incident solar radiation that may contribute to differential ET losses by topographic aspect. Spatial variability of ET in relation to topography has been assessed by data interpolation and modeling methods (Chen et al., 2004; McVicar et al., 2007; Rana et al., 2007). Numerous agro-meteorological variables, including temperature and humidity, are affected by solar radiation and other boundary conditions at the soil surface (Raupach et al., 1992). Modification of these variables occurs when discontinuities arise in regard to topographic characteristics such as elevation, slope, and aspect. Rana et al. (2007) concluded that topography significantly influences energy fluxes, including the latent heat flux (the energy equivalent of ET). By using topography as a correction factor, the accuracy of energy flux simulation models in complex terrain was substantially increased. Chen et al. (2004) suggested that topography is an important variable that hydrologic models used for mapping ET should incorporate, since elevation, slope, and aspect significantly influence soil moisture.

Water relations affected by topography may subsequently influence crop performance. Kravchenko and Bullock (2000) investigated the affects of topography and soil properties on corn (*Zea mays* L.) and soybean [*Glycine max* (L.) Merr.] yields. Topographic features including elevation, slope, curvature, and flow accumulation accounted for approximately 20% of the total yield variability. Soil characteristics were responsible for approximately 30% of the yield variability. Elevation and organic matter content were the most influential factors associated with topography and soil, respectively. Other topographic factors only affected yields in extreme

circumstances, such as saturated depressions or eroded hilltops. Topography has also been documented to influence the distribution of protein contents in soybeans (Kravchenko and Bullock, 2002). Of all the factors associated with topography, aspect had the most significant impact on ET. Rockström et al. (1999) assessed the infiltration rates on up-slope, mid-slope and down-slope areas of a pearl millet [*Pennisetum glaucum* (L.) R. Br.] field with a 1 to 3% slope. The highest infiltration occurred on the mid-sloping plots, while up-sloping plots exhibited the lowest percent infiltration.

Measuring VWC changes in the surface 10-cm zone during a dry-down is a possible means of estimating ET_c spatially across the landscape. However, the VWC measurements would not encompass the complete root zone, as is normal for the soil balance method (Sharma, 1985). The potential for using estimated ET_c based on surface VWC over time is founded on the observation that greater loss of soil moisture through ET initially occurs in the surface zone after irrigation because of higher organic matter content, thereby contributing to greater soil moisture retention, transpiration, and higher root densities in the surface zone. Once soil moisture becomes depleted to the point of reduced plant availability, water extraction becomes progressively greater from deeper zones. Young et al. (1997) reported that 68 and 64% of the daily ET during the first and second days after irrigation, respectively, was attributable to the surface 20% of a 'Tifway' bermudagrass (*Cynodon dactylon* L. Pers. x *Cynodon transvaalensis* Burtt-Davy] root zone, but declined to 30% by day five. Li et al. (2001) illustrated this concept when comparing root-water-uptake models. Various models estimated approximately 60% of the maximum water uptake from agronomic plants originated from the upper 20% of the root zone.

Many complex landscape areas (e.g., golf courses) have an on-site weather station. However, climatic conditions within various microclimate areas may differ from those of the weather station. Climatic factors that influence turfgrass ET_c are those included in weather-based models to estimate plant ET_c.

A potential application for the determination of spatial ET_c differences is incorporating data into irrigation scheduling models using estimated crop reference ET (ET_o) from a weather station. Landscape areas with on-site weather stations can obtain estimated daily ET_o as calculated from weather data. Typical weather station locations are sites with full sunlight, flat topography, and good air movement. Site-specific or precision irrigation requires that water application be adjusted from the weather station ET_o to the microclimate conditions. The ET_o should be adjusted for each microclimate site because grass, soil type, slope aspect, radiation, wind, and other environmental or management conditions will differ from the weather station site. Adjusting the ET_o is performed by multiplying it by a landscape coefficient (K_L), in order to obtain an estimated turf ET_c (where $ET_c = K_L \times ET_o$) (Irrigation Association, 2005). Unfortunately, the K_L differs with grass, season, weather front, and any other site condition that affects ET_c. Obtaining an accurate K_L to make the correction from ET_o to ET_c is a major obstacle preventing the adoption of this approach because of the multitude of microclimates on golf courses and other complex sites.

While many irrigation systems may have a weather station interfaced with the irrigation control system, this feature typically is either ignored or inconsistently utilized for irrigation scheduling. If hand-held sensors could provide an estimate of ET_c within a microclimate by determination of VWC changes during a dry-down, then site-specific K_L values could be

determined from the estimated microclimate ET_c and weather station ET_o to use in controller programming to determine optimal water requirements.

Several studies have focused on the implications of limited solar radiation on turfgrass (Feldhake et al., 1985; Stier et al., 1999; Bell et al., 2000; Koh et al., 2003). When turfgrasses are subjected to shaded environments, the resulting increased leaf succulence and delicateness causes the plant to become more susceptible to traffic stress, wear injury, and prolonged recovery time (Beard, 1973). Feldhake et al. (1985) investigated the effects of preconditioning 'Merion' Kentucky bluegrass to shade on ET rates, determining that ET was not affected by preconditioning to shade, as the canopy temperature and ET were equal for all preconditioned grasses. Though there may be the perception that the importance of sun exposure in morning or afternoon is more or less similar, creeping bentgrass has been reported to be unsustainable at golf course putting green heights without morning sunlight (Vargas, 1994). 'Sea Isle 1' seashore paspalum plots not exposed to wear or soil compaction exhibited turf color, density, and canopy spectral reflectance that did not vary significantly between morning or afternoon shade treatments (Jiang et al., 2003). However, effects of afternoon shade were more significant than morning shade when Sea Isle 1 was subjected to wear stress and/or soil compaction. When 'L93' and 'SR1020' creeping bentgrass (*Agrostis palustris* Huds.) were exposed to reduced shade and airflow, canopy and soil temperature were lowered more by shade than airflow (Koh et al., 2003). Both treatments reduced the color quality and turf density. Shade reduced the root mass more severely than airflow restriction.

Traffic stress includes both turfgrass wear and soil compaction (Beard, 1973). Wear is characterized by scuffing and tearing directed toward the leaves, stems, and crowns of the plant. Disease susceptibility increases when the plant is subjected to wear because the damaged areas

encourage the invasion of pathogens. Warm-season turfgrasses are generally more wear tolerant than their cool-season counterparts. For example, zoysiagrass (*Zoysia* Willd.) and bermudagrass are characterized by a high degree of wear tolerance, while creeping bentgrass and rough bluegrass (*Poa trivialis* L.) are more susceptible to wear.

Compaction, the other primary constituent of traffic stress, involves the pressing together of soil particles, which reduces pore space and increases soil density (Carrow and Petrovic, 1992). On sandy soil, compaction is predominantly considered an insignificant factor; heavier, denser soils comprised of more silt and clay are more susceptible to compaction. In comparison, stress attributable to wear frequently occurs in turf grown in all soils, regardless of particle size.

A reduction in water-use has been found to be a significant effect of turfgrass compaction (Morgan et al., 1966; O'Neil & Carrow 1983; Agnew and Carrow, 1985). Morgan et al. (1966) observed that compaction caused a decrease in ET_c in common bermudagrass [*Cynodon dactylon* (L.) Pers.]. In a study conducted by O'Neil & Carrow (1983), perennial ryegrass (*Lolium perenne* L.) ET_c decreased by 28% in response to compaction. Despite lower water-use, often times turf managers apply more irrigation to turfgrass environments under compacted conditions. This may be in an attempt to compensate for unutilized water moving past the shallow root system or lost during runoff.

Technological Influence

Soil water content and ET have been measured and/or estimated for decades for crop production research and PA (Topp and Davis, 1985; Young et al., 1997; Leib et al., 2003; Wraith et al., 2005; Pauwels and Samson, 2006). One of the more common methods of moisture analysis is performed via time-domain reflectometry (TDR), which measures changes in the soil dielectric constant (ε) as water contents fluctuate (Leib et al., 2003). A TDR sensor produces a

high frequency voltage pulse that is transmitted and reflected along metal probes. The dielectric constant is determined by measuring the velocity of the transmitted pulse in the soil, which is primarily dependent upon the VWC, as water has a significantly higher dielectric constant than air ($\varepsilon = 80$ and 1, respectively). The permittivity and corresponding pulse velocity are closely related to the soil water content (Plauborg et al., 2005). The measurements are taken on a continuous basis, which offers a distinct advantage over instruments that are only capable of periodic moisture content measurements. An added advantage of TDR is that it can be used to measure EC_a and VWC simultaneously (Wraith et al., 2005)

Soil EC_a can also be measured by the four-wenner array method. (Rhoades et al., 1999). A four-wenner array utilizes current (outer) and potential (inner) electrodes. Battery-powered or hand-cranked units produce the current, while the spacing between electrodes determines the measurement depth.

Mobile TDR soil moisture monitoring is a relatively new technique (Western et al., 1998; Wraith et al., 2005). The majority of TDR applications have involved hand-held data acquisition to this point. The most prominent advantage of mobile TDR monitoring (compared to hand-held methods) is the ability to obtain more measurements over a larger area in a shorter period of time.

Optical sensors can use different wavelengths of light to measure plant stress (Bell et al., 2002; Morris et al., 2006; Jiang and Carrow, 2007; Xiong et al. 2007). These sensors measure spectral reflectance from the turf canopy and relate the measurements to a normalized difference vegetative index (NDVI). Near-infrared (NIR) and red light (R) reflected from the turf canopy are measured to calculate NDVI (Major et al., 2003).

$$NDVI = [(NIR - R)/(NIR + R)] \qquad \text{Eq. [2]}$$

The NDVI is a unit-less index that ranges from 0 to 1, where higher values indicate healthier and denser plant canopies.

Canopy density increases as the amount of visible light (R) absorbed increases and the amount of near-infrared light absorbed decreases. Furthermore, healthy plants absorb more visible light and reflect more near-infrared light. The degree of absorption by a plant is controlled by the amount of chlorophyll in the leaves. As chlorophyll production in leaves increases, more visible light is absorbed. Consequently, less visible light is reflected by the plant and more near-infrared light is reflected. There is an inverse relationship between leaf water content and visible light absorption. Higher water contents result in lower visible light reflectance, leading to an overall higher NDVI.

Remotely sensed vegetative indices such as NDVI have been used to estimate ET (Trenholm et al., 1999; Hunsaker et al., 2003). The NDVI can estimate crop cover, green plant biomass, and leaf area index. The NDVI can also be used in algorithms to determine more efficient irrigation scheduling practices. Moreover, NDVI can be measured on a frequent basis at ground level, in the air, or by satellites. Daily NDVI measurements are not typically necessary because of the smooth general shape of the crop coefficient curve over a growing season allows data extrapolation of approximately one week (Hunsaker et al., 2003).

Another method of determining moisture stress involves vehicle-mounted optical sensors (VMOS) (Bell et al., 2002). Vehicle-mounted optical sensors measure R and NIR spectral reflectance from the turf canopy, which can be converted to NDVI. Since higher photosynthetic rates correspond to more chlorophyll, and available moisture is a significant factor in photosynthetic rates, the amount of moisture in the soil can be indirectly measured by NDVI.

Turfgrass managers can use VMOS by incorporating the sensors with equipment such as mowers. On a golf course, a mower with a VMOS would be capable of acquiring data throughout the golf course. These data could be downloaded into the computer that controls the irrigation system. Defined parameters within the irrigation program could adjust each zone (representing a specific number of sprinkler heads) on the golf course according to the VMOS. This would allow the turfgrass manager to adjust the irrigation schedule on a daily basis.

Data derived from soil moisture and plant stress sensors can be spatially mapped using remotely sensed data in GIS (Fenstermaker-Shaulis et al., 1997). Remote sensing is a powerful graphical and quantitative tool to develop cultural practices that maximize efficient water-use. The first application of remote sensing for agricultural management dates back to 1929, when soil types were mapped using aerial photography (Frazier et al., 1997). This aided farmers in selecting land that would be best suited for particular crops based on the soil productivity and input requirements. Later, advances in aerial photography led to images that illustrated stresses caused by insects, diseases, nutrient deficiencies, and moisture extremes.

The Global Positioning System (GPS) is a radio-navigation system providing continuous location (i.e., latitude, longitude, and altitude) information to an unlimited number of users (U.S. Coast Guard Navigation Center). As far as the user is concerned, GPS involves three components: satellites, base stations, and receivers.

The popularity of GPS has grown tremendously in recent years. Applications for GPS include, but are not limited to: transportation (vehicle navigation and emergency response), surveying, mapping (forestry and utilities), recreation (fishing and hiking), and the military (Jordan, 2007). It has become increasing common to find GPS receivers in automobiles, enabling the driver to find the fastest or most economical routes to a destination, or merely to

keep the driver from getting lost. Fishermen, hunters, and hikers have found GPS to be an invaluable tool for marking fishing hot-spots, locating areas of prime hunting ground, and/or locating other areas of interest in the wilderness.

Moreover, GPS has become useful for a variety of research purposes. Among many other applications, GPS has been used to assess fertilization patterns in agricultural environments (Kim et al., 2005). GPS can be used in conjunction with GIS to map, analyze, and interpret a multitude of data.

Remote sensing combined with GPS presents turfgrass managers with a visual representation of the range of soil moisture contents throughout the golf course. This representation illustrates flaws in the irrigation system; areas that receive inadequate and excessive irrigation can be identified. Furthermore, GIS software analyses provide insight into potential SSMUs, especially when developed using VWC at field capacity. Unlike aerial photography, GPS allows for real time data to be analyzed and adjustments can be made accordingly.

Irrigation systems are designed to provide the most efficient distribution of water possible. Throughout the past several decades, countless dollars and hours have been spent developing technologically advanced golf course irrigation systems (Huck, 1997). These systems incorporate computer software and weather stations to make irrigation decisions as accurate and efficient as possible. Unfortunately, a disproportionately small amount of time has been spent researching and assessing the performance of sprinklers, spacing, and nozzle combinations. Frustration on behalf of golf course managers can occur if, following the installation of a million dollar irrigation system, there are still areas of excessively wet or dry areas. Currently it is only possible to adjust individual irrigation heads by the time that they are

activated. This adjustment still leaves substantial room for error. Within a single zone or even a single irrigation head, microclimates exist that have different moisture requirements.

By using GPS-referenced spatial VWC and plant stress data in conjunction with an irrigation scheduling system, this technology can provide turfgrass managers with the ability to make changes in the irrigation program or in the field. He/she will also be able to modify the irrigation system design to alleviate distribution flaws. Spatial data could also be used to determine necessary cultural practices for the site under examination. These changes could lead to more efficient and/or uniform input application.

Objectives

Considering use of mobile platforms for intense spatial and temporal mapping of soil properties (e.g., VWC and penetrometer resistance) and plant performance (NDVI) in complex turfgrass landscapes has not been reported, the purposes of these studies were to: a) determine the most suitable SSMU classification method applicable to the measured data, and b) identify spatial patterns of relationships and inconsistencies involving VWC and NDVI throughout progressions of dry-downs. Additionally, we explored the feasibility of using more limited mapping (compared to full, detailed spatial mapping with rapid, mobile platforms) of topography, light, and traffic microclimate determinations of surface VWC and ET_c estimates for irrigation scheduling decisions involving when to irrigate, where to irrigate, and how much irrigation to apply. Included in these objectives was to present preliminary data analysis and interpretation methods to aid in the development of protocols for future precision turf management (PTM) studies for these field applications.

REFERENCES

Agnew, M.L., and R.N. Carrow. 1985. Soil compaction and moisture stress preconditioning in Kentucky bluegrass. II. Stomatal resistance, leaf water potential, and canopy temperature. Agron. J. 77:878-884.

Beard, J.B. 1973. Turfgrass: Science and culture. Prentice-Hall, Englewood Cliffs, NJ.

Bell, G.E., T.K. Danneberger, and M.J. McMahon. 2000. Spectral irradiance available for turfgrass growth in sun and shade. Crop Sci. 40:189-195.

Bell, G.E., D.L. Martin, M.L. Stone, J.B. Solie, and G.V. Johnson. 2002. Turf area mapping using vehicle-mounted optical sensors. Crop Sci. 42: 648-651.

Boydell, B., and A.B. McBratney. 1999. Identifying potential within-field management zones from cotton yield estimates. p. 331-341. *In* J.V. Stafford (ed.) Precision agriculture ’99. Proc. Eur. Conf. on Precision Agric., 2nd, Odense Congress Cent., Denmark. 11-15 July 1999. SCI, London.

Carrow, R.N., V. Cline, and J.M. Krum. 2007. Monitoring spatial variability in soil properties and turfgrass stress: Applications and protocols. p. 641-645. Proc. Int. Irrig. Show. 28th, 9-11 Dec. 2007. San Diego, CA. [CD-ROM] Irrig. Assoc., Falls Church, VA.

Carrow, R.N. and R.R. Duncan. 2008. Best management practices for turfgrass water resources: Holistic-systems approach. *In* J.B. Beard and M.P. Kenna (ed.) Water quality and quantity issues for turfgrasses in urban landscapes. CAST Special Pub. 27. Counc. for Agric. Sci. and Tech., Ames, IA.

Carrow, R.N., R.R. Duncan, and C. Waltz. 2005a. Golf course water conservation: Best management practices (BMPs). Proc. Golf Course Superintendents Assoc. Am. Conf., Feb. 7-12. GCSAA, Orlando, FL.

Carrow, R.N., R.R. Duncan, and D. Wienecke. 2005b. BMPs: Critical for the golf industry. Golf Course Manage. p. 81-84.

Carrow, R.N., and A.M. Petrovic. 1992. Effects of traffic on turfgrass. Agron. Monogr. 32. ASA-CSSA-SSSA, Madison, WI.

Chen, J.M., X. Chen, W. Ju, and X. Geng. 2004. Distributed hydrological model for mapping evapotranspiration using remote sensing inputs. J. Hydrol. 305:15-39.

Corwin, D.L. and S.M. Lesch. 2005a. Apparent soil electrical conductivity measurements in agriculture. Comput. Electron. Agric. 46:11-43.

Corwin, D.L. and S.M. Lesch. 2005b. Characterizing soil spatial variability with apparent soil electrical conductivity I. Survey protocols. Comput. Electron. Agric. 46:103-133.

Corwin, D.L., S.M. Lesch, P.J. Shouse, R.W. Soppe, and J.E. Ayars. 2006. Delineating site-specific irrigation management units using geospatial EC_a measurements. World Congress of Soil Science. Paper No. 153-19.

Duffera, M., J.G. White, and R. Weisz. 2007. Spatial variability of Southeastern U.S. Coastal Plain soil physical properties: Implications for site-specific management. Geoderma 137:327-339.

Dukes, M.D., M.B. Haley, and S.A. Hanks. 2006. Sprinkler irrigation and soil moisture uniformity. Proc. Int. Irrig. Show, 27th, 5-7 Nov. 2006. San Antonio, TX. [CD-ROM] Irrig. Assoc., Falls Church, VA.

Feldhake, C.M., J.D. Butler, and R.E. Danielson. 1985. Turfgrass evapotranspiration: Responses to shade preconditioning. Irrig. Sci. 6:265-270.

Fenstermaker-Shaulis, L.K., A. Leskys, and D.A. Devitt. 1997. Utilization of remotely sensed data to map and evaluate turfgrass stress associated with drought. J. Turfgrass Manage. 2: 65-81.

Finch, C. 2008. San Antonio water conservation program addresses lawngrass/landscapes. *In* J.B. Beard and M.P. Kenna (ed.) Water quality and quantity issues for turfgrasses in urban landscapes. CAST Special Pub. 27. Counc. for Agric. Sci. and Tech., Ames, IA.

Frazier, B.E., C.S. Walter, and E.M. Perry. 1997. Role of remote sensing in site-specific management. p. 149-161. *In* F.J. Pierce and E.J. Sadler (ed.) The state of site-specific management for agriculture. ASA-CSSA-SSSA, Madison, WI.

Gleick, P.H. 1993. Water in crisis: A guide to the world's fresh water resources. Oxford University Press, New York, NY.

Huck, M. 1997. Irrigation design, rocket science, and the SPACE program. U.S. Golf Assoc. Green Section Record. 35(1):1-7.

Hunsaker, D.J., P.J. Pinter Jr., E.M. Barnes, and B.A. Kimball. 2003. Estimating cotton evapotranspiration crop coefficients with a multispectral vegetation index. Irrig Sci. 22: 95-104.

Irrigation Association. 2005. Landscape irrigation scheduling and water management. Available at http://www.irrigation.org/gov/pdf/liswm_part2of3.pdf (cited 15 Jan 2008; verified 20 Mar. 2008). Irrig. Assoc., Falls Church, Va.

Jiang, Y, and R.N. Carrow. 2007. Broadband spectral reflectance models of turfgrass species and cultivars to drought stress. Crop Sci. 47:1611-1618.

Jiang, Y., R.N. Carrow, and R.R. Duncan. 2003. Effects of morning and afternoon shade in combination with traffic stress on seashore paspalum. HortScience 38:1218-1222.

Jordan, T. 2007. Analysis in geographic information science: The global positioning system. Slideshow presentation, GEOG 4470/6470. Univ. of Georgia. Athens, GA.

Karnok, K.J., E.J. Rowland, and K.H. Tan. 1993. High pH treatments and the alleviation of soil hydrophobicity on golf greens. Agron. J. 85:983-986.

Kim, Y., R.G. Evans, and J. Waddell. 2005. Evaluation of in-field optical sensor for nitrogen assessment of barley in two irrigation systems. ASAE paper No. PNW05-1004. ASAE, St. Joseph, MI.

King, J.A., P.M.R. Dampney, R.M. Lark, H.C. Wheeler, R.I. Bradley, and T.R. Mayr. 2005. Mapping potential crop management zones within fields: Use of yield-map series and patterns of soil physical properties identified by electromagnetic induction sensing. Precision Agric. 6:167-181.

Koh, K.J., G.E. Bell, D.L. Martin, and N.R. Walker. 2003. Shade and airflow restriction effects on creeping bentgrass golf greens. Crop Sci. 43:2182-2188.

Kravchenko, A.N., and D.G. Bullock. 2000. Correlation of corn and soybean grain yield with topography and soil properties. Agron. J. 92:75-83.

Kravchenko, A.N., and D.G. Bullock. 2002. Spatial variability of soybean quality data as a function of field topography. Crop Sci. 42:804-815.

Kurtz, K.W. 2000. California fairways: The history of golf course irrigation. Gale Group, Farmington Hills, MI.

Lascano, R.J., R.L. Baumhardt, S.K. Hicks, and J.A. Landivar. 1999. Spatial and temporal distribution of surface water content in a large agricultural field. p. 19-30. *In* P.C. Robert et al. (ed.) Precision agriculture: A challenge for crop nutrition management. Proc. Int. Conf. Precision Agric., 4th, Minneapolis, MN. 17-20 July 1998. ASA-CSSA-SSSA, Madison, WI.

Leib, B.G., J.D. Jabro, and G.R. Matthews. 2003. Field evaluation and performance comparison of soil moisture sensors. Soil Sci. 168:396-409.

Lesch, S.M., J.D. Rhoades, and D.L. Corwin. 2000. ESAP-95 version 2.0 user manual and tutorial guide. Research Report No. 146, George E. Brown, Jr. Salinity Laboratory, Riverside, CA.

Li, K.Y., R. De Jong, and J.B. Boisvert. 2001. An exponential root-water-uptake model with water stress compensation. J. Hydrol. 252:189-204.

Major, D.J., R. Baumeister, A. Touré, and S.L. Zhao. 2003. Methods of measuring and characterizing the effects of stresses on leaf and canopy signatures. p. 81-92. ASA-CSSA-SSSA., Madison, WI.

McVicar, T.R., T.G. Van Niel, L. Li, M.F. Hutchinson, X. Mu, and Z. Liu. 2007. Spatially distributing monthly reference evapotranspiration and pan evaporation considering topographic influences. J. Hydrol. 338:196-220.

Morgan, W.C., J. Letey, S.J. Richards, and N. Valoras. 1966. Physical soil amendments, soil compaction, irrigation, and wetting agents in turfgrass management I. Effects on compactability, water infiltration rates, evapotranspiration, and numbers of irrigations. Agron. J. 58:525-528.

Morris, K.B., K.L. Martin, K.W. Freeman, R.K. Teal, K. Girma, D.B. Arnall, P.J. Hodgen, J. Mosali, W.R. Raun, and J.B. Solie. 2006. Mid-season recovery from nitrogen stress in winter wheat. J. Plant Nutr. 29:727-745.

Mulla, D.J., and J.S. Schepers. 1997. Key processes and properties for site-specific soil and crop management. p. 1-19. *In* F.J. Pierce and E.J. Sadler (ed.) The state of site-specific management for agriculture. ASA-CSSA-SSSA, Madison, WI.

O'Neil, K.J., and R.N. Carrow. 1983. Perennial ryegrass growth, water use and soil aeration status under soil compaction. Agron. J. 75:177-180.

Pauwels, V.R.N., and R. Samson. 2006. Comparison of different methods to measure and model actual evapotranspiration rates for a wet sloping grassland. Agric. Water Manage. 82:1-24.

Plauborg, F., B.V. Iverson, and P.E. Laerke. 2005. In situ comparison of three dielectric soil moisture sensors in drip irrigated sandy soils. Vadose Zone J. 4:1037-1047.

Rana, G., R.M. Ferrara, N. Martinelli, P. Personnic, and P. Cellier. 2007. Estimating energy fluxes from sloping crops using standard agrometeorological measurements and topography. Agric. For. Meteorol. 146: 116-133.

Raupach, M.R., W.S. Weng, D.J. Carruthers, and J.C.R. Hunt. 1992. Temperature and humidity fields and fluxes over low hills. Q. J. R. Meteorol. Soc. 188:191-225.

Rhoades, J.D, F. Chanduvi, and S. Lesch. 1999. Soil salinity assessment: Methods and interpretation of electrical conductivity measurements. FAO Irrigation and Drainage Paper 57. Food and Agric. Organ. of the United Nations, Rome.

Rockström, J., J. Barron, J. Brouwer, S. Galle, and A. de Rouw. 1999. On-farm spatial and temporal variability of soil and water in pearl millet cultivation. Soil Sci. Soc. Amer. J. 63:1308-1319.

Sharma, M.L. 1985. Estimating evapotranspiration. p. 213-282. *In* D. Hillel (ed.) Advances in irrigation. Vol. 3. Academic Press, New York, NY.

Starr, G.C. 2005. Assessing temporal stability and spatial variability of soil water patterns with implications for precision water management. Agric. Water Manage. 72:223-243.

Stier, J.C., J.N. Rogers III, J.R. Crum, and P.E. Rieke. 1999. Flurprimidol effects on Kentucky bluegrass under reduced irradiance. Crop Sci. 39:1423-1430.

Sudduth, K.A., J.W. Hummel, and S.J. Birrell. 1997. Sensors for site-specific management. p. 183-210. *In* F.J. Pierce and E.J. Sadler (ed.) The state of site-specific management for agriculture. ASA-CSSA-SSSA, Madison, WI.

Topp, G.C., and J.L. Davis. 1985. Measurement of soil water content using time-domain reflectrometry (TDR): A field evaluation. Soil Sci. Soc. Am. J. 49:19-24.

Trenholm, L.E., R.N. Carrow, and R.R. Duncan. 1999. Relationship of multispectral radiometry data to qualitative data in turfgrass research. Crop Sci. 39:763-769.

Tucker R.M. 1999. Clay minerals: Their importance and function in soils. NCDA&CS Soil Fertility Note 13. Available at www.ncagr.com/agronomi/pdffiles/sfn13.pdf (cited 22 Apr. 2008; verified 22 Apr. 2008). North Carolina Dep. Agric. and Consumer Serv., Raleigh, NC.

U.S. Coast Guard Navigation Center. 2008. Global positioning system: Serving the world. Available at http://www.gps.gov (cited 10 Nov. 2005; verified 3 Apr. 2008). U.S. Coast Guard Nav. Cent., Alexandria, VA.

U.S. Geological Survey. 2008. Where is earth's water located? Available at http://ga.water.usgs.gov/edu/earthwherewater.html (cited 3 Apr. 2008; verified 3 Apr. 2008). U.S. Geol. Surv., Washington, DC.

Vargas, J.M., Jr. 1994. Management of turfgrass diseases. 2nd ed. CRC Press, Boca Raton, FL.

Xiong, X, G.E. Bell, J.B. Solie, M.W. Smith, and B. Martin. 2007. Bermudagrass seasonal responses to nitrogen fertilization and irrigation detected using optical sensing. Crop Sci. 47:1603-1610.

Western, A.W., G. Blöschl, and R.B. Grayson. 1998. Geostatistical characterization of soil moisture patterns in the Tarrawarra catchment. J. Hydro. 205:20-37.

Wollenhaupt, N.C., D.J. Mulla, and C.A. Gotway Crawford. 1997. Soil sampling and interpolation for mapping spatial variability of soil properties. p. 19–53. *In* F.J. Pierce and E.J. Sadler (ed.) The state of site-specific management for agriculture. ASA, CSSA, and SSSA, Madison, WI.

Wraith, J.M. D.A. Robinson, S.B. Jones, and D.S. Long. 2005. Spatially characterizing apparent electrical conductivity and water content of surface soils with time domain reflectometry. Comput. Electron. Agric. 46:239-261.

Yan, L., S. Zhou, L. Feng, and L. Hong-Yi. 2007. Delineation of site-specific management zones using fuzzy clustering analysis in a coastal saline land. Comput. Electron. Agric. 56:174-186.

Young, M.H., P.J. Wierenga, and C.F. Mancino. 1997. Monitoring near-surface soil water storage in turfgrass using time domain reflectometry and weighing lysimetry. Soil Sci. Soc. Am. J. 61:1138-1146.

Zoldoske, D.F. 2003. Improving golf course irrigation uniformity: A California case study. p. 1-2. Cent. Irrig. Tech. California State Univ., Fresno, CA.

CHAPTER 2

APPLICATION OF SPATIAL AND TEMPORAL MAPPING OF SOIL PROPERTIES AND TURFGRASS PERFORMANCE IN COMPLEX LANDSCAPES

[1]Joseph M. Krum, Robert N. Carrow, and Keith J. Karnok. To be submitted to *Crop Science*.

ABSTRACT

Golf course landscapes are characterized by a high degree of spatial and temporal variability stemming from plant, soil, and climatic factors. In response, principles of precision agriculture (PA) can be implemented to apply irrigation water only where, when, and in the amount required by the plant. Efficient management of water can help reduce site variability by addressing microclimate irrigation requirements. Site-specific management units (SSMUs) reflect the spatial patterns of microclimates and can be delineated by soil and plant mapping, with subsequent adjustments to the irrigation system addressing the moisture requirements within each SSMU. Volumetric water content (VWC) and normalized difference vegetative index (NDVI) were measured with GPS referencing on two golf course fairways at the Old Collier Golf Club in Naples, FL during the summer of 2006; the study site consisted of 'Salam' seashore paspalum (*Paspalum vaginatum* Sw.). Rapid, large scale mapping of fairways was conducted during numerous dry-downs following significant rain events using a mobile platform; data were displayed, analyzed, and interpreted using GIS methods. Areas of similar VWC and NDVI were the basis of SSMUs determined by several data classification schemes. Lower quartile VWC distribution uniformity (DU_{lq}) was higher in SSMUs than throughout entire fairways, indicating that irrigation scheduling based on SSMUs would lead to more efficient water management. The progressive VWC and NDVI reductions within each SSMU were spatially consistent, suggesting SSMUs were applicable during successive dates and throughout separate dry-downs. Relationships between VWC and NDVI instrumentation resulted in linear $r^2 = 0.27$ and 0.10 and quadratic $r^2 = 0.33$ and 0.15 at field capacity for Fairways 10 and 13, respectively; the apparent low relationship was caused by substantial sample size differences and high VWC variability. Preliminary protocols involving VWC and SSMUs were presented for irrigation management

using field capacity determined on the first day of dry-downs and allowable water depletion (AWD) on subsequent days.

INTRODUCTION

In response to an increased emphasis on environmental stewardship, rising costs, and limited resources, efficient application of inputs has become essential to the evolution of the agricultural industry in general, and the turfgrass industry in particular. Since the advent of agriculture, sites have been predominantly managed in a homogenous, uniform manner (Taylor et al., 2007). Plant growth and yield, however, typically vary significantly within a relatively small area because of the dynamic interactions of climatic, plant, and soil factors. Precision agriculture (PA) has come to the forefront of the agricultural industry in recent years (Bouma et al., 1999: Bullock et al., 2007). The main premise of PA is site-specific management, where inputs (e.g., water, fertilizer, and pesticides) are applied only where, when, and in the amount needed by the plant (Corwin and Lesch, 2005a).

Adaptation of growers to practices promoting site-specific management has generally been slow, a response partially attributable to an extension gap between researchers and growers. McBratney et al. (2005) noted that considerable research had been conducted on yield monitoring and quantifying soil inconsistencies for variable-rate application. However, this information was seldom integrated into formal decision support systems (DSS) to allow incorporation of PA into management decisions in the practical world. Corwin and Lesch (2005b) and Tayor et al. (2007) reported that proven and uniform protocols are necessary to foster the reliability, subsequent acceptance, and utilization of site-specific management techniques in agriculture, but that standardized protocols were lacking. Corwin and Lesch (2005b) suggested protocols based on using apparent soil electrical conductivity (EC_a) survey data that characterized spatial variability for site-specific management. Their detailed protocols consisted of appropriate mobile sensor platforms, defining the mapping purposes or field

applications, mapping procedures, soil sampling, laboratory analyses of soil samples, spatial statistical analysis, and geographic information system (GIS) presentation of results. However, they did not carry the protocols through to development of a DSS or inclusion into a DSS for the end-user.

Mobile sensor platforms are necessary to obtain the site-specific information on soil and plant properties required for site-specific management decisions. While remote sensing can provide valuable information over large areas, field-scale data normally require mobile sensor platforms (Corwin and Lesch, 2005b). King et al. (2005) stated that two broad approaches for site-specific management have been to identify patterns within a field related to crop performance (e.g., yield data and plant stress) or soil factors that affect yield (e.g., soil texture, soil moisture, and salinity). The most widely used field approach to estimate soil properties in PA has been with EC_a measurements, especially by electromagnetic devices, while yield mapping provides crop performance information (Corwin and Lesch, 2005a, 2005b; Rhoades et al., 1999). Electromagnetic devices yield non-intrusive estimates of soil salinity in saline soils, but they estimate soil moisture and bulk density in non-saline soil; the normal zone of determination is approximately 30 cm. Rhoades et al. (1999) also discussed the four-wenner array method, which uses four equally spaced metal electrodes inserted approximately 2 cm into the soil as a means to estimate the same soil properties through electrical resistivity (ER).

Starr (2005) and Duffera et al. (2007) indicated that soil water content maps would be valuable to design efficient irrigation management plans. They also noted that soil water content at field capacity has a relatively consistent spatial pattern and is highly correlated with other stable landscape properties, including particle size classes and topography. A common method used for measuring the volumetric water content (VWC) of soils is time-domain reflectometry

(TDR), which utilizes electromagnetic wave pulses transmitted through the soil (Walker et al., 2004). Direct determination of VWC using TDR has been used in research studies and for smaller landscape areas by hand-held units; but rapid, mobile platforms used for routine spatial mapping has not been common (Dukes et al., 2006; Kieffer and O'Conner, 2007). Thomsen et al. (2007) recently described a mobile TDR device for agricultural applications with 0.50- to 0.75-m probes capable of mapping 15 to 30 ha in 8 hours with a 25-m spacing grid. Pauwels and Samson (2005) used TDR to measure VWC in the evaluation of evapotranspiration (ET) on a sloping grassland. The statistical properties of soil moisture spatial variability were examined by Brocca et al. (2006) using TDR; a trend of decreasing variance with increasing VWC was observed. When evaluating the coefficient of variation (CV) in relation to optimal measurement determination, more measurements were needed as topographic relief increased.

The spectral reflectance of plants is a direct indicator of plant health (Jiang and Carrow, 2007). Vegetative indices typically assess reflectance by implementing two wavelength bands within 660 to 950 nm. However, Jiang and Carrow observed that extending the range to 1480 nm increased the model sensitivity in an assessment of canopy reflectance using a variety of turfgrass species and cultivars. The highest partial r^2 values were associated with broadband wavelengths at 900 and 1200 nm. Furthermore, the study suggested three to five broadbands that could be cultivar specific would more accurately evaluate spectral reflectance than conventional models, especially when mapping turfgrass responses to drought stress. Bell et al. (2002) used a vehicle-mounted optical sensor to map the normalized difference vegetative index (NDVI) of a turf canopy on a creeping bentgrass (*Agrostis palustris* Huds.) golf course putting green. The maps based on NDVI highly correlated ($r^2 = 0.98$) to plots fertilized with varying nitrogen rates, as the turf response and cover mimicked the spatial maps. Poor nutrition, sparse turf cover, and

some irrigation patterns were revealed by the maps. Bell et al. concluded that mapping of NDVI could reduce fertilizer and pesticide use, increase turf uniformity, and potentially provide an early warning system for turf managers. A mobile platform for use in turfgrass situations was developed by the Toro Company (Bloomington, MN) in 2005 compatible with global positioning system (GPS) and GIS technology capable of rapid measurement of turfgrass stress by NDVI, as well as surface zone soil VWC (0- to 10-cm depth) and soil penetrometer resistance (Carrow et al., 2007). Another mobile unit combining a soil sensor and plant spectral sensor for turfgrass applications was described by Stowell and Gelernter (2006) using an electromagnetic device.

Once an appropriate mobile sensor platform with both plant and soil sensing capabilities is available, protocols must focus on specific field applications for spatial and temporal mapping (Corwin and Lesch, 2005b). Within traditional agriculture, the primary field application is to define site-specific management units (SSMUs), where a SSMU is a sub-field area that has similar soil and landscape properties that result in similar plant response, input use efficiency, and environmental impact (Boydell and McBratney, 1999; Corwin and Lesch, 2005a, 2005b; Corwin et al., 2006; Duffera et al., 2007; Yan et al., 2007). By applying PA concepts to precision turfgrass management (PTM), Carrow et al. (2007) proposed six field applications related to improving water-use efficiency on complex turfgrass sites. Specific protocols would be required to achieve the field applications, where the applications are: a) use of initial mapping information to make immediate or relative easy-to-do alterations in irrigation design and/or scheduling for uniformity, where the problems may be associated with head alignment, wrong nozzle size, or incorrect scheduling; b) identification of SSMUs on saline and non-saline sites; c) evaluation of a landscape (e.g., a golf course fairway) for soil VWC uniformity, where uniformity may be influenced by system design, slope influences on effective infiltration of

irrigation and precipitation, and/or other factors that result in non-uniformity of VWC across a landscape; d) determination of the best location for placement of in-situ sensor arrays within representative golf course fairway SSMUs on sites where there may be several distinct SSMUs, with each repeated over several fairways; e) similar to item c, the evaluation of a newly installed system for adequate design for uniformity of water application and soil VWC, where if designers knew that a system would be audited for this purpose, it could improve initial design, as well as serve as a training tool for the site manager to optimize use of the new system; and f) for salt-affected sites, the use of these technologies for monitoring spatial and temporal salinity changes for salt management. Questions such as where to leach, how much water to apply, and is leaching effective would be addressed.

As noted, the most widely used PA field method to determine spatial distribution of soil properties has been with EC_a measurements, especially by electromagnetic devices, with this information used to determine SSMUs (Rhoades et al., 1999; Corwin and Lesch, 2005a, 2005b; Corwin et al., 2006). For example, Corwin et al. (2006) used SSMUs to address spatial variability issues associated with EC_a in an irrigated cotton field using GPS-referenced measurements. The spatial distribution of EC_a was used to determine a soil sampling design to investigate the soil properties that influence seed cotton (*Gossypium hirsutum* L.) yield. Based on this information, SSMUs were developed. There was an r^2 of 0.51 between yield and EC_a. Salinity, plant available water, leaching fraction, and pH were the dominant factors that influenced cotton yield. The SSMUs were directly related to the irrigation distribution variability and its effect on cotton yield. Corwin et al. (2006) concluded that SSMUs provide a basis for variable-rate irrigation technology that can potentially reduce water needs and use.

Fridgen et al. (2004) and Yan et al. (2007) used a software program called Management Zone Analyst, which implements a fuzzy c-means unsupervised clustering algorithm to classify field data. Management Zone Analyst gives the user the ability to determine the appropriate number of SSMUs. Taylor et al. (2007) used a protocol based on analyzing raw data, cleaning, interpolating, and a fuzzy k-means clustering program (FuzMe) to define management classes.

Several other techniques have been used to determine SSMUs in agricultural applications (Suddeth et al., 1996; Fleming et al., 2000; Fraisse et al., 2001; Fridgen et al., 2004). Topographic attributes and/or soil physical properties are useful in the identification of spatial variability because of their correlation to soil moisture conditions (Fridgen et al., 2004). Suddeth et al. (1996) and Fraisse et al. (2001) used EC_a and topographic features to characterize SSMUs. Elevation was linked to organic matter, clay content, P, K, Mg, and yield in a study conducted by Pilesjö et al. (2005), showing that SSMUs could be developed from topographic data. Aerial photography of bare soil and producer knowledge was used by Fleming et al. (2000) for SSMU delineation. The application of satellite imagery was used by Boydell and McBratney (1999) to develop management zones for a cotton field. Weather and plant type were identified as determining factors in the establishment of the number of necessary SSMUs, as fewer zones were needed when adequate plant available water was present (Fraisse et al., 2001). Soil map units identified as Norfolk loamy sand, Goldsboro loamy sand, and Lynchburg sandy loam were used as the basis for SSMU delineation in a study conducted by Duffera et al. (2006). The study found that zones delineated via soil particle size differences could be advantageous for PA, as soil water content, plant available water, and penetrometer cone index were spatially correlated.

Sethuramasamyraja et al. (2007) conducted a study that investigated the spatial variability of soil pH, soluble K, and residual nitrate (NO_3) contents using an on-the-go mapping unit. The

spatial variability of soybean [*Glycine max* (L.) Merr.] protein and oil concentrations and topographic influences were quantitatively characterized for site-specific management by Kravchenko and Bullock (2002). Weaver et al. (2004) mapped soil pH buffering capacity with GIS software and GPS instrumentation to determine sampling zones for site-specific lime applications. There was sufficient general agreement between the mapped pH buffering capacity and directly measured values, as indicated by an r^2 of 0.88.

As the focus on site-specific, precision input application has increased, due in part to rising costs and environmental concerns, spatial variability of soil properties has become a greater topic of interest. The determination of optimal soil sampling schemes has been investigated (Wollenhaupt et al., 1997; Lesch et al., 2000). By evaluating the CV, Wollenhaupt et al. (1997) found that soil pH and, to a lesser extent, crop yield exhibited low spatial variability. Conversely, NO_3-N, organic matter content, plant available P, and plant available K exhibited high spatial variability, as indicated by their correspondingly high CV values. Moreover, organic matter content, soil texture, and cation exchange capacity were associated with little temporal variability, while NO_3-N and soil moisture exhibited high temporal variability. Since temporal variability was highly dependent upon precipitation and temperature, Wollenhaupt et al. concluded that proper timing of soil sampling is essential for site-specific management. Once SSMUs are identified based on soil and plant properties from initial spatial mapping, additional soil property information can be obtained from efficient soil sampling protocols.

The ESAP-95 software is a statistical program that is used for the sampling, assessment and prediction of soil salinity from EC_a survey information, but can be used for other soil information such as VWC (Lesch et al., 2000; Corwin and Lesch, 2005b). The program determines optimal soil sampling designs, estimates calibration equations used to predict values

of soil variables, and produces graphical outputs of conductivity survey data and/or predicted soil variables.

In addition to soil chemical and physical SSMU attributes, inclusion of topographic maps is important for further SSMU refinement (Miao et al., 2005). Topography can influence initial VWC after irrigation or rainfall through infiltration and runoff. It can also affect absorption and reflection of incident solar radiation that may contribute to differential ET losses by topographic aspect. Solar radiation is a major driving force for ET, especially when soil moisture is not limited. The spatial variability of ET in relation to topography (elevation, slope, and aspect) has been assessed by data interpolation and modeling methods (Chen et al., 2004; McVicar et al., 2007; Rana et al., 2007).

One means of assessing VWC spatial uniformity (or variability) within SSMUs could be the distribution uniformity (DU) approach used for irrigation systems. A common method for irrigation uniformity assessment is the catch-can test, which involves the placement of evenly spaced reservoirs in a specified area and measuring the amount of water collected from sprinklers (Dukes et al., 2006). The lower quartile distribution uniformity (DU_{lq}) can be calculated to determine the variability of an irrigation system:

$$DU_{lq} = V_{lq}/V_{tot} \qquad \text{Eq. [1]}$$

where V_{lq} is the average of the lowest quarter of catch-can measurements, and V_{tot} is average of all catch-can measurements.

A lower DU_{lq} corresponds to lower irrigation system efficiency, and consequently, more water required to achieve minimum irrigation levels. Other statistics that provide a quantitative summary can be used to describe spatial data within a SSMU compared to the whole area or other SSMUs (McGrew and Monroe, 2000). The mean, mode, and median are measures of

central tendency. Measures of dispersion include the range, standard deviation, and CV. Skewness and kurtosis indicate the shape or relative position of the data set.

Direct determination of surface zone VWC in turfgrass systems over dry-down periods provides additional insight that could assist in irrigation scheduling decisions of when and where to irrigate. Krum (Chapter 3) noted that VWC obtained after a rainfall that infiltrated into the site elicited an estimation of field capacity within SSMUs and the DU_{lq} at field capacity could be used as a background measure of inherent VWC spatial variability within SSMUs. Once a reliable field capacity baseline is obtained, it should be a relatively stable characteristic based on stable soil (e.g., texture, organic matter content, structure) and topographic (e.g., aspect and slope) factors (Starr, 2005; Brocca et al., 2007; Duffera et al., 2007). The field capacity baseline can then be used to estimate the degree of dry-down within the microclimate if VWC measurements are conducted during dry-downs. While field capacity is a relatively stable parameter, VWC changes during dry-downs are not. The most straight forward means to use surface VWC data for irrigation scheduling would be to determine a surface VWC value that would trigger an irrigation event in the microclimate. This would be similar to the allowable water depletion (AWD, which is also called management allowable depletion or MAD) method, where AWD is the percent of available soil water allowed to be depleted before irrigation is applied (SCS, 1993; Smajstrla et al., 2002). The AWD would be selected by the turfgrass manager based on what would be suitable for the site to avoid undue stress on the turfgrass; it could vary throughout the growing season.

As noted, SSMUs can be delineated based on stable soil and topographic attributes. The patterns associated with VWC during dry-downs add a temporal component into the SSMU. These data should be valuable for determining the minimum number and proper location of in-

situ soil sensor arrays to represent specific SSMUs. Since complex landscapes may have a particular SSMU type at several locations across the broad landscape, careful placement within a single SSMU could be used to represent other SSMUs of the same type (Buss, 1996).

Data presentation and analysis also require specific protocols for each field application. Geographic information system technology has been an essential tool in PA studies as a means to display and analyze large, complex geo-referenced data (i.e., GPS) for spatial and temporal trends (Clark and Lee, 1998; Weaver et al., 2004; Pierce and Clay, 2007: Rana et al., 2007). Interpolation of point measurements has proven to be an effective approach in modeling soil variability (Verhagen and Bouma, 1997). Data are interpolated in GIS to create prediction surface maps in a raster for analysis (ESRI, 2004b). Interpolation involves the prediction of values for cells in a raster using a limited number of data points, employing the assumption that spatially distributed objects are spatially correlated. Sampling every point of interest in a study area is often not feasible because of cost, accessibility, and/or time constraints. By interpolating, all areas are assigned a predicted value based on the measured points.

Interpolation methods include inverse distance weighted (IDW), spline, and kriging. The IDW and spline methods are deterministic; based directly on the surrounding measurements or on specific formulas that determine surface smoothness. Kriging incorporates geostatistical methods and statistical models such as autocorrelation, the statistical relationship among measured points. Kriging and IDW both derive predictions for unmeasured locations from measurements. Furthermore, the measurements nearest to the prediction locations are most influential. The weighted sum formula for IDW and kriging is:

$$\hat{Z}(s_0) = \sum_{i=1}^{n} \lambda_i Z(s_i) \qquad \text{Eq. [2]}$$

where $Z(s_i)$ is the measured value at the *i*th location, λ_i is an unknown weight for the measured value at the *i*th location, s_0 is the prediction location, and n is the number of measured values. In terms of IDW, λ_i is entirely dependent upon the prediction locations and data point distances. Conversely, the weight for kriging is determined by the spatial arrangement of the measured points and values, along with the distance between points and prediction locations. While IDW incorporates a distance based algorithm, kriging weights are affected by a spatially based semivariogram model. Kriging essentially involves a two step process in which an estimation of statistical dependence (spatial autocorrelation) is made, followed by a prediction of unknown values.

The spatial autocorrelation of data is described by semivariograms. A semivariogram is a function of the distance and direction separating measured points used to quantify the spatial autocorrelation of the data set (ESRI, 2004a). Semivariograms are developed by determining the difference-squared of the values between each pair of points at different distances, and fitting a model to the empirically derived points (similar to regression analysis). A basic principle of geography states that closer objects are more alike than those farther apart. Measured points that are closer will generally have a smaller difference-squared than those farther apart. The semivariance, $\gamma(h)$, is quantified as:

$$\gamma(h) = \frac{1}{2n}\sum_{i=1}^{n}\left[Z(u_i) - Z(u_i + h)\right]^2 \qquad \text{Eq. [3]}$$

where n is the number of paired sample points, h is the distance between sample points (i.e., lag distance), and $Z(u_i)$ is the measured value at the *i*th location (Dobermann, 2006).

Spatial mapping of soil EC_a in PA has been conducted using a field sample spacing from 3 to 5 m (Corwin and Lesch, 2005b). However, mobile platform surveys to determine TDR estimates of VWC use a much wider spacing of 10 m or greater (Western et al., 1998; Brocca et

al., 2007; Thomsen et al., 2007). Western et al. (1998) noted that too few samples or large spacing grids would influence spatial correlations and spatially based semivariogram models.

Dissolved salt content, soil moisture, temperature, and clay content determine soil EC_a (McNeill, 1980). Tarr et al. (2005) investigated the potential of using EC_a as a covariate with soil P, K, pH, organic matter, and moisture. Co-kriging each variable with EC_a produced maps with more local detail than the maps of only the kriged variables. Kriging variance was improved when variables more highly correlated with EC_a were used, but the overall characterization accuracy of pasture variability was not consistently and substantially improved with co-kriging.

Since use of mobile platforms for intense mapping of soil properties (e.g., VWC and penetrometer resistance) and plant performance (NDVI) in complex turfgrass landscapes has not been reported, the purposes of this study involved two field applications: a) determine the most suitable SSMU classification method applicable to the measured data, and b) identify spatial patterns of variation and relationships in VWC and NDVI throughout the progression of dry-downs. Included in these objectives was to present preliminary data analysis and interpretation methods to aid in the development of protocols for future PTM studies for these field applications.

MATERIALS and METHODS

The study was conducted at the Old Collier Golf Club in Naples, Florida. The research area consisted of 'Salam' seashore paspalum (*Paspalum vaginatum* Sw.) mowed three times weekly at a height of 0.95 cm with a reel mower. Data collection was initiated following significant rain events, which negated irrigation uniformity issues pertaining to surface VWC (Table A-1, Appendix). Five dry-downs took place during 14 to 16 June, 19 to 20 June, 21 to 23

June, 26 to 29 June, and 12 to 16 July, 2006. No irrigation was applied during dry-downs. Light rain events of 0.43, 0.11, and 0.02 cm occurred during the afternoons of 21 June, 28 June, and 13 July, respectively. Data analysis emphasized the 12 July dry-down because of its duration and absence of significant rainfall in relation to the other dry-downs.

Data collection was performed via the Toro Mobile Multi-Sensor (TMM; patent pending) prototype data acquisition unit (The Toro Company, Bloomington, MN) on Fairways 10 and 13 at the Old Collier Golf Club. Fairway 10 measures 4534 m^2 (0.453 ha), while Fairway 13 comprises an area of 5097 m^2 (0.600 ha). The TMM measures VWC (%), NDVI (unit-less; best = 1.0), and compaction (penetrometer resistance; kg). The TMM was affixed to and maneuvered with a utility vehicle, traversing the fairways by making passes at approximately 2.5-m spacing. An operating speed of 2.7 to 3.3 km h^{-1} was maintained during data acquisition. Data were recorded using an on-board laptop computer and all parameters were displayed in spreadsheet format. Data were obtained during the afternoon of each day within a time period of 1400 to 1800 h EST.

Soil moisture measurements were based TDR, which measures changes in the soil dielectric constant (ε) as water contents fluctuate (Leib et al., 2003). A TDR sensor produces a high frequency voltage pulse that is transmitted and reflected along metal probes. The dielectric constant is determined by measuring the velocity of the transmitted pulse in the soil, which is primarily dependent upon VWC, as water has a significantly higher dielectric constant than air (ε = 80 and 1, respectively). The permittivity and corresponding pulse velocity are closely related to the soil water content (Plauborg et al., 2005).

Soil EC_a can greatly affect TDR readings by promoting erroneous overestimates of water content (Nadler et al., 1999). Salinity is a major contributing factor to EC_a, suggesting that

negligible salinity levels should be verified before taking TDR measurements. A hand-held Landmapper ERM-0l (Landviser, Inc. Westhampton, NJ) measured the electrical resistance (ER; ohm m^{-1}), which was subsequently converted to EC_a, in study plots located in Fairways 10 and 13 to verify the absence of significant salt concentrations in the soil prior to data acquisition (Krum, Chapter 3; Table A-2, Appendix). This device is based on determining EC_a using the four-wenner array method as described by Rhoades et al. (1999).

A Field Scout TDR 100 soil moisture sensor (Spectrum Technologies, Inc. Plainfield, IL) was modified for use on the TMM platform and measured VWC at a 0- to 10-cm depth. Two custom stainless steel probes of 9.53-mm diameter, 3.3-cm spacing, and 10-cm length were installed on the moisture sensor to facilitate a soil penetration depth of 10 cm. The sampling volume is an elliptical cylinder extending 3 cm radially beyond the TDR probes, measuring approximately 825 cm^3. The sensor is attached to one end of a shaft on the TMM, while a bolt is connected to the opposite end. When the TMM moves, the wheel-driven shaft rotates in a circular fashion. As the sensor's probes enter the soil, the bolt passes by a series of magnets that triggers the data logger to take a measurement. The probes are inserted into the soil approximately every 2.5 m, which resulted in an average of 547 readings on Fairway 10 and 765 on Fairway 13. Exceeding 3.5 km h^{-1} significantly increased the probability of obtaining erroneous VWC readings. Possible theories as to the cause of this problem are that the bolt was passing by the magnets too quickly or the TDR probes were being inserted into the soil too quickly to facilitate a VWC measurement.

A GreenSeeker RT100 active sensor (NTech Industries, Inc. Ukiah, CA) evaluated turf canopy NDVI in the study plots. The NDVI, which measures multispectral reflectance, has been shown to be significantly associated with visual turf quality, density, and shoot tissue injury

(Trenholm et al., 1999). The sensor is equipped with internal light emitting diodes and a photodiode optical detector that measures the percent reflectance of red (R = 660 nm) and near-infrared (NIR = 770 nm) spectral bands {NDVI = $[(R_{770} - R_{660})/(R_{770} + R_{660})]$}. Healthy plants are characterized by greater NIR and lower R reflectance than plants under stress. The sensor is mounted on the TMM at a height of approximately 1 m and evaluates a 60- ± 10-cm by 1.52- ± 0.51-cm field of view. The sensor emits light pulses every 100 ms and outputs an averaged value every second. An average of 1779 and 2518 measurements were collected on Fairways 10 and 13, respectively. Measurements are unaffected by solar radiation because of the sensor's internal light source.

An Omega LC302-500 1.90-cm diameter stainless steel compression load cell (Omega Engineering, Inc. Stamford, CT) was used to measure the insertion force (kg) of the TDR moisture sensor probes. As the probes penetrate the soil, pressure is exerted against the load cell, indicating the degree of soil compaction. The load cell converts the load acting on it to electrical signals, which are used to calculate the penetrometer resistance. Penetrometer data are not presented in this paper since the site was very high in sand content and exhibited few high penetrometer resistance measurements.

A Trimble *Ag*GPS 132 receiver (Trimble Navigation Unlimited, Sunnyvale, CA) was used to compile GPS information (i.e., latitude, longitude, and altitude) of each data point. The GPS unit also determined time and speed data. The U.S. Coast Guard Beacon DGPS differential correction service was used to enable the potential of sub-meter precision.

The ESRI ArcGIS GIS and mapping software, versions 9.1 and 9.2 (ArcMap and ArcScene), along with the ArcGIS Spatial Analyst and Geostatistical Analyst extensions, were used to develop, display, analyze, and interpret maps of the TMM data (ESRI, Redlands, CA).

The VWC, NDVI, and compaction data points were displayed on the Old Collier Golf Club base maps and interpolated using the kriging method of interpolation via the Spatial Analyst extension. The ESRI ArcPad software program was used during data acquisition to track the passes of the TMM to aid in the development of a consistent sampling grid.

Initially, six data classification methods were used for SSMU delineation: manual, standard deviation, quantile, Jenk's natural breaks, 1/3 query, and histogram class breaks. The manual method incorporated five VWC groups (<10, 10-15, 15-20, 20-25, and >25%). The histogram class breaks method was performed by analyzing the histogram from each data set and selecting classes based on breaks in the graph and agronomic, soil based considerations. The Jenk's natural breaks scheme identifies clusters of data and maximizes the differences between classes, thereby minimizing the variance within classes. The quantile method used five classes that consisted of an equal number of data points. The 1/3 query method was performed by displaying the lower, middle, and upper 1/3 of data separately in the map view. Then, the SSMUs were drawn based on clusters of data points. Next, all data points were displayed, and all points lying within the SSMUs were selected. The standard deviation classification used divisions of one standard deviation relative to the mean. Based on the comparative strengths and weaknesses of each of these classification methods, an integrated method that encompassed the standard deviation and histogram classifications to delineate SSMUs was developed (termed SD-Integrated).

Several measures of dispersion, central tendency, and shape or relative position were calculated for the 12 and 16 July VWCs of each SSMU and classification method for both fairways (McGrew and Monroe, 2000). These included the mean (average), median (middle

value of the ranked data set), and mode (most frequently occurring value). A significant difference between these measurements usually indicates a skewed data set.

The range of the data set is the difference between the highest and lowest values. The standard deviation is the square root of the sum of the deviations of the square of each value from the mean, divided by number of values in the data set:

$$s = \sqrt{\frac{\Sigma\left(X_i - \overline{X}\right)^2}{n}} \qquad \text{Eq. [4]}$$

where s is the standard deviation, X_i is the value of observation i, $\overline{X}$ is the mean, and n is the number of observations. Unlike standard deviation, the CV is expressed as a percentage of the mean, and consequently allows for analysis between data sets with different absolute values. The CV can be a valuable relative index of dispersion.

$$CV = \frac{s}{\overline{X}}(100) \qquad \text{Eq. [5]}$$

Skewness is a measure of the degree of symmetry in a frequency distribution, and determines the extent of even or uneven data distribution in relation to the mean.

$$\text{Skewness} = \frac{\Sigma\left(Xi - \overline{X}\right)^3}{ns^3} \qquad \text{Eq. [6]}$$

Positively skewed data are skewed to the right, a value of zero indicates symmetry, and negatively skewed values indicate skewness to the left. Kurtosis measures the degree of flatness or peakness of a data set.

$$\text{Kurtosis} = \frac{\Sigma\left(Xi - \overline{X}\right)^4}{ns^4} \qquad \text{Eq. [7]}$$

Normally distributed data have a kurtosis of 3.0, and is termed mesokurtic. A peaked data set is characterized by a high kurtosis, >3.0, and is classified as leptokurtic. Platykurtic distributions are relatively flat and widely dispersed, with a kurtosis value of <3.0. Furthermore, the mean of the VWCs and NDVIs were also determined for each SSMU incorporating each classification method for each day during the 12 to 16 July dry-down.

An additional characterization of SSMUs was conducted using the DU_{lq} of the 12 and 16 July VWC data in an attempt to most accurately define homogenous classes (Dukes, 2006). The first day of the July dry-down was selected because the VWCs on this day estimated field capacity and were not compromised by external factors that affected temporal spatial variability. The SSMUs were categorized by low (L), moderate (M), and high (H) VWCs. The DU_{lq}, r^2 of the TMM VWC and NDVI, and the significance value of the F-statistic were calculated for each SSMU and were compared to the DU_{lq}, r^2, and the significance for the entire fairway.

RESULTS and DISCUSSION

Since the TMM was the first unit developed capable of both soil and plant measurements available for use on turfgrass sites to foster PTM, a central component of this study was to define preliminary protocols similar to that suggested by Corwin and Lesch (2005b) in PA. They noted that protocols included: appropriate mobile sensor platforms, defining the mapping purposes or field applications, mapping procedures, soil sampling to obtain further site information, laboratory analyses of soil samples, spatial statistical analysis, and GIS presentation of results; but, they did not carry the protocols through to an inclusion in a formal DSS. The results and discussion was approached from the standpoint of defining appropriate science-based but practical protocols for integration into a DSS.

Mobile Platform

Map accuracy normally increases as sample number increases, but intensive hand sampling and lab analysis in cost prohibitive (Wollenhaupt et al., 1997). One of the most advantageous characteristics of the TMM over traditional sampling is that it permits relatively quick collection of over 750 VWC measurements and over 2500 NDVI measurements in approximately 60 minutes. The TMM device allows for rapid mapping of a more intensive

spacing grid than typical of PA. In complex turfgrass situations, such as a golf course fairway, earth moving during construction and inclusion of berms, mounds, or other terrain features may influence soil properties, indicating a need for more intensive spatial mapping than used for PA.

Relative to crop fields, turfgrass sites allow easier access for mapping at selected times, such as after rainfall to insure field capacity over the landscape or for temporal mapping over a dry-down period. Also, insertion of TDR probes in the surface 10 cm is possible within turfgrass swards without concern over a fallow or dry surface condition. The TMM unit allows VWC mapping in the surface 10 cm within a few hours after a rainfall of sufficient magnitude and rate to achieve full field capacity measurements across the area. By this means, errors associated with irrigation system distribution on surface VWC were negated and provided for a good estimate of field capacity; a relatively stable soil attribute highly related to soil texture and organic matter content (Starr, 2005; Duffera et al., 2007). Inclusion of a spectral unit to monitor NDVI at field capacity and during dry-downs at the same time as VWC measurements allowed a key soil moisture parameter to be related to an immediate plant response, rather than a delayed yield response as is often the case in PA.

The VWC and NDVI semivariograms (including the spherical models) of Fairways 10 and 13 quantified the spatial autocorrelation of the data on 12 July 2006 (Figures 2.1 to 2.4). The range, nugget, sill, and partial sill are used to describe the models of the semivariograms (ESRI, 2004a). The range is the distance (m) at which the model plateaus, indicating the spatially dependent portion of the semivariogram. The sampling distances were approximately 1 and 2.5 m for NDVI and VWC, respectively. Since the sampling distances were significantly less than the ranges of all semivariograms, this suggests that the sampling scheme was sufficient; sampling distances greater than the range would imply an inadequate sampling scheme.

The nugget is the variability at the origin and indicates spatial measurement errors and/or spatial sources of variation at distances smaller than the sampling interval. The sill represents the total variability, while the partial sill is associated with the spatially correlated component of the data set variability.

SSMU Delineation

A critical aspect of PA is to determine science-based but practical SSMUs (Taylor et al., 2007). Identification of SSMUs related to crop performance requires spatial information sources that are stable over time and that affect crop yield. Many different approaches have been used to delineate SSMUs, including: field observation of soil; soil surveys; EC_a, usually by EM to estimate soil properties (e.g., texture, moisture content, salinity); soil properties (physical or chemical) if spatial data are available or can be easily obtained; topographic maps or attributes; aerial photographs of crops or bare soil; NDVI; yield monitoring; and combination methods (Fridgen et al., 2004; Taylor et al., 2007; Yan et al., 2007). Use of electromagnetic devices to determine EC_a, yield mapping, and NDVI (when mobile NDVI sensors could traverse a crop field), have allowed the most intensive spatial mapping in PA situations.

Measuring VWC via TDR as used in our study is a common research tool and has been applied to small sites, but it has received limited use on mobile platforms for PA as a basis for determining SSMUs. The limited use stems from the time required for probe insertion, but Thomsen et al. (2007) recently described a TDR unit for field mapping (Brocca et al., 2007). Starr (2005) and Duffera et al. (2007) reported that soil water content maps would be valuable to design efficient irrigation management plans, and noted that VWC at field capacity has a relatively stable pattern of spatial variability that is highly correlated with other stable landscape properties, including particle size classes and topography.

The ranges of VWC were 7 to 40% and 7 to 45% for Fairways 10 and 13, respectively, even though the fairway sites were very sandy in nature, as shown by soil texture from samples obtained for studies reported in Chapters 3, 4, and 5, with percent silt and clay at 4% or less (Figures 2.5a and 2.5b; Table A-3, Appendix). Organic matter content ranged from 2.52 to 4.98% (dry weight basis). In addition to possible spatial variation in soil texture and organic matter, some degree of water repellent soil (hydrophobicity), silt layering, and traffic patterns may have had some influence on VWC. During the 12 to 16 July dry-down, visual wilt patterns as reported by Karnok et al. (1993) were observed on the lowest VWC areas of both fairways; delayed rewetting was observed after the 16 July irrigation. Also, during the establishment period, irrigation water from an adjacent canal was used for two periods that resulted in two silt layers of approximately 0.3- to 0.6-cm thickness at approximately 3.8- to 5.1-cm depths. The silt layer was somewhat more pronounced in some areas, most likely because of non-uniformity of irrigation water application at establishment, where greater irrigation overlap would cause more silt deposition. The layered nature of silt would be localized and could result in greater influence on VWC than the percent silt levels would suggest if spread throughout the whole 10-cm soil zone. Traffic patterns off the fairway in front of Green 10 may have contributed to lower percent organic matter in this area even though it was in a depression.

Sometimes SSMU boundaries are delineated by visual means of aerial, soil, or yield maps. The most useful statistical approaches for determining SSMUs are interpolation methods (kriging, co-kriging, IDW) or fuzzy k-means cluster analysis that result in spatial maps to assist in defining SSMU boundaries (Corwin and Lesch, 2005a, 2005b; Cassel, 2007; Taylor et al., 2007; Yan et al., 2007). After interpolation of the spatial VWC data by kriging, we delineated SSMUs based on seven classification procedures (Figures 2.6 to 2.12).

The classification method essentially determines the legend scale for VWC data and therefore the map appearance, which ultimately influences boundary selection for individual SSMUs. For example, Figure 2.6 is the manual classification of VWC data displayed for Fairways 10 and 13 using VWC intervals of 5%, such as 20 to 25% VWC, while Figure 2.7 presents selected VWC intervals based on the fairway histograms (Figures 2.5a and 2.5b) to consider suggested soil type differences or groupings; thus, the intervals are not equal in range, but reflect agronomic considerations. Boundaries were then drawn to incorporate similar areas based on the manual (Figure 2.6) or histogram (Figure 2.7) display of VWC legend groupings. This is the approach used for all seven classification methods to determine the final SSMU boundaries.

Some classification methods were included to illustrate that care should be taken to use the most appropriate data classification schemes, since the associated maps influence SSMU boundaries. For example, the manual, quantile, and 1/3 query classification methods organize data in a rather arbitrary manner because the class breaks are independent of the data set distribution, as reflected in the histograms for each fairway (Figures 2.6, 2.9, 2.10, 2.5a, and 2.5b). The manual method may seem reasonable because of the equal range for each of the five VWC intervals, but soil textures do not follow equal ranges (Figure 2.6). The quantile procedure also resulted in five VWC intervals based on the same number of samples in each interval (Figure 2.9). Comparing the manual (Figure 2.6) to the quantile (Figure 2.9) demonstrates a much more complex map for the quantile classification scheme even though both methods have legends involving five intervals. The 1/3 query method allocates an equal number of samples (roughly) into three groups (Figure 2.10). It is useful when presenting each mapping point as one of three colors to illustrate spatial distribution of the 1/3 highest and lowest VWC sampling

sites. For all three of these classification schemes, the intervals are not based on a science or agronomic basis.

The histogram and Jenk's classification procedures resulted in four VWC intervals (Figures 2.7 and 2.8). The Jenk's method identifies clusters of data that minimizes the variance within classes which is based on locating sharp breaks in the histogram ranges (i.e., natural breaks) (Figure 2.8). The histogram classification method also looks for natural breaks, but these are selected by the researcher based on agronomic considerations of site conditions and characteristics (Figure 2.7). For example, on Fairway 13, the lowest VWC range for the Jenk's method was <17.6%, while for the histogram we selected <15% because this interval represented the lowest VWC range and the 15 to 17% VWC areas appeared to be better associated with the next higher class (Figure 2.5b). Less complex spatial VWC maps using the histogram method relative to the Jenk's were observed for both fairways.

The standard deviation procedure uses the calculated standard deviation value of the data composition of each fairway. The class intervals are based on this value, which resulted in six categories (Figure 2.11). One aspect of this approach is that the two central intervals represent data points within one standard deviation of the mean; a normal distribution should include approximately 68% of the population. For example, in Fairway 10 the 20.4 to 24.4% interval includes VWCs with a range equaling the standard deviation (4.03), centered around the mean (22.37). The standard deviation and mean after kriging interpolation is normally different than those statistics of raw data because the interpolated map in composed of predicted values based on the raw data. A landscape area with a rather uniform VWC should result in fewer class intervals compared to a landscape with a wide VWC range (requiring more classes). Of most importance is that the standard deviation allows the lowest and highest classes to be clearly

defined in a manner that has a relationship corresponding to the degree of data dispersion; the number of class intervals should provide an indication of data dispersion. Defining the most dry and moist areas by using intervals defined by the standard deviation is very valuable, since these areas are the sites that are most distinct in the landscape, and therefore of most interest for management decisions.

It should be noted that all methods provide an estimate of the most dry and moist areas. However, the standard deviation and histogram procedures provide a better basis for defining these values, with the standard deviation including a statistical measure of data dispersion, while the histogram incorporates agronomic experience. Thus, we used both the SD and histogram classification schemes to assist in defining SSMU boundaries.

The SSMU boundaries based only on the particular classification method are denoted on the histogram (Figure 2.7) and standard deviation (Figure 2.11) maps. In Figure 2.12, the final SSMU boundaries for both fairways are presented in the SD-Integrated maps. Mapping intervals retain the standard deviation basis for the class intervals, while using both the individual standard deviation and histogram maps to assist in delineation of SSMU boundaries. Using the standard deviation class intervals allows the lowest and highest VWC areas to be clearly identified, which is critical because these are the sites most likely to require attention to improve water-use efficiency. However, the histogram method, with its agronomic-based but fewer class intervals, illustrates a less cluttered map of potential SSMUs. Since SSMU boundaries are ultimately manually drawn, whether based on the various PA methods for SSMU delineation or by the means proposed in this paper, we believe that the integration of the strengths of both the standard deviation and histogram methods will result in the best SSMU boundary selection. Furthermore,

the SD-Integrated method incorporated SSMUs that were delineated in a more practical implementation manner than the other methods.

Since only two fairways were mapped in this study, it was not possible to determine the actual number of different SSMUs over the entire golf course. Initially, after all fairways are mapped on a site, similar areas of VWC should be investigated For example, in Fairway 10 the low, moderate, and high SSMUs were primarily associated with VWC ranges of <16.3; 16.3 to 24.4; and >24.4%, respectively (Figure 2.12). For Fairway 13, the low, moderate, and high SSMUs were located within VWC ranges of <17.8; 17.8 to 24.0; and >24.0% (Figure 2.12). By comparing the various SSMUs across all fairways (or a large area such as a sod farm) it may be possible to group SSMUs together, such as the <16.3 (Fairway 10) and <17.3% VWC (Fairway 13) SSMUs. Secondly, it may be beneficial to adjust SSMU boundaries to better represent a set of SSMUs that would reflect all possible SSMUs across the site. Or it may be that the histogram method by itself would be a reasonable method to determine SSMUs that are less complicated. Perhaps information regarding whether the SD-Integration or histogram classification methods (or other options) are best may come from studies where a dry-down is mapped to further investigate how potential SSMUs respond over the dry-down and which classification method at field capacity estimates the dry-down SSMU boundaries. Dry-down responses are discussed later, but as dry-downs progressed for Fairway 10 (Figures 2.13 to 2.17) and Fairway 13 (Figures 2.18 to 2.22), the VWC and NDVI responses provide insight into changes within SSMUs and adjacent areas. Since dry-down mapping would not necessarily be common on most sites versus mapping of VWC at field capacity, the objective could be to use selected case studies of mapping of dry-downs to see whether the SD-Integrated or histogram classification method best reflects responses once the site is exposed to a dry-down. Thus, in this study of two fairways, we

are using the SD-Integrated as the standard, but suggesting that the histogram method should be considered until more case studies are investigated.

The optimal SSMU delineation size and detail is influenced by the degree of control that a specific site's irrigation system provides. A system with single-head control (each individual sprinkler head can be adjusted independent of all others) would facilitate the most intricate SSMUs, whereas SSMU detail would be more limited by zoned irrigation systems (multiple sprinklers are grouped and thus all sprinklers within each group operate analogously).

SSMU Characterization

Common descriptive statistics of Fairways 10 and 13 within SSMUs developed for each of the six initial classification methods and the final SD-Integrated SSMUs are presented in Tables 2.1 to 2.4. The descriptive statistics consisted of measures of central tendency (mean, median, and mode), data variability (range, standard deviation, and CV), and nature of frequency distribution (skewness as a measure of degree of symmetry and kurtosis as a measure of flatness or peakness of the data set) (McGrew and Monroe, 2000).

In a unimodal and symmetric data set, the mean, median, and mode would be equal. Positively skewed data are characterized by having a median and mode that are less than the mean; a negatively skewed data set has the opposite attributes. However, if the data set from a fairway is not unimodal, then interpretation is more complex. While presenting all three measures of central tendency could provide insight into the central tendency of data, inclusion would ultimately not be imperative to the end user in a DSS. Additionally, presentation of the fairway histogram illustrates whether the data is unimodal or bimodal, has a normal distribution, or is skewed. Since the mean is the most widely used measure of central tendency and is often

the most appropriate measure for interval data, the mean appears to be the best initial comparison of central tendency.

The range is the simplest measure of data variability (Tables 2.1 to 2.4). Initially, it may be expected that the range of a SSMU would be substantially less than the whole fairway. However, because of the spatial variability of VWC in the field, there are often low or high VWC outliers within each SSMU. Thus, the range is inherently limited is its value in the assessment of data variability. This is illustrated in Tables 2.1 and 2.3, where the SSMU ranges are less than the whole fairway, but are relatively high. There is a tendency for the low SSMUs to exhibit a lower range, indicating less variability within these areas.

Standard deviation and CV are common measures of data variability and allow easy comparison across SSMUs and fairways. For Fairway 10, the standard deviation of all SSMUs by all classification methods were lower than the overall fairway (standard deviation = 5.42), except for the low SSMUs by the SD-Integrated method (Table 2.1). In this fairway, CVs of the low SSMUs were normally higher than for the overall fairway. One reason for this is the somewhat skewed VWC distribution to the lower VWC values as noted in the fairway histogram (Figure 5a). Also, this reflects that fairway areas with lower VWC also showed considerable spatial variability, and that by nature the same increase in VWC (e.g., 5%) in a low VWC area (6 + 5% = 11%) as in a high VWC area (30 + 5% = 35%) results in greater apparent data variability in the low SSMU. The moderate and high SSMUs of Fairway 10 exhibited lower CVs than the overall fairway or the low SSMUs, which was also usually noted for the standard deviations of these areas. This would suggest that these SSMUs have less variability than the overall fairway. Fairway 13 had a more skewed nature for VWC, especially considering the higher VWC values across the fairway relative to Fairway 10 as noted in the histograms (Figures 2.5a and 2.5b).

This is reflected in the tendency for higher standard deviation and CV values for the high SSMUs (Table 2.3).

When comparing the standard deviation and CV trends for the SD–Integrated to the standard deviation and histogram classification methods, they were relatively similar for both fairways (Tables 2.1 and 2.3). This indicated that even though the SD-Integrated classification for SSMUs accounted for more practical SSMU boundaries with the potential to include small areas of diverse VWC values, the resulting SSMUs exhibit similar data variability as the methods contributing to it.

In overview, the data variability within SSMUs was less than what the whole fairway areas exhibited in terms of standard deviation and CV, which would reflect that data within a SSMU are more similar in VWC than the whole area. The exception is when a skewed data distribution is apparent in terms of low VWC (Fairway 10) or high VWC (Fairway 13). In these cases, the SMMU associated with the skewed data exhibited standard deviation and CV values similar to the overall fairway. Thus, a high standard deviation or CV in either the low or high SSMUs would suggest data skewness in this area. The goal for a SSMU is to define an area that is more similar than the whole field area, which should be reflected in lower standard deviation and CV values. While these examples show that outliers or wide dispersion at either end of the VWC range can result in limited change in these values, SSMUs can still be representative of a unique area. Interestingly, for the low SSMU of Fairway 10 that had the higher standard deviation and CV values, the range was lower than for the moderate and high SSMUs; but for Fairway 13 with skewness to the high VWC end, the high SSMU had higher standard deviation, CV, and range values compared to the low and medium SSMUs. We would suggest that all

three measures of data variability be presented for a DSS approach, but with the standard deviation and CV of most importance because of the influence of outliers on the range.

Fairway 10 exhibited a slight negative skewness (-0.18) while Fairway 13 has a positive skewness (1.21) (Tables 2.1 and 2.3). The overall fairway skewness is a valuable measure to describe the nature of the fairway VWC data distribution and should be reported on the histogram figure for a fairway DSS report, along with other relevant descriptive statistics for the whole fairway area, namely: mean, range, standard deviation, CV, skewness, and kurtosis.

In the procedure that we used to define practical SMMU boundaries, the result was formation of three SSMUs for the fairway test sites; however, the standard deviation based legend had six VWC classes. Thus, within a SSMU there is typically at least two adjacent VWC classes; if one dominates, the result would be a negative or positive skewness in the direction of the dominant VWC class within the SSMU. For example, in the SD-Integrated map for the moderate SSMU of Fairway 13 (Figure 2.12), the two adjacent classes that are dominant are the 11.6 to 17.8% and 17.8 to 24.0% VWC classes. Since the skewness for the moderate SSMU is 1.42, this suggests that the 17.8 to 24.0% VWC values are the most prevalent within this SSMU (Table 2.3). In contrast, the skewness of Fairway 10 for the SD-Integrated SSMUs are -0.18, -0.09, and 0.13, respectively, for the low, moderate, and high SSMUs, suggesting that the VWC classes within these SSMUs have an approximately equal number of data points (Table 2.1). While a visual observation of the SSMU map and legend such as in Figure 2.12 shows which VWC classes are present within a SSMU, the skewness value demonstrates the balance of VWC classes within a SSMU. However, for a practical DSS, skewness within the SSMUs may be more complicated to explain relative to the value of the information. Essentially, the value of the mean for a SSMU would denote the bias or “skewness” of VWC values within a SSMU in a

more practical and straight forward fashion, since the mean would be biased toward the most prevalent VWC class included in a particular SSMU.

Kurtosis describes the flatness or peakness of a data distribution curve. Kurtosis for Fairways 10 and 13 were 3.66 and 4.95, respectively, which demonstrated a leptokurtic (peaked) nature of the VWC distribution (Tables 2.1 and 2.3). This is substantiated by their histograms (Figures 2.5a and 2.5b). Within a SSMU, there does not seem to be a value in including the kurtosis within a DSS report.

In terms of basic descriptive statistics for whole fairways or large landscape areas, we suggest the following: mean, range, standard deviation, CV, skewness, and kurtosis. However, for the SSMUs as defined in the SD-Integrated classification scheme, basic descriptive statistics could be confined to the mean, range, standard deviation, and CV. If histograms of individual SSMUs were developed, then the skewness and kurtosis values could be incorporated in the histograms for each individual SSMU.

A non-traditional means to characterize soil VWC spatial variability across a whole area and within specific SSMUs is the DU approach used for determining irrigation system application uniformity. The DU is normally obtained by placing evenly spaced catch-cans in a specified area and measuring the amount of water collected from sprinklers (Dukes, 2006). While the catch-can method only assesses irrigation system distribution, a VWC-based DU would integrate irrigation system non-uniformity, inherent differences in VWC because of soil texture and organic matter, and any factor affecting rain or irrigation infiltration. In the case of VWC data collection when the soil is at field capacity, the VWC-based DU would only reflect soil moisture holding capacity differences that are of direct interest for SSMUs.

Dukes et al., (2006) and Kieffer and O'Conner (2007) applied this approach to smaller landscape areas using hand-held units for direct determination of surface zone VWC by TDR. The lower quartile distribution uniformity (DU_{lq}) is used as a measure of the degree of uniformity (or variability) of the irrigation system, where a DU_{lq} of 0.70 and 0.80 is classified as very good and excellent, respectively, for a rotary irrigation system. The lower half distribution uniformity (DU_{lh}) is often used to determine the Run Time Multiplier (RTM) for irrigation scheduling, where RTM = $100/DU_{lh}$. This adjustment in run time of the system is used to achieve adequate water application over the whole site. If the DU_{lh} is 0.65 and the desired application amount is 1 cm, then 1.54 cm of water would be needed to ensure the entire area receives at least a 1-cm irrigation event.

Using VWC based DU calculations, the DU_{lq} values of Fairways 10 and 13 were 0.69 and 0.66, respectively (Tables 2.5 and 2.6). The low SSMU for Fairway 10 resulted in a range of 0.58 to 0.69 across all classification methods with a 0.59 value for the SD-Integrated method. The lower DU_{lq} values for the low SSMU reflects the considerable range of VWC values within this SSMU. In contrast, for both fairways and all other SSMUs, the DU_{lq} values were consistently greater than the fairway average (Tables 2.5 and 2.6). Mecham (2001), Dukes et al. (2006), and Kieffer and O'Conner (2007) all reported that DU_{lq} based on VWC approximated catch-can DU_{lq}, but was consistently higher. Their test sites were relatively small with little topographic differences.

Since DU is a well understood and frequently used approach for assessing irrigation system uniformity and for scheduling irrigation, inclusion of DU_{lq} and DU_{lh} values for whole fairways and then for individual SSMUs would appear to be beneficial. For example, scheduling irrigation reflective of the VWC based DU_{lh} within individual SSMUs should result in more

efficient water-use than using a catch-can value obtained from a more expansive area where terrain changes make catch-can assessment difficult or impractical. Thus, this value would have an immediate application for irrigation scheduling.

A comparison of VWC and NDVI maps for 12 July when both fairways were at field capacity is presented in Figures 2.13 and 2.18 for Fairways 10 and 13, respectively. One apparent observation is that areas with lower NDVI often coincide with low VWC areas. Linear relationships for VWC and NDVI at 12 July field capacity readings differed within the low, moderate, and high SSMUs for the various classification methods (Tables 2.5 and 2.6). The low SSMU area (i.e., low VWC based SSMU) exhibited the highest linear r^2 regardless of classification method. The residual effect of soil moisture stress on the turfgrass for previous dry-downs may be reflected throughout the fairways, especially in the low SSMU area. Obviously, the low (and high) SSMU areas are of most interest in terms of both improving irrigation scheduling and turf quality. The 1/3 query classification had the highest linear r^2 in the low SSMU, which could be expected since individual VWC readings are used in delineation of SSMUs for this method (Figure 2.10).

VWC Assessment and Protocols for Progressive Dry-Downs

Easy access to a closely mowed turfgrass site with stable surface conditions provides spatial and temporal investigation of VWC and NDVI relations. An examination of the overall fairway and individual SSMUs verified that VWC decreased with each subsequent day through the 12 to 16 July dry-down (Tables 2.7 and 2.8). Dry-down maps for Fairway 10 (Figures 2.13 to 2.17) and Fairway 13 (Figures 2.18 to 2.22) using the SD-Integrated SSMU boundaries also illustrate the progressive decline in VWC noted in the table data. Comparison of dry-down changes in VWC patterns over the whole fairway and within each SSMU highlight locations that

become driest and retain moisture through the end of dry-downs. The greatest reduction in VWC between successive days occurred from 14 to 15 July (4.5%) for Fairway 10 and from 13 to 14 July (4.3%) for Fairway 13 (Tables 2.7 and 2.8). Each low SSMU contained lower VWCs than the moderate SSMUs, and each moderate SSMU contained lower VWCs than each high SSMU, for each date on both fairways. The highest estimated ET loss within the surface 10-cm zone consistently occurred in the high SSMUs; Fairway 10 was associated with higher overall ET than Fairway 13.

Tables 2.1 and 2.2 (Fairway 10) and Tables 2.3 and 2.4 (Fairway 13) illustrate several measures of dispersion for each SSMU for 12 July and 16 July, respectively. Previously, the descriptive statistics for both fairways at field capacity were discussed (Tables 2.1 and 2.3); the following will discuss changes over time. Relative to 12 July, the 16 July range and CV measures of data variability substantially increased for both fairways, while the standard deviation showed less increase. As each fairway dried, SSMUs exhibited an increased positive skewness and a leptokurtic data distribution, especially for the low and moderate SSMUs (Tables 2.1 to 2.4). These trends result from a decreasing soil water potential as the soil dries, so that once VWC achieves 30 to 40% of initial VWC, further water loss is very slow. This causes a positive skewness to higher VWC and an increasing leptokurtic data distribution. The DU_{lq} on the last day of the dry-down was substantially lower than the first day, suggesting that VWC variability increases as dry-downs progress (Table 2.11). Brocca et al. (2006) also observed a trend of increasing variance with decreasing VWC.

As the dry-down progressed, average NDVI across each fairway and within each SSMU (regardless of the method of SSMU classification) increased from 12 to 13 July and then declined for each successive day, with the greatest decrease noted for the low SSMU (Tables 2.9

and 2.10; Figures 2.13 to 2.22). The progressive dry-down maps for each fairway demonstrate that areas with low VWC or NDVI remain in the same general location, but increase in size as dry-down increases. These results also illustrate that as dry-down proceeds, spatial variability of VWC and NDVI increased, as was reported by Brocca et al. (2006).

Linear and quadratic correlation coefficients of VWC versus NDVI across the whole fairways at field capacity were linear $r^2 = 0.27$ and 0.10 and quadratic $r^2 = 0.33$ and 0.15 for Fairways 10 and 13, respectively (Table 2.11; Figures 2.23 and 2.24). At first view, a higher correlation might be anticipated, but the whole fairway areas include a wide range of soil conditions as illustrated by the wide range of VWC values for field capacity on 12 July (Figures 2.13 and 2.18). Except for the limited areas where NDVI values are low, all other VWC ranges were related to relatively high NDVI values over a rather narrow range. Moreover, the NDVI output data consisted of continuous sensing as the TMM traversed the study area, leading to a much larger sample than what the VWC measurements reflected. The VWC sampling scheme was a 2.5-m grid composed of 825-cm^3 samples, as opposed to a continuous 60- ± 10-cm field of view for the NDVI sensor. Successive VWC measurements differing by 5 to 10% was common. Additionally, the course is maintained to foster uniform turf quality across the whole range of soil conditions on a fairway, which provided an inherent limitation on the degree of stress that developed on the site.

Interestingly, as the dry-down progressed, the strength of linear and quadratic correlations of VWC and NDVI across the whole fairway or within SSMUs for the SD-Integrated classification did not improve over that observed on 12 July, even though it was highly significant in most instances (Table 2.11; Figures 2.23 to 2.26). As the dry-down progressed from 12 to 16 July, the occurrence of lower NDVI increased in both fairways,

especially at <10% VWC. Krum (Chapter 3) reported a linear relationship of VWC and NDVI during dry-down across all days and treatments for the 12 to 16 July period with an $r^2 = 0.30$, but r^2 differed with slope aspect microclimates.

While VWC at field capacity is a relatively stable soil parameter, water loss during dry-downs can be highly variable because it is affected by a combination of relatively stable landscape properties and variable temporal climatic properties that directly influence ET (Lascano et al., 1999; McVicar et al., 2007; Starr, 2007; Krum, Chapter 3). Both the stable field capacity information within a SSMU and the temporally variable VWC and NDVI information would be useful for irrigation scheduling. For example, irrigation scheduling based on soil moisture monitoring is often based on allowing soil drying to a certain percent of field capacity (a temporally stable factor), such as 50% soil moisture depletion (ET loss being temporally variable) (Irrigation Association, 2005). Krum (Chapter 3) discussed this approach as a version of the AWD, where AWD is the percent of available soil water allowed to be depleted before irrigation is applied (SCS, 1993; Smajstrla et al., 2002). The AWD suitable for the site would be selected by the turfgrass manager based on avoiding undue stress on the turfgrass. A 50% AWD over the whole root zone is often used as a baseline for sites that require high quality; this may be used even if just based on the surface zone rather than the whole root zone. For example, if AWD was 50% of field capacity, then for Fairway 10, the AWD triggers would be 8.8 (i.e., 0.50 x 17.54% VWC), 10.9 and 12.62% VWC, respectively, for the low, moderate, and high SSMUs, which are similar to the values on 16 July (Table 2.11). This information provides valuable insight concerning when and where to irrigate in a site-specific manner. Thompson et al. (2007) recently reported on the value of determining upper and lower limits for irrigation scheduling using VWC data from soil sensors.

Figures 2.27a to 2.28b are supplemental topographic maps of Fairways 10 and 13 displaying the elevation derived from GPS. Although GPS elevation data involve inherently limited accuracy in relation to horizontal positioning, the relative differences (verified by ground truthing) are reasonable. Based on these maps, a direct relationship between elevation and VWC is not apparent, considering areas of low and high VWCs located in conjunction with both crests and swales.

Protocols relative to the development, presentation, and interpretation of spatial and temporal dry-down data would require mapping at a time when a good estimate of field capacity can be achieved (i.e., the same conditions required for a good mapping to determine SSMUs). However, several days of dry-down conditions without interference of rainfall or precipitation would also be required. Mapping would not be necessary every day, but just at the beginning and end dates. Field dry-down information is valuable because it focuses on temporal changes across the landscape, but is of less importance than the information gained for the SSMU delineation and characterization application. Since mapping of a progressive dry-down would likely not be conducted as a "stand-alone" mapping unless the same conditions are required for SSMU delineation mapping, it may be considered as an option when mapping for SSMU delineation if time, costs, and weather conditions permit. In this context, it would be an add-on option under the SSMU mapping protocols.

The VWC and NDVI maps originating at field capacity and SSMU boundaries defined from this data would be the starting point for the dry-down field application. Mapping on the last day of dry-downs would continue to use the same SSMU delineations. Data for both dates should include the same descriptive statistics previously suggested for the SSMUs. Additionally,

the information shown in Table 2.11 (i.e., VWC_{tot}, VWC_{lq}, DU_{lq}, and VWC-NDVI r^2 for SSMUs and overall fairways) is suggested for this protocol application.

As noted earlier, investigation into whether the SD-integration or histogram classification methods are best may come from further cases studies where a dry-down is mapped. This would develop a better understanding of how potential SSMUs respond over the dry-down and which classification method at field capacity provides the optimum estimates for SSMU boundaries. As dry-downs progressed for Fairway 10 (Figures 2.13 to 2.17) and Fairway 13 (Figures 2.18 to 2.22), the VWC and NDVI responses provide insight into changes within SSMUs and adjacent areas.

Additional Uses of SSMU Spatial Mapping

In this study, the objectives were to develop, present, and interpret protocols for mapping related to SSMU delineation and dry-downs. However, some comments relative to other spatial applications are appropriate. For each specific field application, protocols may require adjustment or refinement to achieve the specific goals for the particular application.

One potential field application involves the use of initial mapping data to identify potential problems, especially ones that may be easily correctable. For example, in Fairway 10, the two areas (Figure 2.13) associated with the lowest VWC and NDVI areas; and in Fairway 13 (Figure 2.18), the four areas with the lowest VWC and NDVI areas. Since low NDVI at field capacity normally is a residual effect from previous stress, the lowest NDVI sites are of special interest. Field observation of the site may reveal the possible problem(s) responsible for each of the smaller areas, such as: a malfunctioning sprinkler head, incorrect nozzle size, insufficient overlap of heads, head alignment, or a head positioned too low causing the spray area to be blocked by the turf canopy. Problems responsible for somewhat larger stress areas may be:

incipient localized dry spot (i.e., soil hydrophobicity), possible runoff area (e.g., a mound), traffic pattern location; or incorrect irrigation frequency (i.e., a sandy area requiring more frequent irrigation or a more fine-textured area receiving irrigation too frequently). Correction of any issues that can be easily alleviated should provide even better SSMUs definitions. Modifications of existing irrigation systems or new system designs could be more efficient if SSMUs with high DU_{lq} are used as decision making tools.

A second field application that arises out of delineation of SSMUs is placement of soil sensors. In-situ soil moisture sensors have been used for several decades in agriculture (Plauborg et al., 2005; Walker et al., 2004). It would not be feasible to install a multitude of in-situ soil moisture sensors throughout fairways to monitor real time conditions. However, with the identification of SSMUs, only a limited number of soil moisture sensors may be required because each sensor would indicate the conditions on that specific SSMU, as well as similar SSMUs on adjacent fairways. The SSMUs can be used as a basis for more science-based and common sense approaches to soil moisture sensor placement. Selection of key indicator sites for wireless, in-situ sensors is essential to maximize the value of the information from the sensors.

A third field application that arises out of SSMU delineation is further characterization of individual SSMUs for soil physical and chemical properties. Corwin and Lesch (2005b) noted that once geo-referenced soil data (i.e., EC_a in their case and VWC in our situation) is available, the data can be used to establish locations of soil core samples for subsequent laboratory analysis of the samples. Spatial distribution of soil properties can be determined that are correlated to the VWC and/or NDVI within the survey area. Lesch et al. (1995) developed a model-based sampling scheme specifically for ground-based EC_a data, but it can also be used for other

ground-based spatial data (e.g., VWC). Lesch et al. (2000) developed a software program (ESAP) to identify the optimal, but minimal soil sample locations from the spatial data.

Fourth, Fleming et al. (2000) noted that besides using SSMUs as indications of equal production potential, variable-rate application maps could be produced via SSMUs. By developing applicable SSMUs based on soil and topographic factors, input applications (beyond water as the input emphasized in this paper) can be more responsibly managed, leading to reduced environmental disruption, costs, labor, and time. There are still strides that need to be made in the management of spatial data, as the adoption of site-specific management will depend in part on the ability to acquire and classify the data in a quick, user-friendly, and cost-effective manner (Fridgen et al. 2004). As data collection, analysis, and interpretation become more efficient, along with the adoption of reliable protocols, PTM will become the standard, not the exception (Stowell and Gelernter, 2006).

The first requirement for PA principles to be applied to turfgrass situations (i.e., PTM) is the ability to obtain site-specific information. This study is the first time that a mobile platform has been used on turfgrass situations capable of rapid determination of both soil (VWC) and plant (NDVI) characteristics. Spatial and temporal characterization of surface zone (0- to 10-cm) VWC along with associated real-time NDVI responses offers the potential for several field applications that could improve water-use efficiency. Two field applications are: a) defining SSMUs based on spatial patterns of VWC at field capacity, and b) using dry-down responses of VWC and NDVI to provide a spatial and temporal understanding of water-use and drought stress. Mapping data from both of these field applications provide valuable information related to irrigation scheduling, especially for scheduling individual SSMU areas based on their rate of dry-down to a selected trigger value of AWD percentage (issues of where and when to irrigate).

In addition to illustrating the potential use of spatial mapping for development of SSMUs and dry-down maps within SSMUs, our objective was to develop suggested protocols for data presentation and analysis that would be both science-based and practical for integration into a DSS approach. When presenting spatial VWC maps based on field capacity used for SSMU delineation, we would suggest the following protocol (using the example of a fairway):

- The histogram of each fairway should be presented with agronomic breaks noted on the histogram. This information provides a visual display of data distribution and dispersion at the low and high end of VWC values.
- The histogram-based map should be presented with the class intervals selected reflecting the best agronomic consideration of the histogram. This map is likely to be less complicated than the standard deviation map for sites with relatively wide VWC ranges, because fewer classes are present and the classes are agronomic-based estimates of possible sites with similar soil texture and organic matter content (based on similar VWC values). No SSMU boundaries would be defined on this map.
- The SD-Integrated map should then be displayed with the SD-based class intervals. The SSMU boundaries would be delineated on this map with consideration of the histogram map in order to obtain the least number of practical SSMUs. When first defining the SSMU boundaries, the lowest and highest VWC areas should be isolated. Then, the remaining area can be evaluated as to whether more than one additional SSMU area is necessary, with the histogram map providing the best guidance for this decision.
- Because our study only involved two fairway areas, we believe that further case studies where dry-down maps can be developed will provide the best insight as to

whether the SD-Integrated or histogram classification methods result in the most reasonable and science-based SSMUs. For this study, the SD-Integrated method was used as the standard.

- Descriptive statistics and information regarding DU are suggested for the whole fairway and within each SSMU based on presentations for a DSS approach.

REFERENCES

Aronson L.J., A.J. Gold, R.J. Hull, and J.L. Cisar. 1987. Evaporation of cool-season turfgrass in the humid northeast. Agron. J. 79:901-904.

Bell, G.E., D.L. Martin, S.G. Wiese, D.D. Dobson, M.W. Smith, M.L. Stone, and J.B. Solie. 2002. Vehicle-mounted optical sensing: An objective means for evaluating turf quality. Crop Sci. 42:197-201.

Bouma, J., J. Stoorvogel, B.J. van Alphen, and H.W.G. Booltink. 1999. Pedology, precision agriculture, and the changing paradigm of agricultural research. Soil Sci. 63:1763-1768.

Boydell, B., and A.B. McBratney. 1999. Identifying potential within-field management zones from cotton yield estimates. p. 331-341. *In* J.V. Stafford (ed.) Precision agriculture ’99. Proc. Eur. Conf. on Precision Agric., 2nd, Odense Congress Cent., Denmark. 11-15 July 1999. SCI, London.

Brocca, L., R. Morbidelli, F. Melone, and T. Moramarco. 2006. Soil moisture spatial variability in experimental areas of central Italy. J. Hydrol. 333:356-373.

Bullock, D.S., N. Kitchen, and D.G. Bullock. 2007. Multidisciplinary teams: A necessity for research in precision agriculture systems. Crop Sci. 47:1765-1769.

Buss, P. 1996. The fourth agriculture revolution – the Australian solution. Proc. Irrig. Assoc. Aust. Conf. 14-16 May, Adelaide SA. IAA, Hornsby, NSW, Australia.

Carrow, R.N., V. Cline, and J.M. Krum. 2007. Monitoring spatial variability in soil properties and turfgrass stress: Applications and protocols. p. 641-645. Proc. Int. Irrig. Show. 28th, 9-11 Dec. 2007. San Diego, CA. [CD-ROM] Irrig. Assoc., Falls Church, VA.

Cary, J.W. 1968. An instrument for in situ measurement of soil moisture flow and suction. Soil Sci. Soc. Am. J. 32:3-5.

Cassel, S.F. 2007. Soil salinity mapping using ArcGIS. p. 141-162. *In* F.J. Pierce and D. Clay (ed.) 2007. GIS applications for agriculture. CRC Press, Boca Raton, FL.

Chen, J.M., X. Chen, W. Ju, and X. Geng. 2004. Distributed hydrological model for mapping evapotranspiration using remote sensing inputs. J. Hydrol. 305:15-39.

Clark, R.L., and R. Lee. 1998. Development of topographic maps for precision farming with kinematic GSP. Transactions of the ASAE 41(4):909-916.

Corwin, D.L. and S.M. Lesch. 2005a. Apparent soil electrical conductivity measurements in agriculture. Comput. Electron. Agric. 46:11-43.

Corwin, D.L. and S.M. Lesch. 2005b. Characterizing soil spatial variability with apparent soil electrical conductivity I. Survey protocols. Comput. Electron. Agric. 46:103-133.

Corwin, D.L., S.M. Lesch, P.J. Shouse, R.W. Soppe, and J.E. Ayars. 2006. Delineating site-specific irrigation management units using geospatial EC_a measurements. World Congress of Soil Science. Paper No. 153-19.

Dobermann, A. 2006. Quantifying spatial variability. Slideshow presentation. AGRO 896. Univ. of Nebraska. Lincoln, NE.

Duffera, M., J.G. White, and R. Weisz. 2007. Spatial variability of Southeastern U.S. Coastal Plain soil physical properties: Implications for site-specific management. Geoderma 137:327-339.

Dukes, M.D., M.B. Haley, and S.A. Hanks. 2006. Sprinkler irrigation and soil moisture uniformity. Proc. Int. Irrig. Show, 27th, 5-7 Nov. 2006. San Antonio, TX. [CD-ROM] Irrig. Assoc., Falls Church, VA.

Ebdon, J.S. A.M. Petrovic, and R.W. Zobel. 1998. Stability of evapotranspiration rates in Kentucky bluegrass cultivars across low and high evaporative environments. Crop Sci. 38:135-142.

ESRI. 2004a. ArcGIS 9: Using ArcGIS geostatistical analyst. ESRI, Redlands, CA.

ESRI. 2004b. ArcGIS 9: Using ArcGIS spatial analyst. ESRI, Redlands, CA.

Fleming, K.L., D.G. Westfall, D.W. Wiens, and M.C. Brodah. 2000. Evaluating farmer developed management zone maps of variable rate fertilizer application. Precision Agric. 2:201-215.

Fraisse, C.W., K.A. Sudduth, and N.R. Kitchen. 2001. Calibration of the Ceres-Maize model for simulating site-specific crop development and yield on claypan soils. Appl. Eng. Agric. 17(4):547–556.

Fridgen, J.J., N.R. Kitchen. K.A. Suddeth, S.T. Drummond, W.J. Wiebold, and C.W. Fraisse. 2004. Management Zone Analyst (MZA): Software for subfield management zone delineation. Agron. J. 96:100-108.

Hsiao, T.C. 1973. Plant responses to water stress. Ann. Rev. Plant Physiol. 24:519-570.

Irrigation Association. 2005. Landscape irrigation scheduling and water management. Available at http://www.irrigation.org/gov/pdf/liswm_part2of3.pdf (cited 15 Jan 2008; verified 20 Mar. 2008). Irrig. Assoc., Falls Church, Va.

Jiang, Y, and R.N. Carrow. 2007. Broadband spectral reflectance models of turfgrass species and cultivars to drought stress. Crop Sci. 47:1611-1618.

Karnok, K.A., E.J. Rowland, and K.H. Tan. 1993. High pH treatments and the alleviation of soil hydrophobicity on golf greens. Agron J. 85:983-986.

Kerry, R. and M.A. Oliver. 2005. Improving prediction of soil properties in precision agriculture by co-kriging with properties that are easily measured. Proc. Eur. Conf. on Precision Agric., 5th, 9-12 June 2005. Uppsala, Sweden.

Kieffer, D.L. and T.S. O'Conner. 2007. Managing soil moisture on golf greens using a portable wave reflectometer. Proc. Int. Irrig. Show, 28th, 9-11 Dec. 2007. San Diego, CA. [CD-ROM] Irrig. Assoc., Falls Church, VA.

King, J.A., P.M.R. Dampney, R.M. Lark, H.C. Wheeler, R.I. Bradley, and T.R. Mayr. 2005. Mapping potential crop management zones within fields: Use of yield-map series and patterns of soil physical properties identified by electromagnetic induction sensing. Precision Agric. 6:167-181.

Kravchenko, A.N., and D.G. Bullock. 2002. Spatial variability of soybean quality data as a function of field topography. Crop Sci. 42:804-815.

Lascano, R.J., R.L. Baumhardt, S.K. Hicks, and J.A. Landivar. 1999. Spatial and temporal distribution of surface water content in a large agricultural field. p. 19-30. *In* P.C. Robert et al. (ed.) Precision agriculture: A challenge for crop nutrition management. Proc. Int. Conf. Precision Agric., 4th, Minneapolis, MN. 17-20 July 1998. ASA-CSSA-SSSA, Madison, WI.

Lee, G., R.N. Carrow, and R.R. Duncan. 2005. Criteria for assessing salinity tolerance of the halophytic turfgrass seashore paspalum. Crop. Sci. 45:251-258.

Leib, B.G., J.D. Jabro, and G.R. Matthews. 2003. Field evaluation and performance comparison of soil moisture sensors. Soil Sci. 168:396-409.

Lesch, S.M., D.J. Strauss, and J.D. Rhoades. 1995. Spatial prediction of soil salinity using electromagnetic induction techniques 2. An efficient spatial sampling algorithm suitable for multiple linear regression model identification and estimation. Water Resour. Res. 31:387-398.

Lesch, S.M., J.D. Rhoades, and D.L. Corwin. 2000. ESAP-95 version 2.0 user manual and tutorial guide. Research Report No. 146, George E. Brown, Jr. Salinity Laboratory, Riverside, CA.

Li, D., K.J. Young, N.E. Christians, and D.D. Minner. 2000. Inorganic soil amendment effects on sand-based sports turf media. Crop Sci. 40:1121-1125.

Marcum, K.B., and M. Pessarakli. 2006. Salinity tolerance and salt gland excretion efficiency of bermudagrass turf cultivars. Crop. Sci. 46:2571-2574.

McBratney, A., B. Whelan, T. Ancev, and J. Bouma 2005. Future directions of precision agriculture. Precision Agric. 6:7-23.

McGrew, J.C. and C.B. Monroe. 2000. An introduction to statistical problem solving in geography. 2nd ed. McGraw-Hill, Dubuque, Iowa.

McNeill, J.D. 1980. Electrical conductivity of soils and rocks. Technical Note TN-5. Geonics Ltd., Mississauga, Ont.

McVicar, T.R., T.G. Van Niel, L. Li, M.F. Hutchinson, X. Mu, and Z. Liu. 2007. Spatially distributing monthly reference evapotranspiration and pan evaporation considering topographic influences. J. Hydrol. 338:196-220.

Mecham, B.Q. 2001. Distribution uniformity results comparing catch-can tests and soil moisture sensor measurements in turfgrass irrigation. Proc. Int. Irrig. Show, 22nd, 4-6 Nov. 2001. San Antonio, TX. [CD-ROM] Irrig. Assoc., Falls Church, VA.

Miao, Y., D.J. Mulla, and P.C. Robert. 2005. Combining soil-landscape and spatial-temporal variability of yield information to delineate site-specific management zones. *In* J. V. Stafford (ed.). Precision Agric. '05. Wageningen Acad. Publ., The Netherlands.

Pauwels, V.R.N., and R. Samson. 2006. Comparison of different methods to measure and model actual evapotranspiration rates for a wet sloping grassland. Agric. Water Manage. 82:1-24.

Pilesjö, P., L. Thylén, and A. Persson. 2005. Topographical data for delineation of agricultural management zones. Proc. Eur. Conf. on Precision Agric., 5th, 9-12 June 2005. Uppsala, Sweden.

Plauborg, F., B.V. Iverson, and P.E. Laerke. 2005. In situ comparison of three dielectric soil moisture sensors in drip irrigated sandy soils. Vadose Zone J. 4:1037-1047.

Rana, G., R.M. Ferrara, N. Martinelli, P. Personnic, and P. Cellier. 2007. Estimating energy fluxes from sloping crops using standard agrometeorological measurements and topography. Agric. For. Meteorol. 146: 116-133.

Rhoades, J.D, F. Chanduvi, and S. Lesch. 1999. Soil salinity assessment: Methods and interpretation of electrical conductivity measurements. FAO Irrigation and Drainage Paper 57. Food and Agric. Organ. of the United Nations, Rome.

Rothe, A., W. Weis, K. Kreutzer, D. Matthies, U. Hess, and B. Ansorge. 1997. Changes in soil structure caused by the installation of time domain reflectometry probes and their influence on the measurement of soil moisture. Water Resour. Res. 33(7):1585–1593.

SCS. 1993. Chapter 2. Irrigation water requirements. *In* SCS technical staff. Part 623 Natl. Engineering Handb. USDA Soil Conser. Serv. Washington, DC.

Sethuramasamyraja, B., V.I. Adamchuk, A. Dobermann, D.B. Marx, D.D. Jones, and G.E. Meyer. 2007. Agitated soil measurement method for integrated on-the-go mapping of soil pH, potassium and nitrate contents. Comput. Electron. Agric. 60(2):212-225.

Shearman, R.C. 1986. Kentucky bluegrass cultivar evapotranspiration rates. HortScience 21:455-457.

Smajstrla, A.G., B.J. Boman, D.Z. Haman, F.T. Izuno, D.J. Pitts, and F.S. Zazueta. 2002. Basic irrigation scheduling in Florida. Ext. Bulletin 249. Instit. of Food and Agric. Sci., Univ. of Florida, Gainsville, FL.

Starr, G.C. 2005. Assessing temporal stability and spatial variability of soil water patterns with implications for precision water management. Agric. Water Manage. 72:223-243.

Stowell, L. and W. Gelernter. 2006. Sensing the future. Golf Course Manage. 74(3):107-110.

Sudduth, K.A., J.W. Hummel, and S.J. Birrell. 1997. Sensors for site-specific management. p. 183-210. *In* F.J. Pierce and E.J. Sadler (ed.) The state of site-specific management for agriculture. ASA-CSSA-SSSA, Madison, WI.

Tarr, A.B., K.J. Moore, D.G. Bullock, P.M. Dixon, and C.L. Burns. 2005. Improving map accuracy of soil variables using soil electrical conductivity as a covariate. Precision Agric. 6:255-270.

Taylor, J.A., A.B. McBratney, and B.M. Whelan. 2007. Establishing management classes for broadacre agricultural productions. Agron. J. 99:1366-1376.

Thompson, R.B., M. Gallardo, L.C. Valdez, and M.D. Fernández. 2007. Determination of lower limits form irrigation management using in situ assessments of apparent crop water uptake made with volumetric soil water content sensors. Agric. Water Manage. 92:13-28

Thomsen, A., K. Schelde, P. Drøscher, and F. Steffensen. 2007. Mobile TDR for geo-referenced measurement of soil water content and electrical conductivity. Precision Agric. 8:213-223.

Trenholm, L.E., R.N. Carrow, and R.R. Duncan. 1999. Relationship of multispectral radiometry data to qualitative data in turfgrass research. Crop Sci. 39:763-769.

Tucker K.A., K.J. Karnok, D.E. Radcliffe, G. Landry Jr., R.W. Roncadori, and K.H. Tan. 1990. Localized dry spots as caused by hydrophobic sands on bentgrass greens. Agron. J. 82:549-555.

Verhagen, J. and J. Bouma. 1997. Modeling soil variability. *In* F.J. Pierce and E.J. Sadler (ed.) The state of site specific management for agriculture. ASA-CSSA-SSSA, Madison, WI.

Walker, J.P., G.R. Willgoose, and J.D. Kalma. 2004. In situ measurement of soil moisture: A comparison of techniques. J. Hydrol. 293:85-99.

Weaver, A.R., D.E. Kissel, F. Chen, L.T. West, W. Adkins, D. Rickman, and J.C. Luvall. 2004. Mapping soil pH buffering capacity of selected fields in the coastal plain. Soil Sci. Soc. Am. J. 68:662-668.

Western, A.W., G. Blöschl, and R.B. Grayson. 1998. Geostatistical characterization of soil moisture patterns in the Tarrawarra catchment. J. Hydro. 205:20-37.

Wollenhaupt, N.C., D.J. Mulla, and C.A. Gotway Crawford. 1997. Soil sampling and interpolation for mapping spatial variability of soil properties. p. 19-53. *In* F.J. Pierce and E.J. Sadler (ed.) The state of site-specific management for agriculture. ASA-CSSA-SSSA, Madison, WI.

Yan, L., S. Zhou, L. Feng, and L. Hong-Yi. 2007. Delineation of site-specific management zones using fuzzy clustering analysis in a coastal saline land. Comput. Electron. Agric 56:174-186.

Table 2.1. Fairway 10: Descriptive statistics of volumetric water content (VWC) in site-specific management units (SSMUs) for classification methods on 12 July 2006.

Classification Method	Mean	Median	Mode	Range	Standard Deviation	CV	Skewness	Kurtosis
SSMU	%							
Manual								
Low	12.0	11	10	13	3.71	30.81	0.85	2.83
Moderate	21.7	22	23	28	4.45	20.50	-0.36	3.66
High	27.9	27	27	30	4.93	17.69	-0.14	5.10
Standard Deviation								
Low	14.1	13.5	10	20	5.25	37.15	0.63	2.45
Moderate	21.3	22	23	26	4.05	19.04	-0.36	3.57
High	27.1	27	27	30	4.47	16.49	0.03	5.03
Quantile								
Low	14.6	14	14	18	4.64	31.89	0.35	2.38
Moderate	22.1	22	23	28	4.00	18.07	-0.14	3.99
High	28.1	27	27	21	4.12	14.67	0.71	4.11
1/3 Query								
Low	17.3	19	20	20	4.14	23.90	-0.56	3.15
Moderate	22.7	23	23	28	3.92	17.25	-0.82	5.37
High	29.1	29	27	20	3.60	12.37	1.00	4.62
Histogram								
Low	15.0	14	14	18	4.79	31.85	0.13	1.94
Moderate	21.8	22	23	28	3.85	17.63	-0.26	3.84
High	27.1	27	27	30	4.60	16.97	0.00	4.77
Jenk's								
Low	17.0	17	22	20	5.34	31.50	-0.13	1.90
Moderate	21.9	22	23	26	3.86	17.59	-0.15	3.49
High	25.7	25	27	31	4.96	19.33	0.04	4.17
SD-Integrated								
Low	17.5	19	22	20	5.44	31.01	-0.18	1.99
Moderate	21.8	22	23	26	3.91	17.95	-0.09	3.53
High	25.2	25	27	31	4.82	19.10	0.13	4.26
Overall								
Fairway	22.1	22	23	33	5.42	24.54	-0.18	3.66

Table 2.2. Fairway 10: Descriptive statistics of volumetric water content (VWC) in site-specific management units (SSMUs) for classification methods on 16 July 2006.

Classification Method	Mean	Median	Mode	Range	Standard Deviation	CV	Skewness	Kurtosis
SSMU	%							
Manual								
Low	6.07	5	4	11	3.08	50.74	1.10	0.26
Moderate	11.10	10	9	42	4.67	42.07	1.89	7.41
High	13.22	12	12	30	5.21	39.41	1.52	3.93
Standard Deviation								
Low	8.48	7.0	4	42	5.87	69.22	3.55	18.27
Moderate	11.06	10	9	32	4.34	39.24	1.73	4.84
High	13.17	12	12	28	4.65	35.31	0.70	0.74
Quantile								
Low	7.94	7	4	42	6.19	77.96	3.96	19.91
Moderate	11.22	10	9	30	4.28	38.15	1.29	2.46
High	13.07	12	12	32	5.00	38.26	1.46	3.88
1/3 Query								
Low	7.52	7	4	28	4.63	61.57	2.53	10.27
Moderate	11.07	10	9	42	4.57	41.28	2.04	8.95
High	12.94	12	10	30	4.93	38.10	1.46	3.27
Histogram								
Low	8.48	7	4	42	5.87	69.22	3.55	18.27
Moderate	10.61	9	9	24	3.81	35.91	1.87	4.67
High	13.17	12	12	28	4.65	35.31	0.70	0.74
Jenk's								
Low	8.52	7	7	42	5.43	63.73	3.54	22.54
Moderate	11.41	10	9	30	4.48	39.26	1.38	5.48
High	12.24	12	12	35	4.60	37.58	1.34	6.97
SD-Integrated								
Low	8.43	8	7	42	4.93	58.48	3.74	27.80
Moderate	11.00	10	9	28	4.07	37.00	1.53	6.73
High	12.62	12	10	35	5.04	39.94	1.23	5.58
Overall								
Fairway	11.12	10	9	42	4.87	43.79	1.68	5.98

Table 2.3. Fairway 13: Descriptive statistics of volumetric water content (VWC) in site-specific management units (SSMUs) for classification methods on 12 July 2006.

Classification Method	Mean	Median	Mode	Range	Standard Deviation	CV	Skewness	Kurtosis
SSMU	%							
Manual								
Low	14.54	14	17	18	3.76	25.86	0.41	2.91
Moderate	18.94	19	17	29	3.68	19.43	0.73	5.16
High	28.39	27	23	26	6.97	24.55	0.71	2.63
Standard Deviation								
Low	15.45	16.0	17	20	3.76	24.34	0.12	2.75
Moderate	19.10	19	19	28	3.73	19.53	0.71	5.03
High	28.16	27	23	37	7.20	25.57	0.53	2.85
Quantile								
Low	13.71	14	14	13	3.14	22.90	0.11	2.38
Moderate	18.82	19	17	28	3.60	19.13	0.84	5.47
High	27.39	25	23	28	6.96	25.41	0.84	2.88
1/3 Query								
Low	15.52	16	17	24	3.81	24.55	0.24	3.50
Moderate	18.69	19	19	28	3.69	19.74	0.90	5.71
High	27.30	25	23	37	6.89	25.24	0.81	3.18
Histogram								
Low	15.68	16	17	20	3.40	21.68	-0.02	2.98
Moderate	19.75	20	19	28	3.62	18.33	0.69	5.55
High	28.23	27	23	37	7.03	24.90	0.60	2.90
Jenk's								
Low	14.51	14	14	16	3.34	23.02	0.09	2.62
Moderate	19.23	19	17	33	3.84	19.97	1.26	8.33
High	27.66	27	23	28	7.05	25.49	0.75	2.74
SD-Integrated								
Low	14.35	14	14	16	3.39	23.62	0.20	2.65
Moderate	19.00	19	17	33	3.86	20.32	1.42	8.84
High	26.87	25	23	29	6.99	26.01	0.87	2.99
Overall								
Fairway	20.40	19	17	38	6.73	32.99	1.21	4.95

Table 2.4. Fairway 13: Descriptive statistics of volumetric water content (VWC) in site-specific management units (SSMUs) for classification methods on 16 July 2006.

Classification Method	Mean	Median	Mode	Range	Standard Deviation	CV	Skewness	Kurtosis
SSMU	%							
Manual								
Low	8.58	7	7	40	5.59	65.15	2.84	11.85
Moderate	10.47	9	7	41	5.56	53.10	2.50	9.59
High	18.87	17	17	39	9.71	51.46	1.08	0.36
Standard Deviation								
Low	9.20	7.0	7	40	5.43	59.02	2.48	9.28
Moderate	10.70	9	9	41	5.84	54.58	2.65	10.21
High	18.58	16	17	40	9.55	51.40	1.14	0.56
Quantile								
Low	8.60	7	5	40	5.82	67.67	2.73	10.70
Moderate	10.26	9	7	41	5.50	53.61	2.68	10.86
High	17.86	16	17	40	9.45	52.91	1.20	0.75
1/3 Query								
Low	8.96	7	7	40	5.45	60.83	2.51	9.91
Moderate	10.40	9	7	40	5.75	55.29	2.70	10.52
High	17.27	14	14	43	9.44	54.66	1.23	0.90
Histogram								
Low	9.20	7	7	40	5.43	59.02	2.48	9.28
Moderate	10.70	9	9	41	5.84	54.58	2.65	10.21
High	18.58	16	17	40	9.55	51.40	1.14	0.56
Jenk's								
Low	9.02	7	7	40	6.73	74.61	3.01	14.23
Moderate	10.25	9	7	43	5.09	49.66	2.19	11.02
High	17.73	14	17	40	9.50	53.58	1.20	3.75
SD-Integrated								
Low	8.82	7	7	40	6.66	75.51	3.18	15.55
Moderate	10.28	9	7	43	5.26	51.17	2.19	10.63
High	16.74	14	10	43	9.29	55.50	1.32	4.17
Overall								
Fairway	12.07	9	7	43	7.78	64.46	1.99	4.43

Table 2.5. Fairway 10: Distribution uniformity (DU) and mobile data correlation of volumetric water content (VWC) and normalized difference vegetative index (NDVI) within site-specific management units (SSMUs) on 12 July 2006.

SSMU	VWC_{tot}	VWC_{lq}	Du_{lq}	r^2-NDVI†
	%			
Low				
Classification Method				
Manual	12.0	8.3	0.69	0.32***
Standard Deviation	14.1	8.6	0.61	0.24***
Quantile	14.6	8.9	0.61	0.33***
1/3 Query	17.3	11.5	0.66	0.44***
Histogram	15.0	9.0	0.60	0.29***
Jenk's	17.0	9.9	0.58	0.39***
SD-Integrated	17.5	10.3	0.59	0.39***
	%			
Moderate				
Classification Method				
Manual	21.7	16.1	0.74	0.11***
SD	21.3	16.1	0.76	0.06***
Quantile	22.1	17.3	0.78	0.04***
1/3 Query	22.7	17.7	0.78	0.07***
Histogram	21.8	17.1	0.78	0.04***
Jenk's	21.9	17.2	0.78	0.01*
SD-Integrated	21.8	17.0	0.78	0.01
	%			
High				
Classification Method				
Manual	27.9	22.3	0.80	0.14***
SD	27.1	22.0	0.81	0.10***
Quantile	28.1	23.5	0.84	0.08**
1/3 Query	29.1	26.0	0.89	0.07***
Histogram	27.1	21.8	0.80	0.05**
Jenk's	25.7	19.6	0.76	0.08***
SD-Integrated	25.2	19.5	0.77	0.11***
	%			
Overall				
Fairway	22.1	15.2	0.69	0.27***

*,**,*** Significant at the 0.05, 0.01, and 0.001 probability levels, respectively.

† Linear correlation coefficient for VWC and NDVI within SSMUs.

Table 2.6. Fairway 13: Distribution uniformity (DU) and mobile data correlation of volumetric water content (VWC) and normalized difference vegetative index (NDVI) within site-specific management units (SSMUs) on 12 July 2006.

SSMU	VWC_{tot}	VWC_{lq}	Du_{lq}	r^2-NDVI†
		%		
Low				
Classification Method				
Manual	14.5	10.1	0.69	0.13***
Standard Deviation	15.4	10.8	0.70	0.24***
Quantile	13.7	9.7	0.71	0.18***
1/3 Query	15.5	10.8	0.70	0.33***
Histogram	15.7	11.4	0.73	0.18***
Jenk's	14.5	10.3	0.71	0.17***
SD-Integrated	14.3	10.2	0.71	0.17***
		%		
Moderate				
Classification Method				
Manual	18.9	14.7	0.78	0.03***
SD	19.1	14.8	0.77	0.03***
Quantile	18.8	14.7	0.78	0.01**
1/3 Query	18.7	14.4	0.77	0.02***
Histogram	19.7	15.5	0.79	0.06***
Jenk's	19.2	15.0	0.78	0.01
SD-Integrated	19.0	14.9	0.78	<0.01
		%		
High				
Classification Method				
Manual	28.4	20.9	0.74	0.06***
SD	28.2	20.3	0.72	0.05***
Quantile	27.4	20.2	0.74	0.04**
1/3 Query	27.3	20.4	0.75	0.06***
Histogram	28.2	20.7	0.73	0.05***
Jenk's	27.7	20.1	0.73	0.05***
SD-Integrated	26.9	19.7	0.73	0.03**
		%		
Overall				
Fairway	20.4	13.4	0.66	0.10***

,* Significant at the 0.01 and 0.001 probability levels, respectively.

† Linear correlation coefficient for VWC and NDVI within SSMUs.

Table 2.7. Fairway 10: Volumetric water content (VWC) and evapotranspiration (ET) within site-specific manangement units (SSMUs) during the 12 to 16 July dry-down.

Date	Manual	Standard Deviation	Quantile	1/3 Query	Histogtram	Jenk's	SD-Integrated
				%			
12 July							
Low	12.04	14.13	14.55	17.32	15.04	16.95	17.54
Moderate	21.71	21.27	22.14	22.72	21.84	21.94	21.78
High	27.87	27.11	28.08	29.11	27.10	25.66	25.24
Fairway				22.09			
				%			
13 July							
Low	12.97	14.21	14.24	14.19	14.99	15.87	15.72
Moderate	19.62	19.26	19.76	19.28	19.53	19.78	19.36
High	23.05	23.46	23.81	23.38	23.63	22.35	22.33
Fairway				19.76			
				%			
14 July							
Low	9.15	11.25	11.09	10.71	11.25	12.47	12.37
Moderate	16.76	16.89	16.95	16.71	16.89	16.96	16.90
High	20.91	20.51	20.88	19.86	20.51	19.59	19.25
Fairway				16.80			
				%			
15 July							
Low	8.09	9.36	8.58	9.10	9.36	10.09	9.93
Moderate	12.59	12.59	12.91	12.27	12.59	12.54	12.26
High	17.62	16.38	16.86	16.39	16.38	15.62	15.43
Fairway				12.32			
				%			
16 July							
Low	6.07	8.48	7.94	7.52	8.48	8.52	8.43
Moderate	11.10	11.06	11.22	11.07	11.06	11.41	11.00
High	13.22	13.17	13.07	12.94	13.17	12.24	12.62
Fairway				11.12			
				cm			
12 - 16 July ET							
Low	0.24	0.23	0.26	0.39	0.26	0.34	0.36
Moderate	0.42	0.41	0.44	0.47	0.43	0.42	0.43
High	0.59	0.56	0.60	0.65	0.56	0.54	0.50
Fairway				0.44			

Table 2.8. Fairway 13: Volumetric water content (VWC) and evapotranspiration (ET) within site-specific manangement units (SSMUs) during the 12 to 16 July dry-down.

Date	Manual	Standard Deviation	Quantile	1/3 Query	Histogtram	Jenk's	SD-Integrated
				%			
12 July							
Low	14.54	15.45	13.71	15.52	15.68	14.51	14.35
Moderate	18.94	19.10	18.82	18.69	19.75	19.23	19.00
High	28.39	28.16	27.39	27.30	28.23	27.66	26.87
Fairway				20.40			
				%			
13 July							
Low	15.88	16.62	15.23	16.21	16.82	15.26	15.10
Moderate	18.86	19.02	18.85	18.88	19.40	19.09	18.79
High	27.09	27.07	26.29	25.85	26.70	26.02	25.12
Fairway				19.93			
				%			
14 July							
Low	11.85	12.25	11.02	12.00	12.25	11.17	10.94
Moderate	14.14	14.81	14.21	14.24	14.81	14.33	14.22
High	22.28	21.92	21.19	21.01	21.92	21.33	20.36
Fairway				15.62			
				%			
15 July							
Low	9.39	10.15	8.62	9.58	10.15	9.07	9.25
Moderate	11.73	12.45	12.00	12.03	12.45	11.99	11.88
High	18.02	17.67	17.10	16.94	17.67	17.10	16.67
Fairway				12.87			
				%			
16 July							
Low	8.58	9.20	8.60	8.96	9.20	9.02	8.82
Moderate	10.47	10.70	10.26	10.40	10.70	10.25	10.28
High	18.87	18.58	17.86	17.27	18.58	17.73	16.74
Fairway				12.07			
12 - 16 July ET				cm			
Low	0.24	0.25	0.20	0.26	0.26	0.22	0.22
Moderate	0.34	0.34	0.34	0.33	0.36	0.36	0.35
High	0.38	0.38	0.38	0.40	0.39	0.40	0.41
Fairway				0.33			

Table 2.9. Fairway 10: Normalized difference vegetative index (NDVI) within site-specific manangement units (SSMUs) during the 12 to 16 July dry-down.

Date	Manual	Standard Deviation	Quantile	1/3 Query	Histogtram	Jenk's	SD-Integrated
12 July							
Low	0.757	0.764	0.780	0.779	0.782	0.789	0.788
Moderate	0.808	0.807	0.808	0.806	0.808	0.806	0.806
High	0.818	0.818	0.820	0.818	0.818	0.818	0.816
Fairway	----------	----------	----------	0.806	----------	----------	----------
13 July							
Low	0.788	0.797	0.809	0.804	0.810	0.816	0.816
Moderate	0.837	0.837	0.838	0.837	0.838	0.837	0.836
High	0.850	0.848	0.850	0.846	0.849	0.847	0.846
Fairway	----------	----------	----------	0.836	----------	----------	----------
14 July							
Low	0.758	0.767	0.785	0.784	0.784	0.793	0.793
Moderate	0.815	0.815	0.815	0.814	0.816	0.814	0.814
High	0.827	0.825	0.827	0.824	0.825	0.825	0.823
Fairway	----------	----------	----------	0.813	----------	----------	----------
15 July							
Low	0.720	0.733	0.761	0.755	0.763	0.774	0.773
Moderate	0.813	0.808	0.809	0.807	0.809	0.808	0.809
High	0.822	0.819	0.821	0.818	0.819	0.818	0.816
Fairway	----------	----------	----------	0.804	----------	----------	----------
16 July							
Low	0.675	0.693	0.730	0.726	0.733	0.748	0.747
Moderate	0.796	0.797	0.798	0.796	0.799	0.799	0.798
High	0.792	0.809	0.811	0.807	0.809	0.808	0.808
Fairway	----------	----------	----------	0.792	----------	----------	----------

Table 2.10. Fairway 13: Normalized difference vegetative index (NDVI) within site-specific manangement units (SSMUs) during the 12 to 16 July dry-down.

Date	Manual	Standard Deviation	Quantile	1/3 Query	Histogtram	Jenk's	SD-Integrated
12 July							
Low	0.792	0.801	0.792	0.798	0.802	0.793	0.791
Moderate	0.818	0.818	0.818	0.818	0.817	0.819	0.818
High	0.816	0.815	0.817	0.818	0.817	0.817	0.818
Fairway	- -			0.813	- -		
13 July							
Low	0.824	0.829	0.824	0.828	0.837	0.823	0.822
Moderate	0.851	0.852	0.851	0.852	0.850	0.853	0.852
High	0.840	0.840	0.842	0.842	0.841	0.841	0.843
Fairway	- -			0.843	- -		
14 July							
Low	0.790	0.796	0.789	0.795	0.806	0.790	0.787
Moderate	0.814	0.815	0.814	0.814	0.813	0.815	0.814
High	0.813	0.813	0.814	0.814	0.814	0.813	0.814
Fairway	- -			0.809	- -		
15 July							
Low	0.776	0.785	0.774	0.783	0.795	0.777	0.773
Moderate	0.807	0.814	0.812	0.814	0.812	0.814	0.813
High	0.815	0.815	0.817	0.816	0.816	0.816	0.816
Fairway	- -			0.806	- -		
16 July							
Low	0.746	0.762	0.743	0.757	0.773	0.748	0.743
Moderate	0.800	0.801	0.800	0.801	0.801	0.802	0.800
High	0.806	0.806	0.807	0.808	0.807	0.806	0.806
Fairway	- -			0.791	- -		

Table 2.11. Fairways 10 and 13: Distribution uniformity (DU) and mobile data correlation of volumetric water content (VWC) and normalized difference vegetative index (NDVI) for the SD-Integrated classification method.

SSMU	VWC_{tot}	VWC_{lq}	Du_{lq}	Linear r^2-NDVI†	Quadratic r^2-NDVI‡
	%				
Fairway 10					
Low					
12 July	17.54	10.31	0.59	0.39***	0.43
16 July	8.43	4.13	0.49	0.14***	0.31
Moderate					
12 July	21.78	17.02	0.78	0.01	0.03
16 July	11.00	7.20	0.65	<0.01	0.01
High					
12 July	25.24	19.47	0.77	0.11***	0.11
16 July	12.62	7.54	0.60	0.03**	0.05
Fairway					
12 July	22.09	15.22	0.69	0.27***	0.33
16 July	11.11	6.32	0.57	0.10***	0.21
Fairway 13					
Low					
12 July	14.35	10.21	0.71	0.17***	0.18
16 July	8.82	4.22	0.48	0.01	0.14
Moderate					
12 July	19.00	14.86	0.78	<0.01	<0.01
16 July	10.28	5.77	0.56	0.03***	0.03
High					
12 July	26.87	19.67	0.73	0.03**	0.04
16 July	16.74	8.10	0.48	0.01	0.01
Fairway					
12 July	20.40	13.39	0.66	0.10***	0.15
16 July	12.06	5.59	0.46	0.05***	0.12

,* Significant at the 0.01 and 0.001 probability levels, respectively.

† Linear correlation coefficient for VWC and NDVI within site-specific management units (SSMUs).

‡ Quadratic correlation coefficient for the VWC and NDVI within SSMUs.

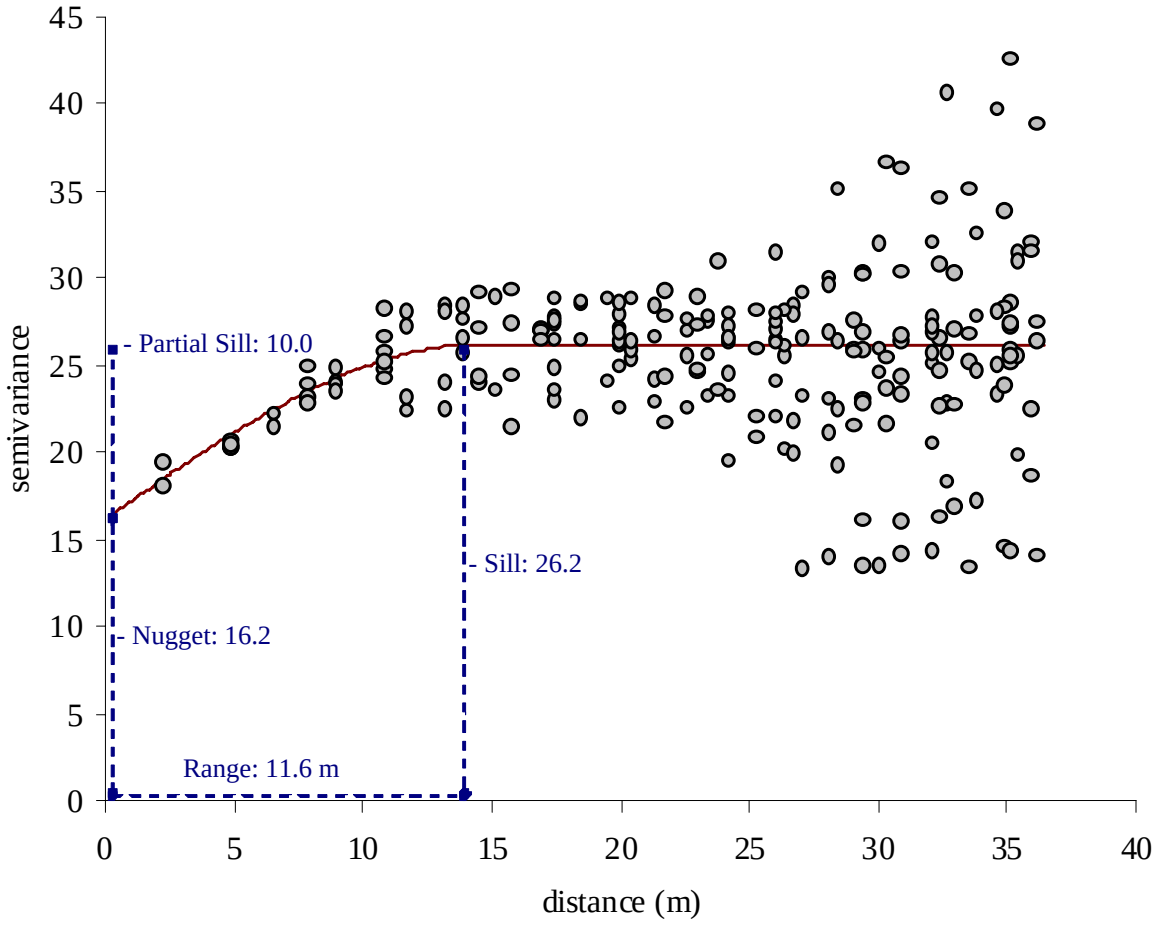

Figure 2.1. Semivariogram of Fairway 10 volumetric water content (VWC) including the fitted spherical model curve on 12 July 2006.

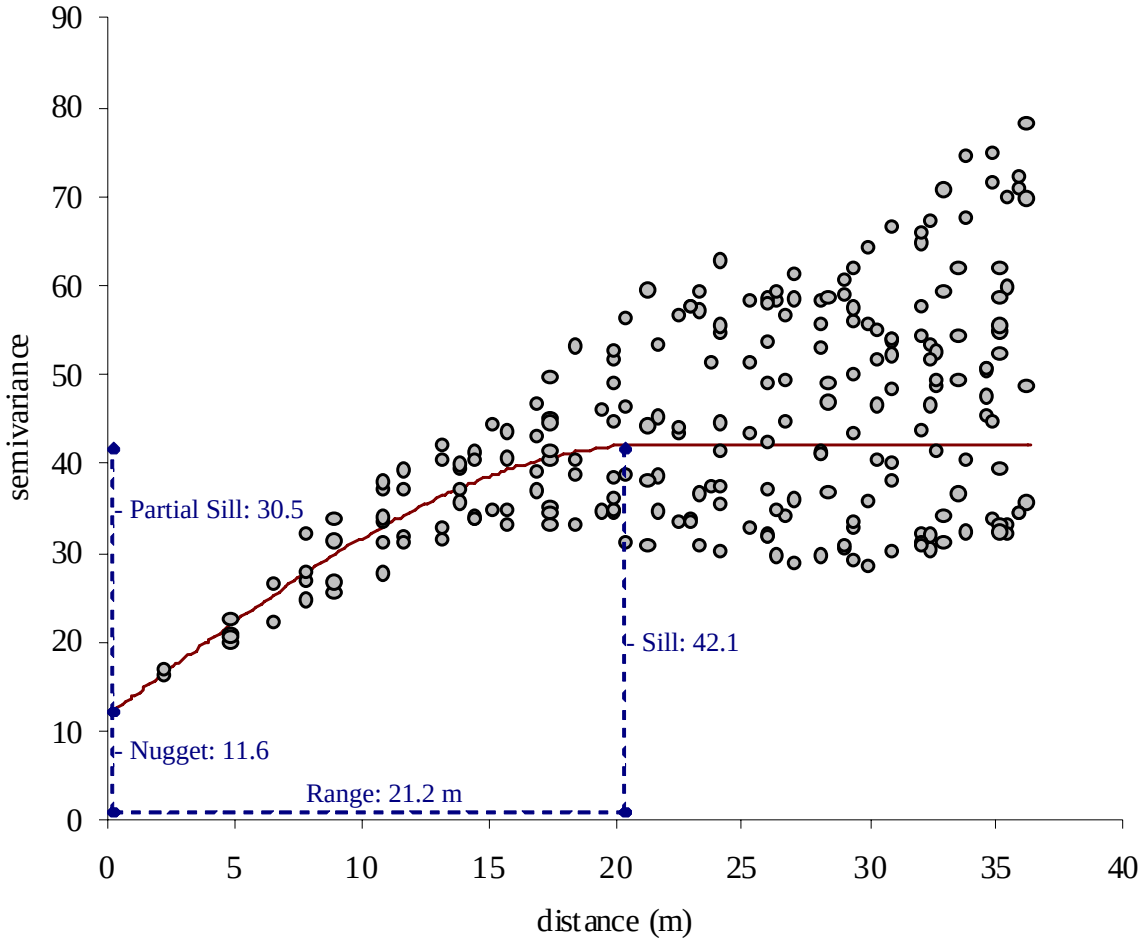

Figure 2.2. Semivariogram of Fairway 13 volumetric water content (VWC) including the fitted spherical model curve on 12 July 2006.

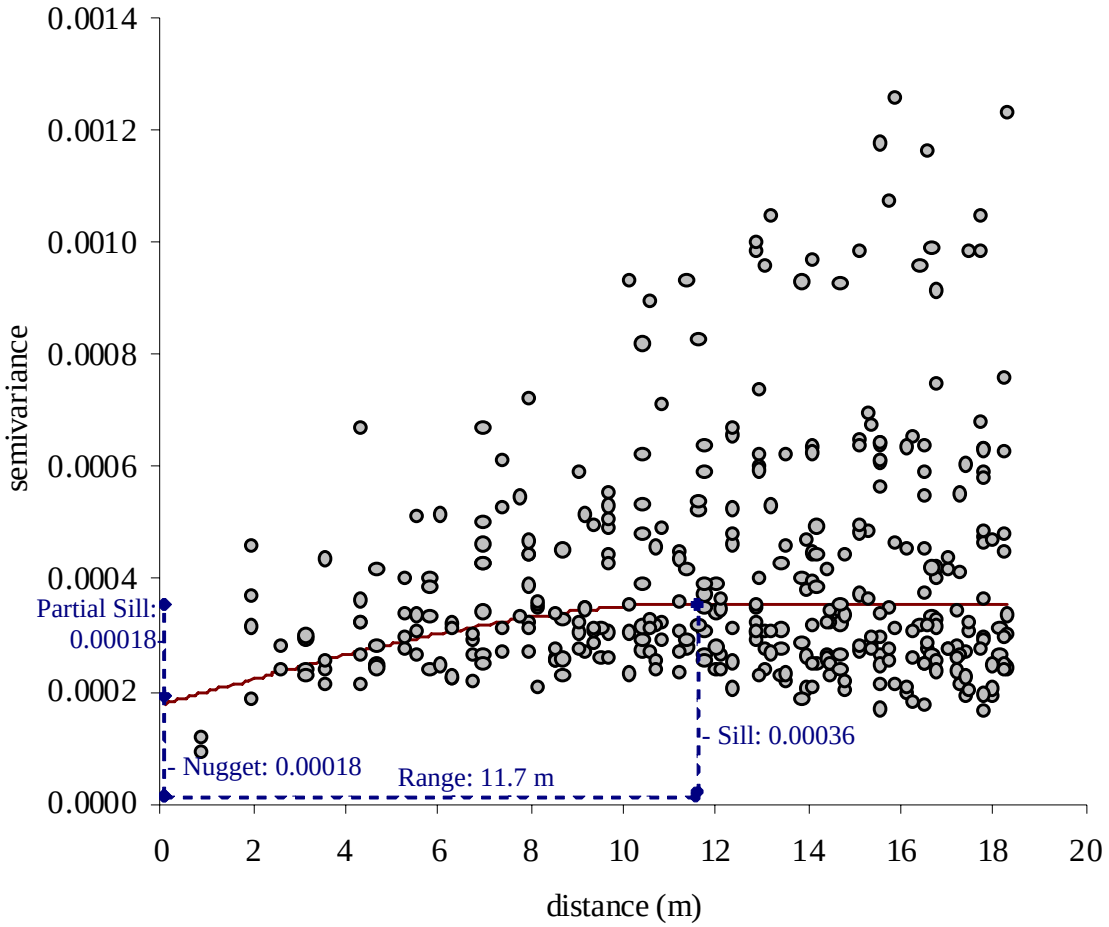

Figure 2.3. Semivariogram of Fairway 10 normalized difference vegetative index (NDVI) including the fitted spherical model curve on 12 July 2006.

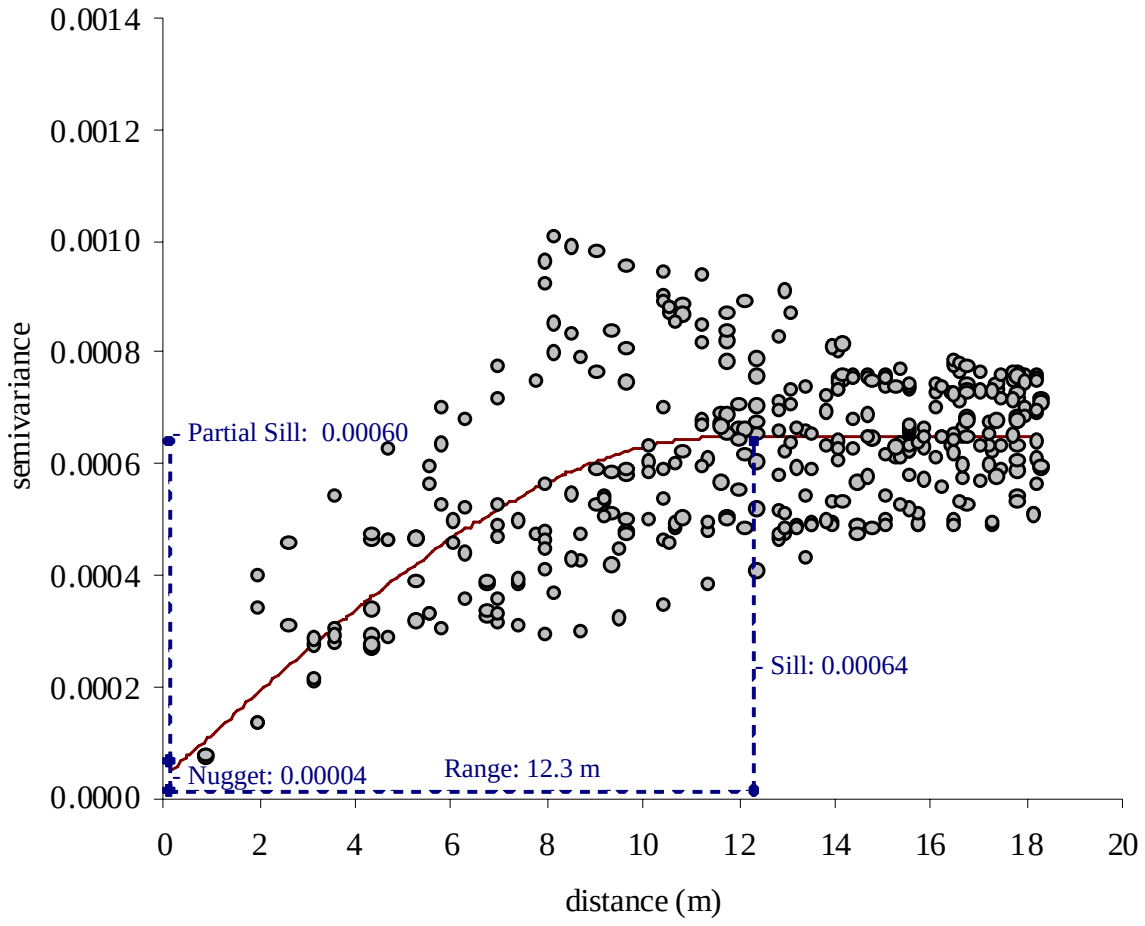

Figure 2.4. Semivariogram of Fairway 13 normalized difference vegetative index (NDVI) including the fitted spherical model curve on 12 July 2006.

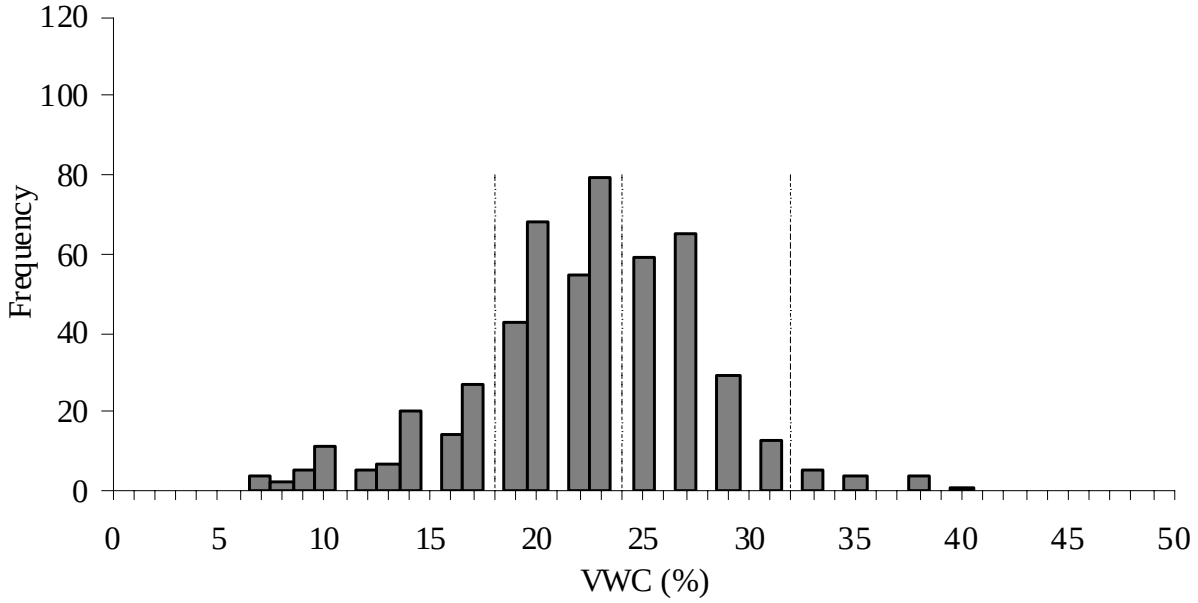

Figure 2.5a. Histogram of Fairway 10 volumetric water content (VWC) distribution on 12 July 2006. Class breaks used in site-specific management unit (SSMU) classification are indicated by dashed lines.

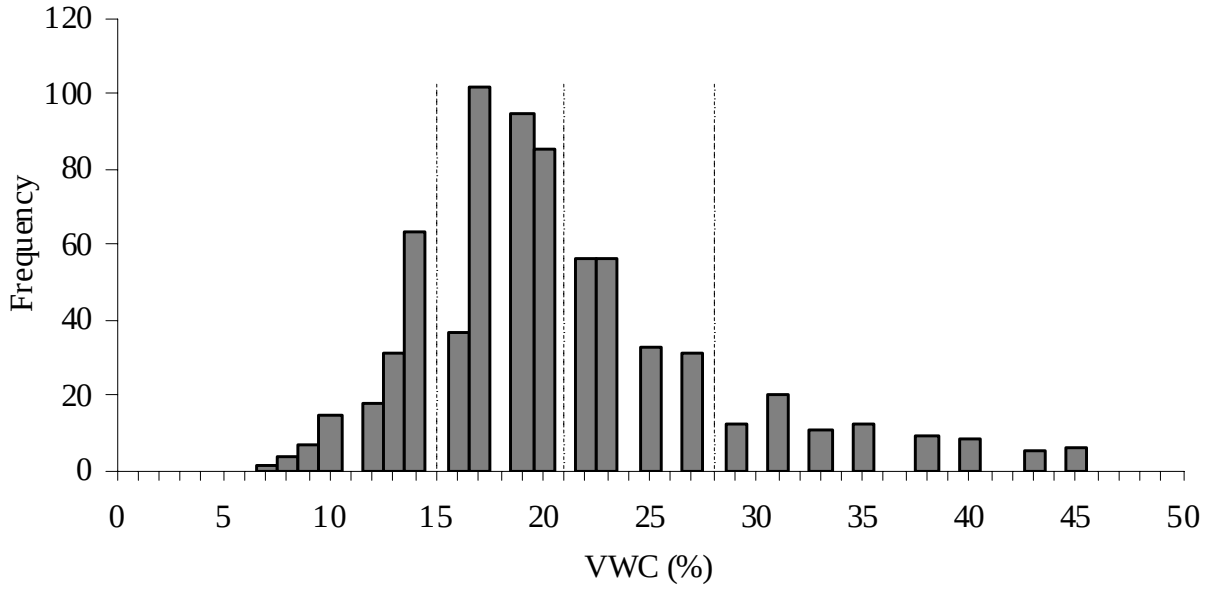

Figure 2.5b. Histogram of Fairway 13 volumetric water content (VWC) distribution on 12 July 2006. Class breaks used in site-specific management unit (SSMU) classification are indicated by dashed lines.

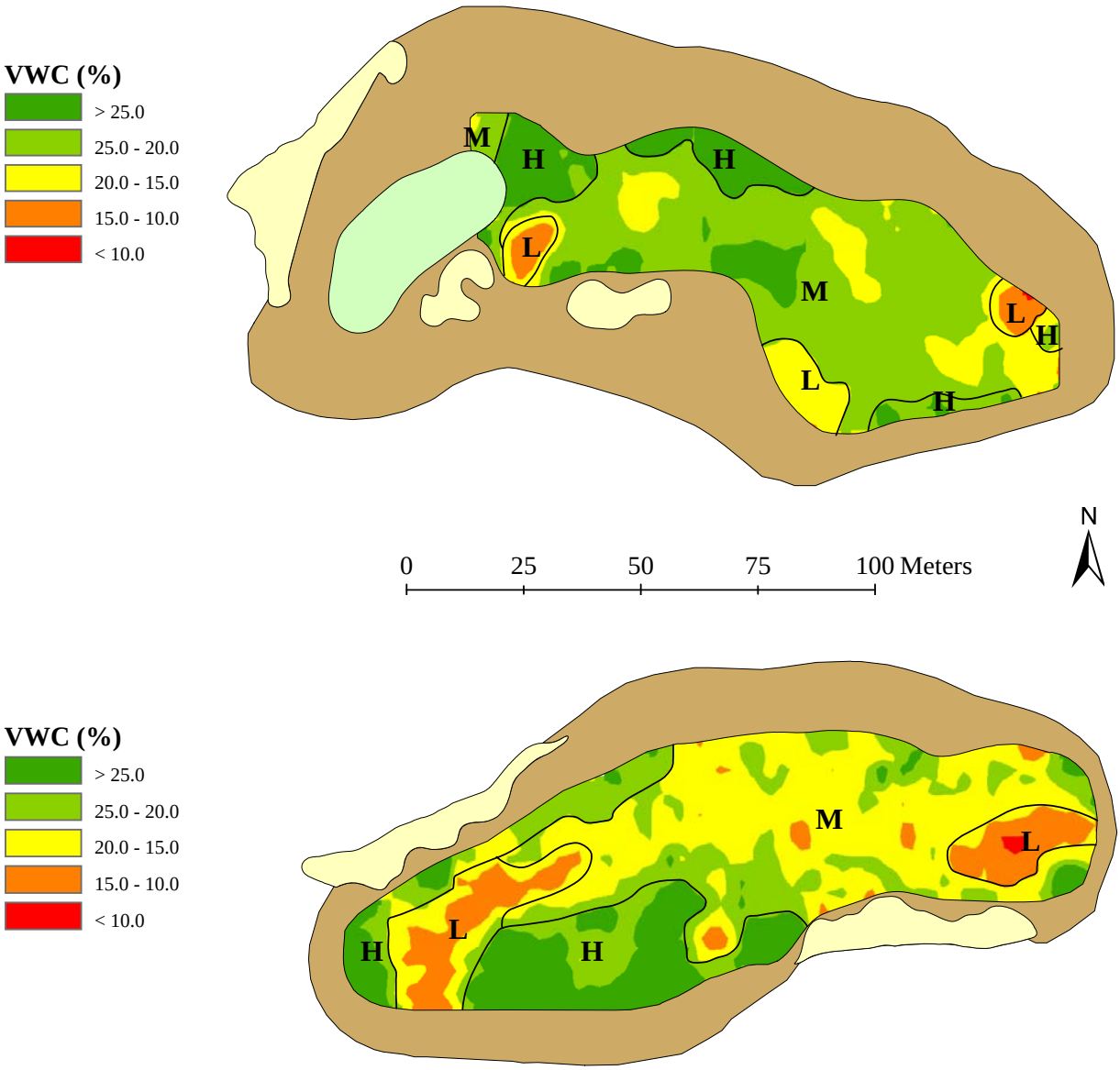

Figure 2.6. Site-specific management units (SSMUs) of Fairways 10 and 13 (upper and lower maps, respectively) based on the manual classification method on 12 July 2006. Low, moderate, and high SSMUs are denoted as L, M, and H, respectively. VWC = volumetric water content.

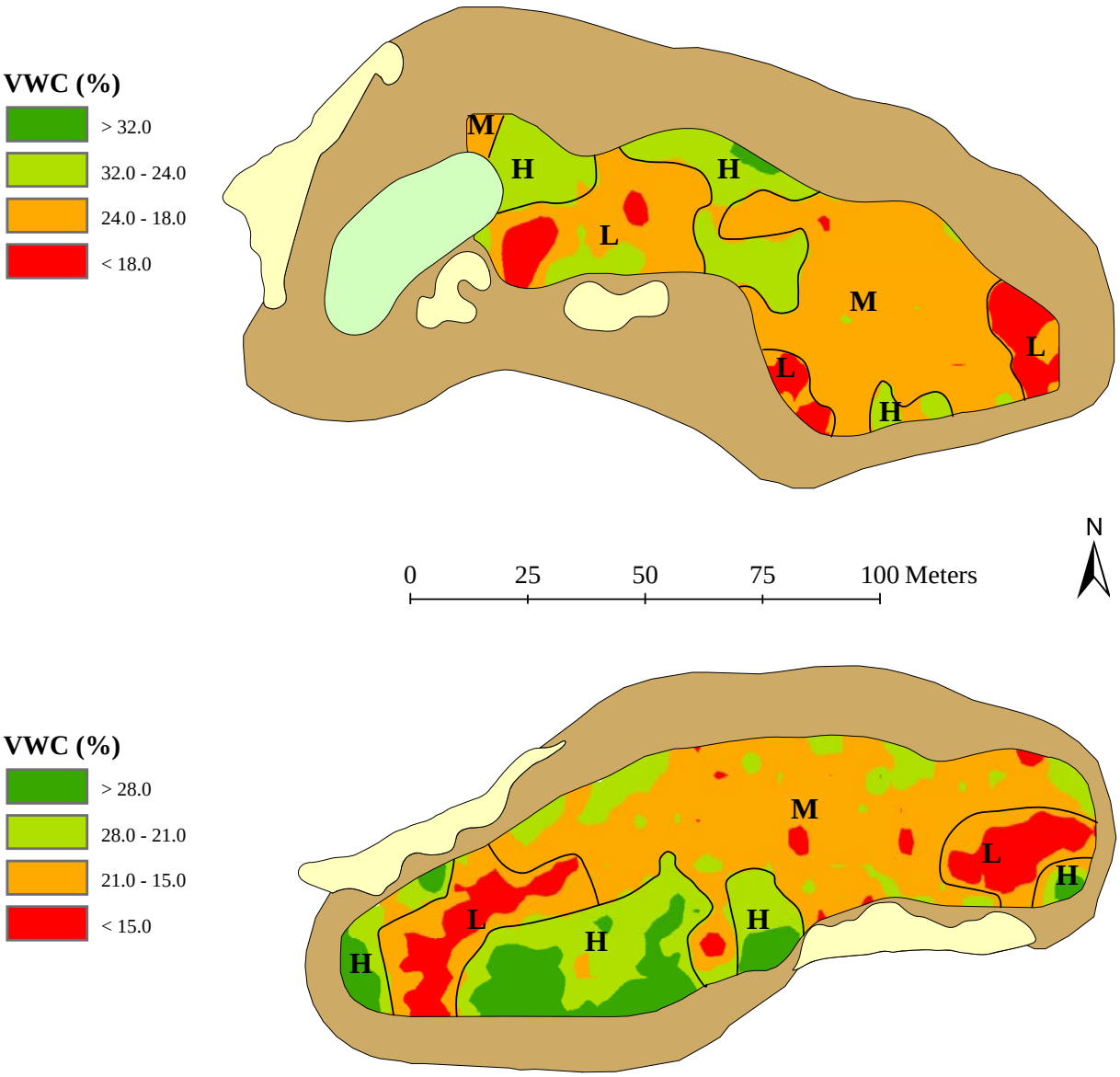

Figure 2.7. Site-specific management units (SSMUs) of Fairways 10 and 13 (upper and lower maps, respectively) based on the histogram classification method on 12 July 2006. Low, moderate, and high SSMUs are denoted as L, M, and H, respectively. VWC = volumetric water content.

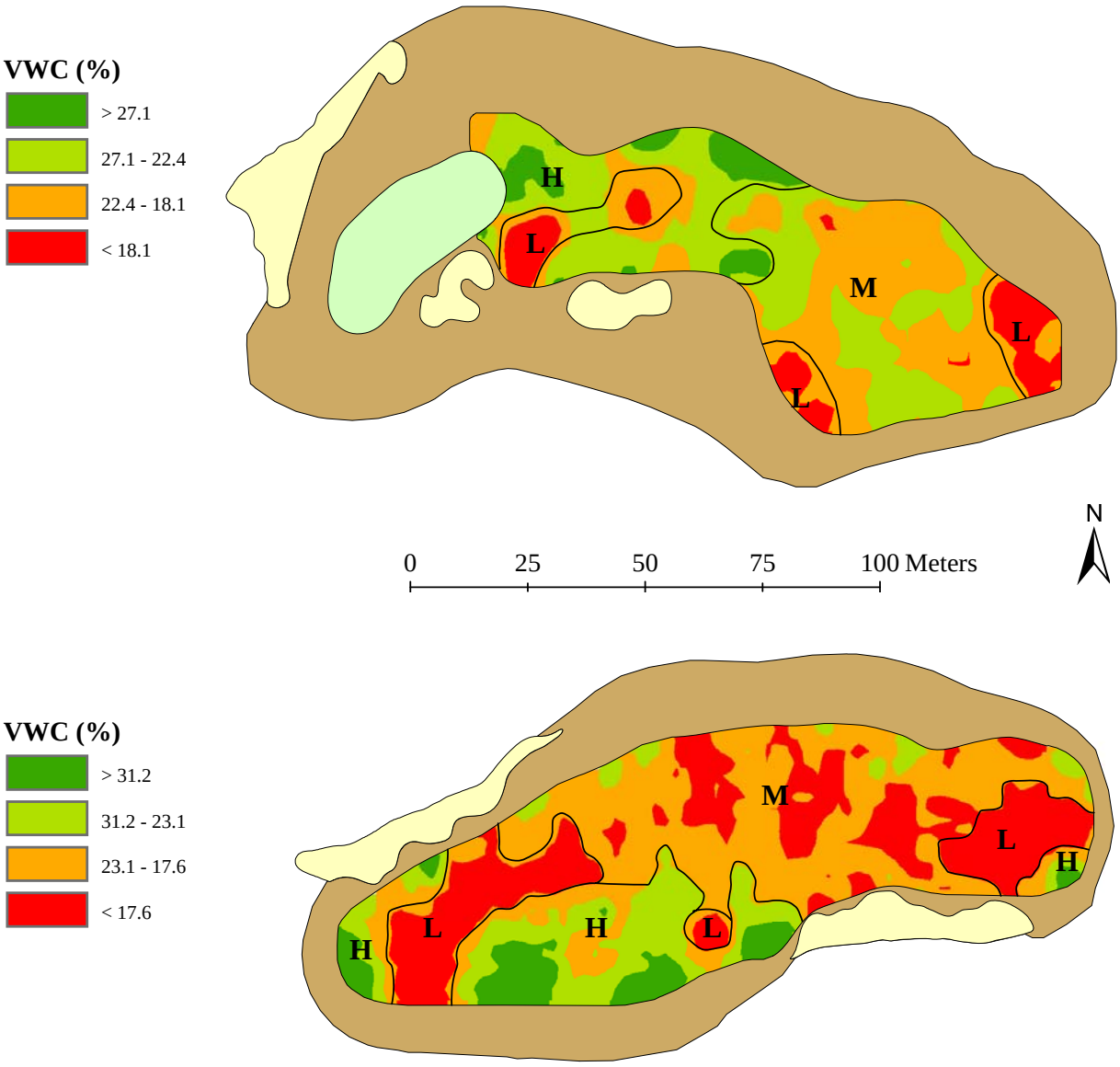

Figure 2.8. Site-specific management units (SSMUs) of Fairways 10 and 13 (upper and lower maps, respectively) based on the Jenk's classification method on 12 July 2006. Low, moderate, and high SSMUs are denoted as L, M, and H, respectively. VWC = volumetric water content.

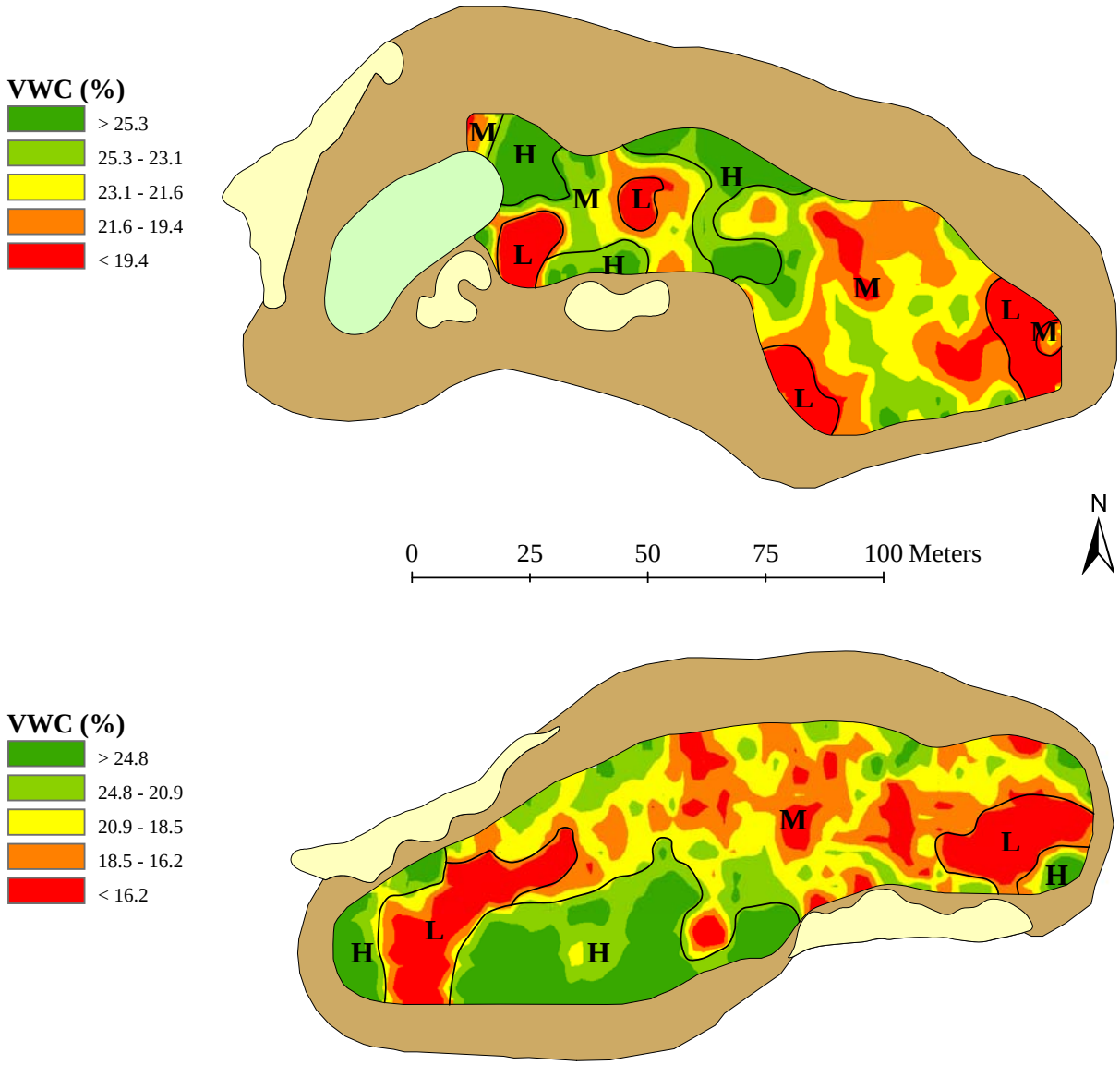

Figure 2.9. Site-specific management units (SSMUs) of Fairways 10 and 13 (upper and lower maps, respectively) based on the quantile classification method on 12 July 2006. Low, moderate, and high SSMUs are denoted as L, M, and H, respectively. VWC = volumetric water content.

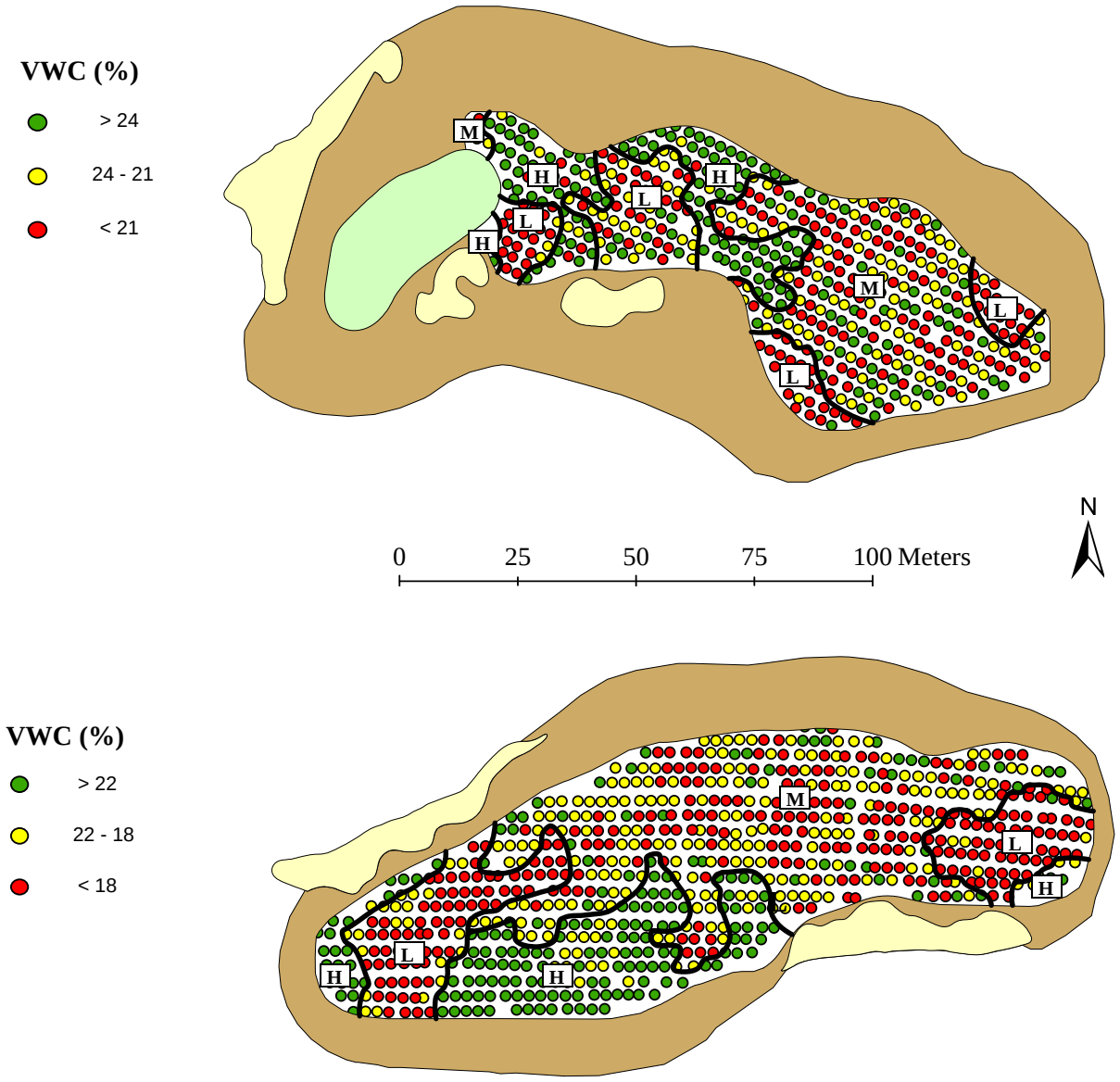

Figure 2.10. Site-specific management units (SSMUs) of Fairways 10 and 13 (upper and lower maps, respectively) based on the 1/3 query classification method on 12 July 2006. Low, moderate, and high SSMUs are denoted as L, M, and H, respectively. VWC = volumetric water content.

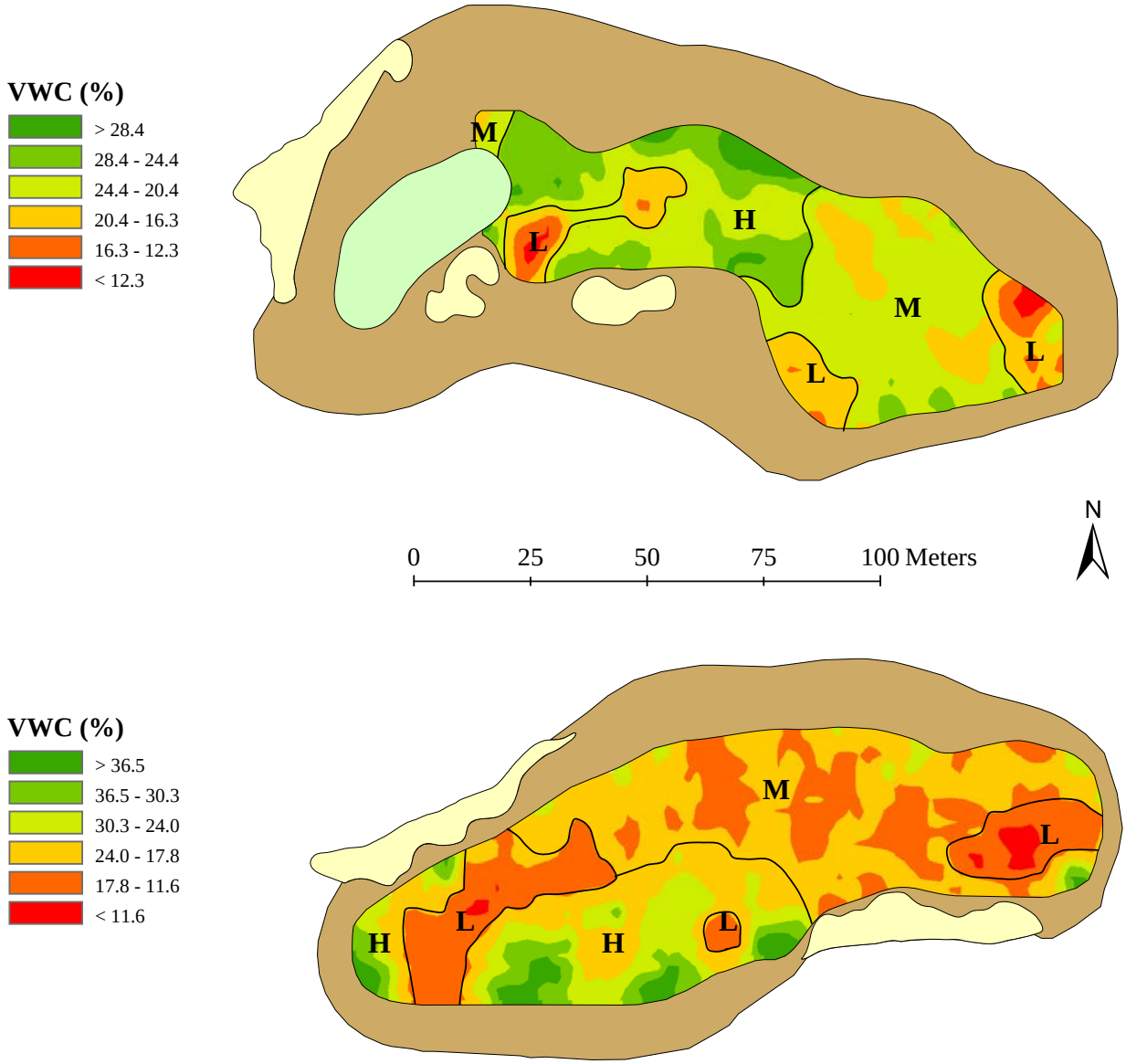

Figure 2.11. Site-specific management units (SSMUs) of Fairways 10 and 13 (upper and lower maps, respectively) based on the standard deviation classification method on 12 July 2006. Low, moderate, and high SSMUs are denoted as L, M, and H, respectively. VWC = volumetric water content.

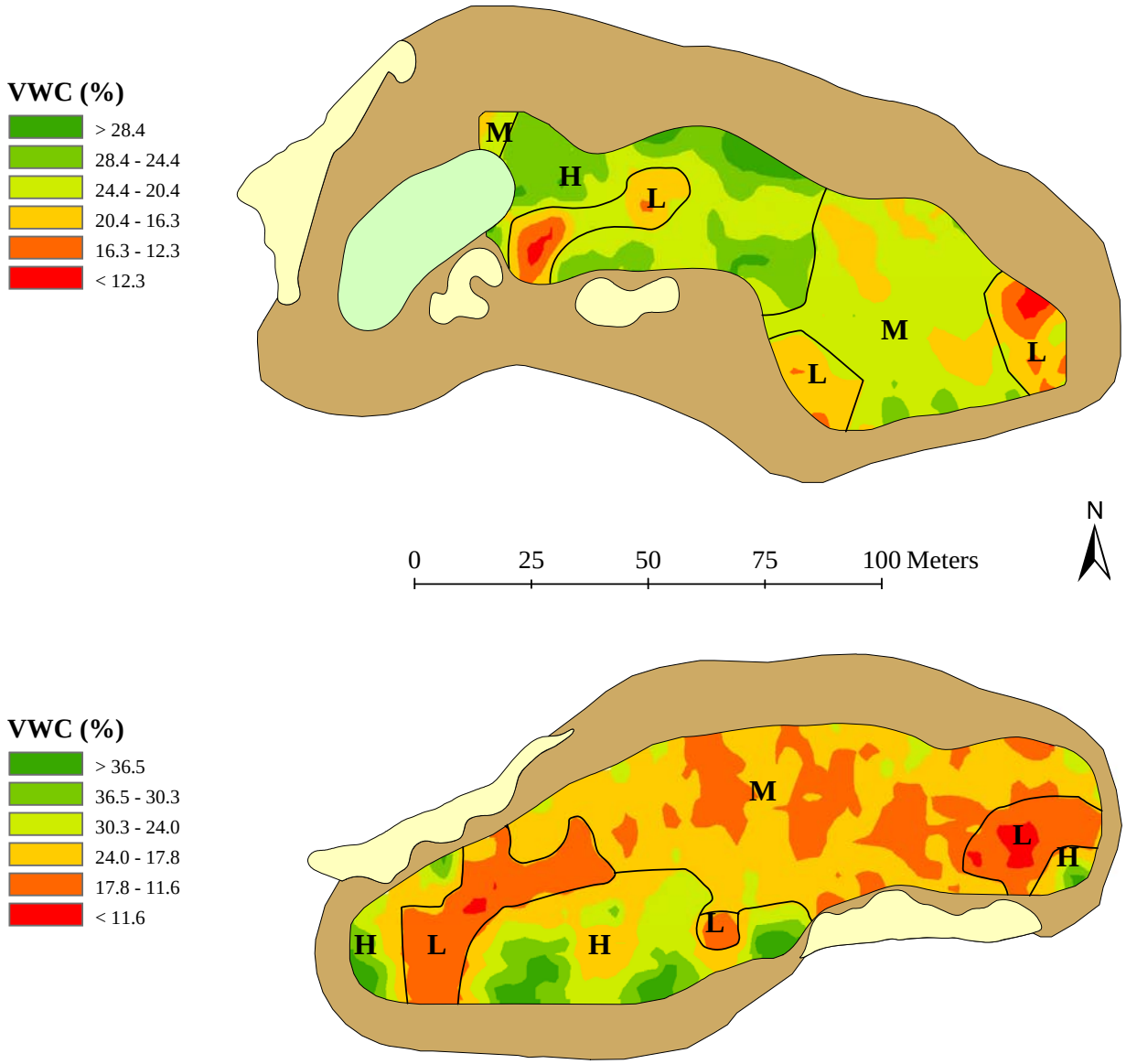

Figure 2.12: Site-specific management units (SSMUs) of Fairways 10 and 13 (upper and lower maps, respectively) based on the SD-Integrated classification method on 12 July 2006. Low, moderate, and high SSMUs are denoted as L, M, and H, respectively. VWC = volumetric water content.

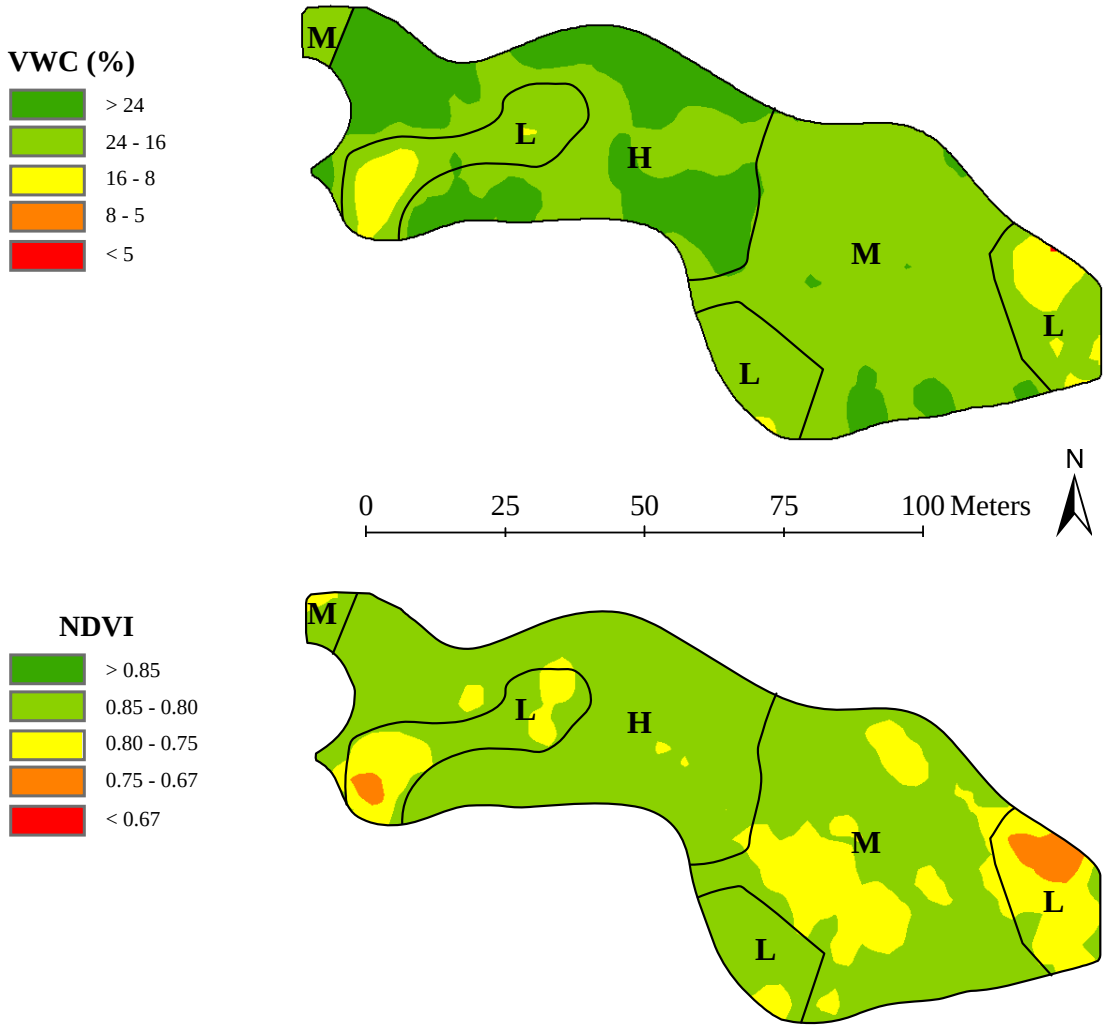

Figure 2.13. Volumetric water content (VWC) and normalized difference vegetative index (NDVI) of Fairway 10 on 12 July 2006. Low, moderate, and high SSMUs for the SD-Integrated classification method are denoted as L, M, and H, respectively.

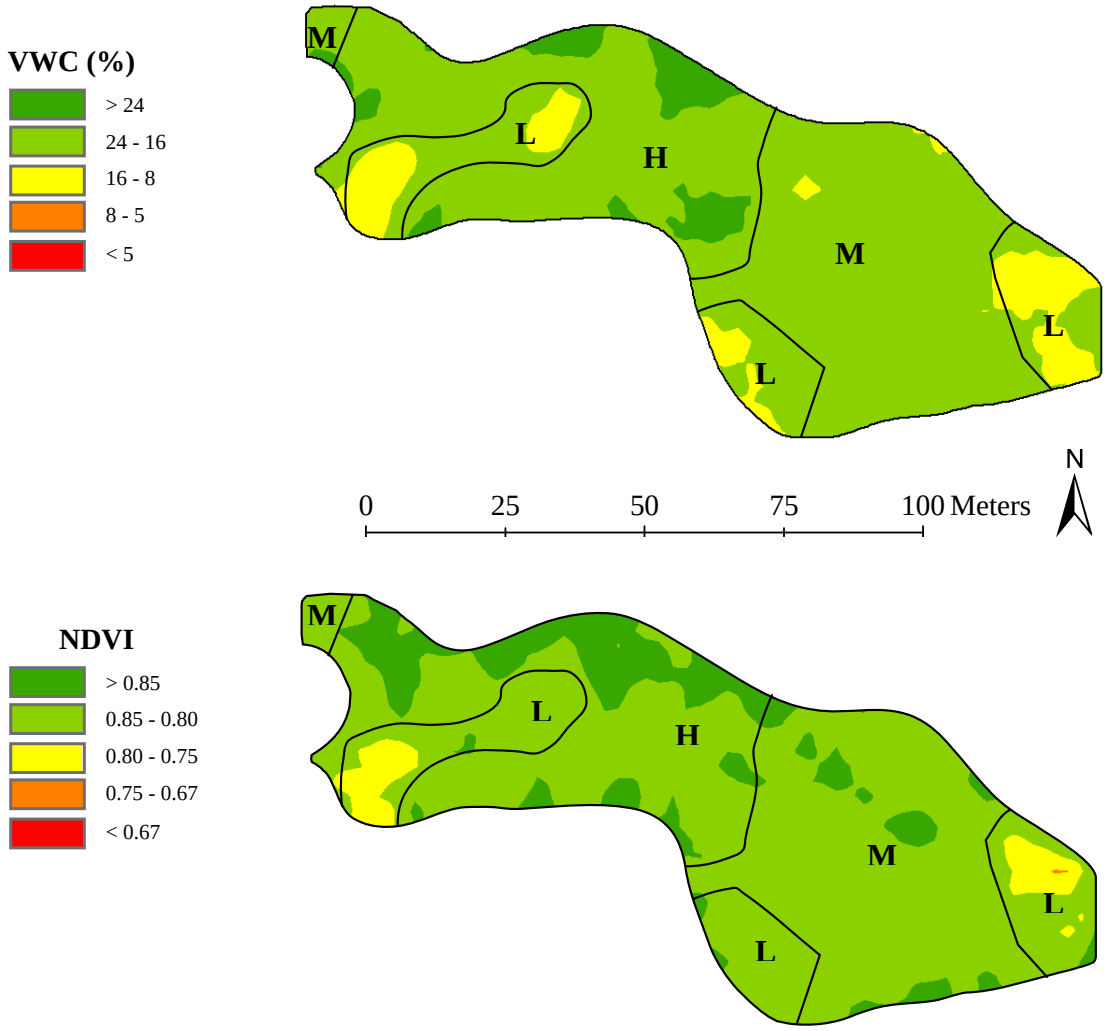

Figure 2.14. Volumetric water content (VWC) and normalized difference vegetative index (NDVI) of Fairway 10 on 13 July 2006. Low, moderate, and high SSMUs for the SD-Integrated classification method are denoted as L, M, and H, respectively.

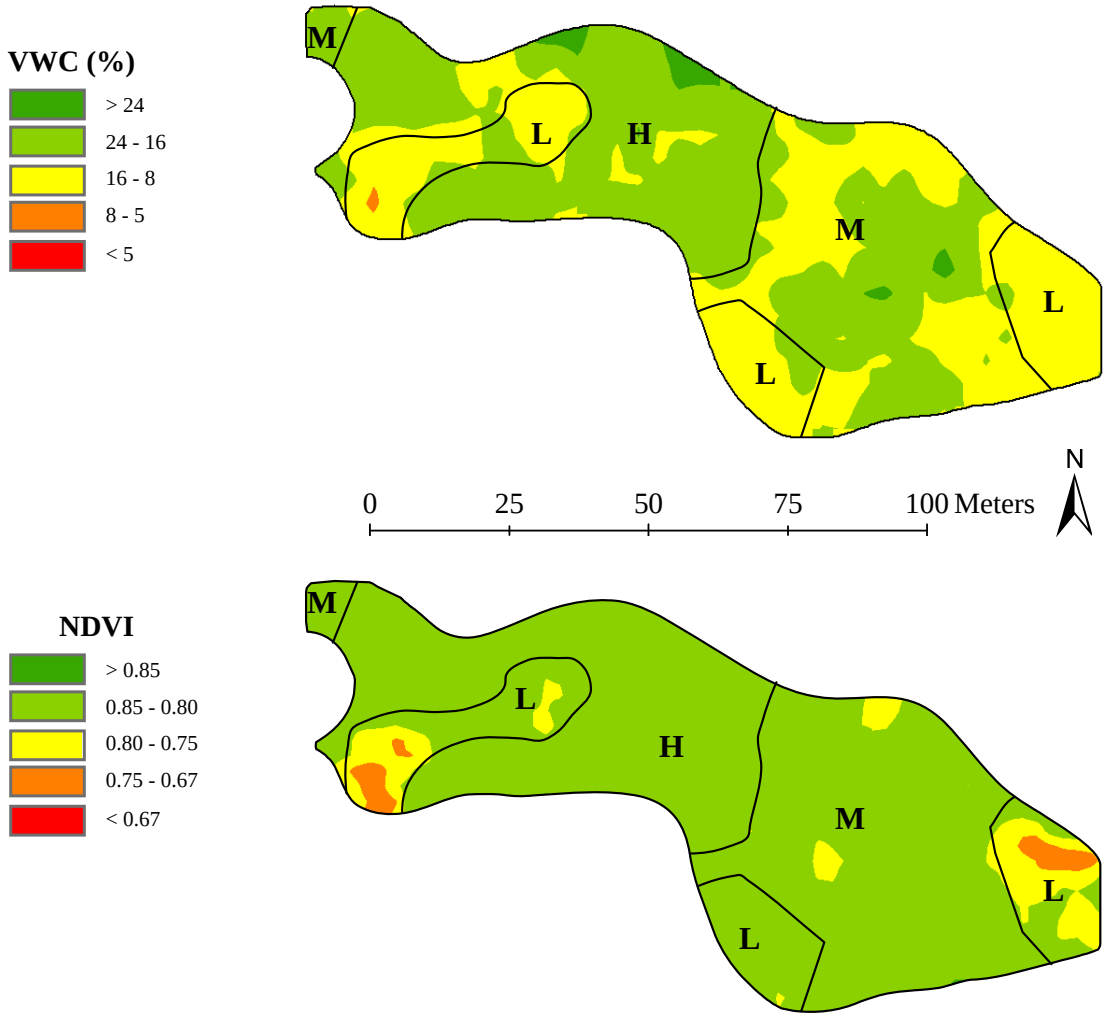

Figure 2.15. Volumetric water content (VWC) and normalized difference vegetative index (NDVI) of Fairway 10 on 14 July 2006. Low, moderate, and high SSMUs for the SD-Integrated classification method are denoted as L, M, and H, respectively.

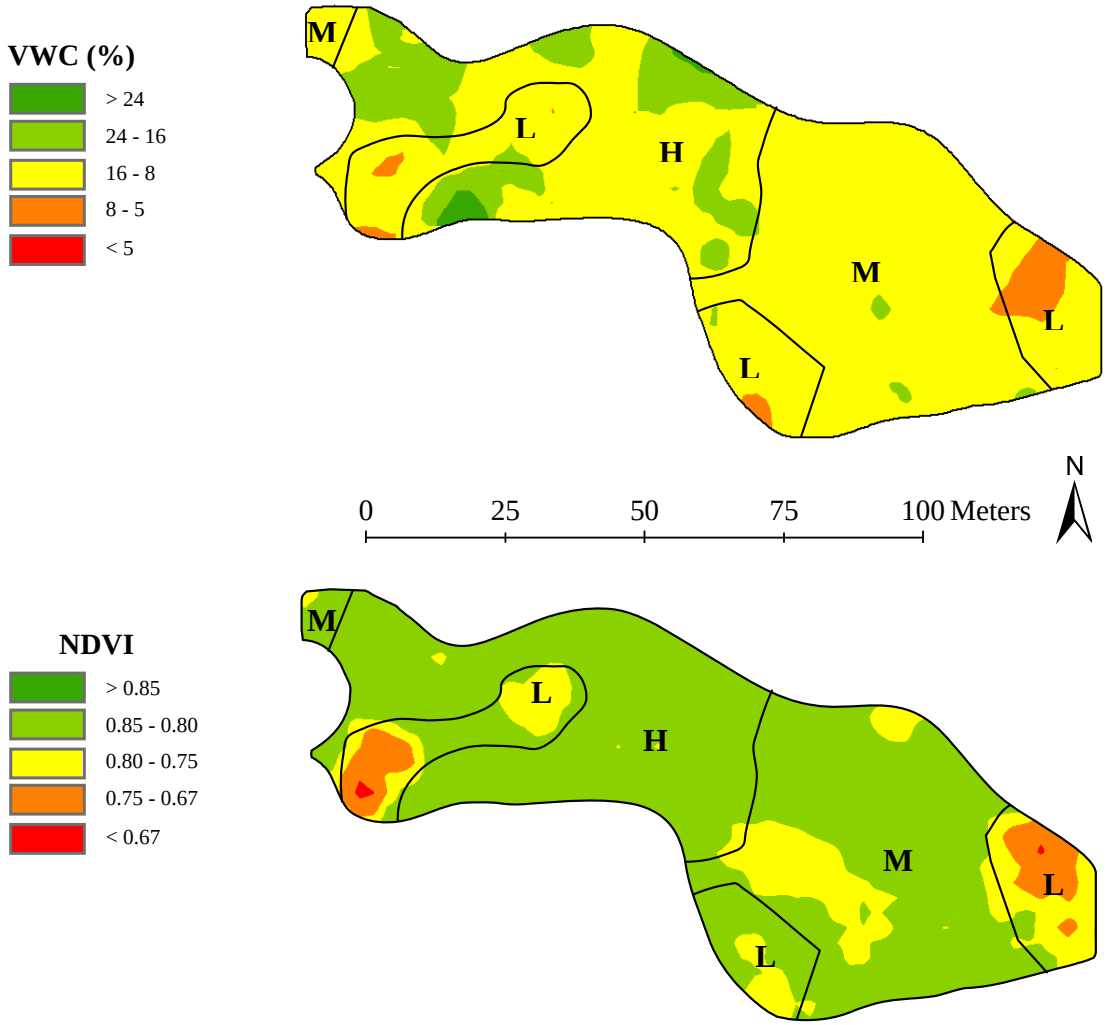

Figure 2.16. Volumetric water content (VWC) and normalized difference vegetative index (NDVI) of Fairway 10 on 15 July 2006. Low, moderate, and high SSMUs for the SD-Integrated classification method are denoted as L, M, and H, respectively.

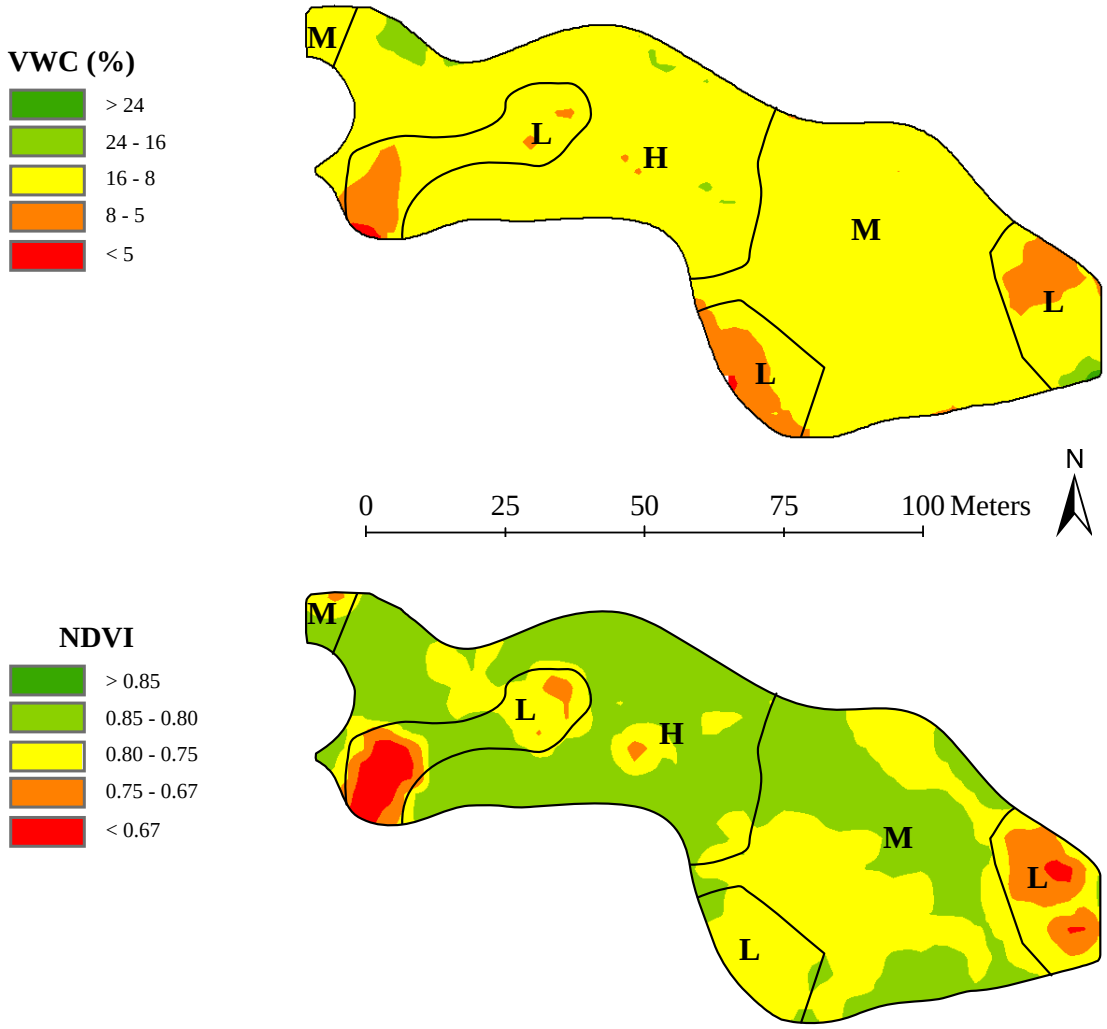

Figure 2.17. Volumetric water content (VWC) and normalized difference vegetative index (NDVI) of Fairway 10 on 16 July 2006. Low, moderate, and high SSMUs for the SD-Integrated classification method are denoted as L, M, and H, respectively.

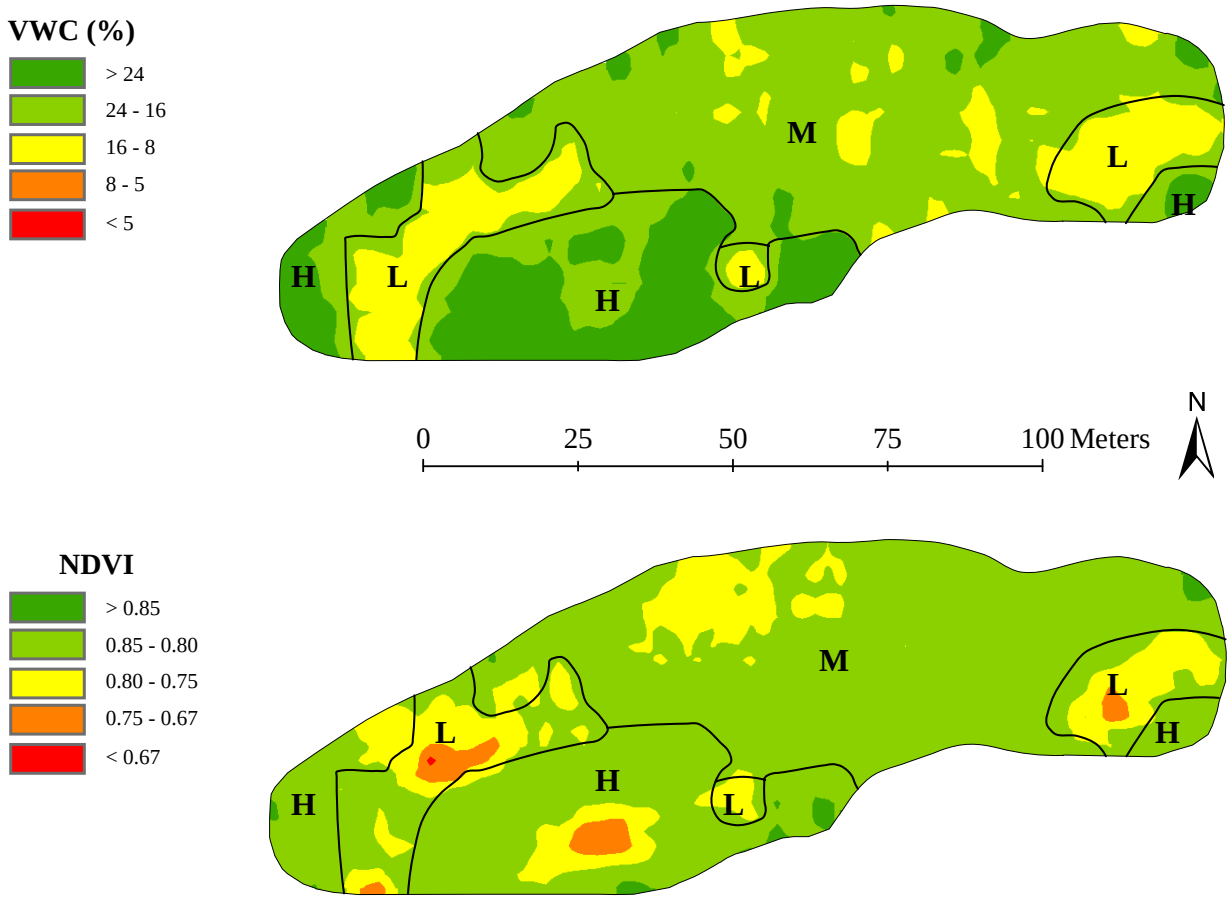

Figure 2.18. Volumetric water content (VWC) and normalized difference vegetative index (NDVI) of Fairway 13 on 12 July 2006. Low, moderate, and high SSMUs for the SD-Integrated classification method are denoted as L, M, and H, respectively.

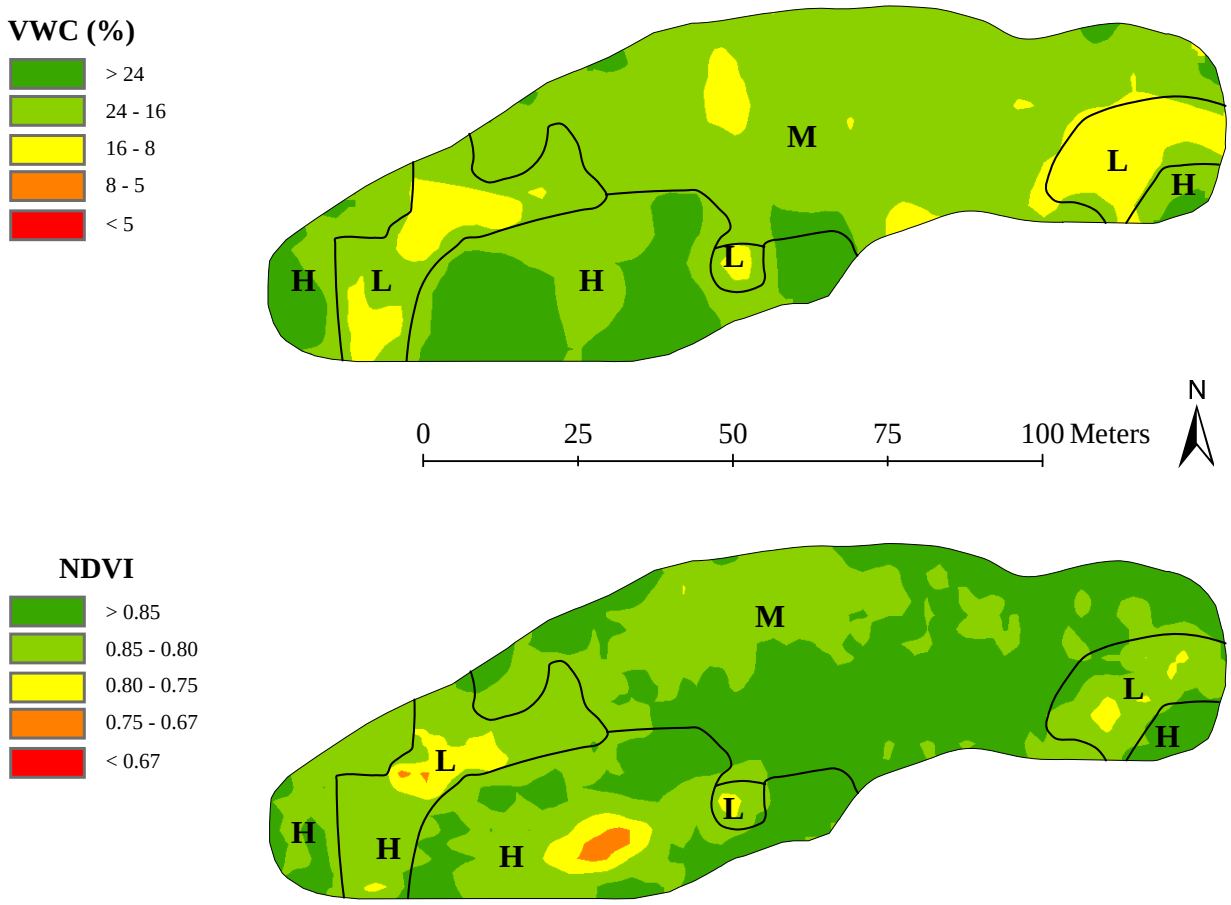

Figure 2.19. Volumetric water content (VWC) and normalized difference vegetative index (NDVI) of Fairway 13 on 13 July 2006. Low, moderate, and high SSMUs for the SD-Integrated classification method are denoted as L, M, and H, respectively.

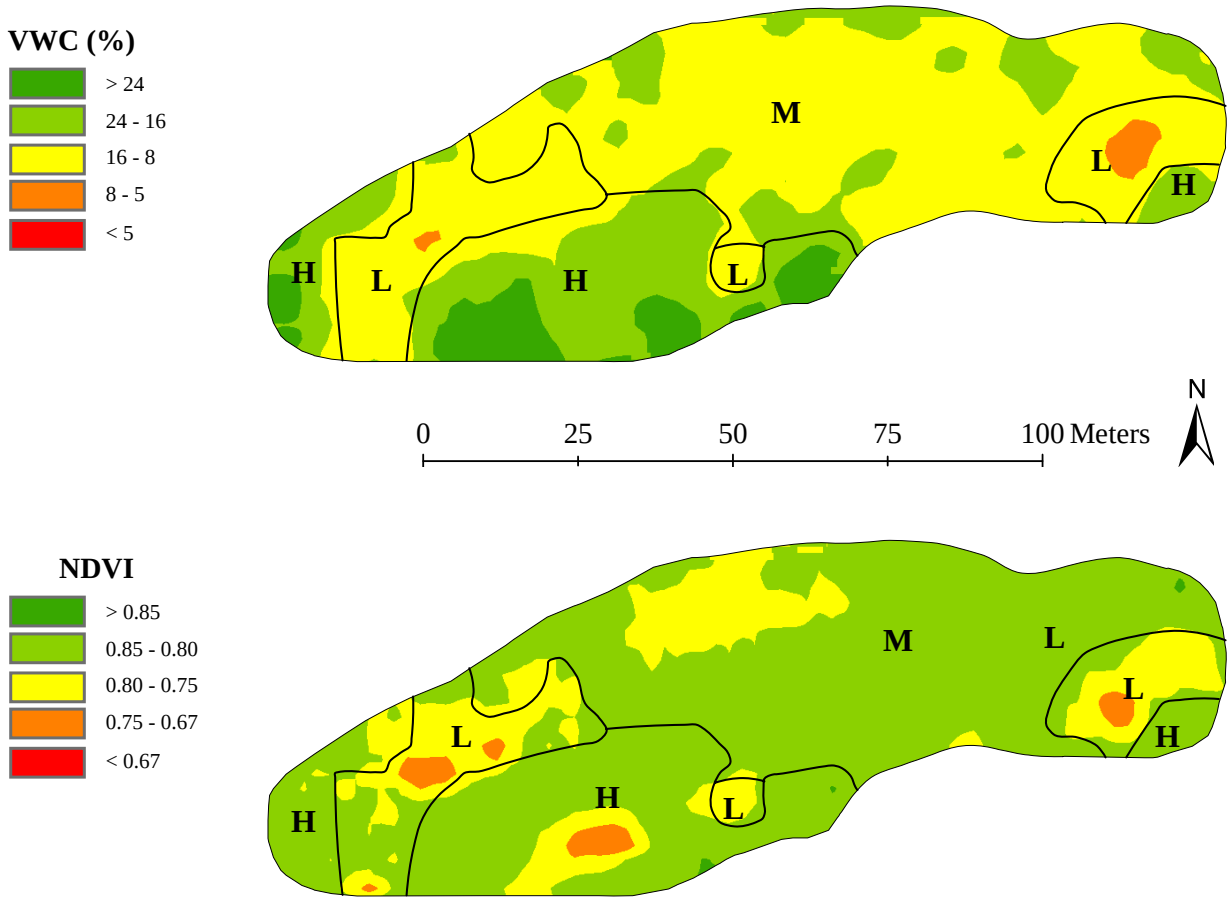

Figure 2.20. Volumetric water content (VWC) and normalized difference vegetative index (NDVI) of Fairway 13 on 14 July 2006. Low, moderate, and high SSMUs for the SD-Integrated classification method are denoted as L, M, and H, respectively.

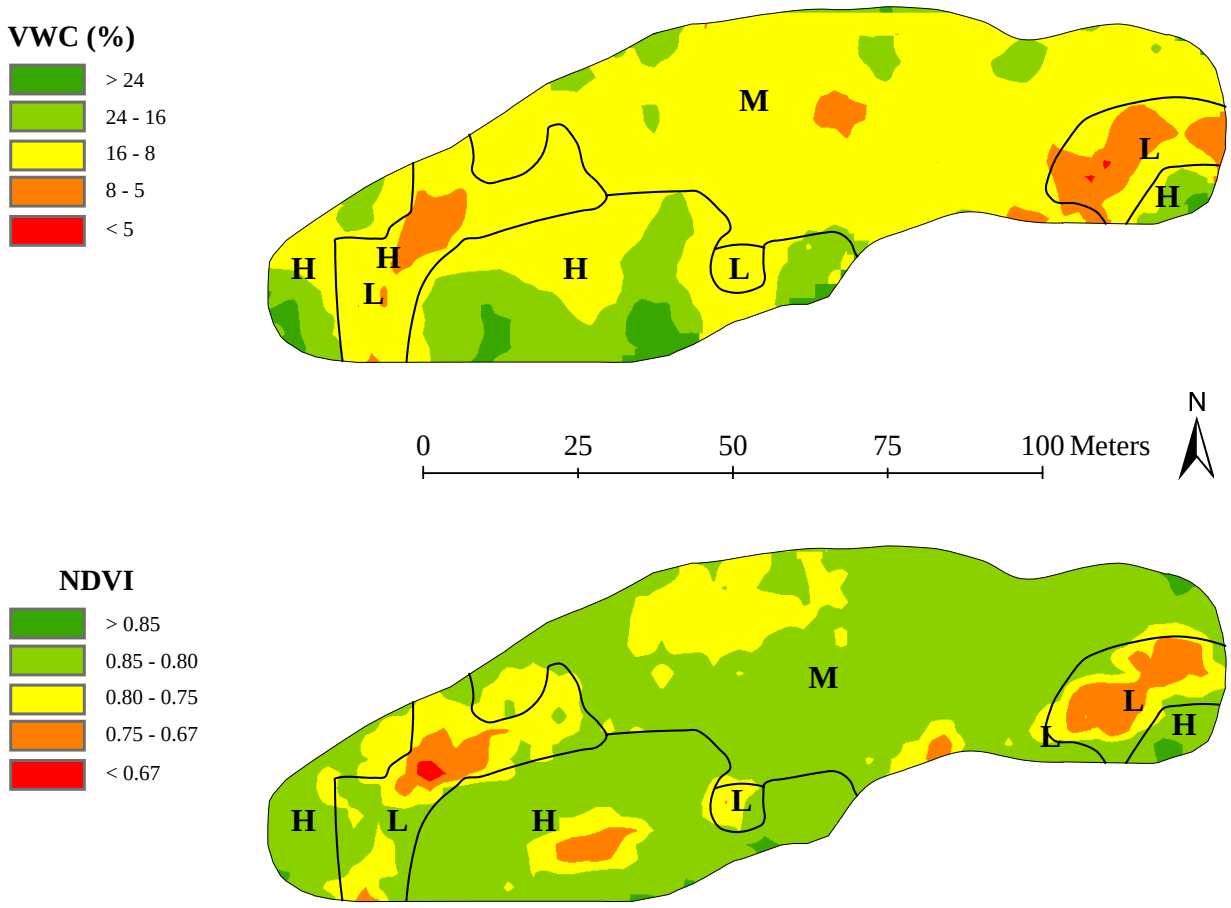

Figure 2.21. Volumetric water content (VWC) and normalized difference vegetative index (NDVI) of Fairway 13 on 15 July 2006. Low, moderate, and high SSMUs for the SD-Integrated classification method are denoted as L, M, and H, respectively.

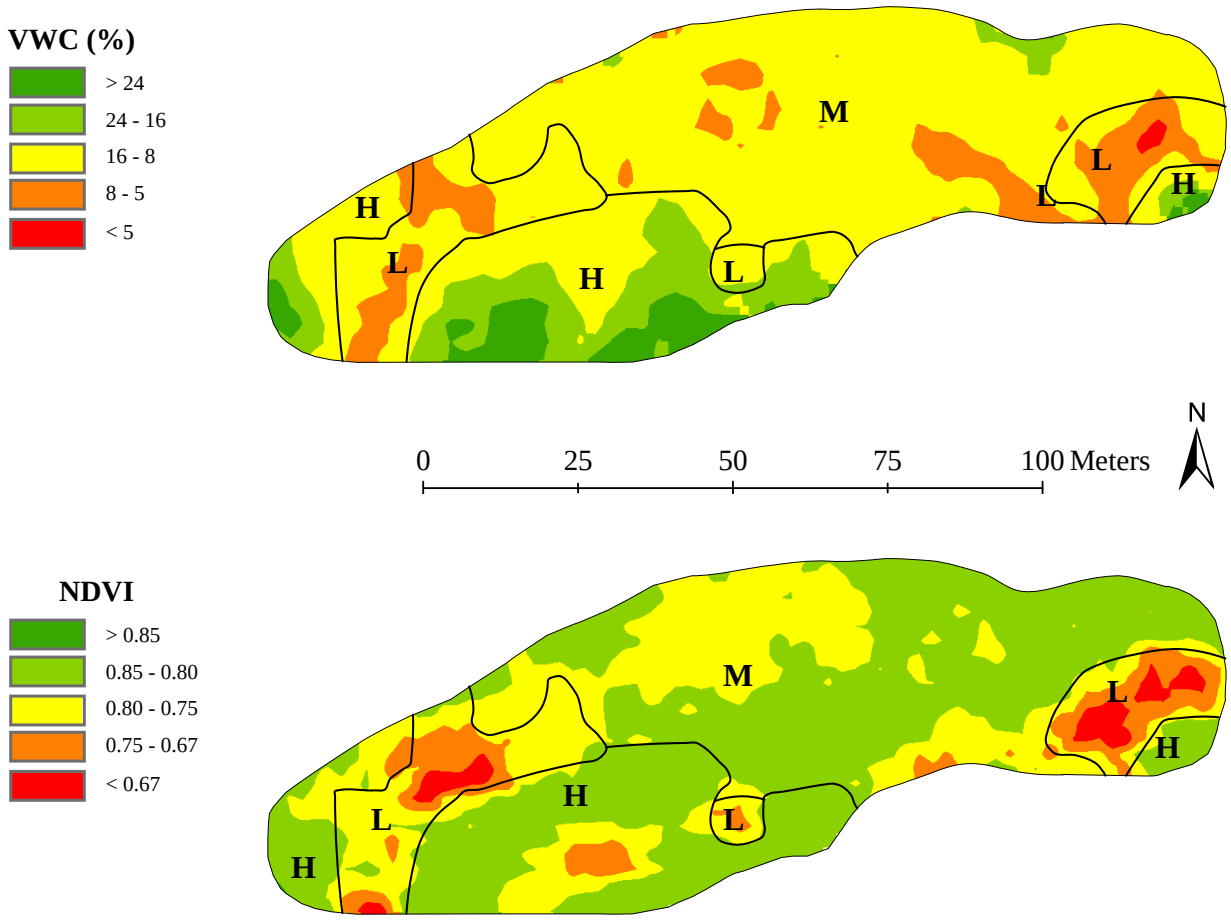

Figure 2.22. Volumetric water content (VWC) and normalized difference vegetative index (NDVI) of Fairway 13 on 16 July 2006. Low, moderate, and high SSMUs for the SD-Integrated classification method are denoted as L, M, and H, respectively.

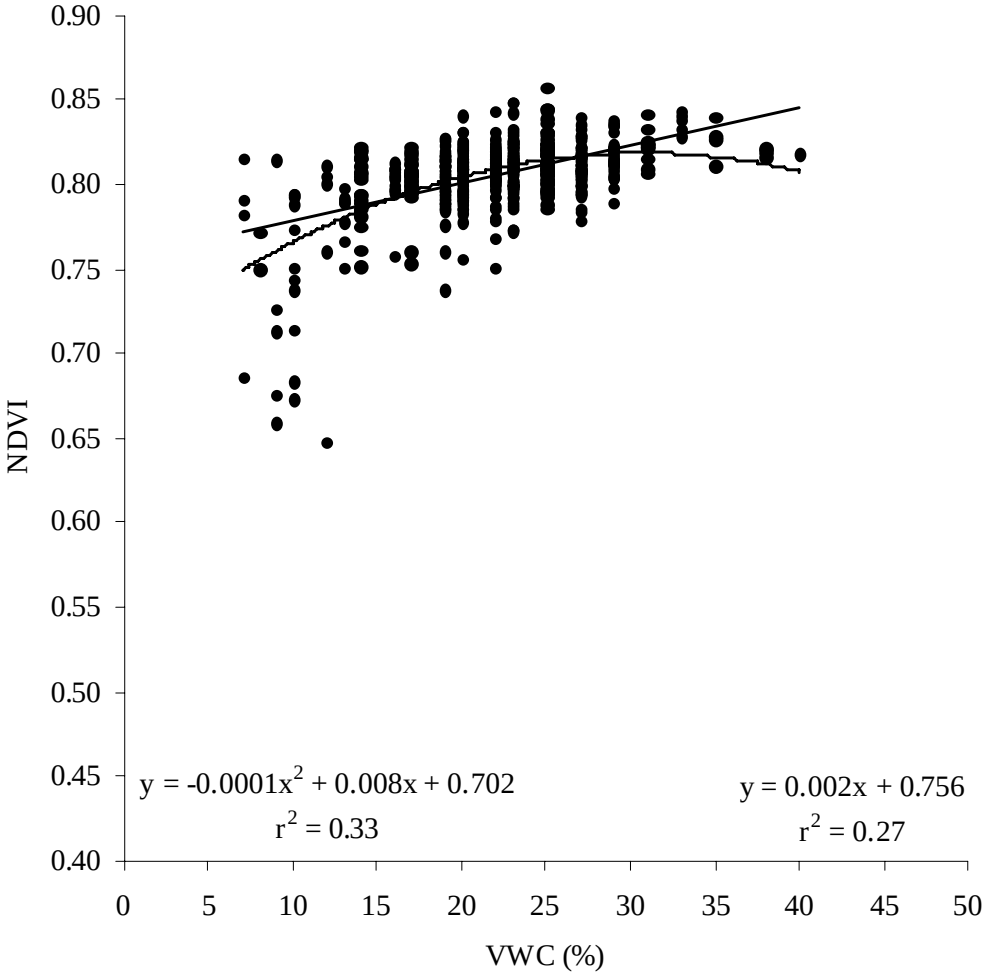

Figure 2.23. Linear and quadratic relationships between volumetric water content (VWC) and normalized difference vegetative index (NDVI) of Fairway 10 on 12 July 2006.

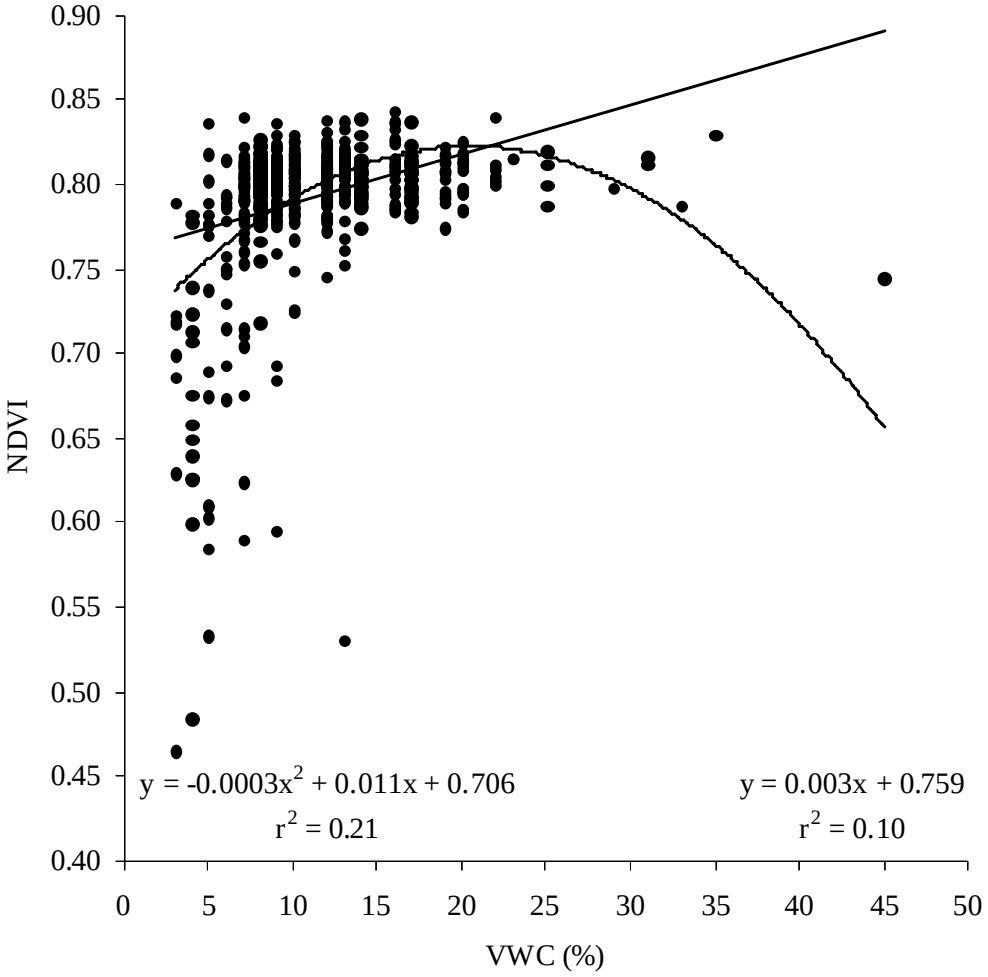

Figure 2.24. Linear and quadratic relationships between volumetric water content (VWC) and normalized difference vegetative index (NDVI) of Fairway 10 on 16 July 2006.

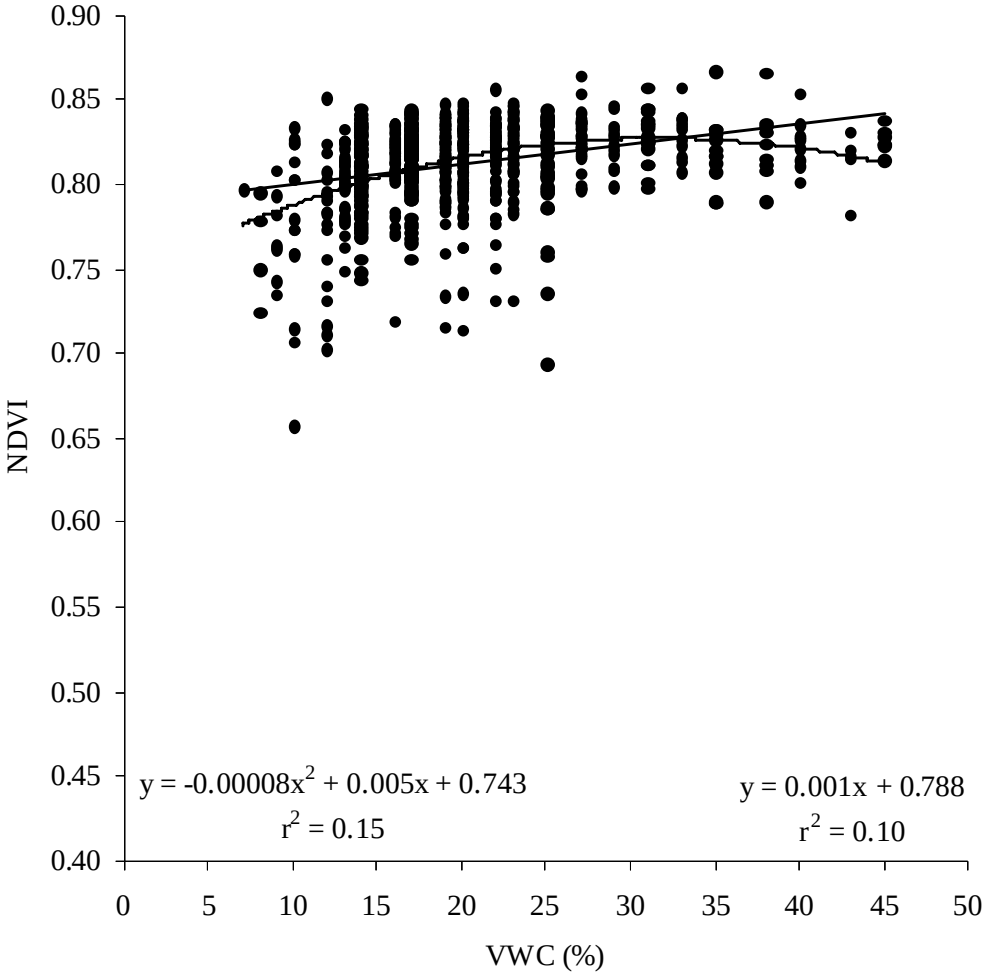

Figure 2.25. Linear and quadratic relationships between volumetric water content (VWC) and normalized difference vegetative index (NDVI) of Fairway 13 on 12 July 2006.

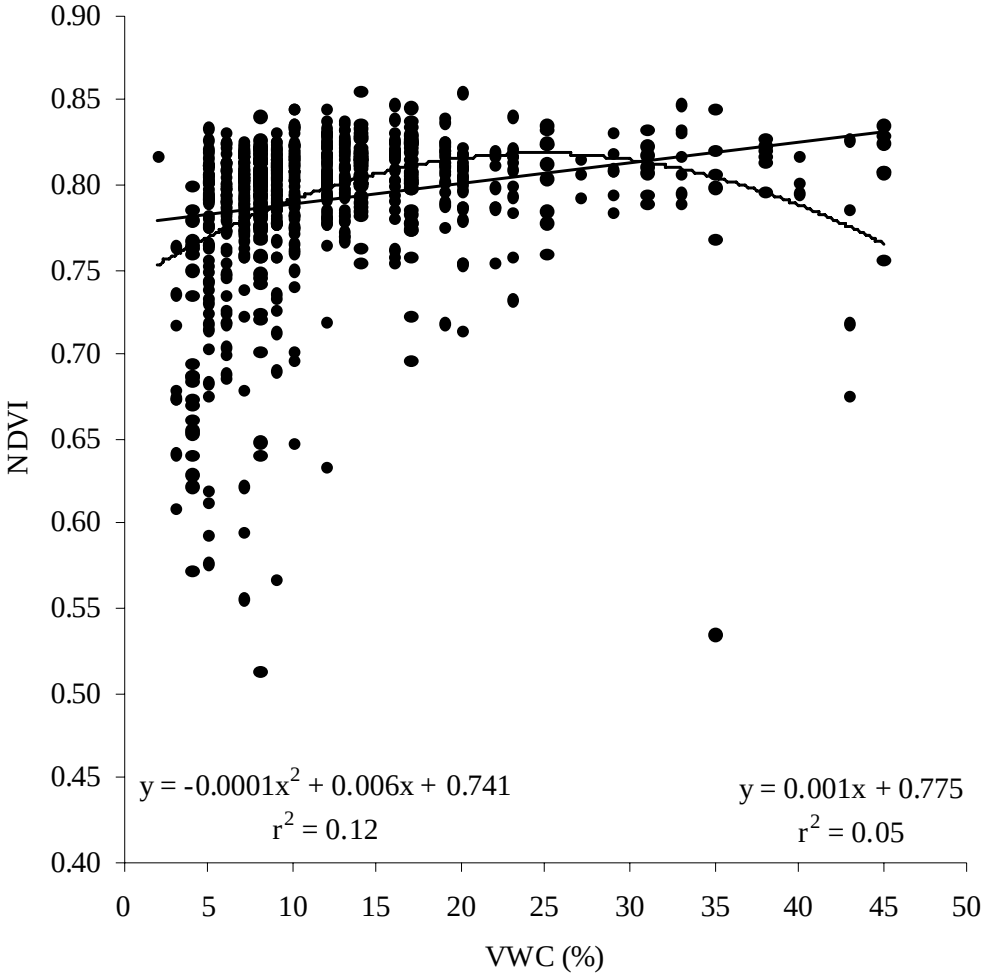

Figure 2.26. Linear and quadratic relationships between volumetric water content (VWC) and normalized difference vegetative index (NDVI) of Fairway 13 on 16 July 2006.

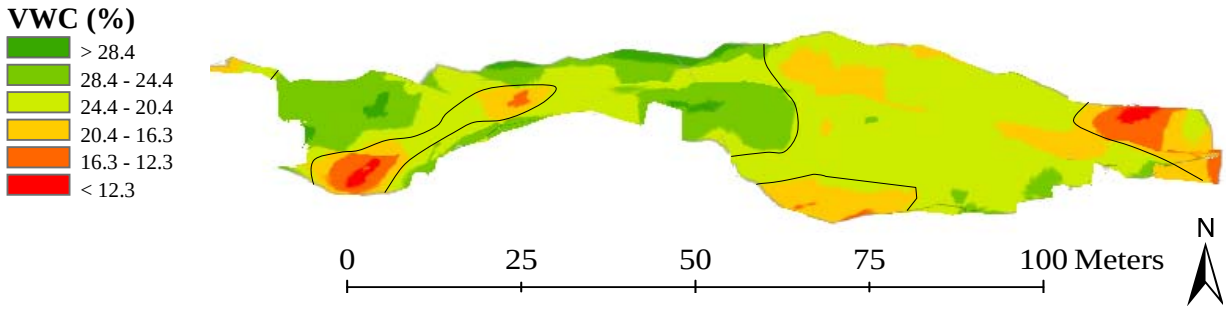

Figure 2.27a. Vertically exaggerated elevation map of Fairway 10 using a Triangulated Irregular Network (TIN) to depict terrain gradations. Volumetric water content (VWC) using the SD-Integrated site-specific management units (SSMUs) on 12 July 2006 is displayed. Elevation data are derived from the GPS receiver of the Toro Mobile Multi-Sensor (TMM).

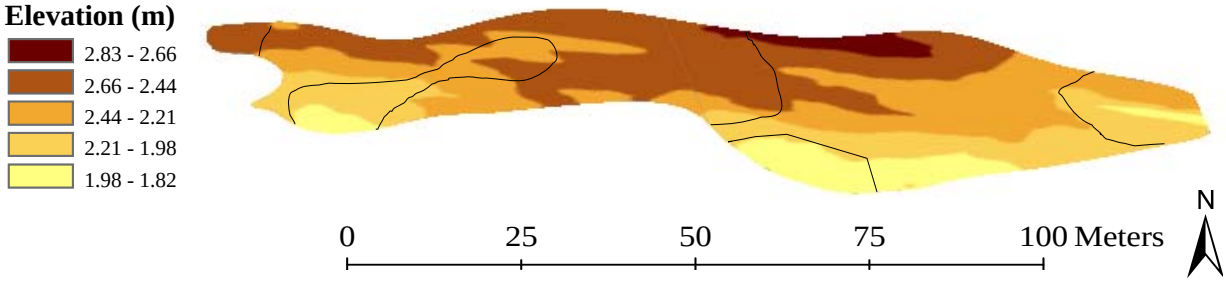

Figure 2.27b. Interpolated map of elevation data derived from the GPS receiver of the Toro Mobile Multi-Sensor (TMM) of Fairway 10 on 12 July 2006. Data are classified by standard deviation.

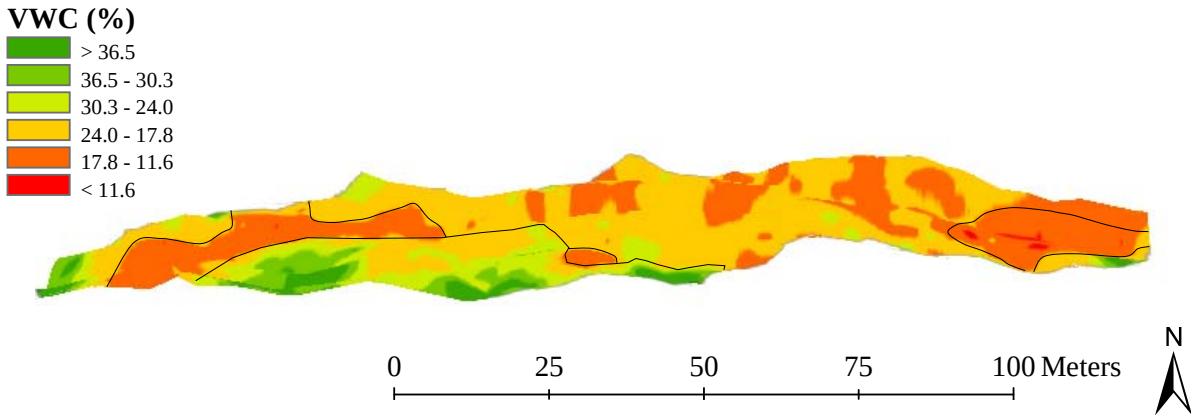

Figure 2.28a. Vertically exaggerated elevation map of Fairway 13 using a Triangulated Irregular Network (TIN) to depict terrain gradations. Volumetric water content (VWC) using the SD-Integrated site-specific management units (SSMUs) on 12 July 2006 is displayed. Elevation data are derived from the GPS receiver of the Toro Mobile Multi-Sensor (TMM).

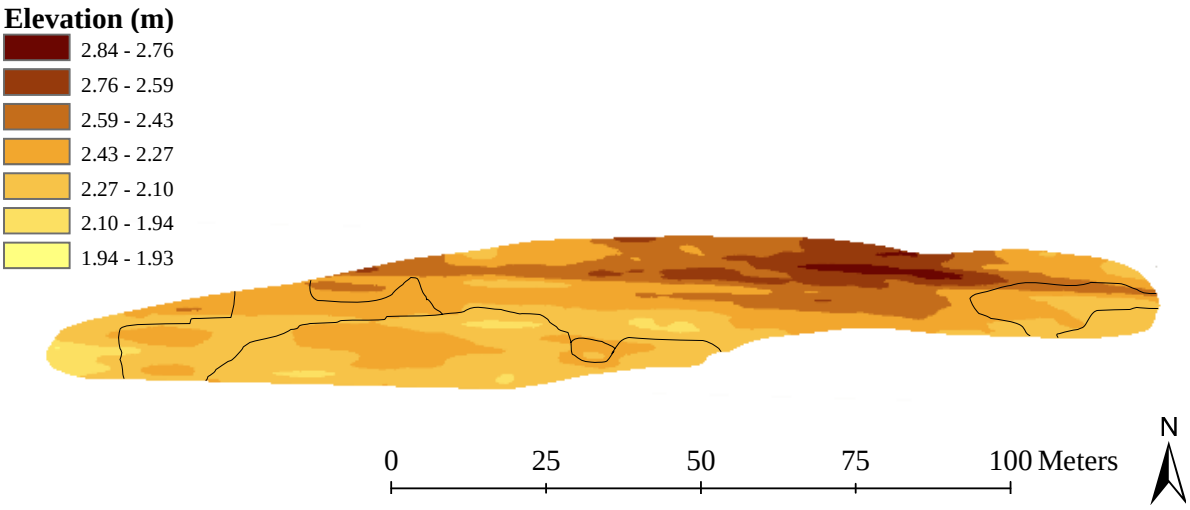

Figure 2.28b. Interpolated map of elevation data derived from the GPS receiver of the Toro Mobile Multi-Sensor (TMM) of Fairway 13 on 12 July 2006. Data are classified by standard deviation.

CHAPTER 3

INFLUENCE OF TOPOGRAPHIC ASPECT ON SOIL WATER RELATIONS AND TURFGRASS STRESS

[1]Joseph M. Krum, Robert N. Carrow, and Keith J. Karnok. To be submitted to *Crop Science*.

ABSTRACT

While plant water-use is affected by variable climatic factors such as solar radiation, wind, air temperature, and precipitation, inherent soil factors throughout landscapes are also influential. Several important soil factors are relatively stable, including soil particle size, infiltration rate, organic matter, topography, and compaction; these also reflect water-relations. The effects of topographic aspect on volumetric water content (VWC), estimated evapotranspiration (ET), and plant performance during dry-downs were assessed on selected microclimate sites at the Old Colliers Golf Club in Naples, FL during the summer of 2006; the study site consisted of 'Salam' seashore paspalum (*Paspalum vaginatum* Sw.). A mobile platform and hand-held instrumentation measured VWC at 10-, 12-, and 20-cm depths, along with mobile and hand-held normalized difference vegetative index (NDVI) determinations. The greatest water loss involved the north, west, and low slope aspects, while the east and south slope aspects exhibited the lowest water loss. Instrument comparisons of time-domain reflectometry (TDR) VWC data during the 12 to 16 July exhibited an r^2 of 0.85. We suggest that percent field capacity VWC measurements could be used as a baseline to determine available water depletion (AWD) trigger values for irrigation events in microclimates and could have an immediate impact on irrigation scheduling.

INTRODUCTION

Whether the focus is a golf course, athletic field, crop field, or pasture, spatial and temporal variability of soil moisture and other soil attributes are ever present realities and primary challenges for efficient management of inputs, especially irrigation water. Climatic, plant, and soil variability must be assessed, analyzed, and addressed in order to maximize plant health and yield with the efficient application of inputs. The National Academy of Sciences (1997, p. 21) emphasized the necessity of addressing spatial and temporal variability in their report on the potential for precision agriculture: "The potential for individually managing small areas, whose size is determined by local characteristics and crop value, is one of the most enticing aspects of precision agriculture. The ability to repeatedly locate a specific site and measure agronomic characteristics provides an opportunity to optimize management throughout the production area. Subdividing a field into small management units may improve both the economic and environmental sustainability of crop production systems." Similar to precision agriculture (PA), precision turfgrass management (PTM) or site-specific turfgrass management must develop the means to obtain information on a site-specific basis to make the best management decisions on inputs.

Krum (Chapter 2) demonstrated the application of spatial and temporal mapping of surface VWC (volumetric water content) and NDVI (normalized difference vegetation index) over a complex landscape site such as a golf course fairway. Mapping after a sufficient rainfall when the soil would be at field capacity allowed SSMUs (site-specific management units) to be identified based on similar VWC at field capacity. During progressive dry-downs, the surface 10-cm VWC declined, as did the NDVI within each SMMU. Relative to the key questions of site-specific irrigation (i.e., when to irrigate, where to irrigate, and how much irrigation water to

apply for each SSMU), a VWC value for each SSMU could be selected as a "trigger" value to initiate irrigation within the SSMU, which would deal with the issues of when and where to irrigate (Corwin and Lesch, 2005). However, the question of whether the difference between initial versus final VWC within the top 10 cm can be a reliable indicator of quantity of water to apply is not clear, since the entire root system is not monitored.

A SSMU can be thought of as a "microclimate" that would have specific irrigation requirements compared to other SSMUs that differ in soil, plant, or climatic characteristics. In the case of SSMUs as defined by Krum (Chapter 2), these were primarily based on using VWC data at field capacity to estimate soil type, while slope was incorporated as a secondary factor. There will be situations, however, where rapid mobile device mapping is not available to provide intensive spatial and temporal data over a large landscape that is necessary to define SSMUs. In these cases, hand-held VWC and NDVI units could potentially be used to obtain more limited soil and plant spatial data within selected microclimates to assist in irrigation decisions. The application of VWC and NDVI data for the assessment of selected microclimate conditions (via small area sampling) is discussed in this paper and companion papers by Krum (Chapters 4 and 5). Topography is the emphasis of this paper, while shade (Krum, Chapter 4) and traffic microclimate areas (Krum, Chapter 5) are the focal points of the remaining papers.

Van Pelt and Wierenga (2001) pointed out that spatial variability of soil water presents a significant challenge for irrigation scheduling because of the difficulty associated with obtaining measurements representative of agricultural field areas. Duffera et al. (2007) and Starr (2005) indicated that soil water content maps would be valuable to design efficient irrigation management plans. Furthermore, they noted that soil water content at field capacity has a relatively stable pattern of spatial variability that is highly correlated with other stable landscape

properties, such as particle size classes and topography. Thus, soil VWC determined within a few hours of rainfall or irrigation and under conditions where water infiltrates the soil, so that the soil is able to achieve field capacity, is primarily influenced by the stable parameters of soil texture, organic matter content, and soil structure. Under less ideal conditions for infiltration where runoff may occur, topography (elevation, slope, and aspect) may influence whether field capacity is achieved. However, the topographic characteristics would be stable properties.

Evapotranspiration (ET) is the loss of water from the soil and plants by evaporation and transpiration, respectively (Beard, 1973). The VWC reduction during a dry-down throughout the root zone of a crop can be used to estimate ET by the soil water balance method (Sharma, 1985). During dry-down periods following an irrigation or rain event, temporal variation of VWC (i.e., changes in VWC over time) is influenced by a mix of relatively stable landscape properties and variable temporal properties, such as the climatic parameters that drive ET (Lascano et al., 1999; Starr, 2007). McVicar et al. (2007) reported substantial spatial and temporal ET variability at the watershed scale, while Pauwels and Samson (2005) and Rana et al. (2007) found similar results at the field level.

Beard (1973) noted that turfgrass ET across the landscape is influenced by factors that drive ET demand (solar radiation and duration, temperature, humidity, and wind), water absorption rate, soil moisture potential, soil water content, and plant aspects such as cover and vigor. As solar radiation intensifies and temperatures rise, the leaf vapor pressure gradient exhibits a corresponding increase, thereby enhancing transpiration. Similarly, as humidity declines, the vapor pressure gradient increases. Topography not only influences initial VWC after irrigation or rain through infiltration and runoff, but it affects the absorption and reflection of incident solar radiation that may contribute to differential ET losses by topographic aspect.

Solar radiation is a major driving force for ET, especially when soil moisture is not limited. The spatial variability of ET in relation to topography has been assessed by data interpolation and modeling methods (Chen et al., 2004; McVicar et al., 2007; Rana et al., 2007). Numerous agro-meteorological variables, including temperature and humidity, are affected by solar radiation and other boundary conditions at the soil surface (Raupach et al., 1992). Modification of these variables occurs when discontinuities arise in regard to topographic characteristics such as elevation, slope, and aspect. Rana et al. (2007) concluded that topography significantly influences energy fluxes, including the latent heat flux (i.e., the energy equivalent of ET). By using topography as a correction factor, the accuracy of simulation models of energy fluxes in complex terrain was substantially increased. Chen et al. (2004) suggested that topography is an important variable that hydrologic models used for mapping ET should incorporate, since elevation, slope, and aspect significantly influence soil moisture.

Water relations affected by topography may subsequently influence crop performance. Kravchenko and Bullock (2000) investigated the affects of topography and soil properties on corn (*Zea mays* L.) and soybean [*Glycine max* (L.) Merr.] yields. Topographic features, including elevation, slope, curvature, and flow accumulation, accounted for approximately 20% of the total yield variability. Soil features were responsible for approximately 30% of the yield variability. Elevation and organic matter content were the most influential factors associated with topography and soil, respectively. Other topographic factors only affected yields in extreme circumstances, such as saturated depressions or eroded hilltops. Topography has also been documented to influence the distribution of protein contents in soybeans (Kravchenko and Bullock, 2002). Of all the factors associated with topography, aspect had the most significant impact on ET. Rockström et al. (1999) assessed the infiltration rates on up-slope, mid-slope and

down-slope areas of a pearl millet [Pennisetum glaucum (L.) Br.] field with a 1 to 3% slope. The highest infiltration occurred on the mid-sloping plots, while up-sloping plots exhibited the lowest percent infiltration.

Many complex landscape areas (e.g., golf courses) have an on-site weather station. However, climatic conditions within various microclimates may differ from those of the weather station. Climatic factors that influence turfgrass ET are those included in weather-based models to estimate plant ET.

The Penman-Monteith approach is widely regarded as the method of choice for estimating reference crop ET (ET_o) and was endorsed by the Food and Agricultural Organization (FAO) (Allen et al., 1998; McVicar et al., 2007). The ET_o formulation was derived from the Penman-Monteith equation by incorporating assumptions based on the definition of a reference surface. Allen et al.'s (1998, p. 23) FAO-56 report described the composition of the reference conditions as: "A hypothetical reference crop with an assumed height of 0.12 m, a fixed surface resistance of 70 s m^{-1}, and an albedo of 0.23. The reference surface closely resembles an extensive surface of green grass of uniform height, actively growing, completely shading the ground, and with adequate water. The requirements that the grass surface should be extensive and uniform result from the assumption that all fluxes are one-dimensional upwards." The FAO-56 formulation for ET_o (mm day^{-1}) is:

$$ET_o = \frac{0.408\Delta(R_n - G) + \gamma \frac{900}{T + 273} u_2 (e_s - e_a)}{\Delta + \gamma(1 + 0.34u_2)} \quad \text{Eq. [1]}$$

where Δ is the slope of the saturation vapor pressure curve (kPa $°C^{-1}$); R_n is the net radiation (MJ m^{-2} day^{-1}); G is the soil heat flux (MJ m^{-2} day^{-1}); γ is the psychrometric constant (kPa $°C^{-1}$); T is the mean daily air temperature at 2 m above the ground (°C); u_2 is the wind speed at 2 m

above the ground (m s^{-1}); e_s is the saturation vapor pressure (kPa); and e_a is the actual vapor pressure (kPa).

Measuring VWC changes in the surface 10-cm zone during a dry-down is a possible means of estimating actual crop or turfgrass ET (ET_c) spatially across the landscape. However, the VWC measurements would not encompass the complete root zone, as is normal for the soil balance method (Sharma, 1985). The potential for using estimated ET_c based on the surface VWC over time is founded on the observation that greater loss of soil moisture through ET initially occurs in the surface zone after irrigation because of higher organic matter content; thereby contributing to greater soil moisture retention, transpiration, and high root length densities in the surface zone. Once soil moisture becomes depleted to the point of reduced plant availability, water extraction becomes progressively greater from deeper zones. Young et al. (1997) reported that 68 and 64% of daily ET during the first and second days after irrigation, respectively, was attributable to the surface 20% of a 'Tifway' bermudagrass [(*Cynodon dactylon* (L.) Pers. x *Cynodon transvaalensis* (Burtt-Davy)] root zone, but declined to 30% by day five. Li et al. (2001) illustrated this concept when comparing root-water-uptake models. Various models estimated that approximately 60% of the maximum water uptake from agronomic plants originated from the top 20% of the root zone.

A potential application for the determination of spatial ET_c differences is incorporating the data into irrigation scheduling models using estimated ET_o from a weather station. Landscape areas with an on-site weather station can obtain an estimated daily ET_o, as calculated from weather data. Typical weather station locations are sites with full sunlight, flat topography, and good air movement. Site-specific or precision irrigation requires that water application be adjusted from the weather station ET_o to the microclimate conditions. The ET_o should be

adjusted for each microclimate site because grass, soil type, slope aspect, radiation, wind, and other environmental or management conditions will differ from the weather station site. Adjusting the ET_o is performed by multiplying it by a landscape coefficient (K_L), in order to obtain an estimated turf ET_c (where $ET_c = K_L \times ET_o$) (Irrigation Association, 2005). Unfortunately, the K_L differs with grass, season, weather front, and any other site condition that affects ET_c. Obtaining an accurate K_L to make the correction from ET_o to ET_c is a major obstacle preventing the adoption of this is approach because of the multitude of microclimates on golf courses and other complex sites.

While many irrigation systems may have a weather station interfaced with the irrigation control system, this feature typically is either ignored or inconsistently utilized for irrigation scheduling. If hand-held sensors could provide an estimate of ET_c within a microclimate by determination of VWC changes during a dry-down, then site-specific K_L values could be determined from the estimated microclimate ET_c and weather station ET_o to use in controller programming to determine optimal water requirements.

The purposes of this research were: a) using slope aspect as a "microclimate" type, to determine the degree of influence of slope aspect under golf course fairway conditions on surface VWC, estimated ET_c, and turfgrass stress during dry-downs after rain events; b) to explore the feasibility of using microclimate determinations of surface VWC and ET_c estimates for irrigation scheduling decisions involving when to irrigate, where to irrigate, or how much irrigation water to apply; and c) since both mobile and hand-held instruments were used to determine VWC and NDVI, this facilitated the comparison of methods as a secondary objective, with the assumption that hand-held devices would be used on situations where more intensive mobile mapping data are not available.

MATERIALS and METHODS

The study was conducted at the Old Collier Golf Club in Naples, Florida. The research area consisted of 'Salam' seashore paspalum (*Paspalum vaginatum* Sw.) mowed three times weekly at a height of 0.95 cm with a reel mower. Data collection was initiated following significant rain events, which negated any irrigation uniformity issues pertaining to surface VWC (Table A-1, Appendix). Five dry-downs took place during 14 to 16 June, 19 to 20 June, 21 to 23 June, 26 to 29 June, and 12 to 16 July, 2006. No irrigation was applied during dry-downs. Light rain events of 0.43, 0.11, and 0.02 cm occurred during the afternoons of 21 June, 28 June, and 13 July, respectively.

A completely randomized design of six treatments and four replications was used, with plots located on Fairways 10 and 13. The six treatments were high elevation (H; control), low elevation (L), east (E), west (W), north (N), and south (S) facing slopes. Plot dimensions were 3 by 6 m.

Basic data collection was performed via the Toro Mobile Multi-Sensor (TMM; patent pending) prototype data acquisition unit (The Toro Company, Bloomington, MN). The TMM measures VWC (%), NDVI (unit-less; best = 1.0), and compaction (penetrometer resistance; kg). The TMM was affixed to and maneuvered with a utility vehicle. An operating speed of 2.7 to 3.3 km h^{-1} was maintained during data acquisition. Study plots were dew-whipped prior to TMM use to reduce the potential influence of dew on NDVI. Plot length was such that two readings per plot were obtained when the TMM traversed the plots. Data were recorded using an on-board laptop computer and all parameters were displayed in spreadsheet format.

Soil moisture measurements were based on time-domain reflectometry (TDR), which measures changes in the soil dielectric constant (ε) as water contents fluctuate (Leib et al., 2003).

A TDR sensor produces a high frequency voltage pulse that is transmitted and reflected along metal probes. The dielectric constant is determined by measuring the velocity of the transmitted pulse in the soil, which is primarily dependent upon the VWC, as water has a significantly higher dielectric constant than air ($\varepsilon = 80$ and 1, respectively). The permittivity and corresponding pulse velocity are closely related to the soil water content (Plauborg et al., 2005).

The electrical conductivity (EC_a) of soil can greatly affect TDR measurements by promoting erroneous overestimates of water content (Nadler et al., 1999). Salinity is a major contributing factor to EC_a, suggesting that negligible salinity levels should be verified before taking TDR measurements. A hand-held Landmapper ERM-0l (Landviser, Inc. Westhampton, NJ) measured the electrical resistance (ER; ohm m^{-1}) in the study plots, which was subsequently converted to EC_a (Table A-2, Appendix). The EC_a was measured to verify the absence of significant salt concentrations in the soil prior to data acquisition. This device is based on determining apparent EC_a using the four-wenner array method as described by Rhoades et al. (1999).

A Field Scout TDR 100 soil moisture sensor (Spectrum Technologies, Inc. Plainfield, IL; TMM_{10}) was modified for use on the TMM platform and used to determine VWC at a 0- to 10-cm depth. Two custom stainless steel probes of 9.53-mm diameter, 3.3-cm spacing, and 10-cm length were installed on the moisture sensor to facilitate a soil penetration depth of 10 cm. The sampling volume is an elliptical cylinder extending 3 cm radially beyond the TDR probes, measuring approximately 825 cm^3. The sensor is attached to one end of a shaft on the TMM, while a bolt is connected to the opposite end. When the TMM moves, the wheel-driven shaft rotates in a circular fashion. As the sensor's probes enter the ground, the bolt passes by a series of magnets that triggers the data logger to take a measurement. The probes are inserted into the

soil approximately every 2.5 m. Two readings per plot were taken between the time period of 0700 to 0830 h EST. Additional readings were taken within a time period of 1700 to 2000 h EST on select days. Exceeding 3.5 km h^{-1} significantly increased the probability of obtaining erroneous VWC readings. Possible theories as to the cause of this problem are that the bolt was passing by the magnets too quickly or the TDR probes were being inserted too quickly to facilitate a VWC measurement.

A GreenSeeker RT100 active sensor (NTech Industries, Inc. Ukiah, CA; TMM_{NDVI}) evaluated turf canopy NDVI in the study plots. The NDVI, which measures multispectral reflectance, has been shown to be significantly associated with visual turf quality, density, and shoot tissue injury (Trenholm et al., 1999). The sensor is equipped with internal light emitting diodes and a photodiode optical detector that measures the percent reflectance of the red (R = 660 nm) and near-infrared (NIR = 770 nm) spectral bands {$NDVI = [(R_{770} - R_{660})/(R_{770} + R_{660})]$}. The sensor is mounted on the TMM at a height of approximately 1 m and evaluates a 60- ± 10-cm by 1.52- ± 0.51-cm field of view. The sensor emits light pulses every 100 ms and outputs an averaged value every second. Depending on operating speed, six to eight measurements per plot were recorded between the time period of 0700 to 0830 h EST. Additional readings were taken within a time period of 1700 to 2000 h EST on select days. Measurements are unaffected by solar radiation because of the sensor's internal light source.

An Omega LC302-500 1.90-cm diameter stainless steel compression load cell (Omega Engineering, Inc. Stamford, CT) was used to measure insertion force (kg) of the TDR moisture sensor probes. As the probes penetrate the soil, pressure is exerted against the load cell, indicating the degree of soil compaction. The load cell converts the load acting on it to electrical signals, which are used to calculate the penetrometer resistance. Penetrometer data are not

presented in this paper since the site was very high in sand content and exhibited few high penetrometer resistance measurements.

Additional data were obtained with various hand-held devices to facilitate comparison with the TMM device as well as to supplement the data obtained by the TMM. All hand-held data acquisition utilized the same sampling method as the TMM, as measurements were taken in the same general areas of the study plots to maximize the integrity of the research. A hand-held Spectrum Field Scout TDR 300 unit (HH_{12} and HH_{20}) measured VWC of the 0- to 12-cm and 0- to 20-cm depths. The sensor is equipped with two stainless steel probes of 5-mm diameter, 3.3-cm spacing, and 12- or 20-cm length. The sampling volumes are elliptical cylinders extending 3 cm radially beyond the TDR probes, measuring approximately 905 and 1510 cm^3 for the 12- and 20-cm probes, respectively. Measurements were taken at the 0- to 12-cm depth daily within a time period of 0700 to 0830 h EST. Additional data were acquired within a time period of 1700 to 2000 h EST on select days. Two readings per plot were taken during the first four dry-downs, while five readings per plot were recorded for the 12 July to 16 July dry-down. The VWC of the 0- to 20-cm soil depth was measured once daily at 1230 to 1330 h EST. Two readings per plot were taken at the 0- to 20-cm depth. The 10-, 12-, and 20-cm VWC measurements were used to estimate ET_c during various durations of the study: $ET_c = [(VWC_{inititial} - VWC_{final})/100] \times depth$.

A hand-held, Spectrum Field Scout TCM 500 (turf color meter, HH_{NDVI}) evaluated the turf canopy NDVI $[(R_{850} - R_{680})/(R_{850} + R_{680})]$ in the study plots. Similarly, the leaf area index (IR/R; best = highest value) was calculated (R_{850}/R_{680}). The TCM 500 measures a 7.6-cm diameter target (45.36-cm^2 area). The instrument contains an internal light source, thereby eliminating external effects of sunny or cloudy conditions. The TCM 500 is placed directly on

the ground to make a measurement. Two readings per plot were taken once daily within a time period of 1230 to 1330 h EST.

An Everest Interscience 100.3ZL hand-held infrared thermometer measured the canopy temperature (°C) of the plots (Everest Interscience, Inc. Tucson, AZ). The thermometer measures the infrared radiation (approximately 700 to 1000 nm) that is emitted from the turfgrass by using an optical infrared detector. The detector converts the radiation to a proportional signal. The temperature is the electrical analog of the infrared radiation. Two readings per plot, one north facing and one south facing, were taken once daily within a time period of 1230 to 1330 h EST, under sunny conditions. The instrument was held at a height of approximately 1 m at a 45° angle.

Data were analyzed using the Statistical Analysis System (SAS Institute, Inc. Cary, NC; version 9.1) and statistical differences were determined by the Generalized Linear Model (GLM) procedure in conjunction with Duncan's Multiple Range Test at a 0.10 significance level.

RESULTS and DISCUSSION

Site Conditions

There was substantial soil disruption on the study site that was attributed to golf course construction activities when the course was built. However, the general soil texture is a sand to loamy sand. Slope, soil texture, and organic matter content data are presented in Table A-3 (Appendix). Slope aspect plot locations were selected in early June prior to the availability of spatial soil VWC maps encompassing whole fairways (Chapter 2) and at a time when soil salinity was still evident (Table A-2, Appendix). Salinity concentrations in the upper soil profile (i.e., the 0- to 10-cm depth) greatly diminished by 14 June in response to significant rain events. Treatment results for VWC were reported by incorporating all dry-downs and by focusing on the

12 to 16 July dry-down separately. The 12 to 16 July dry-down experienced the longest duration without irrigation, while only receiving minimal rainfall (0.03 cm on 13 July). Furthermore, the dry-down VWC was least likely to be affected by salinity due to the numerous rain events and dry-downs that occurred prior to 12 July.

Ideally, VWC at field capacity (measurements taken within 3 to 4 hours of a rain or irrigation event) should not differ across slope aspect treatments. Using the TMM, initial VWC data as a measure of field capacity on 14, 19, and 21 June did not reveal any statistical differences between treatments (Table 3.1). However, the 26 June and 12 July measurements indicated treatment differences in VWC at field capacity, with the lowest VWC occurring on the L (26 June), and W and H slope aspect treatments (12 July). Salinity data obtained on 16 June indicated that salinity should not have affected the TDR readings, but there may have been some influence on 19 and 21 June if capillary rise occurred from below the 10-cm depth. The rainfall occurring prior to the 26 June and 12 July periods would suggest that by these dates salinity concentrations in the zone of analysis (i.e., the 0 to 20-cm depth) would not be significant. While it is doubtful that salinity was a contributing factor to TDR data variability for the 12 to 16 July dry-down, treatment differences in VWC at field capacity (i.e., initial dry-down measurements) suggested that comparisons of raw VWC data between treatments would be confounded. This, however, should not influence comparisons of treatments for water extracted from this zone during dry-downs or comparisons on a percent of field capacity basis.

Instrument Comparisons for VWC and NDVI

Krum (Chapter 2) illustrated the usefulness of intensive VWC and NDVI mapping of large and complex landscapes. With intensive mapping of VWC displayed in GIS interpolated maps, areas of similar VWC could be identified as SSMUs. In contrast, the emphasis in this

study was to investigate use of less intensive determination of VWC and plant performance data within microclimates, such as may be accomplished by hand-held devices, to guide in irrigation decisions. Different slope aspects were used as examples of microclimates in a complex landscape as represented by a golf course fairway. However, with hand-held devices the mapping would normally be on a more limited basis within an expected microclimate, where microclimate locations are based on experience and observation of the site.

Comparison of the TMM_{10} and HH_{12} VWC throughout the 10- and 12-cm sampling depths, respectively, across all dates exhibited a correlation of $r^2 = 0.67$ when using the replication averages (treatment averages); or $r^2 = 0.53$ based on data from each plot replication (Tables 3.1 and 3.2; Figures 3.1 and 3.2). The linear equations were:

$VWC_{HH} = 0.800VWC_{TMM} + 6.172$; based on treatment replication averages.

$VWC_{HH} = 0.665VWC_{TMM} + 9.107$; based on data from each replication.

Linear correlations within specific dry-down periods based on treatment averages and replications, respectively, were: for the 14 to 16 June dry-down, correlations of $r^2 = 0.06$ and 0.14; 19 to 20 July dry-down, $r^2 = 0.65$ and 0.44; 21 to 23 June dry-down, $r^2 = 0.73$ and 0.52; 26 to 29 June dry-down, $r^2 = 0.82$ and 0.70; and the 12 to 16 July dry-down resulted in correlations of $r^2 = 0.85$ and 0.71 (Figures 3.3 and 3.4). The linear relationships for the 12 to 16 July period were:

$VWC_{HH} = 0.848VWC_{TMM} + 6.780$; based on treatment replication averages.

$VWC_{HH} = 0.769\,VWC_{TMM} + 8.111$; based on data from each replication.

Since the correlations were lower earlier in the study period, this would suggest that salinity may have affected the two devices differently, despite that the mobile TDR device was a modification of the TDR device used for hand-held determinations. Initial VWC as a measure of

field capacity on 14 June was 30.0 and 32.1%, respectively for the TMM_{10} and HH_{12}, while on 12 July values were 24.6 and 27.2%, respectively (Tables 3.1 and 3.2). On a percent basis, this measure of surface zone field capacity declined by 18.0 (TMM_{10}) and 15.0% (HH_{12}) from 14 June to 12 July, which are relatively similar changes in terms of magnitude. Five HH_{12} measurements per plot were obtained during the 12 to 16 July period, whereas two HH_{12} measurements were taken for all other dates. This may have contributed to better correlations during the last dry-down.

When comparing the HH_{12} and HH_{20} VWC data across all treatments and using data from each replication for 12 to 16 July, $r^2 = 0.62$ for the quadratic regression relationship: $VWC_{HH12} = -0.037VWC_{HH20}^2 + 2.283VWC_{HH20} - 4.923$ (Tables 3.2 and 3.3; Figure 3.5). The quadratic (as opposed to linear) relationship appeared to result from the influence of high VWC values. Using the quadratic and linear regression equations based on data from each replication, and if $VWC_{HH12} = 20\%$, the predicted $VWC_{HH20} = 14.4\%$ and $VWC_{TMM} = 15.9\%$. Since the site was sandy and organic matter in the surface 5 to 7 cm contributed significantly to soil moisture retention, average VWC for surface measurements (i.e., the 10- and 12-cm depths) after a rainfall would be expected to be higher, while the longer TDR VWC probes would average lower moisture retention from the deeper zone.

The relationship between the TMM_{10} and HH_{12} VWC data during the 12 to 16 July period was likely not influenced by salinity, which may account for the higher correlations relative to the other dates. Therefore, the 12 to 16 July instrument correlations should be more representative of the true instrument relationship, as opposed to the evaluations during the remaining measurement periods. Since VWC measurements were point determinations encompassing a small soil volume, were not taken in the exact same area of each plot, and

assessed different soil depths, the degree of correlation between methods would appear to be reasonable. Dukes et al. (2007) reported an r^2 of 0.76 for the same type of TDR unit using the 20-cm probes versus 10-cm gravimetric moisture readings.

Comparison of the TMM_{NDVI} and HH_{NDVI} across all dates resulted in low correlations of $r^2 = 0.16$ and $r^2 = 0.10$ for treatment averages and across all replications, respectively (Tables 3.4 and 3.5; Figures 3.6 and 3.7). Within each dry-down period, correlations based on treatment averages and across all replications, respectively, were: 14 to 16 June dry-down resulted in correlations of $r^2 = 0.04$ and $r^2 = 0.06$; 26 to 29 June dry-down resulted in correlations of $r^2 = 0.18$ and $r^2 = 0.23$; 12 to 16 July dry-down resulted in correlations of $r^2 = 0.14$ and $r^2 = 0.43$ (Figures 3.8 and 3.9). The Spectrum hand-held NDVI device is placed directly on the turfgrass canopy, has a field of view of 45.4 cm^2, and used 680 and 850 nm for NDVI determinations. Conversely, the GreenSeeker NDVI unit on the TMM platform does not contact the canopy to cause any physical impact that may influence canopy reflective properties, has a field of view of approximately 91 cm^2, and uses the 660- and 770-nm wavelengths for NDVI. Moreover, the NDVI output data consisted of continuous sensing as the TMM traversed the plots, leading to a much larger sample area. The low NDVI correlation could be partially attributable to the unit differences, but a better correlation would be expected than what we observed. The GreenSeeker demonstrated sufficient resolution in relation to soil drying conditions when it was used for spatial mapping in Krum, Chapter 2.

The Spectrum NDVI unit allowed for calculation of the IR/R stress index, which is a leaf area index (LAI) that has been show to correlate with turfgrass quality (Table 3.6) (Trenholm et al., 1999). Since the same wavelengths are used for both the Spectrum NDVI and IR/R stress

indices, they are essentially the same across treatments but expressed in a different manner (i.e. $r^2 = 0.99$).

Slope Aspect Effects

As each dry-down progressed, VWC declined, as would be expected (Tables 3.1, 3.2, and 3.3). One approach used to characterize slope aspect affects on VWC is to determine the percentage of readings in the lowest VWC statistical group (i.e., the "b" or "c" notation based on Duncan's Multiple Range Test when treatment differences occurred). This group would represent the lowest VWC values, reflecting greater ET loss and slope aspect influences on ET. The lowest statistical VWC groups for the three means of determining VWC based on all dates were:

- 38(N), 0(S), 0(E), 46(W), 54(L), and 23%(H); TMM_{10} (Table 2).
- 37(N), 4(S), 4(E), 15(W), 89(L), and 22%(H); HH_{12} (Table 3).
- 79(N), 14(S), 7(E), 43(W), 93(L), and 29%(H); HH_{20} (Table 4).

Based on using the lowest VWC as a means of assessing slope influence on ET loss across all time periods where statistical treatment differences occurred, the greatest drying appeared to be on the L, N, and W slope aspects; the least occurred on the E and S slope aspects.

Comparisons during the 12 to 16 dry-down encompassing a longer duration and not influenced by any rain or salinity, revealed the following based on the lowest VWC statistical group:

- 43(N), 0(S), 0(E), 57(W), 57(L), and 43%(H); TMM_{10} (Table 3.1).
- 20(N), 0(S), 0(E), 0(W), 100(L), and 10%(H); HH_{12} (Table 3.2).
- 100(N), 40(S), 0(E), 60(W), 60(L), and 60%(H); HH_{20} (Table 3.3).

During the 12 to 16 July dry-down, the greatest degree of drying occurred on the N, W, L, and H slope aspect, while S and E facing slopes exhibited the least amount of water loss.

Since there were statistical differences between slope aspect treatments between the first day VWC values for the 26 to 29 June and 12 to 16 July period, a better comparison for ET losses (as opposed to raw VWC) should be percent of field capacity (initial VWC = 100%) at the end of dry-downs (Table 3.7). Using these criteria to compare the slope aspect influence across the various TDR devices and all dry-downs, the percent of times that the slope aspect treatments were in the lowest statistical category (greatest water loss) for the 12 dates with significant treatment differences were: 33(N), 0(S), 0(E), 58(W), 75(L), 25(H). During the last dry-down (using the TMM_{10}), the W and L slope aspects exhibited 30.6 and 30.2% field capacity, respectively, while the E slope aspect was at 50.8% field capacity.

Slope aspect comparisons in terms of VWC differences, whether expressed as raw VWC or percent of field capacity, demonstrated that the S and E exposures were consistently associated with the least water loss, while the N, W and L slope aspects exhibited greatest water loss; the H slope aspect exhibited intermediate water loss (Tables 3.1, 3.2, 3.3, and 3.7). High water loss by the W exposure would be expected. The L slope aspect, while lower in elevation compared to the H treatment, was in a full sun location and could be expected to have reasonably high ET, but why this treatment differed from the H slope aspect could not be determined based on the site condition information available, since these areas were similar except for elevation (Table A-3, Appendix). The consistently lower water-use from the S slope aspect, while the N slope aspect was highest, is opposite of what would be expected, but consistent over the duration of the study. These results indicate that microclimates differing in water status could be consistently identified based on raw VWC data. To investigate microclimate differences in

water loss over a dry-down, VWC and the corresponding field capacity data can be used.

In the previous discussion, soil water status was compared using raw VWC data and percent of field capacity at the end of a dry-down. A third means of comparing slope aspect treatments for water status could be by estimation of ET_c. Two different methods were used to calculate estimated ET_c. One method involved using the beginning and ending VWC values, which ignores daily changes (gross ET), while the other was to sum each day's morning (a.m.) to evening (p.m.) water-use (net ET) (Tables 3.8 to 3.10).

The TDR data obtained on an a.m. and p.m. basis over the 12 to 16 July period using the TMM_{10} and HH_{12} revealed recharge of the surface zone soil moisture from the p.m. measurements to the following a.m. measurements by either capillary rise or movement of water within the roots from deeper in the profile (Tables 3.1 and 3.2). This complicates the use of surface zone VWC measurements to estimate ET_c, compared to the normal soil water balance method, which accounts for VWC changes in the entire root zone (Sharma, 1985).

Estimated ET_c across all dates and by both means of reporting ET_c resulted in percent readings in the top statistical (highest ET_c values, which represent highest water extraction) group for slope aspect treatments of:

- 50(N), 0(S), 25(E), 13(W), 50(L), and 13%(H); TMM_{10} (Table 3.8).
- 18(N), 29(S), 12(E), 41(W), 24(L), and 24%(H); HH_{12} (Table 3.9).
- 20(N), 30(S), 30(E), 40(W), 10(L), and 30%(H); HH_{20} (Table 3.10).

For the 12 to 16 July dry-down, there were significant slope aspect responses when using estimated ET_c summed for daily a.m. and p.m. readings of the TMM_{10} and HH_{12} (Tables 3.8 and 3.9). Daily summation of a.m. and p.m. ET_c for the TMM_{10} resulted in the highest estimated ET_c observed for the L slope aspect (2.78 cm) and least for the W exposure (0.99 cm) (Table 3.8). In

terms of the HH_{12}, S (3.09 cm) slopes exhibited the highest ET_c and E (2.02 cm) slopes were associated with the lowest ET_c (Table 3.9).

For the 12 to 16 July dry-down, estimated ET_c calculated by both means of reporting ET_c resulted in percent readings in the top statistical group for slope aspect treatments of:

- 25(N), 0(S), 25(E), 0(W), 75(L), and 25%(H); TMM_{10} (Table 9).
- 17(N), 67(S), 0(E), 17(W), 0(L), and 17%(H); HH_{12} (Table 10).
- 33(N), 33(S), 0(E), 67(W), 0(L), and 33%(H); HH_{20} (Table 11).

The HH_{20} provides a measurement of a greater portion of the root zone compared to the 10 or 12-cm probes. However, from the various negative values for ET_c, capillary rise of water into the zone of VWC measurement must have been occurring, which would confound use of the soil water balance method (Table 3.10). When comparing the three devices, the results for estimated ET_c of the various slope aspect treatments based across all dates and within the 12 to 16 July period did not elicit a consistent treatment response. Thus, attempting to assess microclimate differences in soil water status by presenting data in estimated ET_c format does not appear to be useful.

The canopy temperature data across all dates resulted in 25(N), 50(S), 8(E), 8(W), 8(L), and 42%(H) for the highest statistical group (highest values) (Table 3.11). The canopy temperature tended to increase as a dry-down progressed. Correlations of the VWC and canopy temperature determined by the HH_{20} during the 12 to 16 July period revealed an r^2 of only 0.02. Since canopy temperatures were only obtained from 1230 to 1330 h EST, this could confound any real slope aspect effect based on VWC information obtained early or late in the day.

Slope aspect treatment effects on turfgrass performance were assessed by the NDVI stress indice using the TMM GreenSeeker. This unit was considered to be more accurate than

the Spectrum device, as discussed in the section on comparison of the units. Trenholm et al. (1999) demonstrated that NDVI is strongly related to turfgrass quality. GreenSeeker NDVI decreased as a dry-down progressed as indicated by the 12 to 16 July response of NDVI versus VWC across all treatments (Table 3.5; Figure 3.9). The NDVI data analysis from the TMM unit across all dates determined that the highest statistical group (i.e. highest NDVI, which is the best in terms of turf performance) was composed of 0(N), 50(S), 33(E), 17(W), 0(L), and 0%(H) (Table 3.5). Meanwhile, the lowest statistical group involved 0(N), 33(S), 50(E), 0(W), 17(L), and 17%(H). Over the course of the 12 to 16 July dry-down, no slope aspect treatment differences were observed in terms of the raw NDVI readings. On the first two days of the dry-down, the greatest a.m. to p.m. change in NDVI occurred on the S exposure and the least on the E exposure for 12 and 13 July.

Across all treatments and replications during the 12 to 16 July period, TMM_{10} and TMM_{NDVI} data exhibited a linear correlation of $r^2 = 0.30$ (Figure 3.10). When VWC versus NDVI correlations were made for this period by slope aspect, the strength of the relationship varied with slope aspect. The linear r^2 values by slope aspect were: 0.55(L), 0.52(N), 0.50(H), 0.42(W), 0.31(E), and 0.18(S). These results would suggest that as a dry-down occurred, the L, N, H, and W slope aspects would exhibit the greatest reduction as VWC decreased, while the E and S slope aspects would be less affected. This may be a reflection of the L, N, H, and W slope aspects exhibiting the highest degree of drying, as reported in the VWC section, which would indicate an apparent stronger relationship. If the dry-down was extended, it is anticipated that a stronger relationship between NDVI and VWC would have become evident for the E and S slope aspects (Tables 3.1, 3.2, and 3.3).

Relative to the identification of slope aspect effects on soil water relations and turfgrass performance, surface VWC measurements were able to identify slope aspects differences (microclimates) by using raw VWC values or expressed as a percent of field capacity. The highest amount of water loss involved the N, W, and L slope aspects, while the H treatment rated at an intermediate level, and the E and S slope aspects exhibited the lowest water loss. Turfgrass performance as determined by the TMM_{NDVI} for each slope aspect reflected greater NDVI declines on those slope aspects with the greatest water loss. Using estimated ET_c to determine slope aspect differences did not yield consistent results, primarily because of water recharge into the zone of measurement from day to day.

Applications

With intensive spatial mapping after a rainfall, the initial VWC was useful for mapping SSMUs with similar field capacity (i.e., similar VWC values) and observation of VWC changes during dry-downs provided information regarding areas of relatively high and low VWC (Krum, Chapter 2). In a similar manner, for a microclimate area, VWC data could be used to determine field capacity differences and whether the degree of water loss during dry-downs would differ from one microclimate to another. While field capacity is a relatively stable soil parameter, water loss during drying is not since it is affected by a combination of relatively stable landscape properties and variable temporal climatic properties that directly influence ET (Lascano et al., 1999; McVicar et al., 2007; Starr, 2007). Both types of information would be useful for irrigation scheduling. For example, irrigation scheduling based on soil moisture monitoring is often based on allowing soil drying to a certain percent of field capacity (a temporally stable factor), such as 50% soil moisture depletion (ET being temporally variable) (Irrigation

Association, 2005). A question arises as to how to best use the changes in water status of the surface 10- to 12-cm zone during dry-downs for irrigation scheduling purposes.

An essential baseline for interpreting microclimate soil moisture is to estimate field capacity, so the first issue is how to best determine this factor. Starr (2005) discussed the importance of determining the nature of spatial and temporal soil water content variability of the surface soil zone in order to use the information for site-specific irrigation. In our study, VWC data were obtained at the beginning of dry-downs to provide an estimate of field capacity as a baseline for assessing changes over time, where knowledge of field capacity as a temporally stable factor is a critical component of determining plant available water and irrigation scheduling using soil moisture data (Irrigation Association, 2005; Starr, 2005). This procedure would minimize the spatial and temporal VWC variability within the surface zone, which can be greater in field crop situations where VWC is mapped without regard to rain or irrigation events (Western et al., 1998; Starr, 2005; Gabrielle et al., 2006).

Earlier in the study period, it appeared that residual salinity affected VWC measurements, resulting in higher field capacity estimates than evident in the last two dry-downs. These earlier VWC readings indicated that field capacity was consistent across all slope aspect treatments. However, data from the last two dry-downs revealed that field capacities of the slope aspect treatments did differ once the confounding factor of salinity was removed (Tables 2 and 3). Knowledge of slope aspect field capacity differences would be useful from the standpoint of viewing each slope aspect as a microclimate situation; but when attempting to determine slope aspect influence on surface water relations, it presents a problem if raw VWC data are used for treatment comparisons. Another potential slope aspect influence on estimated field capacity VWC values is the effect of topography on infiltration and runoff. For example,

Tomer and Anderson (1995) reported that 51 to 77% of spatial variability in soil water content could be explained by topography. The sandy nature of the soil and nature of the rainfall prior to our dry-downs negated this influence in our study.

These results suggest that when obtaining VWC data to estimate field capacity of microclimates, attention should be given to: obtaining measurements when the soil should be at field capacity due to a recent rain or irrigation event, avoiding the influence of salinity on TDR determinations, and ensuring runoff does not prevent adequate recharge of the surface area. With attention to these factors, surface VWC measurements within slope aspect microclimates provided a reliable field capacity estimate. Once a reliable field capacity baseline is obtained, it should be a relatively stable characteristic based on stable soil (texture, organic matter content, structure) and topographic (aspect, slope) factors (Starr, 2005; Brocca et al., 2007; Duffera et al., 2007). The field capacity baseline can be used to estimate the degree of dry-down within the microclimate if VWC measurements are conducted during dry-downs.

While field capacity is relatively stable, VWC changes during dry-downs can be highly variable. The most straight forward means to use surface VWC data for irrigation scheduling would be to determine a surface VWC value that would trigger an irrigation event in the microclimate. This would be a version of the allowable water depletion (AWD, which is also referred to as the management allowable depletion or MAD) method, where AWD is the percent of available soil water allowed to be depleted before irrigation is applied (SCS, 1993; Smajstrla et al., 2002). The AWD would be selected by the turfgrass manager based on what would be suitable for the site to avoid undue stress on the turfgrass, and may change with season. A 50% AWD is often used as a baseline, but this assumes depletion over the whole root zone. In the case of surface measurements, the surface AWD may be greater than 50%. For example, the

AWD was 30% of field capacity on the W and L slope aspects for the surface 10 cm on 16 July, while the AWD was 50% on the E slope treatment (Table 3.7). Thus, if a 30% AWD was the trigger value for irrigation, only the W and L microclimates would be irrigated. The issues of "when to irrigate" and "where to irrigate" could be determined by this approach.

As a guide for the quantity of irrigation to apply, spatial assessment of estimated ET_c from the VWC data would be valuable, as is done in the soil water balance method (Sharma, 1985). As noted in the results, slope aspect treatments were not consistent across the various instruments or means of estimating ET_c. Linear correlations of estimated ET_c for the 12 to 16 July period based on the initial minus final VWC for each treatment with the different methods were: TMM_{10} versus HH_{12} ($r^2 = 0.68$); TMM_{10} versus HH_{20} ($r^2 = 0.19$); and HH_{12} versus HH_{20} ($r^2 = 0.63$). Over this 5-day period, estimated ET_c averaged across all treatments were 1.51, 1.57, 0.95, and 2.25 cm for the TMM_{10}, HH_{12}, HH_{20}, and weather station ET_o (FAO-56), respectively. The low estimated ET_c from the HH_{20} measurements may be attributable to capillary rise from below the 20-cm zone, as indicated by several negative values (i.e., net gains of water) for certain days and treatments (Table 3.10). Even at the surface 10- to 12-cm zone, comparison of VWC data from the p.m. of one day to the a.m. reading of the next day demonstrated recharge of water either by capillary rise or by movement in roots. Thus, attempting to spatially estimate ET_c via surface zone VWC data for the purpose of determining the quantity of water to apply for irrigation appears to be a difficult issue. However, by using the raw VWC data to determine when to irrigate at a selected trigger AWD value, selected soil VWC measurements over the whole root zone at that time should provide a better estimate of the irrigation required to recharge the soil moisture status to field capacity. Such measurements could be taken by hand-held units or carefully placed in-situ sensors within microclimates.

Chen et al. (2005) and Pauwels and Samson (2006) discuss the importance of spatial and temporal mapping of ET for hydrological modeling purposes. The raw VWC information on turfgrass sites with a close mowed canopy, involving the ability to access a site and rapidly map surface VWC conditions over time and space, may provide a good case study for modeling purposes.

REFERENCES

Allen, R.G., L.S. Pereira, D. Raes, and M. Smith. 1998. Crop evapotranspiration. FAO Irrigation and Drainage Paper 56. FAO, Rome, Italy.

Beard, J.B. 1973. Turfgrass: Science and culture. Prentice-Hall, Englewood Cliffs, NJ.

Brocca, L., R. Morbidelli, F. Melone, and T. Moramarco. 2006. Soil moisture spatial variability in experimental areas of central Italy. J. Hydrol. 333:356-373.

Chen, J.M., X. Chen, W. Ju, and X. Geng. 2004. Distributed hydrological model for mapping evapotranspiration using remote sensing inputs. J. Hydrol. 305:15-39.

Clarke, F.R., R.J. Baker, and R.M. DePauw. 2000. Plot direction and spacing effects on interplot interference in spring wheat cultivar trials. Crop Sci. 40:655-658.

Corwin, D.L., and S.M. Lesch. 2005. Apparent soil electrical conductivity measurements in agriculture. Comp. Electron. Agric. 46:11-43.

Duffera, M., J.G. White, and R. Weisz. 2007. Spatial variability of Southeastern U.S Coastal Plain soil physical properties: Implications for site-specific management. Geordema 137:327-339.

Dukes, M.D., M.B. Haley, and S.A. Hanks. 2006. Sprinkler irrigation and soil moisture uniformity. Proc. Int. Irrig. Show, 27th, San Antonio, TX. 5-7 Nov. 2006. [CD-ROM]. Irrig. Assoc., Falls Church, VA.

Gabriëlle, J.M. De Lannoy, N.E.C. Verhoest, P.R. Houser, T.J. Gish, and M. Van Meirvenne. 2006. Spatial and temporal characteristics of soil moisture in an intensively monitored agricultural field (OPE^3). J. Hydrol. 331:719-730.

Irrigation Association. 2005. Landscape irrigation scheduling and water management. Available at http://www.irrigation.org/gov/pdf/liswm_part2of3.pdf (cited 15 Jan 2008; verified 20 Mar. 2008). Irrig. Assoc., Falls Church, Va.

Kravchenko, A.N., and D.G. Bullock. 2000. Correlation of corn and soybean grain yield with topography and soil properties. Agron. J. 92:75-83.

Kravchenko, A.N., and D.G. Bullock. 2002. Spatial variability of soybean quality data as a function of field topography. Crop Sci. 42:804-815.

Lascano, R.J., R.L. Baumhardt, S.K. Hicks, and J.A. Landivar. 1999. Spatial and temporal distribution of surface water content in a large agricultural field. p. 19-30. *In* P.C. Robert et al. (ed.) Precision agriculture: A challenge for crop nutrition management. Proc. Int. Conf. Precision Agric., 4th, Minneapolis, MN. 17-20 July 1998. ASA-CSSA-SSSA, Madison, WI.

Leib, B.G., J.D. Jabro, and G.R. Matthews. 2003. Field evaluation and performance comparison of soil moisture sensors. Soil Sci. 168:396-409.

Li, K.Y., R. De Jong, and J.B. Boisvert. 2001. An exponential root-water-uptake model with water stress compensation. J. Hydrol. 252:189-204.

McVicar, T.R., T.G. Van Niel, L. Li, M.F. Hutchinson, X. Mu, and Z. Liu. 2007. Spatially distributing monthly reference evapotranspiration and pan evaporation considering topographic influences. J. Hydrol. 338:196-220.

Nadler, A., A. Gamliel, and I. Peretz. 1999. Practical aspects of salinity effect on TDR-measured water content: A field study. Soil Sci. Soc. Am. J. 63:1070-1076.

National Academy of Sciences. 1997. Precision agriculture in the 21st century: Geospatial and information technologies in crop management. Natl. Acad. Press, Washington, D.C.

Pauwels, V.R.N., and R. Samson. 2006. Comparison of different methods to measure and model actual evapotranspiration rates for a wet sloping grassland. Agric. Water Manage. 82:1-24.

Plauborg, F., B.V. Iverson, and P.E. Laerke. 2005. In situ comparison of three dielectric soil moisture sensors in drip irrigated sandy soils. Vadose Zone J. 4:1037-1047.

Rana, G., R.M. Ferrara, N. Martinelli, P. Personnic, and P. Cellier. 2007. Estimating energy fluxes from sloping crops using standard agrometeorological measurements and topography. Agric. For. Meteorol. 146:116-133.

Raupach, M.R., W.S. Weng, D.J. Carruthers, and J.C.R. Hunt. 1992. Temperature and humidity fields and fluxes over low hills. Q. J. R. Meteorol. Soc. 188:191-225.

Rhoades, J.D, F. Chanduvi, and S. Lesch. 1999. Soil salinity assessment: Methods and interpretation of electrical conductivity measurements. FAO Irrigation and Drainage Paper 57. Food and Agric. Organ. of the United Nations, Rome.

Rockström, J., J. Barron, J. Brouwer, S. Galle, and A. de Rouw. 1999. On-farm spatial and temporal variability of soil and water in pearl millet cultivation. Soil Sci. Soc. Amer. J. 63:1308-1319.

SAS Institute. 2003. The SAS system for Windows. Release 9.1. SAS Inst., Cary, NC.

SCS. 1993. Chapter 2. Irrigation water requirements. *In* SCS technical staff. Part 623 Natl. Engineering Handb. USDA Soil Conser. Serv. Washington, DC.

Sharma, M.L. 1985. Estimating evapotranspiration. p. 213-282. *In* D. Hillel (ed.). Advances in irrigation. Vol. 3. Academic Press, New York, NY.

Smajstrla, A.G., B.J. Boman, D.Z. Haman, F.T. Izuno, D.J. Pitts, and F.S. Zazueta. 2002. Basic irrigation scheduling in Florida. Ext. Bulletin 249. Instit. of Food and Agric. Sci., Univ. of Florida, Gainsville, FL.

Starr, G.C. 2005. Assessing temporal stability and spatial variability of soil water patterns with implications for precision water management. Agric. Water Manage. 72:223-243.

Tomer, M.D., and J.L. Anderson. 1995. Variation of soil water storage across a sand hill slope. Soil Sci. Soc. Am. J. 59:1091-1100.

Trenholm, L.E., R.N. Carrow, and R.R. Duncan. 1999. Relationship of multispectral radiometry data to qualitative data in turfgrass research. Crop Sci. 39:763-769.

Van Pelt, R.S. and P.J. Wierenga. 2001. Temporal stability of spatially measured soil matric potential probability density function. Soil Sci. Soc. Am. J. 65:668-677.

Western, A.W., G. Blöschl, and R.B. Grayson. 1998. Geostatistical characterization of soil moisture patterns in the Tarrawarra catchment. J. Hydro. 205:20-37.

Young, M.H., P.J. Wierenga, and C.F. Mancino. 1997. Monitoring near-surface soil water storage in turfgrass using time domain reflectometry and weighing lysimetry. Soil Sci. Soc. Am. J. 61:1138-1146.

Table 3.1. Influence of topography on 10-cm volumetric water content (VWC) during dry-down periods (mobile unit).

Date	Topography						F-test	CV
	North	South	East	West	Low	High		
14 - 16 June	%							%
14 June	28.8	30.5	27.3	32.3	32.3	28.9	0.97	32
15 June	24.8	27.9	24.8	23.4	25.8	25.0	0.99	37
16 June	19.5b	30.3a	24.8ab	22.4ab	21.4ab	26.8ab	0.43	32
19 - 20 June	%							%
19 June	27.9	30.5	29.0	28.4	24.8	25.4	0.63	19
20 June	25.6abc	28.0ab	29.9a	25.3abc	20.8c	22.0bc	0.15	20
21 - 23 June†	%							%
21 June	28.3	28.9	26.9	26.5	24.8	27.1	0.90	19
22 June	24.0	27.6	27.6	24.1	22.9	24.8	0.68	20
23 June am	20.5	23.8	25.8	22.6	19.6	22.0	0.51	21
23 June pm	17.8	20.0	21.4	18.0	16.5	18.0	0.67	24
26 - 29 June‡	%							%
26 June	29.4ab	28.9ab	35.8a	27.9ab	24.5b	27.6ab	0.37	24
27 June	23.9	27.3	28.3	23.1	22.0	26.3	0.67	25
28 June am	20.0ab	24.8ab	27.6a	20.5ab	18.6b	20.1ab	0.25	26
28 June pm	21.5ab	26.5ab	28.5a	18.4b	20.3ab	24.1ab	0.34	30
29 June am	19.0	25.3	26.8	19.1	19.9	21.4	0.29	26
29 June pm	13.3b	21.6a	21.9a	13.1b	12.6b	17.6ab	0.01	24
12 - 16 July§	%							%
12 July am	23.8ab	26.6ab	28.5a	23.1b	23.5ab	22.1b	0.23	16
12 July pm	17.9b	24.1a	24.9a	20.5ab	16.4b	18.8b	0.05	20
13 July am	18.0	21.3	22.9	17.5	18.5	19.6	0.57	24
13 July pm	17.1ab	22.1a	21.6a	18.3ab	15.5b	17.9ab	0.29	24
14 July am	16.6ab	19.9ab	23.1a	14.4b	17.9ab	18.6ab	0.38	30
14 July pm	12.3b	16.1ab	19.3a	12.9ab	12.0b	13.9ab	0.28	33
15 July am	16.6	21.8	21.9	14.8	16.8	18.3	0.47	33
15 July pm	11.0	14.0	13.0	11.6	10.5	10.9	0.73	31
16 July am	11.3ab	15.0ab	17.6a	10.5b	12.5ab	12.5ab	0.38	37
16 July pm	9.3b	10.1ab	15.5a	7.1b	7.0b	8.1b	0.17	50

† A 0.43-cm rainfall occurred during the afternoon of 21 June following data aquisition.

‡ A 0.11-cm rainfall occurred during the afternoon of 28 June prior to pm data acquisition.

§ A 0.08-cm rainfall occurred during the afternoon of 13 July prior to pm data acquisition.

Table 3.2. Influence of topography on 12-cm volumetric water content (VWC) during dry-down periods (hand-held unit).

Date	Topography						F-test	CV
	North	South	East	West	Low	High		
14 - 16 June	%							%
14 June am	31.1ab	37.5ab	27.1b	39.5a	27.5b	29.6ab	0.21	26
14 June pm	29.5	33.1	27.1	34.6	26.1	28.3	0.48	24
15 June	37.5a	32.6ab	31.5ab	34.0ab	27.4b	30.3b	0.20	17
16 June	26.5	29.0	27.6	28.6	25.6	24.4	0.71	17
19 - 20 June	%							%
19 June am	27.4ab	29.9a	32.9a	30.3a	22.0b	27.1ab	0.11	18
19 June pm	22.1ab	27.6a	25.6a	22.8ab	19.8b	23.0ab	0.16	18
20 June am	23.5	27.8	28.5	27.1	23.4	22.8	0.49	21
20 June pm	20.3b	27.4a	23.1ab	20.8ab	16.4b	21.3ab	0.14	24
21 - 23 June†	%							%
21 June am	27.9bc	35.0a	31.0ab	27.4bc	24.3c	27.3bc	0.09	17
21 June pm	30.8	35.6	33.9	31.4	29.4	32.0	0.64	17
22 June am	24.9ab	28.6a	25.5ab	24.6ab	23.3b	23.6ab	0.42	15
22 June pm	23.4	25.0	22.5	23.8	20.1	20.4	0.41	17
23 June am	19.8b	19.6b	24.3a	19.5b	20.4ab	17.5b	0.18	17
23 June pm	17.1bc	24.4a	21.6ab	20.5abc	15.4c	18.3bc	0.06	21
26 - 29 June‡	%							%
26 June am	25.8b	34.0ab	34.5a	28.9ab	26.3ab	30.6ab	0.25	21
26 June pm	21.4c	29.0ab	30.9a	22.8bc	24.0bc	21.4c	0.07	21
27 June am	23.0bc	28.4ab	29.4a	24.1abc	21.3c	24.0abc	0.10	17
27 June pm	15.6b	22.9ab	29.9a	18.8b	15.9b	18.1b	0.04	32
28 June am	19.4ab	21.6ab	24.4a	19.6ab	17.6b	19.3ab	0.45	23
28 June pm	15.9b	22.3ab	25.4a	17.0b	15.5b	17.1b	0.11	29
29 June am	18.3b	26.6a	26.0a	18.3b	19.0b	21.3ab	0.08	23
29 June pm	13.4b	20.3a	20.5a	14.5ab	11.9b	15.3ab	0.13	32
12 - 16 July§	%							%
12 July am	24.4bc	30.9a	29.8ab	29.1abc	23.9c	25.3bc	0.11	16
12 July pm	22.4ab	25.5a	25.5a	22.9ab	19.8b	22.7ab	0.40	18
13 July am	21.1bc	28.1a	26.8ab	23.8abc	19.9c	24.2abc	0.19	20
13 July pm	20.6ab	25.1a	25.9a	23.4ab	19.6b	21.7ab	0.22	18
14 July am	22.3ab	26.9a	26.1ab	24.3ab	20.8b	23.2ab	0.31	17
14 July pm	16.8b	21.8ab	23.1a	20.0ab	16.8b	18.4ab	0.23	22
15 July am	19.7bc	25.8a	24.9ab	22.2abc	18.9c	21.3abc	0.22	20
15 July pm	14.4bc	19.0ab	20.3a	16.3abc	12.8c	15.5abc	0.17	26
16 July am	16.7ab	21.0ab	21.9a	18.6ab	15.2b	18.6ab	0.28	23
16 July pm	11.8b	16.0ab	18.3a	13.4ab	10.4b	12.4b	0.14	31

† A 0.43-cm rainfall occurred during the afternoon of 21 June prior to pm data aquisition.

‡ A 0.11-cm rainfall occurred during the afternoon of 28 June prior to pm data acquisition.

§ A 0.08-cm rainfall occurred during the afternoon of 13 July prior to pm data acquisition.

Table 3.3. Influence of topography on 20-cm volumetric water content (VWC) during dry-down periods (hand-held unit).

Date	Topography						F-test	CV
	North	South	East	West	Low	High		
14 - 16 June	%							%
14 June	30.5ab	28.9ab	27.1b	37.5a	26.5b	33.0ab	0.24	22
15 June	26.5	29.1	23.3	30.8	24.8	28.8	0.79	30
16 June	21.6ab	22.3ab	19.8ab	26.0a	16.8b	18.3ab	0.33	28
19 - 20 June	%							%
19 June	22.3b	25.0ab	29.6a	25.1ab	21.5b	23.5ab	0.26	20
20 June	19.6b	23.0ab	26.6a	19.0b	19.6b	23.6ab	0.11	19
21 - 23 June†	%							%
21 June	24.3ab	28.4a	26.5ab	25.3ab	19.6b	25.0ab	0.35	22
22 June	24.5	27.0	27.0	25.1	22.1	23.0	0.38	15
23 June	18.9b	26.1a	20.1ab	19.1b	16.5b	19.4ab	0.23	26
26 - 29 June‡	%							%
26 June	20.4b	27.5ab	31.1a	23.4b	21.1b	23.6b	0.11	23
27 June	19.1	23.6	25.9	20.9	17.4	21.8	0.46	29
28 June	15.4b	23.3a	23.0a	19.3ab	15.3b	20.4ab	0.11	25
29 June	11.6b	17.5ab	20.5a	14.1ab	12.3b	17.3ab	0.14	32
12 - 16 July§	%							%
12 July	18.1b	21.5ab	26.3a	21.1ab	18.3b	19.6ab	0.31	25
13 July	14.9b	18.3b	24.8a	16.6b	15.8b	16.9b	0.05	24
14 July	14.5b	18.6ab	23.6a	17.8b	17.1b	16.1b	0.15	25
15 July	11.9c	16.5bc	23.9a	19.3ab	15.6bc	14.0bc	0.02	27
16 July	13.8b	16.9b	21.9a	15.3b	13.8b	15.3b	0.07	24

† A 0.43-cm rainfall occurred during the afternoon of 21 June following data aquisition.

‡ A 0.11-cm rainfall occurred during the afternoon of 28 June following data acquisition.

§ A 0.08-cm rainfall occurred during the afternoon of 13 July following data acquisition.

Table 3.4. Influence of topography on the normalized difference vegetative index (NDVI) during dry-down periods (hand-held unit).

	Topography							
Date	North	South	East	West	Low	High	F-test	CV
14 - 16 June								%
14 June	0.716	0.724	0.706	0.724	0.729	0.711	0.43	2
15 June	0.733	0.726	0.727	0.741	0.729	0.725	0.82	2
16 June	0.706	0.691	0.707	0.705	0.682	0.708	0.66	4
14 - 16 June†	0.010	0.033	-0.002	0.019	0.047	0.003	0.43	202
19 - 20 June								%
19 June	0.756ab	0.755ab	0.773a	0.774a	0.778a	0.744b	0.21	3
20 June	0.711	0.714	0.734	0.734	0.732	0.705	0.48	4
19 - 20 June†	0.046	0.041	0.039	0.040	0.046	0.038	1.00	62
21 - 23 June‡								%
21 June	0.726	0.723	0.727	0.745	0.731	0.716	0.66	3
22 June	0.734abc	0.714c	0.741ab	0.755a	0.752a	0.721bc	0.06	3
23 June	0.715	0.693	0.734	0.741	0.718	0.703	0.59	6
21 - 23 June†	0.011	0.030	-0.007	0.004	0.013	0.013	0.79	325
26 - 29 June§								%
26 June	0.743ab	0.724ab	0.748a	0.746a	0.755a	0.714b	0.15	3
27 June	0.759a	0.747ab	0.754ab	0.766a	0.750ab	0.729b	0.18	3
28 June	0.747ab	0.717b	0.742ab	0.753a	0.738ab	0.722ab	0.27	3
29 June	0.745a	0.714ab	0.731a	0.734a	0.730a	0.686b	0.09	4
26 - 29 June†	-0.002a	0.010ab	0.017ab	0.013ab	0.025ab	0.029b	0.37	137
12 - 16 July¶								%
12 July	0.788	0.763	0.767	0.778	0.778	0.768	0.44	2
13 July	0.778	0.777	0.763	0.777	0.779	0.766	0.82	3
14 July	0.781a	0.750c	0.759abc	0.776ab	0.766abc	0.754bc	0.17	2
15 July	0.782	0.780	0.765	0.774	0.772	0.769	0.42	2
16 July	0.773	0.762	0.766	0.784	0.765	0.759	0.65	3
12 - 16 July†	0.016	0.002	0.002	-0.006	0.012	0.009	0.55	310

† NDVI change.

‡ A 0.43-cm rainfall occurred during the afternoon of 21 June following data acquisition.

§ A 0.11-cm rainfall occurred during the afternoon of 28 June following data acquisition.

¶ A 0.08-cm rainfall occurred during the afternoon of 13 July following data acquisition.

Table 3.5. Influence of topography on the normalized difference vegetative index (NDVI) during dry-down periods (mobile unit).

Date	Topography						F-test	CV
	North	South	East	West	Low	High		
14 - 16 June								%
14 June	0.844ab	0.861a	0.833b	0.842ab	0.847ab	0.843ab	0.46	2
15 June	0.802abc	0.824a	0.777c	0.793bc	0.804abc	0.809ab	0.13	3
16 June	0.795ab	0.810a	0.769b	0.788ab	0.792ab	0.796ab	0.21	3
14 - 16 June†	0.049	0.050	0.064	0.054	0.055	0.048	0.43	23
19 - 24 June‡								%
19 June	0.838	0.847	0.829	0.837	0.838	0.830	0.56	2
24 June	0.824ab	0.817ab	0.822ab	0.828a	0.807b	0.809b	0.26	2
26 - 29 June§								%
26 June	0.857	0.853	0.861	0.862	0.858	0.845	0.54	2
27 June	0.819	0.819	0.813	0.820	0.815	0.810	0.93	2
28 June am	0.827	0.819	0.818	0.825	0.819	0.811	0.79	2
28 June pm	0.830	0.821	0.823	0.832	0.820	0.816	0.77	2
29 June am	0.834	0.826	0.830	0.835	0.826	0.823	0.74	2
29 June pm	0.782	0.769	0.788	0.778	0.775	0.766	0.80	3
26 - 29 June†	0.075	0.084	0.072	0.084	0.084	0.079	0.87	21
12 - 16 July¶								%
12 July am	0.872	0.870	0.860	0.876	0.861	0.864	0.59	2
12 July pm	0.829	0.815	0.824	0.831	0.818	0.814	0.49	2
13 July am	0.851	0.845	0.840	0.852	0.842	0.838	0.74	2
13 July pm	0.841	0.829	0.833	0.840	0.831	0.826	0.71	2
14 July am	0.860	0.851	0.853	0.862	0.851	0.846	0.59	2
14 July pm	0.831	0.820	0.823	0.831	0.819	0.817	0.68	2
15 July am	0.857	0.851	0.850	0.859	0.845	0.845	0.58	2
15 July pm	0.820	0.818	0.819	0.822	0.807	0.811	0.83	2
16 July am	0.844	0.836	0.839	0.841	0.830	0.832	0.77	2
16 July pm	0.808	0.814	0.817	0.818	0.799	0.810	0.89	3
12am - 12pm†	0.043ab	0.055c	0.035a	0.044ab	0.043ab	0.050bc	0.06	18
13am - 13pm†	0.009ab	0.016b	0.007a	0.012ab	0.011ab	0.012ab	0.41	54
14am - 14pm†	0.029	0.031	0.030	0.031	0.032	0.029	0.95	18
15am - 15pm†	0.037	0.033	0.031	0.037	0.038	0.033	0.80	23
16am - 16pm†	0.036	0.021	0.022	0.023	0.031	0.022	0.75	64
12am - 16pm†	0.064	0.056	0.043	0.058	0.063	0.054	0.72	36

† NDVI change.

‡ The mobile NDVI data were not recorded during the 21 to 23 June dry-down. Rainfalls totaling 1.66 cm occurred from 20 to 23 June.

§ A 0.11-cm rainfall occurred during the afternoon of 28 June prior to pm data acquisition.

¶ A 0.08-cm rainfall occurred during the afternoon of 13 July prior to pm data acquisition.

Table 3.6. Influence of topography on the ratio of infrared and red light (IR/R) during dry-down periods (hand-held unit).

	Topography							
Date	North	South	East	West	Low	High	F-test	CV
14 - 16 June								%
14 June	6.11	6.28	5.88	6.26	6.39	5.92	0.48	7
15 June	6.50	6.37	6.39	6.72	6.39	6.37	0.88	7
16 June	5.86	5.54	5.85	5.83	5.44	5.89	0.79	10
14 - 16 June†	0.26	0.75	0.03	0.43	0.95	0.04	0.52	199
19 - 20 June								%
19 June	7.26ab	7.26ab	7.88ab	7.92a	8.06a	6.89b	0.22	10
20 June	5.95	6.19	6.61	6.57	6.52	5.84	0.49	11
19 - 20 June†	1.30	1.07	1.27	1.35	1.54	1.05	0.94	60
21 - 23 June‡								%
21 June	6.42	6.27	6.41	6.89	6.46	6.17	0.65	9
22 June	6.59ab	6.05b	6.82ab	7.22a	7.11a	6.19b	0.06	9
23 June	6.20	5.57	6.63	6.75	6.45	5.77	0.43	15
21 - 23 June†	0.21	0.70	-0.22	0.13	0.01	0.41	0.64	373
26 - 29 June§								%
26 June	6.91abc	6.29bc	7.04ab	6.89abc	7.20a	6.11c	0.17	10
27 June	7.34a	6.92ab	7.26ab	7.59a	7.04ab	6.50b	0.19	8
28 June	7.02ab	6.08b	6.88ab	7.14a	6.72ab	6.23ab	0.23	10
29 June	6.93a	6.03ab	6.62a	6.57a	6.50ab	5.41b	0.11	12
26 - 29 June†	-0.02	0.26	0.43	0.33	0.70	0.70	0.45	140
12 - 16 July¶								%
12 July	8.47a	7.55b	7.72ab	8.05ab	8.00ab	7.64ab	0.39	8
13 July	8.00	7.98	7.64	7.97	8.07	7.66	0.90	9
14 July	8.16a	7.05c	7.40abc	7.95ab	7.60abc	7.13bc	0.12	8
15 July	8.23a	8.11ab	7.56b	7.87ab	7.80ab	7.66ab	0.38	6
16 July	7.94	7.43	7.64	8.31	7.63	7.34	0.51	10
12 - 16 July†	0.53	0.11	0.09	-0.26	0.37	0.29	0.57	325

† IR/R change.

‡ A 0.43-cm rainfall occurred during the afternoon of 21 June following data acquisition.

§ A 0.11-cm rainfall occurred during the afternoon of 28 June following data acquisition.

¶ A 0.08-cm rainfall occurred during the afternoon of 13 July following data acquisition.

Table 3.7. Percent of field capacity on the last day of dry-downs for the mobile (TMM) 10-cm, and hand-held (HH) 12- and 20-cm soil moisture probes.

Date	Topography						F-test	CV
	North	South	East	West	Low	High		
TMM 10 cm	%							%
16 June	70.7bc	105.4a	92.1ab	69.0c	65.5c	93.9a	0.02	21
20 June	93.4ab	91.7ab	104.0a	90.9ab	83.8b	85.6b	0.36	14
23 June	62.6b	69.8ab	79.2a	68.2ab	66.9b	65.3b	0.21	13
29 June	45.4d	76.3a	61.4bc	47.8d	51.6cd	63.7b	<0.01	14
16 July	38.9ab	38.3ab	50.8a	30.6b	30.2b	37.3ab	0.34	36
HH 12 cm	%							%
16 June	85.8	79.1	102.4	80.3	98.3	81.7	0.49	24
20 June	73.2b	91.5a	70.9b	67.6b	74.8b	78.1ab	0.15	16
23 June	62.2b	69.7ab	69.4ab	75.5a	63.3b	66.8ab	0.36	13
29 June	50.9ab	59.5a	58.1a	48.2ab	43.7b	50.7ab	0.23	19
16 July	48.0ab	52.1ab	59.9a	45.3b	43.5b	48.1ab	0.29	21
HH 20 cm	%							%
16 June	70.6ab	79.8a	72.7a	67.7ab	63.4ab	54.7b	0.99	22
20 June	89.2a	92.4a	91.0a	75.8b	91.5a	100.9a	0.19	13
23 June	78.2	93.1	75.6	75.1	86.6	77.2	0.70	23
29 June	57.6b	63.6ab	64.2ab	59.8b	57.7b	71.6a	0.07	11
16 July	77.2	78.5	84.1	77.7	76.2	77.4	0.16	19

Table 3.8. Influence of topography on 10-cm estimated evapotranspiration (ET) during dry-down periods (mobile unit).

Date	Topography						F-test	CV
	North	South	East	West	Low	High		
14 - 16 June	cm							%
14 - 15 June	0.40	0.26	0.25	0.89	0.65	0.39	0.57	119
15 - 16 June	0.53	-0.24	0.00	0.10	0.44	-0.18	0.57	653
14 - 16 June (N)†	0.93a	0.03b	0.25b	0.99a	1.09a	0.21b	0.04	93
19 - 20 June	cm							%
19 - 20 June (N)	0.23	0.25	-0.09	0.31	0.4	0.34	0.55	158
21 - 23 June‡	cm							%
21 - 22 June	0.43	0.13	-0.08	0.24	0.19	0.24	0.56	192
22 - 23 June	0.28	0.38	0.44	0.47	0.32	0.41	0.96	86
21 - 23 June (N)	1.05a	0.89ab	0.55b	0.85ab	0.83ab	0.91ab	0.28	33
26 - 29 June§	cm							%
26 - 27 June	0.56ab	0.17cd	0.76a	0.48abc	0.25bcd	0.14d	0.01	64
28am - 28pm	-0.15	-0.18	-0.09	0.22	-0.17	-0.41	0.69	-397
29am - 29pm	0.58	0.37	0.50	0.61	0.74	0.38	0.79	78
26 - 29 June (N)	1.60a	0.73c	1.39ab	1.48ab	1.19abc	1.00bc	0.06	33
12 - 16 July¶	cm							%
12am - 12pm	0.59ab	0.25c	0.36bc	0.26c	0.71a	0.34bc	0.04	53
13am - 13pm	0.09	-0.09	0.13	-0.08	0.30	0.18	0.52	366
14am - 14pm	0.44a	0.38ab	0.39ab	0.15b	0.59a	0.48a	0.13	51
15am - 15pm	0.56ab	0.78ab	0.89a	0.31b	0.63ab	0.74ab	0.31	54
16am - 16pm	0.20	0.49	0.21	0.34	0.55	0.44	0.51	83
∑12 - 16 July (G)	1.88b	1.80b	1.98ab	0.99c	2.78a	2.16ab	0.03	33
12am - 16pm (N)	1.45	1.65	1.30	1.60	1.65	1.40	0.69	25

† (G) and (N) indicate estimated gross and net ET at dry-down termination, respectively.

‡ A 0.43-cm rainfall occurred during the afternoon of 21 June following data aquisition.

§ A 0.11-cm rainfall occurred during the afternoon of 28 June prior to pm data acquisition.

¶ A 0.08-cm rainfall occurred during the afternoon of 13 July prior to pm data acquisition.

Table 3.9. Influence of topography on 12-cm estimated evapotranspiration (ET) during dry-down periods (hand-held unit).

Date	Topography						F-test	CV
	North	South	East	West	Low	High		
14 - 16 June	cm							%
14am - 14pm	0.20	0.53	0.00	0.59	0.17	0.17	0.88	290
14 - 15 June	-0.78c	0.59ab	-0.53bc	0.67a	0.02abc	-0.08abc	0.18	-4970
15 - 16 June	1.34a	0.44ab	0.47ab	0.66ab	0.21b	0.72ab	0.31	106
14 - 16 June (N)†	0.56ab	1.04ab	-0.06b	1.33a	0.23ab	0.64ab	0.40	156
19 - 20 June	cm							%
19am - 19pm	0.64	0.27	0.88	0.92	0.27	0.50	0.25	81
20am - 20pm	0.40abc	0.05c	0.66ab	0.78a	0.85a	0.18bc	0.07	85
∑19 - 20 June (G)	1.04abc	0.32c	1.54a	1.69a	1.13ab	0.69bc	0.04	56
19am - 20pm (N)	0.87ab	0.31b	1.19a	1.16a	0.69ab	0.72ab	0.08	52
21 - 23 June‡	cm							%
21am - 21pm	-0.35	-0.08	-0.35	-0.49	-0.63	-0.58	0.62	-115
22am - 22pm	0.18	0.44	0.37	0.11	0.38	0.40	0.88	146
23am - 23pm	0.32ab	-0.58c	0.32ab	-0.12bc	0.61a	-0.09bc	0.01	553
∑21 - 23 June (G)	0.15	-0.21	0.34	-0.50	0.37	-0.27	0.48	-3216
21am - 23pm (N)	1.31	1.30	1.14	0.84	1.08	1.10	0.48	32
26 - 29 June§	cm							%
26am - 26pm	0.53b	0.61ab	0.44b	0.75ab	0.27b	1.13a	0.13	67
27am - 27pm	0.90a	0.67a	-0.06b	0.66a	0.66a	0.72a	0.19	87
28am - 28pm	0.43	-0.08	-0.12	0.32	0.26	0.26	0.61	293
29am - 29pm	0.59ab	0.78ab	0.67ab	0.46b	0.87a	0.73ab	0.40	41
∑26 - 29 June (G)	2.04ab	1.16bc	0.73c	1.86abc	1.53abc	2.38a	0.16	55
26am - 29pm (N)	1.51	1.68	1.71	1.75	1.75	1.88	0.85	22
12 - 16 July¶	cm							%
12am - 12pm	0.25b	0.66a	0.52ab	0.77a	0.50ab	0.31b	0.08	51
13am -13pm	0.05b	0.37a	0.11ab	0.04b	0.03b	0.31ab	0.12	137
14am - 14pm	0.68a	0.62ab	0.37b	0.53ab	0.49ab	0.58ab	0.44	39
15am - 15pm	0.65ab	0.83a	0.57b	0.73ab	0.74ab	0.70ab	0.50	26
16am - 16pm	0.60ab	0.61ab	0.45b	0.64ab	0.59ab	0.76a	0.54	36
∑12 - 16 July (G)	2.23b	3.09a	2.02b	2.71ab	2.36ab	2.66ab	0.20	24
12am - 16pm (N)	1.54	1.82	1.41	1.92	1.65	1.57	0.48	24

† (G) and (N) indicate estimated gross and net ET at dry-down termination, respectively.
‡ A 0.43-cm rainfall occurred during the afternoon of 21 June prior to pm data aquisition.
§ A 0.11-cm rainfall occurred during the afternoon of 28 June prior to pm data acquisition.
¶ A 0.08-cm rainfall occurred during the afternoon of 13 July prior to pm data acquisition.

Table 3.10. Influence of topography on 20-cm estimated evapotranspiration (ET) during dry-down periods (hand-held unit).

Date	Topography						F-test	CV
	North	South	East	West	Low	High		
14 - 16 June	cm							%
14 - 15 June	0.81	-0.05	0.79	1.37	0.36	0.86	0.56	157
15 - 16 June	0.99ab	1.40ab	0.71b	0.97ab	1.63ab	2.13a	0.37	75
14 - 16 June	1.80b	1.35b	1.50b	2.34ab	1.98ab	3.00a	0.09	40
19 - 20 June	cm							%
19 - 20 June	0.53b	0.41b	0.61ab	1.24a	0.38b	-0.03b	0.08	102
21 - 23 June†	cm							%
21 - 22 June	-0.05	0.28	-0.10	0.03	-0.51	0.41	0.75	10363
22 - 23 June	1.14ab	0.18b	1.40a	1.22ab	1.14ab	0.74ab	0.34	83
21 - 23 June	1.09	0.46	1.30	1.24	0.64	1.14	0.65	87
26 - 29 June‡	cm							%
26 - 27 June	0.25b	0.79ab	1.07a	0.51ab	0.76ab	0.38b	0.27	81
27 - 28 June	0.76	0.08	0.58	0.33	0.43	0.28	0.67	147
28 - 29 June	0.76ab	1.17a	0.51b	1.04ab	0.61ab	0.64ab	0.34	60
26 - 29 June	1.78a	2.03a	2.16a	1.88a	1.80a	1.30b	0.08	21
12 - 16 July§	cm							%
12 - 13 July	0.66ab	0.66ab	0.30b	0.91a	0.51ab	0.56ab	0.44	67
13 - 14 July	0.08	-0.08	0.23	-0.23	-0.28	0.15	0.57	-2208
14 - 15 July	0.53a	0.43a	-0.05ab	-0.30b	0.30ab	0.43a	0.19	226
15 - 16 July	-0.38c	-0.08bc	0.41ab	0.81a	0.38ab	-0.25bc	0.03	339
12 - 16 July	0.89	0.94	0.89	1.19	0.91	0.89	0.99	83

† A 0.43-cm rainfall occurred during the afternoon of 21 June following data aquisition.
‡ A 0.11-cm rainfall occurred during the afternoon of 28 June following data acquisition.
§ A 0.08-cm rainfall occurred during the afternoon of 13 July following data acquisition.

Table 3.11. Influence of topography on canopy temperature during dry-down periods.

Date	Topography						F-test	CV
	North	South	East	West	Low	High		
14 - 16 June	°C							%
14 June	30.0	30.4	30.5	29.1	29.3	29.4	0.34	4
15 June	31.9ab	31.2abc	30.9bc	30.0c	30.4c	32.4a	0.02	3
16 June	31.8a	30.1b	29.9b	27.5c	27.8c	31.6a	<0.01	3
19 - 20 June	°C							%
19 June	31.6ab	38.3a	27.3b	31.4ab	30.6ab	35.2ab	0.40	23
20 June	37.0ab	39.9a	36.5b	37.7ab	37.4ab	39.5ab	0.27	6
21 - 23 June†	°C							%
21 June	37.0ab	41.0a	34.7b	37.5ab	38.2ab	40.1a	0.12	8
22 June	39.4ab	41.6a	37.2b	38.9ab	37.5b	40.3ab	0.12	6
23 June	37.2ab	41.0a	35.7b	37.2ab	37.3ab	39.6ab	0.18	8
26 - 29 June‡	°C							%
26 June	35.8a	33.5ab	35.7a	34.8a	35.2a	32.1b	0.06	5
27 June	27.0b	28.4ab	29.5ab	27.2b	27.1b	29.9a	0.21	7
28 June	32.8	33.8	33.0	33.0	33.2	33.3	0.77	3
29 June	32.3	33.4	31.6	32.2	31.7	33.2	0.53	5
12 - 16 July§	°C							%
12 July	29.7	32.9	28.7	29.6	31.5	31.9	0.44	10
13 July	24.7ab	27.4ab	24.0b	25.3ab	24.7ab	28.0a	0.25	10
14 July	30.9	31.6	31.4	30.4	31.4	31.2	0.62	3
15 July	34.2a	31.4ab	29.9b	30.8ab	32.8ab	31.1ab	0.44	10
16 July	32.0ab	34.5a	30.2ab	30.0b	31.6ab	33.2ab	0.34	10

† A 0.43-cm rainfall occurred during the afternoon of 21 June following data aquisition.

‡ A 0.11-cm rainfall occurred during the afternoon of 28 June following data acquisition.

§ A 0.08-cm rainfall occurred during the afternoon of 13 July following data acquisition.

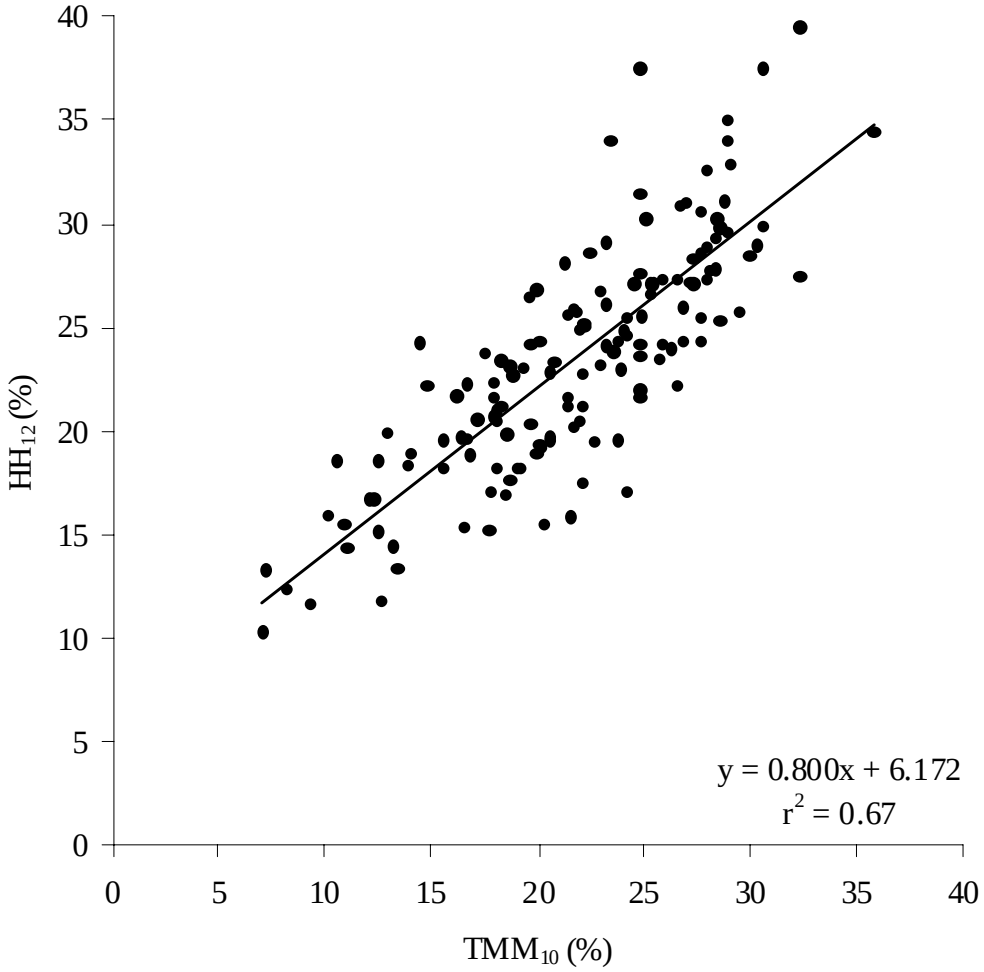

Figure 3.1. Linear relationship between TMM_{10} (mobile) and HH_{12} (hand-held) volumetric water content (VWC) consisting of all topography treatments and dry-downs.

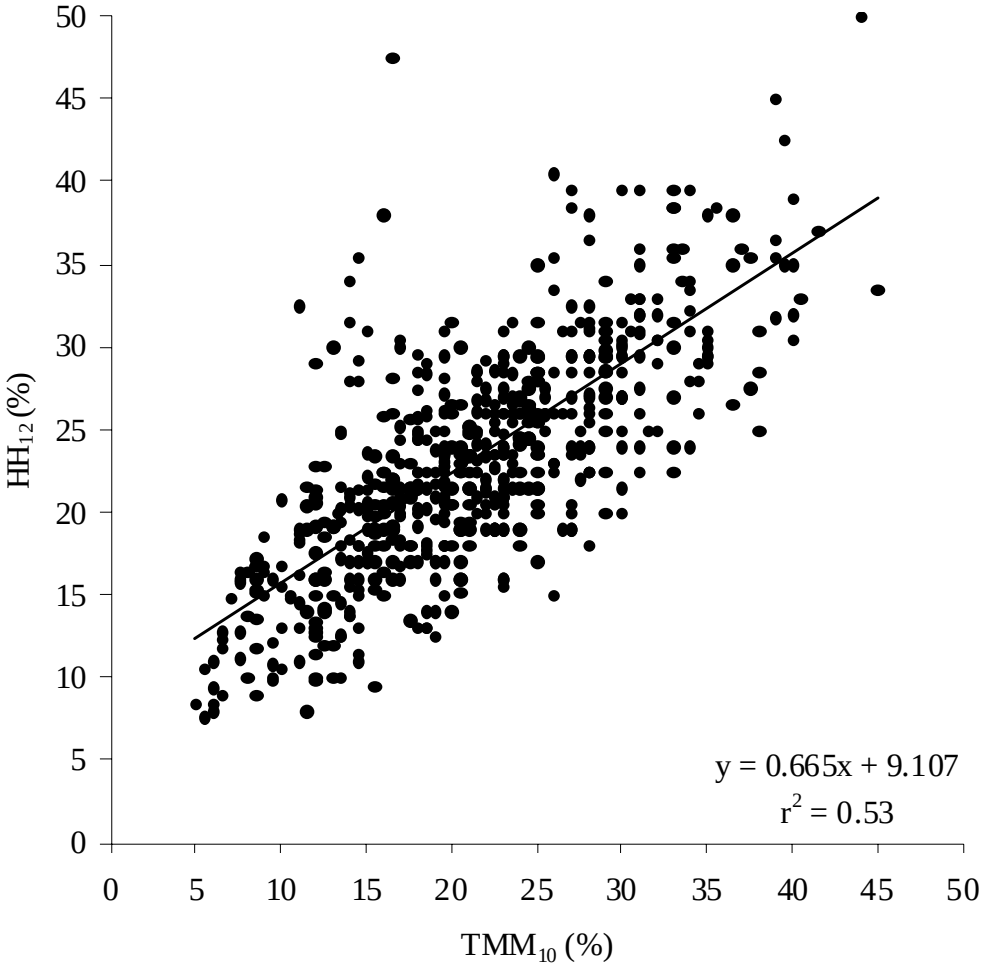

Figure 3.2. Linear relationship between TMM_{10} (mobile) and HH_{12} (hand-held) volumetric water content (VWC) consisting of all topography treatments, replications, and dry-downs.

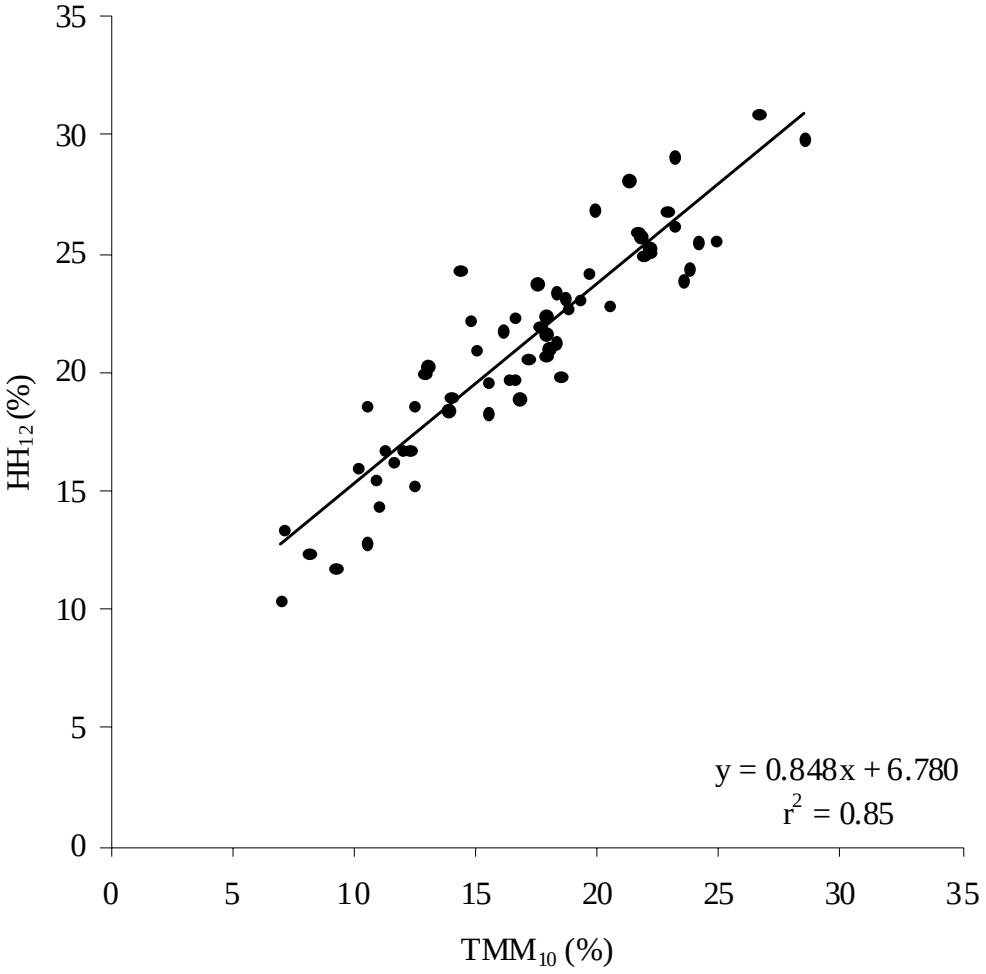

Figure 3.3. Linear relationship between TMM_{10} (mobile) and HH_{12} (hand-held) volumetric water content (VWC) consisting of all topography treatments during the 12 to 16 July dry-down.

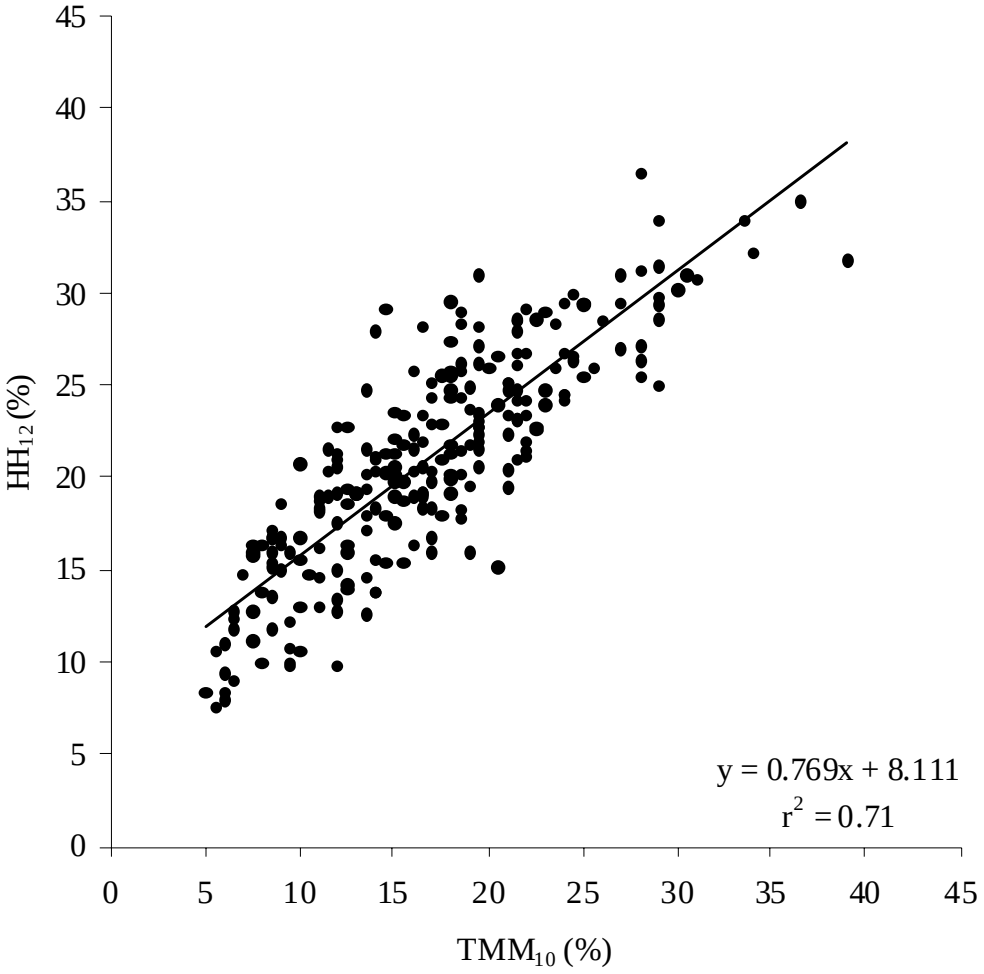

Figure 3.4. Linear relationship between TMM_{10} (mobile) and HH_{12} (hand-held) volumetric water content (VWC) consisting of all topography treatments and replications during the 12 to 16 July dry-down.

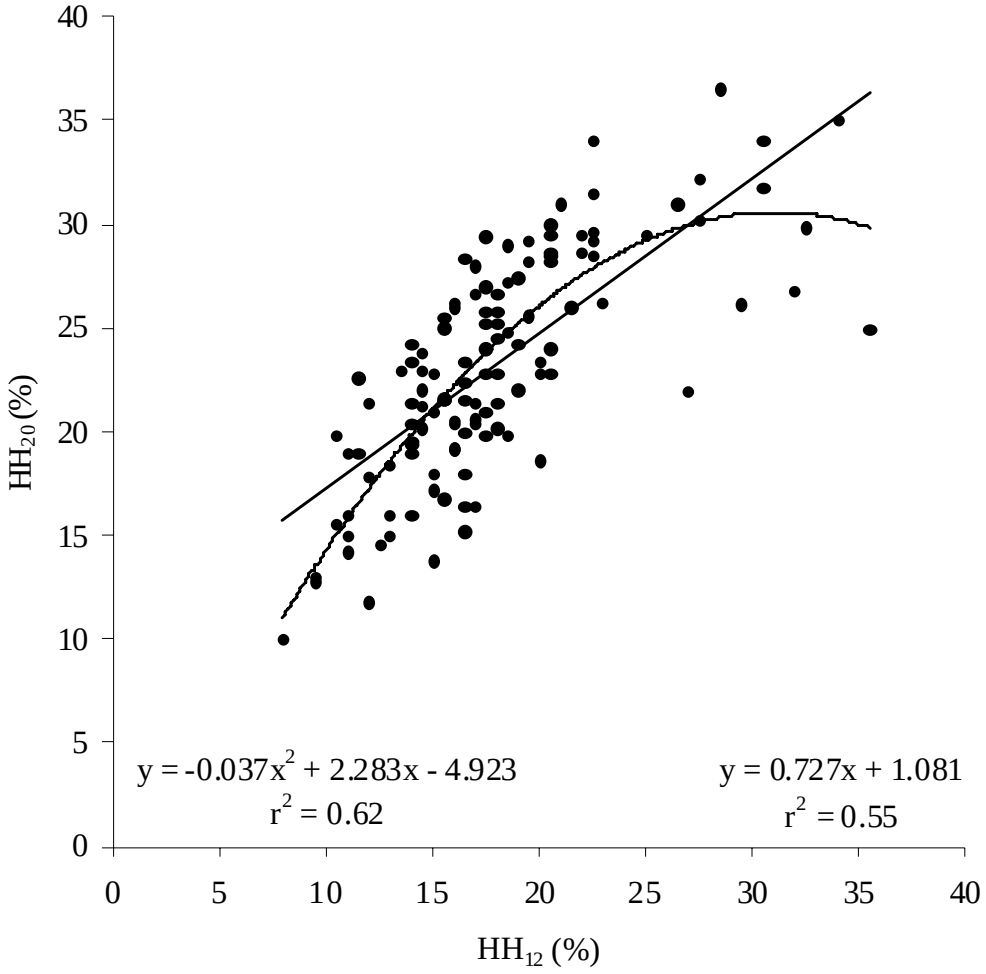

Figure 3.5. Linear and quadratic relationships between HH_{12} (hand-held) and HH_{20} (hand-held) volumetric water content (VWC) consisting of all topography treatments and replications during the 12 to 16 July dry-down.

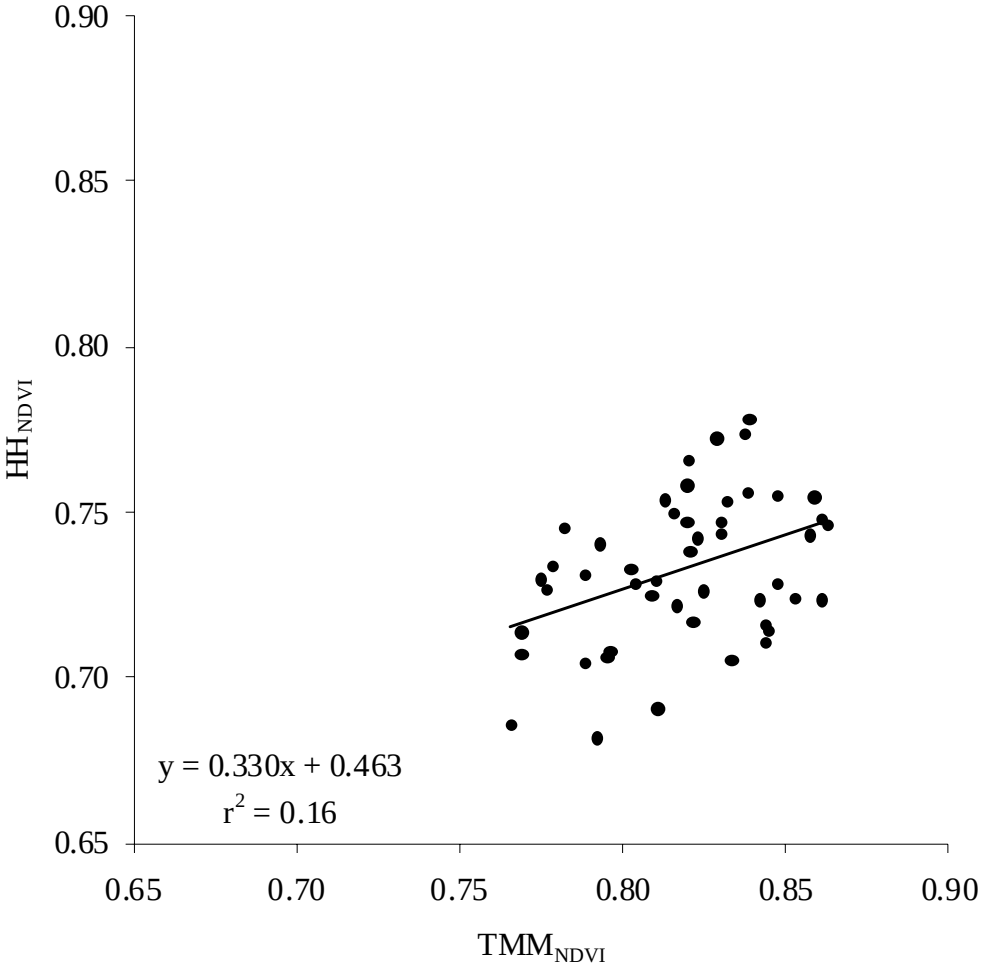

Figure 3.6. Linear relationship between TMM_{NDVI} (mobile) and HH_{NDVI} (hand-held) normalized difference vegetative index (NDVI) consisting of all topography treatments during all dry-downs.

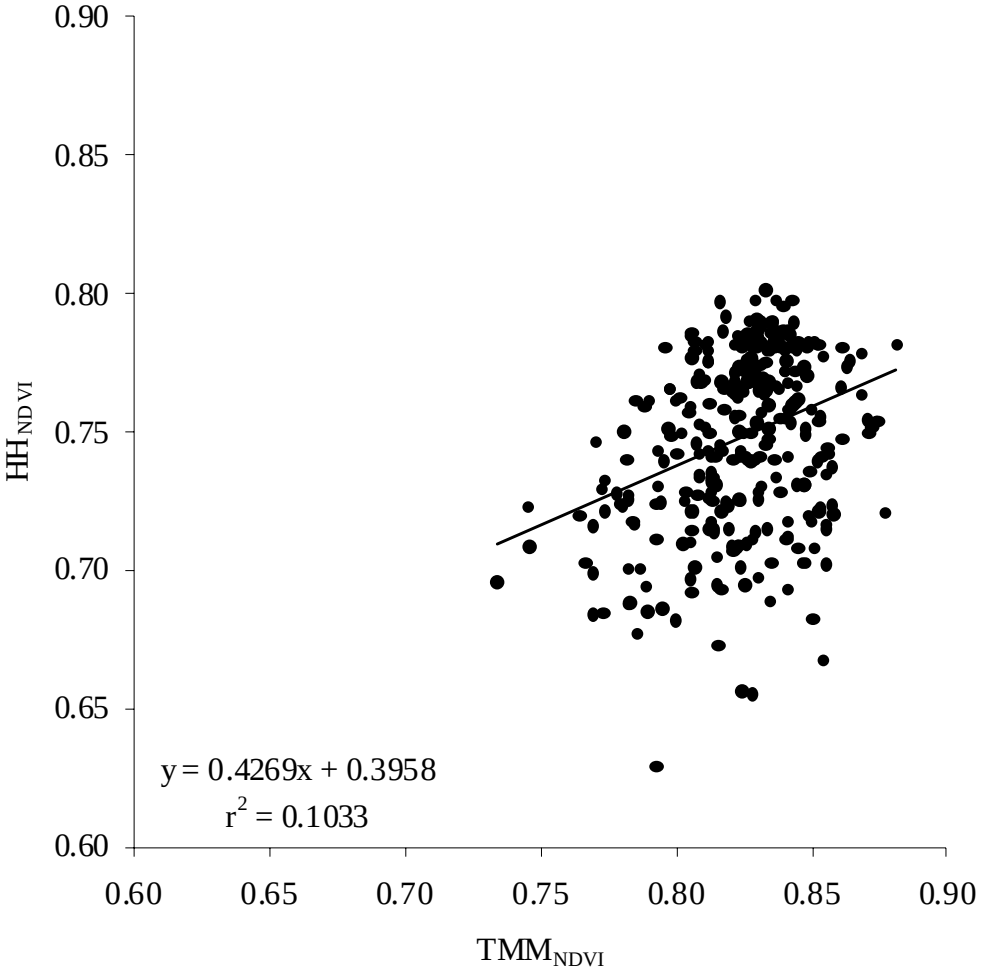

Figure 3.7. Linear relationship between TMM_{NDVI} (mobile) and HH_{NDVI} (hand-held) normalized difference vegetative index (NDVI) consisting of all topography treatments and replications during all dry-downs.

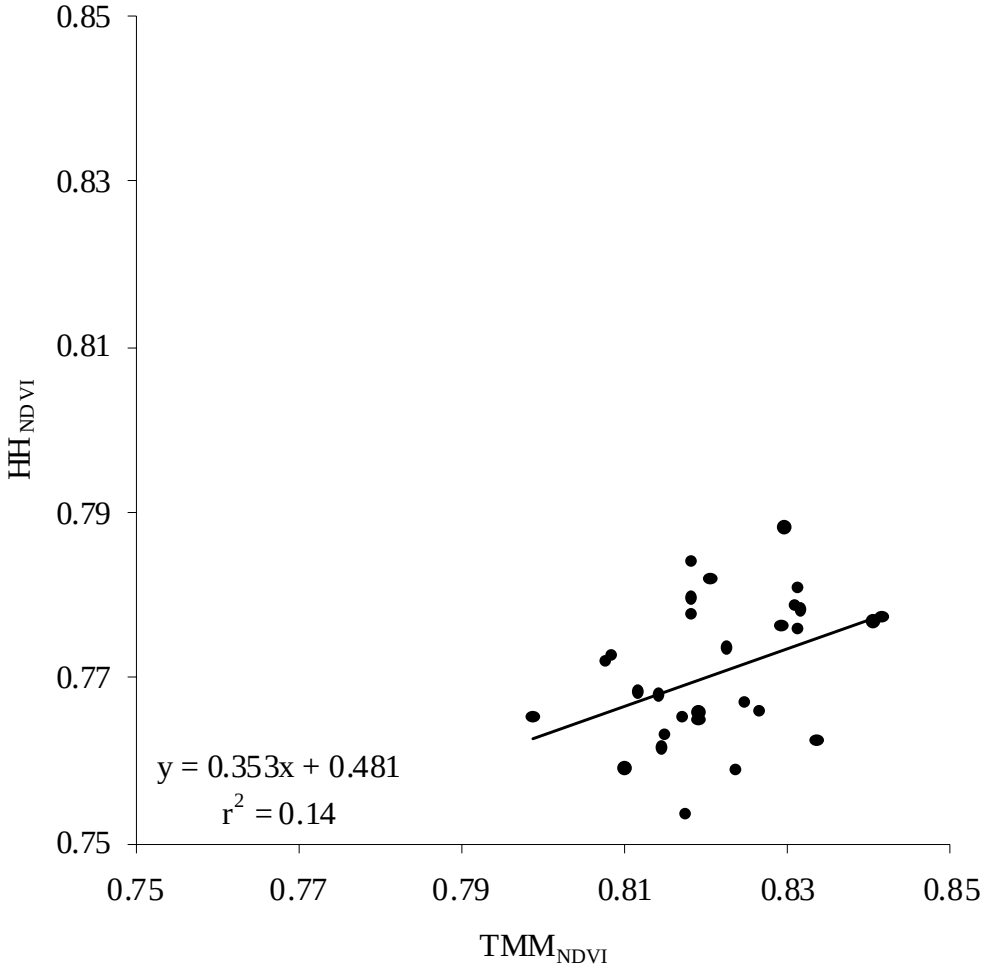

Figure 3.8. Linear relationship between TMM_{NDVI} (mobile) and HH_{NDVI} (hand-held) normalized difference vegetative index (NDVI) consisting of all topography treatments during the 12 to 16 July dry-down.

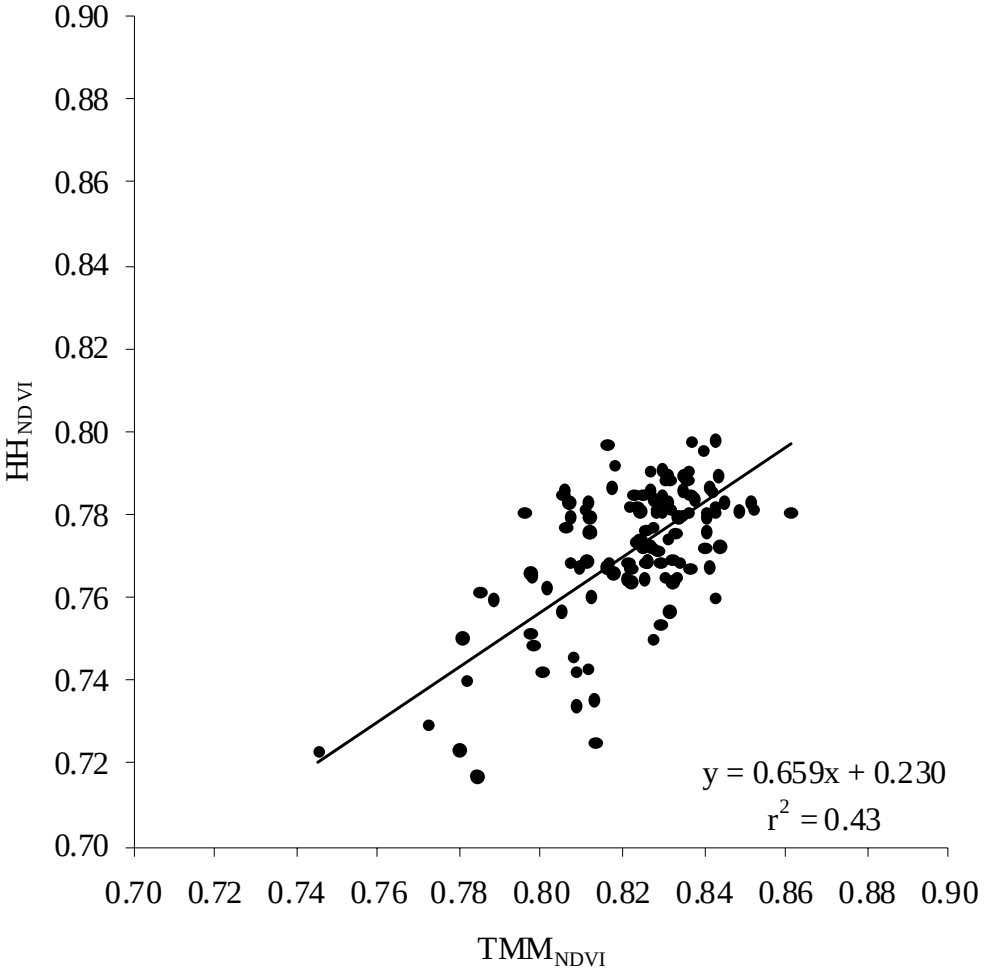

Figure 3.9. Linear relationship between TMM_{NDVI} (mobile) and HH_{NDVI} (hand-held) normalized difference vegetative index (NDVI) consisting of all topography treatments and replications during the 12 to 16 July dry-down.

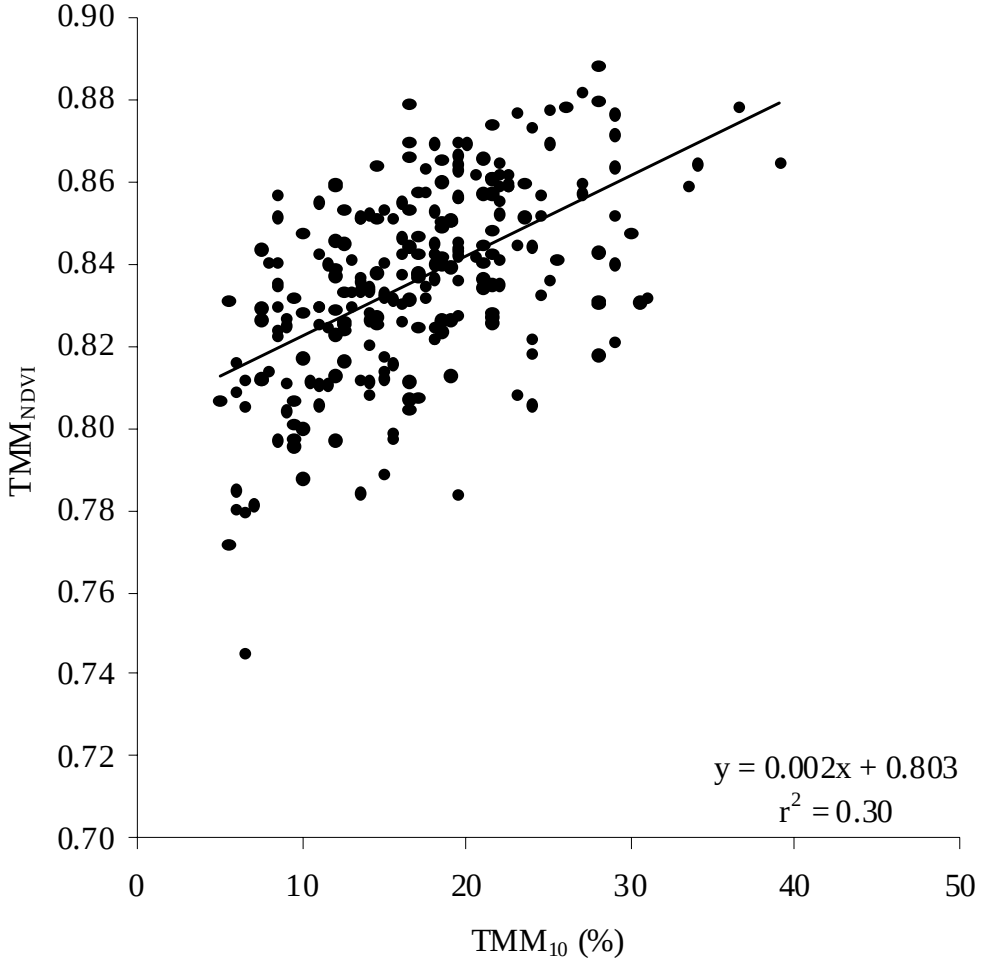

Figure 3.10. Linear relationship between TMM_{10} (mobile) volumetric water content (VWC) and TMM_{NDVI} (mobile) normalized difference vegetative index (NDVI) consisting of all topography treatments during all dry-downs.

CHAPTER 4

INFLUENCE OF SOLAR RADIATION ON SOIL WATER RELATIONS AND TURFGRASS STRESS

[1]Joseph M. Krum, Robert N. Carrow, and Keith J. Karnok. To be submitted to *Crop Science*.

ABSTRACT

Solar radiation affects plant water-use and can directly impact plant growth. Turfgrass breeding has produced cultivars that require less water in intense light environments, while other cultivars have been developed that are better adapted to reduced light conditions. Shaded microclimates require different management strategies than adjacent areas exposed to abundant sunlight, especially in terms of irrigation. Furthermore, the degree of morning versus afternoon shade can affect turfgrass. Water-use and corresponding plant performance was assessed in morning shade and full sunlight microclimates in this study at the Old Collier Golf Club in Naples, FL on 'Salam' seashore paspalum (*Paspalum vaginatum* Sw.) during the summer of 2006 during times of dry-downs following rain events. For time periods exhibiting significant differences, morning shade demonstrated 40% lower water-use relative to full sunlight. The adequate degree of shade tolerance associated with seashore paspalum may have contributed to a lower degree of turf response differences between treatments as revealed by similar normalized difference vegetative index (NDVI) values. Because of the confounding influence of different volumetric water content (VWC) field capacity baselines for directly comparing water-use, raw VWC data does not appear to be appropriate. However, field capacity as an irrigation baseline for each microclimate and available water depletion (AWD) concepts could be valuable for irrigation scheduling.

INTRODUCTION

Numerous factors affect the physiology, morphology, and growth of turfgrasses (Bell and Danneberger, 1999). Plant available water, nutrient availability, and canopy temperature are just a few variables that can induce turfgrass stress (Dudeck and Peacock, 1992). Furthermore, limited solar radiation is a factor which commonly defines plant vigor and spatial extent in a landscape (Beard, 1973; Bell et al., 2000).

Reduction in light intensity is the most obvious result of shade (Beard, 1973). Other effects of reduced light conditions on microclimates include changes in light quality, moderation of seasonal and diurnal extremes, decreased wind speed, increased relative humidity, and competition for water and nutrients by trees. A reduction in the photosynthetic photon flux density of plants also occurs as a result of shade (Zhao and Oosterhuis, 1998).

Reduced light intensity leads to decreased turf density, less turgid leaves that become more susceptible to mechanical injury, and disease development (Dudeck and Peacock, 1992). When subjected to shaded environments, the compromised photosynthetic rate results in slower growth and tillering. Along with reduced evapotranspiration (ET), microclimates are created that are conducive to disease development. Fungal pathogens such as *Rhizoctonia solani* (the causal agent of brown patch) and *Sclerotinia homoecarpa* (the causal agent of dollar spot) are promoted by shaded environments (Koh et al., 2003). Shade also encourages the development of powdery mildew on Kentucky bluegrass (*Poa pretensis* L.) (Beard, 1973). *Puccinia* spp. (the causal agent of rust diseases) is more prevalent under reduced light, especially in the southern United States. Conversely, *Fusarium* blight is enhanced by persistent sun exposure. Moreover, ultraviolet light increases sporulation of *Typhula* blight.

Turfgrasses differ in respect to shade tolerance at the species and cultivar level (Beard, 1973; Harivandi et al., 1984; Jiang et al., 2004). Seashore paspalum (*Paspalum vaginatum* Sw.) displayed better low light (LL) tolerance than hybrid bermudagrass (*Cynodon dactylon* L. x *C. transvaalensis* Burtt Davy) when exposed to 70% and 90% shade (LL) (Jiang et al., 2004). Among cultivars, 'Sea Isle 1' paspalum responded best to LL conditions, followed by 'Cloister' paspalum = 'Sea Isle 2000' paspalum > 'Temple 1' paspalum = 'Salam' paspalum > 'Q36131' paspalum = '561-79' paspalum = 'Hybrid 5' paspalum. 'TifSport' and 'TifEagle' bermudagrass exhibited the most stress due to LL conditions. Responses to 65% shade differed significantly between creeping red fescue (*Festuca rubra* L. subsp. *rubra*), chewings fescue (*Festuca rubra* var. commutata Gaud.) and perennial ryegrass (*Lolium perenne* L.) (Van Huylenbroeck and Bockstaele, 2001).

While turfgrasses such as Kentucky bluegrass and creeping bentgrass (*Agrostis palustris* Huds.) are not well adapted to shaded conditions, creeping red fescue, annual bluegrass (*Poa annua* L.) and rough bluegrass (*Poa trivialis* L.) grow well when sunlight is limited (Beard, 1973). Creeping red fescue is characterized by its exceptional shade tolerance and drought resistance, making it the best cool season turfgrass for use under dry, shaded conditions. Of the warm season turfgrasses, St. Augustinegrass [*Stenotaphrum secundatum* (Walt.) Kuntze] is used extensively in shaded areas, while bermudagrass (*Cynodon* spp.) performs poorly under limited light.

'Diamond' zoysiagrass [*Zoysia matrella* (L.) Merr.] is noted for its superior shade tolerance in comparison to other zoysiagrass cultivars (Qian and Engelke, 1999). However, with shade levels above 80%, turf decline occurs as the result of excessive etiolated shoot growth and insufficient carbohydrate levels. Trinexapac-ethyl (TE) is a plant growth regulator utilized for its

shoot growth control, and has been examined to determine if it could improve turfgrass performance under reduced light conditions. Treatments subjected to TE applications maintained acceptable turf quality throughout the duration of the 6- to 7-month studies, while the control exhibited unacceptable commercial turf quality after 6- to 10-weeks. It was concluded that low rates of TE applied on short intervals provides the most consistent shoot growth suppression. Under 80% shade, TE increased creeping bentgrass turf cover from 6 to 33%, tiller growth increased from 40 to 52%, and fructose content increased by as much as 40% (Goss et al., 2002). Meanwhile, under 60% shade, TE did not have a significant effect on turf cover.

Another growth regulator, flurprimidol, can also help to minimize the negative implications of reduced light levels on turfgrass (Stier et al., 1999). In this study, established Kentucky bluegrass was subjected to an indoor environment that simulated a covered athletic stadium. Turf quality reached unacceptable levels within 30 days, but with a flurprimidol rate of 0.56 kg ha^{-1}, the period was increased to as much as 60 days. Although turf shear resistance and rooting was not enhanced by flurprimidol, increased tillering was observed.

The degree of light exposure causes varying turfgrass responses. Continuous shade caused a 38% color reduction and 33% density loss in creeping bentgrass (Bell and Danneberger, 1999). Chlorophyll concentrations declined by 50% in continuous shade compared to full sunlight. However, treatments exposed to 6 hours of shade did not show substantial differences in color, density, root mass, pigment concentrations, or total nonstructural carbohydrates when compared to treatments receiving full sunlight. Plots also did not show significant differences in response to morning vs. afternoon shade, or 80 versus 100% shade.

Evapotranspiration is the loss of water from soil and plants by evaporation and transpiration, respectively (Beard, 1973). Transpiration accounts for the majority of water lost

via ET from dense turfgrass stands. Evapotranspiration varies on a diurnal and seasonal basis. Diurnally, ET corresponds to the daily solar radiation flux; it increases after sunrise, plateaus around mid-day, and diminishes toward sunset. Seasonally, ET is generally highest in the summer and lowest in the winter.

Climatic and soil factors influencing ET include solar radiation, temperature, atmospheric vapor pressure, wind, water absorption rate, and soil moisture potential. Solar radiation is typically the dominant factor when soil moisture in not limited. Transpiration and the vapor pressure gradient are positively correlated unless temporary closure of the plant stomata occurs as a response to extremely high temperatures. Shaded environments are associated with low ET as a result of less incident radiation, which modifies temperature in shaded areas.

The water-use rate combines ET and turfgrass water requirements. Turfgrass water-use is dependent upon climatic conditions, turfgrass species, soil type, traffic, and available soil moisture. Fine fescues (*Festuca rubra* L.) have a significantly lower water-use rate and superior drought resistance as opposed to Kentucky bluegrass and creeping bentgrass. Irrigation frequency and nitrogen fertilization are positively correlated with water-use. Shearman (2008) recently reviewed turfgrass cultural practices and their influence on water-use.

Mowing heights of turfgrasses can interact with shade effects (Dudeck and Peacock, 1992). As the height decreases, plant surface area is lowered, thereby limiting photosynthetic ability. Combined with limited light availability, a loss of shoot density occurs, which compromises the health and uniformity of the turf. Raising the mowing height increases turfgrass water-use (Beard, 1973).

Though there may be the perception that the importance of sun exposure in morning or afternoon is more or less similar, creeping bentgrass has been reported to not be sustainable at

golf course putting green heights (approximately 0.30 cm) without morning sunlight (Vargas, 1994). It can survive well though the first several months of the growing season in northern climates, but as the sun angle decreases in the latter portions of the summer (August), the overall quality and health of creeping bentgrass diminishes. Eventually the turf will thin out and die. No matter how much afternoon sunlight the turfgrass is exposed to, sufficient morning sunlight was reported to be imperative.

When turfgrasses are subjected to shaded environments, the resulting increased leaf succulence and delicateness causes the plant to become more susceptible to traffic stress, wear injury, and prolonged recovery time (Beard, 1973). Under no wear or soil compaction conditions, turf color, density, and canopy spectral reflectance did not vary significantly between Sea Isle 1 seashore paspalum plots receiving morning shade or afternoon shade (Jiang et al., 2003). However, morning shade had less of an adverse effect than afternoon shade on turfgrass subjected to wear stress and/or soil compaction. When 'L93' and 'SR1020' creeping bentgrass were exposed to reduced shade and airflow, canopy and soil temperature were lowered more by shade than airflow (Koh et al., 2003). Both treatments reduced the color quality and turf density. Shade reduced the root mass more severely than airflow restriction.

Photosynthetically active radiation (PAR) is the light in the 400 to 700 nm wavelengths that plants utilize (Bell et al., 2000). Light absorption varies throughout the spectral band for pigments such as chlorophyll and carotenoids, which influence a variety of plant responses. Cell elongation and chloroplast development are associated with phytocrome, a photoreceptor pigment that has an optimum absorption at 660 to 730 nm. Blue light is the PAR from 400 to 500 nm, while red light occurs from 600 to 700 nm. The spectral band from 500 to 600 nm is composed of green light and is not primarily used by plants. When analyzing the spectral quality

of deciduous shade, coniferous shade, building shade, and full sunlight, results showed that both types of trees filtered more red and blue light than buildings. There was a direct relationship between the proportion of blue light and shade density. The relationships between different spectral bands that induce plant responses were influenced by shade source and shade density.

Feldhake et al. (1985) investigated the effects of preconditioning 'Merion' Kentucky bluegrass to shade on ET rates. The turf was preconditioned to 100, 71, 51, and 27% of possible PAR and subjected to full sunlight (100% PAR) or full shade (2% PAR) for one day periods. As PAR increased from 27 to 100%, dry weight tripled. The study determined that ET was not affected by preconditioning to shade, as the canopy temperature and ET were equal for all preconditioned grasses.

The objective of this study was to assess the microclimatic effects of morning shade and full sunlight on ET and the normalized difference vegetative index (NDVI) in order to optimize the irrigation system design and scheduling for efficiency and uniformity in environments influenced by variable light intensity and/or duration.

MATERIALS AND METHODS

The study was conducted at the Old Collier Golf Club in Naples, Florida. The research area consisted of 'Salam' seashore paspalum mowed once weekly at a height of 3.18 cm with a rotary mower. Data collection was initiated following significant rain events, which negated any irrigation uniformity issues pertaining to surface volumetric water content VWC (Table A-1, Appendix). Four dry-downs took place during 19 to 20 June, 21 to 23 June, 26 to 29 June, and 12 to 16 July, 2006. No irrigation was applied during dry-downs. Light rain events of 0.35, 0.21, and 0.03 cm occurred during the afternoons of 21 June, 28 June, and 13 July, respectively.

A completely randomized design of two treatments and four replications was used, with plots located on the fairway rough area of Fairway 3. The two treatments were full sunlight (control) and morning shade lasting for a period of 5 to 6 h. Plot dimensions were 3 by 6 m. Shade was attributed to the presence of slash pine trees (*Pinus elliottii* Englem.).

A LI-COR LI-250 hand-held light meter was used to assess the PAR received by the turf canopy in the 400 to 700 nm waveband using a connected LI-190SA quantum sensor (LI-COR, Inc. Lincoln, NE). The LI-190SA contains a silicone photodiode and a visible bandpass interference filter with colored glass filters in a cosine corrected head. The unit of measurement is $\mu mols^{-1}m^{-2}$ with a relative error of ± 5%. The sensor was placed at the apex of the turf canopy to take readings. Five measurements per plot were taken from 12 to 28 July 2006 on select days at various times between 0730 and 1500 h EST under clear skies (Table 4.1).

Basic data collection was performed via the Toro Mobile Multi-Sensor (TMM; patent pending) prototype data acquisition unit (The Toro Company, Bloomington, MN). The TMM measures VWC (%), NDVI (unit-less; best = 1.0), and compaction (penetrometer resistance; kg). The TMM was affixed to and maneuvered with a utility vehicle. An operating speed of 2.7 to 3.3 km h^{-1} was maintained during data acquisition. Study plots were dew-whipped prior to TMM use to reduce the potential influence of dew on NDVI. Plot length was such that two readings per plot were obtained when the TMM traversed the plots. Data were recorded using an on-board laptop computer and all parameters were displayed in spreadsheet format.

Soil moisture measurements were based on time-domain reflectometry (TDR), which measures changes in the soil dielectric constant (ε) as water contents fluctuate (Leib et al., 2003). A TDR sensor produces a high frequency voltage pulse that is transmitted and reflected along metal probes. The dielectric constant is determined by measuring the velocity of the transmitted

pulse in the soil, which is primarily dependent upon the VWC, as water has a significantly higher dielectric constant than air ($\varepsilon = 80$ and 1, respectively). The permittivity and corresponding pulse velocity are closely related to the soil water content (Plauborg et al., 2005).

The electrical conductivity (EC_a) of soil can greatly affect TDR measurements by promoting erroneous overestimates of water content (Nadler et al., 1999). Salinity is a major contributing factor to EC_a, suggesting that negligible salinity levels should be verified before taking TDR measurements. A hand-held Landmapper ERM-0l (Landviser, Inc. Westhampton, NJ) measured the electrical resistance (ER; ohm m^{-1}) in the study plots, which was subsequently converted to EC_a (Table A-2, Appendix). The EC_a was measured to verify the absence of significant salt concentrations in the soil prior to data acquisition. This device is based on determining apparent EC_a using the four-wenner array method as described by Rhoades et al. (1999).

A Field Scout TDR 100 soil moisture sensor (Spectrum Technologies, Inc. Plainfield, IL; TMM_{10}) was modified for use on the TMM platform and used to determine VWC at a 0- to 10-cm depth. Two custom stainless steel probes of 9.53-mm diameter, 3.3-cm spacing, and 10-cm length were installed on the moisture sensor to facilitate a soil penetration depth of 10 cm. The sampling volume is an elliptical cylinder extending 3 cm radially beyond the TDR probes, measuring approximately 825 cm^3. The sensor is attached to one end of a shaft on the TMM, while a bolt is connected to the opposite end. When the TMM moves, the wheel-driven shaft rotates in a circular fashion. As the sensor's probes enter the ground, the bolt passes by a series of magnets that triggers the data logger to take a measurement. The probes are inserted into the soil approximately every 2.5 m. Two readings per plot were taken between the time period of 0900 to 1030 h EST. Additional readings were taken within a time period of 1800 to 2000 h

EST on select days. Exceeding 3.5 km h^{-1} significantly increased the probability of obtaining erroneous VWC readings. Possible theories as to the cause of this problem are that the bolt was passing by the magnets too quickly or the TDR probes were being inserted too quickly to facilitate a VWC measurement.

A GreenSeeker RT100 active sensor (NTech Industries, Inc. Ukiah, CA; TMM_{NDVI}) evaluated turf canopy NDVI in the study plots. The NDVI, which measures multispectral reflectance, has been shown to be significantly associated with visual turf quality, density, and shoot tissue injury (Trenholm et al., 1999). The sensor is equipped with internal light emitting diodes and a photodiode optical detector that measures the percent reflectance of the red (R = 660 nm) and near-infrared (NIR = 770 nm) spectral bands {$NDVI = [(R_{770} - R_{660})/(R_{770} + R_{660})]$}. The sensor is mounted on the TMM at a height of approximately 1 m and evaluates a 60- ± 10-cm by 1.52- ± 0.51-cm field of view. The sensor emits light pulses every 100 ms and outputs an averaged value every second. Depending on operating speed, six to eight readings per plot were recorded between the time period of 0900 to 1030 h EST. Additional readings were taken within a time period of 1800 to 2000 h EST on select days. The sensor only detects the light emitted, thereby preventing any possible influence of sunlight on the measurements.

An Omega LC302-500 1.90-cm diameter stainless steel compression load cell (Omega Engineering, Inc. Stamford, CT) was used to measure insertion force (kg) of the TDR moisture sensor probes. As the probes penetrate the soil, pressure is exerted against the load cell, indicating the degree of soil compaction. The load cell converts the load acting on it to electrical signals, which are used to calculate the penetrometer resistance. Penetrometer data are not presented in this paper since the site was very high in sand content and exhibited few high penetrometer resistance measurements.

Additional data were obtained with various hand-held devices to facilitate comparison with the TMM device as well as to supplement the data obtained by the TMM. All hand-held data acquisition utilized the same sampling method as the TMM, as measurements were taken in the same general areas of the study plots to maximize the integrity of the research. A hand-held Spectrum Field Scout TDR 300 unit (HH_{12} and HH_{20}) measured VWC of the 0- to 12-cm and 0- to 20-cm depths. The sensor is equipped with two stainless steel probes of 5-mm diameter, 3.3-cm spacing, and 12- or 20-cm length. The sampling volumes are elliptical cylinders extending 3 cm radially beyond the TDR probes, measuring approximately 905 and 1510 cm^3 for the 12- and 20-cm probes, respectively. Measurements were taken at the 0- to 12-cm depth daily within a time period of 0900 to 1030 h EST. Additional data were acquired within a time period of 1800 to 2000 h EST on select days. Two readings per plot were taken during the first three dry-downs, while five readings per plot were recorded for the 12 to 16 July, 2006 dry-down. The VWC of the 0- to 20-cm soil depth was measured once daily at 1300 to 1400 h EST. Two readings per plot were taken at the 0- to 20-cm depth. The 10-, 12-, and 20-cm VWC measurements were used to estimate ET_c during various durations of the study: $ET_c = [(VWC_{inititial} - VWC_{final})/100] \times depth$.

A hand-held, Spectrum Field Scout TCM 500 (turf color meter) evaluated the turf canopy NDVI $[(R_{850} - R_{680})/(R_{850} + R_{680})]$ in the study plots. Similarly, the leaf area index (IR/R, best = highest value) was calculated (R_{850}/R_{680}). The TCM 500 measures a 7.6-cm diameter target (45.36-cm^2 area). The instrument contains an internal light source, thereby eliminating external effects of sunny or cloudy conditions. The TCM 500 is placed directly on the ground to make a measurement. Two readings per plot were taken once daily within a time period from 1300 to 1400 h EST. Based on the results in Krum (Chapter 2), which demonstrated inconsistent results,

and because of the small sampling area (compared to the TMM_{NDVI}), the hand-held NDVI results were not presented for this study.

An Everest Interscience 100.3ZL hand-held infrared thermometer measured the canopy temperature (°C) of the plots (Everest Interscience, Inc. Tucson, AZ). The thermometer measures the infrared radiation (approximately 700 to 1000 nm) that is emitted from the turfgrass by using an optical infrared detector. The detector converts the radiation to a proportional signal. The temperature is the electrical analog of the infrared radiation. Two readings per plot, one north facing and one south facing, were taken once daily within a time period from 1300 to 1400 h EST, under sunny conditions. The instrument was held at a height of 1 m at a 45° angle.

Data were analyzed using the Statistical Analysis System (SAS Institute, Inc. Cary, NC; version 9.1) and statistical differences were determined by the Generalized Linear Model (GLM) procedure in conjunction with the least significant difference (LSD) t-test at a 0.10 significance level.

RESULTS and DISCUSSION

The morning shade treatment demonstrated lower solar radiation compared to the full sunlight treatment on most days, except in early morning or late afternoon (Table 4.1). Throughout all measurements taken at 1000 to 1300 h, an averaged solar radiation of 427 versus 874 μmol s^{-1} m^{-2} occurred on morning shade versus full sunlight plots, respectively, suggesting approximately 50% reduction in solar radiation during this time period.

Volumetric water content measurements taken on the first day of dry-downs were estimates of field capacity, especially during the 26 to 29 June and 12 to 16 July periods when salinity was not a confounding issue as discussed in Chapter 3 (Tables 4.2 to 4.4). Field capacity estimates varied with TDR instruments because of different sampling volumes. All instruments,

however, showed that field capacity was lower for morning shade relative to full sunlight plots. This may reflect less biomass production under lower light conditions that resulted in lower soil organic matter content in the morning shade plots relative to the full sunlight plots with 3.46 and 4.23% organic matter by dry weight, respectively (Table A-3, Appendix). Since the soil texture of the site was 96% sand, organic matter would have a significant influence on total moisture retention. Differences in the inherent VWC at field capacity illustrate how microclimate areas within a larger landscape, in this case a solar radiation microclimate, may vary in important characteristics that could influence irrigation scheduling. Van Pelt and Wierenga (2001), Starr (2005), and Duffera et al. (2007) pointed out that spatial variability of soil water presents a significant challenge for irrigation scheduling and soil water content maps would be valuable to design efficient irrigation management plans. They also noted that soil water content at field capacity has a relatively stable pattern of spatial variability that is highly correlated with other stable landscape properties such as particle size classes and topography.

Some significant differences in VWC of full sunlight versus morning shade treatments were observed over the various dry-downs using the three different TDR devices, namely: 7 of 22, 3 of 28, and 2 of 14 readings for the TMM_{10}, HH_{12}, and HH_{20} units, respectively (Tables 4.2 to 4.4). All VWC measurements throughout all analysis depths were lower for the shade treatment. However, because of the confounding influence of different VWC field capacity baselines for comparing water-use, direct comparison of treatment raw VWC data is not appropriate.

Krum (Chapter 3) noted that when the field capacity baselines differ across microclimates, the allowable water depletion method (AWD, also called management allowable depletion, or MAD) can be used, where AWD is the percent of available soil water allowed to be

depleted before irrigation is applied (SCS, 1993; Smarjstria et al., 2006). Field capacity for a microclimate area represents 100%, so dry-downs are set at a suitable level for the site to avoid undue stress on the turfgrass and may change with season. Once AWD is reached it would be a trigger for irrigation. The values in parentheses in Tables 4.2 to 4.4 indicate the percent dry-down from initial VWC (field capacity). For example, for the 26 to 29 June dry-down using the TMM_{10}, full sunlight plots exhibited surface drying to 54% of field capacity, while shade plots were at 65% (Table 4.2). However, there was no consistent treatment pattern when full sunlight and morning shade plots were compared for percent drying across the various dry-downs regardless of the TDR unit (Tables 4.2 to 4.4).

Differences in VWC from one time period to another by soil depth allow water-use to be compared between treatments. Daily ET (i.e., ET calculated from the difference in daily a.m. to p.m. VWC) and the summation of daily gross ET over a time period (i.e., daily a.m. to p.m. ET values summed for the particular dry-down) provide two measures of estimated ET. A third estimate of ET is net ET (i.e., ET calculated from the first day VWC to the last day VWC of each dry-down). The net ET differs from the gross ET due to a consistent increase in VWC from one evening to the following morning, as exhibited in the 12 to 16 July dry-down by comparing the p.m. VWC to the following day's a.m. VWC value for either the TMM_{10} (Table 4.2) or HH_{12} (Table 4.3) devices. Capillary rise or dew could be responsible for this pattern, despite plots being dew-whipped prior to data acquisition. Even when using the longer HH_{20} probes, there were instances of increased VWC from one day to another, such as from 13 to 14 July (Table 4.4). Moreover, the rain events (noted in the tables) during dry-downs typically correspond to rises in VWC from the morning to afternoon and low or negative ET values.

For daily a.m. to p.m. comparison of ET, 27 June, 14 July, and 16 July ET based on the HH_{12} showed significant treatment differences between the full sunlight versus morning shade plots at daily ET of 0.79 vs. 0.21, 0.64 vs. 0.37, and 0.87 vs. 0.45 cm, respectively (Table 4.6). For the same TDR device and the 12 to 16 July period, the gross ET was also greater for full sunlight (2.95 cm) compared to the morning shade (1.97 cm) plots, as was the net ET at 1.78 and 1.25 cm, respectively (Table 4.6). When ET was averaged over the dates when significant differences occurred, the morning shade plots exhibited an ET of 60% that of full sun conditions. Net ET differences using the TMM_{10} were observed for the 21 to 23 June and 26 to 29 June periods (Table 4.5). The only significant treatment difference using the HH_{20} occurred from 12 to 13 July, where the full sunlight plots exhibited lower ET than the morning shade plots (Table 4.7). The reason for this response is not clear.

These results correlate to other studies that found that shaded environments use less water than those which are continually exposed to sunlight (Dudeck and Peacock, 1992; Dipaola and Beard, 1992). However, using relatively few readings to quantify estimated ET based on the surface 10- to 12-cm zone resulted in high CVs for most of the ET determinations regardless of device used. Perhaps spatial mapping with a mobile platform (e.g., the spatial study of Chapter 2) over a whole shaded microclimate and an adjacent full sunlight area would offer more consistent results and insight into the influence of shaded environments in real world situations. This may be especially applicable when attempting to use rapid surface zone measurements, necessary in a precision turf management (PTM) approach, to provide a better understanding of spatial water relations.

The TMM_{NDVI} and canopy temperature data were taken to provide a measure of turf performance and possible stress (Tables 4.8 and 4.9). Lower plant stress on 28 $June_{am}$ under

morning shade was measured by the $NDVI_{tmm}$ (Table 4.8). No statistical differences in NDVI were found during the 12 to 16 July dry-down; VWC and NDVI exhibited a weak linear relationship of $r^2 = 0.11$ (Figure 4.1). Thus, the morning shade microclimate, while differing from the full sunlight microclimate (in terms of VWC and light), revealed only slight influence on turf performance. The canopy temperature measurements did not reveal any statistical differences except on 16 July, where canopy temperatures were 26.8 and 21.1°C for the full sunlight and morning shade plots, respectively (Table 4.9). Both NDVI and canopy temperature data had low CVs. The lack of influence of this degree of low light on the seashore paspalum is likely a result of greater tolerance to low light for seashore paspalum compared to bermudagrass (Jiang et al., 2003; 2004; 2005).

These results illustrate that ET in shade microclimates of field situations is often lower than full sunlight; in this study, ET was 60% of full sunlight when significant differences occurred. Also, this study suggests rapid field measurement of VWC in the surface 10- to 12-cm zone could provide guidance to make irrigation adjustments in shaded areas relative to full sunlight areas. In areas where the baseline field capacity of a shade microclimate or other type of microclimate area differs from the adjacent locations, we discussed various means of using VWC and estimated ET to avoid confounding effects from different baselines.

REFERENCES

Amato, M., and J.T. Ritchie. 2002. Spatial distribution of roots and water uptake of maize (*Zea mays* L.) as affected by soil structure. Crop Sci. 42:773-780.

Beard, J.B. 1973. Turfgrass: Science and culture. Prentice-Hall, Englewood Cliffs, NJ.

Bell, G.E., and T.K. Danneberger. 1999. Temporal shade on creeping bentgrass turf. Crop Sci. 39:1142-1146.

Bell, G.E., T.K. Danneberger, and M.J. McMahon. 2000. Spectral irradiance available for turfgrass growth in sun and shade. Crop Sci. 40:189-195.

Dudeck, A.E., and C.H. Peacock. 1992. Shade and turfgrass culture. Agron. Monogr. 32. ASA, CSSA, and SSSA, Madison, WI.

Dipaola J.M., and J.B. Beard. 1992. Physiological effects of temperature stress. Agron. Monogr. 32. ASA, CSSA, and SSSA, Madison, WI.

Feldhake, C.M., J.D. Butler, and R.E. Danielson. 1985. Turfgrass evapotranspiration: Responses to shade preconditioning. Irrig. Sci. 6:265-270.

Goss, R.M., J.H. Baird, S.L. Kelm, and R.N. Calhoun. 2002. Trinexapac-ethyl and nitrogen effects on creeping bentgrass grown under reduced light conditions. Crop Sci. 42:472-479.

Harivandi, M.A. 1984. Turfgrass irrigation efficiency. Int. Turfgrass Conf, 55th, Las Vegas, NV. Jan. 1984. 34(4):21-23. California Turfgrass Culture.

Jiang, Y., R.N. Carrow, and R.R. Duncan. 2003. Effects of morning and afternoon shade in combination with traffic stress on seashore paspalum. HortScience 38:1218-1222.

Jiang, Y., R.N. Carrow, and R.R. Duncan. 2005. Physiological acclimation of seashore paspalum and bermudagrass to low light. Scientia Horticulturae 105:101-115.

Jiang, Y., R.R. Duncan, and R.N. Carrow. 2004. Assessment of low light tolerance of seashore paspalum and bermudagrass. Crop Sci. 44:587-594.

Koh, K.J., G.E. Bell, D.L. Martin, and N.R. Walker. 2003. Shade and airflow restriction effects on creeping bentgrass golf greens. Crop Sci. 43:2182-2188.

Leib, B.G., J.D. Jabro, and G.R. Matthews. 2003. Field evaluation and performance comparison of soil moisture sensors. Soil Sci. 168:396-409.

Qian, Y.L., and M.C. Engelke. 1999. Influence of trinexapac-ethyl on diamond zoysiagrass in a shade environment. Crop Sci. 39:202-208.

Plauborg, F., B.V. Iverson, and P.E. Laerke. 2005. In situ comparison of three dielectric soil moisture sensors in drip irrigated sandy soils. Vadose Zone J. 4:1037-1047.

Rothe, A., W. Wies, K. Kreutzer, D. Matthies, U. Hess, and B. Ansorge.1997. Changes in soil structure caused by the installation of time domain reflectometry probes and their influence on the measurement of soil moisture. Water Resour. Res. 33(7):1585-1593.

SAS Institute. 2003. The SAS system for Windows. Release 9.1. SAS Inst., Cary, NC.

Shearman, R.C. 2008. Turfgrass cultural practices for water conservation. p. 205-222. *In* J.B. Beard and M.P. Kenna (ed.) Water quality and quantity issues for turfgrasses in urban landscapes. Proc. Workshop on Water Quality and Quantity Issues for Turfgrasses in Urban Landscapes, Las Vegas, NV. Jan. 2006. Counc. Agric. Sci. Technol., Ames, IA.

Stier, J.C., J.N. Rogers III, J.R. Crum, and P.E. Rieke. 1999. Flurprimidol effects on Kentucky bluegrass under reduced irradiance. Crop Sci. 39:1423-1430.

Trenholm, L.E., R.N. Carrow, and R.R. Duncan. 1999. Relationship of multispectral radiometry data to qualitative data in turfgrass research. Crop Sci. 39:763-769.

Van Huylenbroeck, J.M., and E. Van Bockstaele. 2001. Effects of shading on photosynthetic capacity and growth of turfgrass species. Int. Turfgrass Soc. Res. J. 9:353-362.

Van Pelt, R.S. and P.J. Wierenga. 2001. Temporal stability of spatially measured soil matric potential probability density function. Soil Sci. Soc. Am. J. 65:668-677.

Vargas, J.M. 1994. Management of turfgrass diseases. 2nd ed. CRC Press, Boca Raton, FL.

Zhao, D., and D. Oosterhuis. 1998. Cotton responses to shade at different growth stages: Nonstructural carbohydrate composition. Crop Sci. 38:1196-1203.

Table 4.1. Turfgrass canopy photosynthetically active radiation (PAR).

Date Time (EST)	Treatment Full Sunlight	Treatment Morning Shade	F-test	CV
	μmol s^{-1} m^{-2}			%
12 July				
0800 h	81	65	0.26	26
14 July				
1000 h	728	292	<0.01†	21
1300 h	881	518	0.04†	29
16 July				
1000 h	570	240	<0.01†	20
1230 h	1102	594	0.02†	27
17 July				
0830 h	124	134	0.74	30
1200 h	1058	431	0.01†	31
1500 h	1060	1025	0.01†	1
20 July				
0800 h	87	96	0.60	25
1030 h	837	443	0.01†	22
24 July				
0900 h	207	154	0.13	23
1100 h	894	368	0.02†	36
1400 h	1078	985	0.21	9
25 July				
0700 h	47	40	0.35	23
28 July				
1130 h	921	532	0.01†	20

† Significant at a 0.10 probability level.

Table 4.2. Influence of sunlight on 10-cm volumetric water content (VWC) during dry-down periods (mobile unit).

Date	Treatment		F-test	CV
	Full Sunlight	Morning Shade		
19 - 20 June	%			%
19 June	39.1	25.9	0.16	36
20 June	38.6	26.0	0.21	40
21 - 23 June‡	%			%
21 June	44.6	31.0	0.25	40
22 June	42.5	29.6	0.32	46
23 June am	34.0	30.8	0.82	60
23 June pm	31.9 (72)#	25.4 (82)	0.55	51
26 - 29 June§	%			%
26 June	37.3	24.6	0.02†	18
27 June	28.1	18.6	0.02†	19
28 June am	25.3	17.4	0.08†	24
28 June pm	29.3	22.0	0.09†	20
29 June am	26.5	19.9	0.12	23
29 June pm	20.3 (54)	17.4 (71)	0.26	18
12 - 16 July¶	%			%
12 July am	28.0	22.0	0.15	21
12 July pm	25.7	19.5	0.10†	20
13 July am	26.2	19.2	0.09†	22
13 July pm	26.8	19.8	0.09†	21
14 July am	27.9	21.8	0.14	20
14 July pm	23.0	17.1	0.13	24
15 July am	26.6	20.1	0.15	24
15 July pm	20.3	14.5	0.15	28
16 July am	22.7	16.2	0.12	26
16 July pm	18.0 (64)	11.9 (54)	0.18	38

† Significant at a 0.10 probability level.

‡ A 0.35-cm rainfall occurred during the afternoon of 21 June following data acquisition.

§ A 0.21-cm rainfall occurred during the afternoon of 28 June prior to pm data acquisition.

¶ A 0.03-cm rainfall occurred during the afternoon of 13 July prior to pm data acquisition.

Data in parentheses indicate percent of field capacity (100%) at dry-down termination.

Table 4.3. Influence of sunlight on 12-cm volumetric water content (VWC) during dry-down periods (hand-held unit).

Date	Treatment		F-test	CV
	Full Sunlight	Morning Shade		
19 - 20 June	%			%
19 June am	43.9	29.1	0.15	34
19 June pm	32.8	24.4	0.21	30
20 June am	39.5	28.4	0.20	32
20 June pm	33.9 (77)#	21.8 (75)	0.19	41
21 - 23 June‡	%			%
21 June am	43.9	34.1	0.36	36
21 June pm	43.6	34.5	0.49	45
22 June am	42.5	31.1	0.31	39
22 June pm	35.1	25.0	0.28	40
23 June am	41.0	26.1	0.23	47
23 June pm	33.0 (75)	22.9 (67)	0.30	45
26 - 29 June§	%			%
26 June am	30.6	25.5	0.18	17
26 June pm	27.1	20.9	0.13	21
27 June am	26.6	19.6	0.09†	21
27 June pm	20.1	17.9	0.45	21
28 June am	22.8	18.3	0.22	23
28 June pm	24.4	19.8	0.14	17
29 June am	28.4	23.1	0.27	24
29 June pm	18.8 (61)	15.0 (59)	0.30	28
12 - 16 July¶	%			%
12 July am	28.9	22.6	0.07†	15
12 July pm	24.5	20.1	0.16	18
13 July am	24.8	20.3	0.14	17
13 July pm	22.6	19.1	0.11	13
14 July am	24.8	20.4	0.17	18
14 July pm	19.6	17.4	0.45	21
15 July am	23.6	19.8	0.19	17
15 July pm	18.3	14.0	0.13	21
16 July am	21.4	16.1	0.09†	20
16 July pm	14.3 (49)	12.4 (55)	0.32	18

† Significant at a 0.10 probability level.

‡ A 0.35-cm rainfall occurred during the afternoon of 21 June prior to pm data acquisition.

§ A 0.21-cm rainfall occurred during the afternoon of 28 June prior to pm data acquisition.

¶ A 0.03-cm rainfall occurred during the afternoon of 13 July prior to pm data acquisition.

Data in parentheses indicate percent of field capacity (100%) at dry-down termination.

Table 4.4. Influence of sunlight on 20-cm volumetric water content (VWC) during dry-down periods (hand-held unit).

Date	Treatment		F-test	CV
	Full Sunlight	Morning Shade		
19 - 20 June	%			%
19 June	36.4	26.6	0.27	36
20 June	32.6	25.1	0.35	36
21 - 23 June‡	%			%
21 June	35.6	27.8	0.36	35
22 June	38.4	30.0	0.36	35
23 June	23.4 (66)#	19.3 (69)	0.51	39
26 - 29 June§	%			%
26 June	23.3	19.0	0.03†	10
27 June	21.0	17.8	0.27	20
28 June	17.3	15.8	0.34	12
29 June	18.8 (81)	15.9 (84)	0.21	17
12 - 16 July¶	%			%
12 July	21.1	18.9	0.11	8
13 July	18.1	14.8	0.02†	9
14 July	18.9	17.3	0.23	10
15 July	19.0	16.3	0.20	15
16 July	14.4 (68)	11.5 (61)	0.13	18

† Significant at a 0.10 probability level.
‡ A 0.35-cm rainfall occurred during the afternoon of 21 June following data acquisition.
§ A 0.21-cm rainfall occurred during the afternoon of 28 June following data acquisition.
¶ A 0.03-cm rainfall occurred during the afternoon of 13 July following data acquisition.
# Data in parentheses indicate percent of field capacity (100%) at dry-down termination.

Table 4.5. Influence of sunlight on 10-cm evapotranspiration (ET) during dry-down periods (mobile unit).

Date	Treatment		F-test	CV
	Full Sunlight	Morning Shade		
19 - 20 June	cm			%
19 - 20 June (N)‡	0.05	-0.01	0.76	1488
21 - 23 June§	cm			%
21 - 22 June	0.22	0.14	0.88	380
22 - 23 June	0.22	0.55	0.62	232
21 - 23 June (N)	1.28	0.56	0.09†	55
26 - 29 June¶	cm			%
26 - 27 June	0.93	0.61	0.54	89
28am - 28pm	-0.41	-0.47	0.86	-111
29am - 29pm	0.64	0.25	0.19	83
26 - 29 June (N)	1.70	0.73	0.06†	49
12 - 16 July#	cm			%
12am - 12pm	0.29	0.31	0.84	56
13am - 13pm	-0.07	-0.07	1.00	-227
14am - 14pm	0.60	0.58	0.76	14
15am - 15pm	0.77	0.68	0.66	39
16am - 16pm	0.57	0.52	0.71	32
∑12 - 16 July (G)	2.16	2.03	0.62	17
12am - 16pm (N)	1.22	1.23	0.97	37

† Significant at a 0.10 probability level.

‡ (G) and (N) indicate estimated gross and net ET at dry-down termination, respectively.

§ A 0.35-cm rainfall occurred during the afternoon of 21 June following data acquisition.

¶ A 0.21-cm rainfall occurred during the afternoon of 28 June prior to pm data acquisition.

A 0.03-cm rainfall occurred during the afternoon of 13 July prior to pm data acquisition.

Table 4.6. Influence of sunlight on 12-cm evapotranspiration (ET) during dry-down periods (hand-held unit).

Date	Treatment		F-test	CV
	Full Sunlight	Morning Shade		
19 - 20 June	cm			%
19am - 19pm	1.36	0.58	0.17	72
20am - 20pm	0.69	0.81	0.82	96
∑19 - 20 June (G)‡	2.04	1.39	0.21	39
19am - 20pm (N)	1.22	0.90	0.51	60
21 - 23 June§	cm			%
21am - 21pm	0.03	-0.05	0.88	-9026
22am - 22pm	0.90	0.75	0.63	52
23am - 23pm	0.98	0.40	0.28	100
∑21 - 23 June (G)	1.91	1.10	0.21	54
21am - 23pm (N)	1.33	1.37	0.87	28
26 - 29 June¶	cm			%
26am - 26pm	0.43	0.56	0.63	78
27am - 27pm	0.79	0.21	0.01†	46
28am - 28pm	-0.20	-0.18	0.96	-245
29am - 29pm	1.17	0.99	0.45	29
∑26 - 29 June (G)	2.20	1.59	0.23	34
26am - 29pm (N)	1.45	1.28	0.56	28
12 - 16 July#	cm			%
12am - 12pm	0.53	0.31	0.40	83
13am - 13pm	0.27	0.15	0.34	75
14am - 14pm	0.64	0.37	0.08†	36
15am - 15pm	0.64	0.70	0.72	34
16am - 16pm	0.87	0.45	0.02†	28
∑12 - 16 July (G)	2.95	1.97	0.06†	24
12am - 16pm (N)	1.78	1.25	0.03†	17

† Significant at a 0.10 probability level.

‡ (G) and (N) indicate estimated gross and net ET at dry-down termination, respectively.

§ A 0.35-cm rainfall occurred during the afternoon of 21 June prior to pm data acquisition.

¶ A 0.21-cm rainfall occurred during the afternoon of 28 June prior to pm data acquisition.

A 0.03-cm rainfall occurred during the afternoon of 13 July prior to pm data acquisition.

Table 4.7. Influence of sunlight on 20-cm evapotranspiration (ET) during dry-down periods (hand-held unit).

Date	Treatment		F-test	CV
	Full Sunlight	Morning Shade		
	cm			%
19 - 20 June				
19 - 20 June	0.76	0.31	0.42	141
	cm			%
21 - 23 June‡				
21 - 22 June	-0.56	-0.46	0.76	-87
22 - 23 June	3.05	2.18	0.26	38
21 - 23 June	2.49	1.73	0.32	48
	cm			%
26 - 29 June§				
26 - 27 June	0.46	0.25	0.59	141
27 - 28 June	0.76	0.41	0.33	81
28 - 29 June	-0.30	-0.03	0.23	-179
26 - 29 June	0.91	0.64	0.18	33
	cm			%
12 - 16 July¶				
12 - 13 July	0.61	0.84	0.04†	17
13 - 14 July	-0.15	-0.51	0.18	-101
14 - 15 July	-0.03	0.20	0.41	409
15 - 16 July	0.94	0.97	0.93	44
12 - 16 July	1.37	1.50	0.41	14

† Significant at a 0.10 probability level.

‡ A 0.35-cm rainfall occurred during the afternoon of 21 June following data acquisition.

§ A 0.21-cm rainfall occurred during the afternoon of 28 June following data acquisition.

¶ A 0.03-cm rainfall occurred during the afternoon of 13 July following data acquisition.

Table 4.8. Influence of sunlight on normalized difference vegetative index (NDVI) during dry-down periods (mobile unit).

Date‡	Treatment		F-test	CV
	Full Sunlight	Morning Shade		
26 - 29 June§				%
26 June	0.897	0.903	0.37	1
27 June	0.860	0.867	0.24	1
28 June am	0.865	0.878	0.01†	1
28 June pm	0.883	0.888	0.23	1
29 June am	0.883	0.891	0.17	1
29 June pm	0.848	0.856	0.13	1
26 - 29 June#	0.049	0.047	0.78	23
12 - 16 July¶				%
12 July am	0.872	0.877	0.36	1
12 July pm	0.842	0.844	0.79	1
13 July am	0.847	0.849	0.61	1
13 July pm	0.845	0.841	0.49	1
14 July am	0.864	0.864	0.99	1
14 July pm	0.847	0.843	0.59	1
15 July am	0.871	0.869	0.66	1
15 July pm	0.847	0.845	0.85	1
16 July am	0.861	0.866	0.23	1
16 July pm	0.836	0.836	0.95	1
12am - 12pm#	0.030	0.033	0.51	20
13am - 13pm#	0.002	0.009	0.33	176
14am - 14pm#	0.018	0.021	0.40	28
15am - 15pm#	0.025	0.024	0.90	26
16am - 16pm#	0.025	0.030	0.40	26
12am - 16pm#	0.100	0.117	0.38	24

† Significant at a 0.10 probability level.

‡ The mobile NDVI data were not recorded from 19 to 23 June.

§ A 0.21-cm rainfall occurred during the afternoon of 28 June prior to pm data acquisition.

¶ A 0.03-cm rainfall occurred during the afternoon of 13 July prior to pm data acquisition.

NDVI change.

Table 4.9. Influence of sunlight on canopy temperature during dry-down periods.

Date	Treatment		F-test	CV
	Full Sunlight	Morning Shade		
19 - 20 June	°C			%
19 June	24.5	23.8	0.11	2
20 June	26.5	23.0	0.32	18
21 - 23 June‡	°C			%
21 - 22 June	29.8	27.8	0.33	9
22 - 23 June	31.0	27.1	0.11	10
21 - 23 June	27.9	27.2	0.74	10
26 - 29 June§	°C			%
26 June	28.3	28.5	0.93	10
27 June	26.4	25.9	0.57	4
28 June	27.7	25.6	0.41	12
29 June	27.6	25.4	0.40	13
12 - 16 July¶	°C			%
12 July	26.2	25.2	0.41	7
13 July	22.2	21.6	0.37	4
14 July	27.1	24.9	0.14	7
15 July	30.3	29.5	0.56	6
16 July	26.8	21.1†	0.06	15

† Significant at a 0.10 probability level.

‡ A 0.35-cm rainfall occurred during the afternoon of 21 June following data acquisition.

§ A 0.21-cm rainfall occurred during the afternoon of 28 June following data acquisition.

¶ A 0.03-cm rainfall occurred during the afternoon of 13 July following data acquisition.

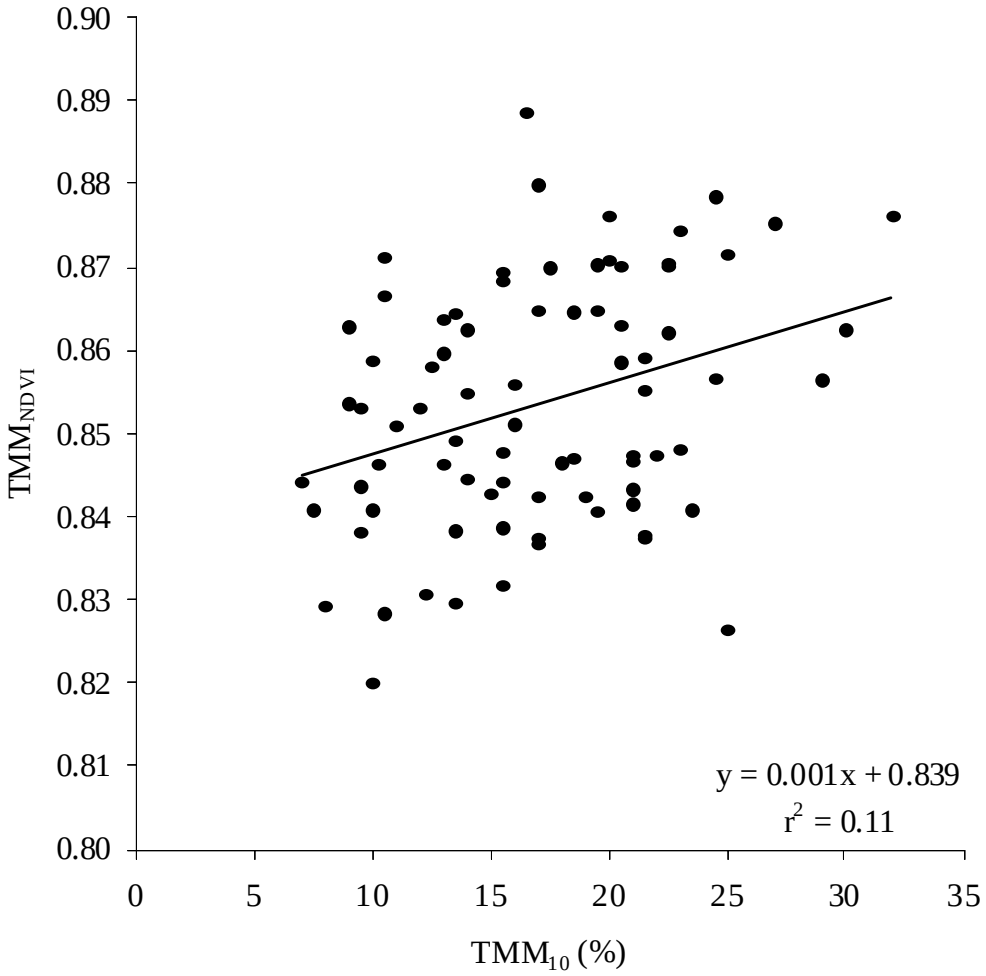

Figure 4.1. Linear relationship between TMM_{10} (mobile) volumetric water content (VWC) and TMM_{NDVI} (mobile) normalized difference vegetative index (NDVI) consisting of morning shade and full sunlight treatments and replications during the 12 to 16 July dry-down.

CHAPTER 5

INFLUENCE OF TRAFFIC ON SOIL WATER RELATIONS AND TURFGRASS STRESS

[1]Joseph M. Krum, Robert N. Carrow, and Keith J. Karnok. To be submitted to *Crop Science*.

ABSTRACT

The aesthetic and functional attributes of turfgrasses can be dramatically affected by traffic stresses, which are commonly subdivided into soil compaction and turfgrass wear. The effects of traffic on soil moisture, water-use, and plant performance were investigated on a sandy site where wear was the dominant traffic stress. The study took place during the summer of 2006 at the Old Collier Golf Club in Naples, FL on 'Salam' seashore paspalum (*Paspalum vaginatum* Sw.). High and low traffic treatment microclimates were selected based on vehicular traffic patterns on the site. Volumetric water content (VWC) and normalized difference vegetative index (NDVI) were measured during dry-downs with hand-held and mobile platform instrumentation. The hand-held VWC yielded estimated evapotranspiration (ET) differences between treatments, as ET was lower for the high traffic plots compared to the low traffic plots during the 12 to 16 July dry-down, with ET of 1.82 and 2.16 cm, respectively. The high traffic treatment also exhibited lower NDVI relative to the low traffic treatment.

INTRODUCTION

Turfgrasses are subjected to a variety of stresses that can directly or indirectly compromise aesthetic and functional quality, health, or even lead to plant mortality (Beard, 1973). Traffic stresses primarily pertain to turfgrass wear and soil compaction (Carrow and Petrovic, 1992). Soil displacement and turf removal also occur as a result of traffic, but are less prevalent than wear and compaction.

Turfgrass wear is associated with scuffing and tearing directed toward the leaves, stems, and crowns of the plant. Disease susceptibility increases when the plant is subjected to wear because the damaged areas encourage the invasion of pathogens.

Wear tolerance varies significantly among species and cultivars because of anatomical and morphological characteristics (Shearman and Beard, 1975; Carrow and Petrovic, 1992; Trenholm et al., 2000). Leaf structure, shoot density, lignin content, and location of strengthening tissues (e.g., sclerenchyma) are among several factors that determine wear tolerance. Warm season turfgrasses are generally more wear tolerant than their cool season counterparts. For example, zoysiagrass (*Zoysia* spp.) and bermudagrass (*Cynodon* spp.) are characterized by a high degree of wear tolerance, while creeping bentgrass (*Agrostis palustris* Huds.) and rough bluegrass (*Poa trivialis* L.) are much more susceptible to wear. However, Kentucky bluegrass (*Poa pretensis* L.), a cool season species, performs better under wear than centipedegrass [*Eremochloa ophiuroides* (Munro.) Hack.], a warm season turfgrass. Among strictly cool season grasses, Shearman and Beard (1973) noted that 'Manhattan' perennial ryegrass (*Lolium perenne* L.) was most wear tolerant, followed by 'Kentucky 31' tall fescue (*Festuca arundinacea* Schreb.), 'Merion' Kentucky bluegrass, 'Pennlawn' red fescue (*Festuca*

rubra L.), and Italian ryegrass (*Lolium multiflorum* Lam.). 'Cascade' chewings fescue (*Festuca rubra* var. *commutata* Gaud.) and rough bluegrass were most susceptible to wear stress.

Excessive nitrogen, moisture content extremes, and shade all increase the succulent, delicate nature of turfgrass. Conversely, increased cutting heights, moderate thatch depth, and adequate potassium levels have been reported to increase wear tolerance (Cockerham et al., 1994). Under saline soil conditions, potassium is important for turgor pressure control and maintaining cell wall integrity (Lee et al., 2007). Potassium is the predominate ion that dictates solute potential regulation, and was observed to contribute to over 29% of the total inorganic osmolytes in halophytic seashore paspalum (*Paspalum vaginatum* Sw.). Furthermore, potassium was found to be responsible for enhanced wear tolerance, as a reduction in injury from 35% to 14% occurred from potassium applications (Trenholm et al., 2000, 2001). Wear tolerance was also enhanced by shoot density, leaf lignin content, manganese, and magnesium. A reduction in the leaf total cell wall content was the most prominent factor that compromised seashore paspalum wear tolerance. When comparing the bermudagrasses and seashore paspalums for wear tolerance, ecotype differences were apparent for seashore paspalums; the most wear tolerant seashore paspalums were comparable to bermudagrasses.

Maintaining adequate turgor pressure involves a high solute content, which helps to promote water flow through cells (Carrow, 1995). However, if too much water is present in soils, succulent cells develop that are high in water content, low in solutes, and composed of weaker cell walls. Conversely, dry conditions increase the upper soil profile salt concentration, leading to decreased water uptake.

Compaction, the other primary constituent of traffic stress, involves the pressing together of soil particles, which reduces pore space and increases soil density (Carrow and Petrovic,

1992). On sandy soil, compaction is predominantly considered an insignificant factor. However, fine-textured soils comprised of more silt and clay are more susceptible to compaction. In comparison, stress attributable to wear frequently occurs in turf grown in all soils, regardless of particle size or texture. The upper 7 to 8 cm of soil exhibits the most compaction in turfgrass environments (Beard, 1973). Water content, applied pressure, frequency of pressure, and the extent of vegetative cover also determine the magnitude of compaction.

Modification of the pore-size distribution occurs with compaction as the number of micropores increase at the expense of macropores (Carrow and Petrovic, 1992). The air-water relationship is altered with an increase in moisture retention. In a study that investigated the quality of creeping bentgrass under traffic, increasing the traffic frequency resulted in an increase in bulk density and soil strength in the surface 3 cm (Cuddeback and Petrovic, 1985). Soils higher in bulk density typically hold more water (Baver et al., 1972). While the physical characteristics of the soil can be dramatically altered by compaction, observations of microbial activity have shown that compaction does not influence biological indices of the soil environment (Shestak and Busse, 2005). Along with reduced porosity and increased bulk density, compaction results in the loss of soil structure, increased toxic gases, reduced percolation, and increased surface runoff (Beard, 1973). Moreover, compaction can restrict root growth to the point of plant death.

Primary factors contributing to soil compaction are vehicular and foot traffic on recreational sites. Water droplet impact is a third, less common cause of compaction, and mainly occurs on bare soil. Cohron (1971) observed that bulk density increased by 15% in the surface 2.5 cm during the establishment period due to rain droplets.

Vehicular traffic is determined by tire characteristics and equipment operation (Beard, 1973). As the surface area of tires increases, the pressure on the turf is distributed over a larger area. The pressure per unit area can be reduced by using tires without lugs, low pressure tires, and increasing the number of tires. Avoiding sharp turns, quick starts, and abrupt stops can limit the tearing effects of equipment. Stafford and de Carvalho Mattos (1981) noted that increasing vehicular speed from 0.2 to 5 m s^{-1} reduced compaction by as much as 50% in the upper 5 cm of soil.

Foot traffic from shoes with flat soles leads to abrasive wear, while spiked soles create more damage by tearing and divot removal (Beard, 1973). A 25-fold difference in compacting pressure was observed by Watson (1961) when comparing a person wearing football shoes and street shoes. Also, a 38-fold difference was determined by van Wijk et al. (1977) when assessing the pressure exerted by a running athlete, as compared to when stationary.

Traffic can be reduced and/or controlled by implementing various cultural practices and by strategic landscape design (Beard, 1973). On a golf course, minimizing concentrated, narrow areas of traffic can be done by providing numerous entrances and exits to high use locations such as fairways and greens. Spreading traffic over broad areas and positioning hazards sufficiently far away from greens can also greatly decrease traffic stress on turf.

Cultivation practices can alleviate compaction by improving air and water exchange in the soil. Beard (1973), O'Neil and Carrow (1982), and Sills and Carrow (1982) observed that surface cultivation can be very useful within the same upper 3-cm zone where compaction most significantly affects bulk density. Core and solid-tine aeration, along with slicing, are common procedures used to modify the soil environment and reduce compaction (Beard 1973). The Toro HydroJect (The Toro Company, Bloomington, MN) utilizes a high-pressure water injection

system to aerate soil without causing disruption to the putting surface (Carrow, 2003). The water also helps to alleviate salt accumulation. Carrow (2003) observed that the use of the HydroJect increased the saturated hydraulic conductivity in creeping bentgrass greens by 27 to 45 cm hr^{-1}. Saturated hydraulic conductivity declined after approximately 3 weeks. Using high-pressure water injection on 3-week intervals to supplement other cultivation practices was suggested to maintain high saturated hydraulic conductivity and gas exchange.

Sand topdressing is another common cultural practice used to improve soil characteristics, and consequently, turfgrass conditions. Topdressing aids in the development of a smooth, consistent surface, while providing an effective means of thatch control, soil modification, and winter protection. Topdressing is especially important for putting greens and athletic fields, as a smooth, uniform surface is critical (Rogers et al., 1998). Though the application of sand provides acceptable macroporosity and hydraulic conductivity, sand abrasiveness compromises turfgrass by damaging plant tissue. Rogers et al. (1998) examined the effects of crumb rubber derived from recycled tires as a topdressing material. Two size ranges of 2.0 to 6.0 mm and 0.05 to 2.0 mm were used at various application rates. Shear resistance increased by 20% after the rubber particles settled into the soil surface, and rates exceeding 34.1 t ha^{-1} increased turf cover under trafficked conditions. The smaller size was more effective in protecting the crown tissue area. The study suggested that crumb rubber can be used as a less abrasive topdressing material than sand as a soil amendment to increase turfgrass wear tolerance.

Soil compaction is highly dependent on the soil water content (Beard, 1973). Water films surrounding soil particles facilitate compacting and sliding together of plate-like clay particles, forming a dense, impervious state. Therefore, vehicle use should be avoided during wet conditions, especially on fine-textured soils.

Merkel (1952) found that the soil structure is affected more under saturated conditions than moist conditions. A small degree of compaction can displace soil under saturated conditions because the pore space is filled with water. Irrigation events should be timed in accordance to high traffic intervals to minimize compaction during wet periods (Beard 1973). Moreover, since surface water contents are commonly highest in the spring in most regions, careful attention needs to be directed toward high risk areas during this time.

Precision agriculture involving site-specific management using mobile measurement instrumentation is a relatively new technique (Lui et al., 1996; Bell et al., 2002). Lui et al. (1996) conducted a study using a mobile device equipped with load cells, a depth sensor, radar gun, moisture sensor, and global positioning system (GPS) unit. The moisture sensor was implemented to correct the reference tillage tool draft requirements to estimate the degree of compaction. It was found that the instrument, if operated at a constant speed and depth, could be used to provide a soil texture and compaction index, with adjustments based on moisture content.

Bell et al. (2002) assessed the use of vehicle-mounted optical sensors (VMOS) to measure red (R) and near-infrared (NIR) reflectance. The R and NIR readings were converted to normalized difference vegetative indices (NDVI). The NDVI was closely correlated with turf color and moderately correlated to percent live color evaluations using visual analysis. Turf color and percent live color measurements were evaluated more consistently with the VMOS than by visual readings. It was determined that the VMOS reliably and quickly assessed turfgrass characteristics, and should be considered as a supplemental or replacement procedure for measuring turfgrass characteristics.

Smectite clays (e.g., montmorillonite) exhibit an expanding clay lattice that swells under moist conditions and shrinks during drying periods (Carrow and Petrovic, 1992). Expanding clays are more susceptible to compaction than non-expanding clays (e.g., kaolinite).

Soil O_2 can become a limiting factor when gas exchange between the soil and atmosphere becomes insufficient. Following a rain event, interaggregated air-filled pores are needed for adequate gas exchange. Compaction can destroy the pores, which in turn increases micropores (water-filled pores), decreases macopores (air-filled pores), lowers the total porosity, and disrupts pore continuity. In coarse-textured soils with poor inherent moisture-holding capacity, this could be advantageous. However, excessive and predominantly unavailable moisture would result in finer soils due to enhanced matric potentials under compacted situations. Moreover, there is a loss of infiltration, percolation, and root penetration when macropores are lost. Subsequent problems include standing water, runoff, a perched water table, higher evaporation rates, and reduced irrigation flexibility. As a result, aeration can be substantially compromised, considering O_2 diffusion occurs 10^5 times faster through air than through water. Compacted, moist soils also maintain warm temperatures longer, while taking more time to warm up in the spring.

Reduced water-use has been found to be a significant effect of turfgrass compaction. Morgan et al. (1966) observed that compaction caused a decrease in crop evapotranspiration (ET_c) in common bermudagrass [*Cynodon dactylon* (L.) Pers.]. Perennial ryegrass ET_c decreased by 28% in a compaction study conducted by O'Neil and Carrow (1983).

Despite lower water-use, turf managers often apply more irrigation to turfgrass environments under compacted conditions. This may be in an attempt to compensate for unutilized water moving past the shallow root system, runoff losses, or to stimulate turf recovery.

However, when compaction is the limiting stress, especially due to low soil O_2, additional water can result in further turf deterioration.

Leaf water potential (Ψ_L) can be adversely affected by soil compaction, leading to limited water uptake and drought stress (Agnew and Carrow, 1985). Under compacted conditions, Kentucky bluegrass exhibited lower (more negative) Ψ_L than when grown under uncompacted conditions. Although stomatal response was not associated with decreasing Ψ_L as soil water potential (Ψ_S) decreased, higher stomatal resistance occurred.

The combined affects of wear and compaction in conjunction with limited light has been investigated (Jiang et al., 2003b). In the study, 'Sea Isle1' seashore paspalum was subjected to wear (WD treatment) imposed by a differential slip wear device that applied pressure of 0.90 kg s^{-1} to the study area. The other traffic treatment implemented a studded roller device that mimicked football cleat studs, subjecting study plots to both wear and compaction (WSC treatment). Turf color and density were compromised under both WD and WSC treatments when compared to the control. Furthermore, the WSC treatment exhibited a slower color and density recovery rate than the WD treatment. Morning shade combined with WD resulted in a 9% higher color rating and an 11% higher density than WD with afternoon shade. A 12% higher color rating and 9% higher density occurred when WSC was combined with morning shade, as compared to WSC with afternoon shade.

The assessment of Sea Isle 1 turf quality and canopy spectral reflectance under WD and WSC was conducted by utilizing the first derivative of reflectance (Jiang et al., 2003a). The WSC treatment demonstrated a more significant reduction in shoot density and percent canopy coverage than the WD treatment. Moreover, the first derivative of reflectance was more accurately correlated with canopy temperature than original reflectance. The traffic treatments

were associated with an increase in the significance level of the correlation coefficient. These results draw a parallel to other studies that came to similar conclusions, as it was determined that there is a strong correlation between the first derivative of reflectance and pigment content, biomass, and canopy water content (Blackburn, 1998; Rollin and Milton, 1998).

Chapter 2 presented research on mobile platform spatial mapping to assess water and plant performance across all areas of a golf course fairway. The remaining three studies emphasize using hand-held or limited mapping to determine microclimate differences in selected "microclimates" on a golf course, namely: topographic aspect (Chapter 3), morning shade (Chapter 4), and in this chapter, traffic pattern areas as a microclimate. The golf course study site was predominately sand; wear would be considered the dominant traffic stress. The objective of this study was to assess the microclimatic effects of limited traffic to more intense traffic areas on turfgrass water-use and performance as measured by NDVI in order to optimize the irrigation system design and scheduling for efficiency and uniformity.

MATERIALS AND METHODS

The study was conducted at the Old Collier Golf Club in Naples, FL. The research area consisted of 'Salam' seashore paspalum mowed once weekly at a height of 3.18 cm with a rotary mower. Data collection was initiated following significant rain events, which negated any irrigation uniformity issues pertaining to surface volumetric water content (VWC) (Table A-1, Appendix). Five dry-downs took place during 14 to 16 June, 19 to 20 June, 21 to 23 June, 26 to 29 June, and 12 to 16 July, 2006. No irrigation was applied during dry-downs. Light rain events of 0.48, 0.10, and 0.03 cm occurred during the afternoons of 21 June, 28 June, and 13 July, respectively.

A completely randomized design of two treatments and four replications was used with plots located on the fairway rough area of Fairway 13. The two treatments were low traffic (control) and high traffic. High traffic areas were selected based on frequency of maintenance utility vehicles, mowers, and golf carts traversing the designated plot areas. Plot dimensions were 3 by 6 m.

A hand-held, Field Scout SC 900 (soil compaction meter) evaluated the soil compaction (kPa) between the depths of 0 to 20 cm at 2.5-cm intervals (Spectrum Technologies, Inc. Plainfield, IL). A cone is affixed to the bottom of the stainless steal shaft, which is steadily inserted into the soil to the desired depth. The SC 900 measures the cone index data to determine compaction. The penetration depth is measured by an ultrasonic depth sensor located at the base of the meter. The sensor emits a sound wave and measures the return time of the reflected wave. Two measurements per plot were taken after rain events on the first day of each dry down (Table 5.1).

Basic data collection was performed via the Toro Mobile Multi-Sensor (TMM; patent pending) prototype data acquisition unit (The Toro Company, Bloomington, MN). The TMM measures VWC (%), NDVI (unit-less; best = 1.0), and compaction (penetrometer resistance; kg). The TMM was affixed to and maneuvered with a utility vehicle. An operating speed of 2.7 to 3.3 km h^{-1} was maintained during data acquisition. Study plots were dew-whipped prior to TMM use to reduce the potential influence of dew on NDVI. Plot length was such that two readings per plot were obtained when the TMM traversed the plots. Data were recorded using an on-board laptop computer and all parameters were displayed in spreadsheet format.

Soil moisture measurements were based on time-domain reflectometry (TDR), which measures changes in the soil dielectric constant (ε) as water contents fluctuate (Leib et al., 2003).

A TDR sensor produces a high frequency voltage pulse that is transmitted and reflected along metal probes. The dielectric constant is determined by measuring the velocity of the transmitted pulse in the soil, which is primarily dependent upon the VWC, as water has a significantly higher dielectric constant than air ($\varepsilon = 80$ and 1, respectively). The permittivity and corresponding pulse velocity are closely related to the soil water content (Plauborg et al., 2005).

The electrical conductivity (EC_a) of soil can greatly affect TDR measurements by promoting erroneous overestimates of water content (Nadler et al., 1999). Salinity is a major contributing factor to EC_a, suggesting that negligible salinity levels should be verified before taking TDR measurements. A hand-held Landmapper ERM-0l (Landviser, Inc. Westhampton, NJ) measured the electrical resistance (ER; ohm m^{-1}) in the study plots, which was subsequently converted to EC_a (Table A-2, Appendix). The EC_a was measured to verify the absence of significant salt concentrations in the soil prior to data acquisition. This device is based on determining apparent EC_a using the four-wenner array method as described by Rhoades et al. (1999).

A Spectrum Field Scout TDR 100 soil moisture sensor (TMM_{10}) was modified for use on the TMM platform and used to determine VWC at a 0- to 10-cm depth. Two custom stainless steel probes of 9.53-mm diameter, 3.3-cm spacing, and 10-cm length were installed on the moisture sensor to facilitate a soil penetration depth of 10 cm. The sampling volume is an elliptical cylinder extending 3 cm radially beyond the TDR probes, measuring approximately 825 cm^3. The sensor is attached to one end of a shaft on the TMM, while a bolt is connected to the opposite end. When the TMM moves, the wheel-driven shaft rotates in a circular fashion. As the sensor's probes enter the ground, the bolt passes by a series of magnets that triggers the data logger to take a measurement. The probes are inserted into the soil approximately every 2.5

m. Two readings per plot were taken between the time period of 0900 to 1030 h EST. Additional readings were taken within a time period of 1800 to 2000 h EST on select days. Exceeding 3.5 km h^{-1} significantly increased the probability of obtaining erroneous VWC readings. Possible theories as to the cause of this problem are that the bolt was passing by the magnets too quickly and/or the TDR probes were being inserted too quickly to facilitate a VWC measurement.

A GreenSeeker RT100 active sensor (NTech Industries, Inc. Ukiah, CA; TMM_{NDVI}) evaluated turf canopy NDVI in the study plots. The NDVI, which measures multispectral reflectance, has been shown to be significantly associated with visual turf quality, density, and shoot tissue injury (Trenholm et al., 1999). The sensor is equipped with internal light emitting diodes and a photodiode optical detector that measures the percent reflectance of the red (R = 660 nm) and near-infrared (NIR = 770 nm) spectral bands {$NDVI = [(R_{770} - R_{660})/(R_{770} + R_{660})]$}. The sensor is mounted on the TMM at a height of approximately 1 m and evaluates a 60- ± 10-cm by 1.52- ± 0.51-cm field of view. The sensor emits light pulses every 100 ms and outputs an averaged value every second. Depending on operating speed, six to eight readings per plot were recorded between the time period of 0900 to 1030 h EST. Additional readings were taken within a time period of 1800 to 2000 h EST on select days. The sensor only detects the light emitted, thereby preventing any possible influence of sunlight on the measurements.

An Omega LC302-500 1.90-cm diameter stainless steel compression load cell (Omega Engineering, Inc. Stamford, CT) was used to measure insertion force (kg) of the TDR moisture sensor probes. As the probes penetrate the soil, pressure is exerted against the load cell, indicating the degree of soil compaction. The load cell converts the load acting on it to electrical signals, which are used to calculate the penetrometer resistance. Load cell penetrometer data are

not presented in this paper since the site was very high in sand content and exhibited few high penetrometer resistance measurements.

Additional data were obtained with various hand-held devices to facilitate comparison with the TMM device as well as to supplement the data obtained by the TMM. All hand-held data acquisition utilized the same sampling method as the TMM, as measurements were taken in the same general areas of the study plots to maximize the integrity of the research. A hand-held Spectrum Field Scout TDR 300 unit (HH_{12} and HH_{20}) measured VWC of the 0- to 12-cm and 0- to 20-cm depths. The sensor is equipped with two stainless steel probes of 5-mm diameter, 3.3-cm spacing, and 12- or 20-cm length. The sampling volumes are elliptical cylinders extending 3 cm radially beyond the TDR probes, measuring approximately 905 and 1510 cm^3 for the 12- and 20-cm probes, respectively. Measurements were taken at the 0- to 12-cm depth daily within a time period of 0900 to 1030 h EST. Additional data were acquired within a time period of 1800 to 2000 h EST on select days. Two readings per plot were taken during the first four dry-downs, while five readings per plot were recorded for the 12 to 16 July, 2006 dry-down. The VWC was measured from 0 to 20 cm once daily at 1300 to 1400 h EST. Two readings per plot were taken at the 0- to 20-cm depth. The 10-, 12-, and 20-cm VWC measurements were used to estimate ET_c during various durations of the study: $ET_c = [(VWC_{inititial} - VWC_{final})/100] \times depth$.

A hand-held, Spectrum Field Scout TCM 500 (turf color meter) evaluated the turf canopy NDVI $[(R_{850} - R_{680})/(R_{850} + R_{680})]$ in the study plots. Similarly, the leaf area index (IR/R, best = highest value) was calculated (R_{850}/R_{680}). The TCM 500 measures a 7.6-cm diameter target (45.36-cm^2 area). The instrument contains an internal light source, thereby eliminating external effects of sunny or cloudy conditions. The TCM 500 is placed directly on the ground to make a measurement. Two readings per plot were taken once daily within a time period from 1300 to

1400 h EST. Based on the results in Krum (Chapter 2), which demonstrated inconsistent results, and because of the small sampling area (compared to the TMM_{NDVI}), the hand-held NDVI results were not presented for this study.

An Everest Interscience 100.3ZL hand-held infrared thermometer measured the canopy temperature (°C) of the plots (Everest Interscience, Inc. Tucson, AZ). The thermometer measures the infrared radiation (approximately 700 to 1000 nm) that is emitted from the turfgrass by using an optical infrared detector. The detector converts the radiation to a proportional signal. The temperature is the electrical analog of the infrared radiation. Two readings per plot, one north facing and one south facing, were taken once daily within a time period from 1300 to 1400 h EST, under sunny conditions. The instrument was held at a height of 1 m at a 45° angle.

Data were analyzed using the Statistical Analysis System (SAS Institute, Inc. Cary, NC; version 9.1) and statistical differences were determined by the Generalized Linear Model (GLM) procedure in conjunction with the least significant difference (LSD) t-test at a 0.10 significance level.

RESULTS and DISCUSSION

The research study area averaged 97 and 96% sand for the low and high traffic plots with organic matter content of 3.65 and 3.18% (dry wt.), respectively (Table A-3, Appendix). Carrow and Petrovic (1992) reported that wear could reduce thatch on turfgrasses. This or perhaps greater wear stress causing lower biomass production may account for the relatively low organic matter content. While wear was the dominant stress, there were differences in penetrometer resistance averaged over the 0- to 20-cm zone through the 21 June readings (Table 5.1). Higher penetrometer readings would indicate some compaction even in this high sand, where the compaction would likely be in the form of more settling of sand particles into a denser mass.

Volumetric water content measurements using the three TDR devices (TMM_{10}, HH_{12}, and HH_{20}) obtained on the first day of dry-downs provided an estimate of VWC at field capacity (Tables 5.2 to 5.4). Field capacity estimates varied with TDR instruments because of different sampling volumes. Field capacity VWC for the low traffic plots was significantly higher than in the high traffic plots on most dates for all TDR devices. A different field capacity baseline when comparing microclimates is an example of spatial variability of soil water. This is one of the challenges for implementation of precision agriculture (PA) or precision turf management (PTM) concepts to irrigation scheduling as reported by Van Pelt and Wierenga (2001), Starr (2005), and Duffera et al. (2007). Krum (Chapter 4) noted (on the same golf course that the traffic microclimate study was conducted) that field capacity VWC was less for a shaded microclimate versus full sunlight and discussed how a different baseline for field capacity is an important site characteristic to recognize, since it may influence site-specific irrigation frequency or rate.

VWC data were also reported on a basis of percent of field capacity at the end of dry-downs, such as used in the allowable water depletion (AWD) approach (Tables 5.2 to 5.4) (SCS, 1993; Smarjstria et al., 2006). There was not any apparent treatment response trend regardless of the TDR device when comparing VWC using field capacity as a 100% baseline.

Estimated turfgrass ET was compared using three approaches. Daily readings (i.e., calculated from the difference in a.m. to p.m. VWC) and gross ET (i.e., the summation of daily a.m. to p.m. ET values for the particular dry-down period) provide two measures of estimated ET. A third estimate of ET is the net ET calculated from the first to last day VWC of each dry-down. The net ET differs from the gross ET because of a tendency for VWC to increase from the evening to the following morning. The VWC reading exhibited this tendency on 13 July p.m compared to the 14 July a.m. VWC for both the TMM_{10} (Table 5.2) and HH_{12} (Table 5.3)

devices. Capillary rise or dew could be responsible for this pattern, despite plots being dew-whipped prior to data acquisition.

When using the TMM_{10} to determine VWC from the plots, no differences between treatments were noted for daily, net, or gross ET (Table 5.5). For the HH_{12} unit, significant daily differences were observed on two dates (19 June a.m. and p.m.; 27 June a.m. and p.m.) and during two time periods (15 to 16 June; 19 to 20 June), with the high traffic plots showing lower estimated ET (Table 5.6). For the 12 to 16 July dry-down, the gross ET was lower for the high traffic plots compared to the low traffic plots, with gross ET of 1.82 and 2.16 cm, respectively. When averaged over all dates or time periods when significant treatment differences occurred, low traffic and high traffic estimated ET values were 1.22 and 0.72 cm, respectively. Thus, high traffic plots exhibited an average of 59% ET compared to the low traffic plots on dates when significant traffic treatment differences were observed. Similar results occurred using the HH_{20} probe, where a 59% reduction in net ET in the high traffic plots over the 26 to 29 June period was noted (Table 5.7).

Turfgrass performance was evaluated using NDVI spectral reflectance because it provides an indication of turfgrass quality, density, and color (Table 5.8) (Trenholm et al., 1999; Bell et al., 2002). Canopy temperature was monitored as another indicator or stress (Table 5.9). High traffic caused a reduction in NDVI during the 12 to 16 July dry-down on several of the p.m. measurements; high traffic exhibited a greater NDVI reduction between the a.m. and p.m. ratings on two days. The statistical treatment differences for NDVI found during the 12 to 16 July dry-down were also apparent in the VWC versus NDVI linear relationship of $r^2 = 0.30$ (Figure 5.1). Thus, the high traffic microclimate, which differed from the low traffic microclimate in terms of lower VWC, also displayed lower turf performance. Canopy temperature differences between

treatments were observed on 13 July and over the 21 to 23 July period, with high traffic plots exhibiting higher canopy temperatures (Table 5.9). This would suggest that high traffic was resulting is some degree of turfgrass stress.

Both soil compaction and wear can occur when turfgrass sites are subjected to stress, but usually only one is dominant; wear is predominant on sands that resist soil compaction. Carrow and Petrovic (1992) reviewed traffic stresses on turfgrass and reported several studies that showed a reduction in water-use under soil compaction, including early work by Morgan et al. (1966) on common bermudagrass. However, the author could not find any research reporting the influence of wear on turfgrass water-use. The reduced ET under higher traffic could be caused by somewhat lower canopy biomass or leaf area index as suggested by the reduction in NDVI, or slower shoot growth rate observed for turfgrass under traffic stresses (Carrow and Petrovic, 1992).

REFERENCES

Agnew, M.L., and R.N. Carrow. 1985. Soil compaction and moisture stress preconditioning on Kentucky bluegrass. II. Stomatal resistance, leaf water potential, and canopy temperature. Agron. J. 77:878-884.

Baver, L.D., W.H. Gardner, and W.R. Gardner. 1972. Soil Physics, 4th ed. John Wiley and Sons, New York. p. 498.

Beard, J.B. 1973. Turfgrass: Science and culture. Prentice-Hall, Englewood Cliffs, NJ.

Bell, G.E., D.L. Martin, S.G. Wiese, D.D. Dobson, M.W. Smith, M.L. Stone, and J.B. Solie. 2002. Vehicle-mounted optical sensing: an objective means for evaluating turf quality. Crop Sci. 42:197-201.

Blackburn, G.A. 1998. Quantifying chlorophylls and carotenoids at leaf and canopy scales: An evaluation of some hyperspectral approaches. Remote Sens. Environ. 66:273-285.

Carrow R.N. 1995. Wear stress on turfgrass. Golf Course Manage. 63(9):49-53.

Carrow, R.N. 2003. Surface organic matter in bentgrass greens. USGA Turfgrass and Environmental Research Online. 2(17):1-12.

Carrow, R.N., and A.M. Petrovic. 1992. Effects of traffic on turfgrass. Agron. Monogr. 32. ASA-CSSA-SSSA, Madison, WI.

Cockerham, S.T., V.A. Gibeault, and M. Borgonovo. 1994. Effects of nitrogen and potassium on high-trafficked sand rootzone turfgrass. California Turfgrass Culture. 44:4-6.

Cohron, G.T. 1971. Forces causing soil compaction. p. 106-122. *In* K.K. Barnes (ed.) Compaction of agricultural soil. Am. Soc. Agric. Eng., St. Joseph, MI.

Cuddeback, S., and A.M. Petrovic. 1985. Traffic effects on the growth and quality of *Agrostis palustris* Huds. p. 411-416. *In* F. Lemaire (ed.) Proc. Int. Turfgrass Res. Conf., 5th, Avignon. 1-5 July 1985. INRA Publ., Versailles, France.

GCSAA News Weekly. 13 Jan. 2005. Product News. Available at www.gcsaa.org/newsweekly/2005/jan/2/divmix.asp (cited 27 July 2007; verified 21 Apr. 2008)

Jiang, Y., R.N. Carrow, and R.R. Duncan. 2003a. Correlation analysis procedures for canopy spectral reflectance data of seashore paspalum under traffic stress. HortScience. 128(3):343-348.

Jiang, Y., R.N. Carrow, and R.R. Duncan. 2003b. Effects of morning and afternoon shade in combination with traffic stress on seashore paspalum. HortScience. 38:1218-1222.

Lee, G.J., R.R. Duncan, and R.N. Carrow. 2007. Nutrient uptake responses and inorganic ion contribution to solute potential under salinity stress in halophytic seashore paspalums. *In review*.

Leib, B.G., J.D. Jabro, and G.R. Matthews. 2003. Field evaluation and performance comparison of soil moisture sensors. Soil Sci. 168:396-409.

Lui, W., S.K. Upadhyaya, T. Kataoka, and S. Shibusawa. 1996. Development of a texture/soil compaction sensor. p. 617-630. *In* P.C. Robert et al. (ed.) Proc. Int. Prec. Agric. Conf., 3rd, Minneapolis, MN. 23-26 Jun. 1996. ASA-CSSA-SSSA, Madison, WI.

Merkel, E.J. 1952. The effect of aerification on water absorption and runoff. Pennsylvania State College 21st Annual Turf Conference. p. 1-2.

Morgan, W.C., J. Letey, S.J. Richards, and N. Valoras. 1966. Physical soil amendments, soil compaction, irrigation, and wetting agents in turfgrass management I. Effects on compactability, water infiltration rates, evapotranspiration, and numbers of irrigations. Agron. J. 58:525-535.

O'Neil, K.J., and R.N. Carrow. 1982. Kentucky bluegrass growth and water-use under different soil compaction and irrigation regimes. Agron. J. 74:933-936.

O'Neil, K.J., and R.N. Carrow. 1983. Perennial ryegrass growth, water-use and soil aeration status under soil compaction. Agron. J. 75:177-180.

Plauborg, F., B.V. Iverson, and P.E. Laerke. 2005. In situ comparison of three dielectric soil moisture sensors in drip irrigated sandy soils. Vadose Zone J. 4:1037-1047.

Rogers, J.N. III, J.T. Vanini, and J.R. Crum. 1998. Simulated traffic on turfgrass topdressed with crumb rubber. Agron. J. 90:215-221.

Rollin, E.M., and E.J. Milton. 1998. Processing of high spectral resolution reflectance data for the retrieval of canopy water content information. Remote Sens. Environ. 65:86-92.

Shearman R.C., and J.B. Beard. 1975. Turfgrass wear tolerance mechanisms: I. Wear tolerance of seven turfgrass species and quantitative methods for determining turfgrass wear injury. 1975. Agron. J. 67:208-211.

Shestak C.J., and M.D. Busse. 2005. Compaction alters physical but not biological indices of soil health. Soil Sci. Soc. Am. J. 69:236-246.

Sills, M.J., and R.N. Carrow. 1982. Soil compaction effects on turfgrass use in tall fescue. J. Am. Soc. Hortic. Sci. 107:934-937.

Stafford, J.V, and P. de Carvalho Mattos. 1981. The effect of forward speed on tractor wheel-induced soil compaction: Laboratory simulation and field experiments. J. Agric. Eng. Res. 26:333-347.

Trenholm, L.E., R.N. Carrow, and R.R. Duncan. 1999. Relationship of multispectral radiometry data to qualitative data in turfgrass research. Crop Sci. 39:763-769.

Trenholm L.E., R.R. Duncan, and R.N. Carrow. 2000. Mechanisms of wear tolerance in seashore paspalum and bermudagrass. Crop Sci. 40:1350-1357.

Trenholm L.E., R.R. Duncan, R. N. Carrow, and G.H. Snyder. 2001. Influence of silica on growth, quality, and wear tolerance of seashore paspalum. J. Plant Nutr. 24(2):245-259.

Van Wijk, A.L.M., W.B. Verhaegh, and J. Beuving. 1977. Grass sportsfields: Top layer compaction and soil aeration. Rasen Turf Gazon 8:47-52.

Watson, J.R. 1961. Soil physical effects of traffic. p. 1-9. *In* Proc. Texas Turf Conf., 16th, College Station. TX. Texas A&M Univ., College Station, TX.

Table 5.1. Soil compaction throughout the 0- to 20-cm depth at the initiation of dry-downs.

Date	Treatment		F-test	CV
	Low Traffic	High Traffic		
	kPa			%
14 June	1379	1696	0.04†	11
19 June	1385	1673	<0.01†	4
21 June	1346	1623	0.01†	8
26 June	1513	1698	0.18	11
12 July	1567	1697	0.28	10

† Significant at a 0.10 probability level.

Table 5.2. Influence of traffic on 10-cm volumetric water content (VWC) during dry-down periods (mobile unit).

Date	Treatment		F-test	CV
	Low Traffic	High Traffic		
14 - 16 June	%			%
14 June	26.8	23.5	0.35	18
15 June	23.1	19	0.27	23
16 June	19.5 (73)#	15.8 (67)	0.32	27
19 - 20 June	%			%
19 June	26.8	18.3	0.01†	12
20 June	23.1 (86)	15.0 (82)	0.03†	22
21 - 23 June‡	%			%
21 June	27.8	18.5	0.01†	15
22 June	24.0	15.2	0.01†	16
23 June am	21.3	14.8	0.01†	13
23 June pm	17.1 (62)	12.2 (66)	0.03†	17
26 - 29 June§	%			%
26 June	29.0	20.7	0.01†	12
27 June	23.6	15.5	<0.01†	10
28 June am	22.5	13.8	0.01†	16
28 June pm	23.9	15.2	<0.01†	15
29 June am	22.3	14.0	0.02†	20
29 June pm	19.3 (67)	11.8 (57)	0.03†	24
12 - 16 July¶	%			%
12 July am	24.4	18.5	0.13	22
12 July pm	21.5	17.2	0.12	17
13 July am	19.3	14.0	0.09†	22
13 July pm	19.8	16.0	0.30	26
14 July am	21.1	19.0	0.55	23
14 July pm	22.8	15.0	0.12	32
15 July am	22.1	18.8	0.37	24
15 July pm	14.5	11.0	0.33	37
16 July am	15.5	12.2	0.36	34
16 July pm	12.5 (51)	9.8 (53)	0.28	29

† Significant at a 0.10 probability level.

‡ A 0.48-cm rainfall occurred during the afternoon of 21 June following data acquisition.

§ A 0.10-cm rainfall occurred during the afternoon of 28 June prior to pm data acquisition.

¶ A 0.03-cm rainfall occurred during the afternoon of 13 July prior to pm data acquisition.

Data in parentheses indicate percent of field capacity (100%) at dry-down termination.

Table 5.3. Influence of traffic on 12-cm volumetric water content during dry-down periods (hand-held unit).

Date	Treatment		F-test	CV
	Low Traffic	High Traffic		
14 - 16 June	%			%
14 June am	28.9	21.5	0.09†	21
14 June pm	29.8	17.8	<0.01†	8
15 June	29.6	19.8	<0.01†	9
16 June	19.1 (68)#	15.8 (73)	0.18†	17
19 - 20 June	%			%
19 June am	28.4	18.5	<0.01†	12
19 June pm	22.8	16.5	0.02†	13
20 June am	23.6	14.7	0.05†	26
20 June pm	17.5 (62)	10.8 (58)	<0.01†	15
21 - 23 June‡	%			%
21 June am	32.1	19.2	0.01†	18
21 June pm	28.0	18.5	0.01†	15
22 June am	27.3	17.8	<0.01†	13
22 June pm	19.6	12.8	0.12	33
23 June am	22.1	14.3	0.01†	17
23 June pm	18.0 (56)	11.3 (59)	<0.01†	10
26 - 29 June§	%			%
26 June am	29.3	21.3	0.01†	12
26 June pm	26.9	17.0	<0.01†	13
27 June am	24.9	14.5	<0.01†	17
27 June pm	19.4	12.8	0.06†	25
28 June am	21.6	13.8	0.02†	20
28 June pm	23.4	14.7	0.01†	18
29 June am	19.8	12.2	0.01†	18
29 June pm	18.5 (63)	11.5 (54)	0.04†	26
12 - 16 July¶	%			%
12 July am	28.0	19.5	0.02†	16
12 July pm	25.7	17.6	0.02†	17
13 July am	26.2	17.3	0.02†	19
13 July pm	26.8	17.7	0.02†	18
14 July am	27.9	19.7	0.03†	17
14 July pm	23.0	15.3	0.04†	21
15 July am	26.6	18.5	0.06†	22
15 July pm	20.3	13.3	0.08†	27
16 July am	22.7	15.0	0.06†	25
16 July pm	18.0 (64)	11.2 (57)	0.13	38

† Significant at a 0.10 probability level.

‡ A 0.48-cm rainfall occurred during the afternoon of 21 June prior to pm data acquisition.

§ A 0.10-cm rainfall occurred during the afternoon of 28 June prior to pm data acquisition.

¶ A 0.03-cm rainfall occurred during the afternoon of 13 July prior to pm data acquisition.

Data in parentheses indicate percent of field capacity (100%) at dry-down termination.

Table 5.4. Influence of traffic on 20-cm volumetric water content (VWC) during dry-down periods (hand-held unit).

Date	Treatment		F-test	CV
	Low Traffic	High Traffic		
	%			%
14 - 16 June				
14 June	27.0	23.3	0.33	19
15 June	20.9	17.7	0.23	18
16 June	16.5 (61)	14.5 (62)	0.30	16
	%			%
19 - 20 June				
19 June	25.4	18.2	0.09†	23
20 June	19.0 (75)	11.8 (65)	0.02†	21
	%			%
21 - 23 June‡				
21 June	23.3	16.7	0.01†	11
22 June	22.6	15.7	0.01†	13
23 June	17.8 (76)	10.8 (65)	0.03†	24
	%			%
26 - 29 June§				
26 June	25.8	15.7	<0.01†	10
27 June	21.9	15.0	0.07†	24
28 June	18.0	11.2	0.03†	23
29 June	16.4 (64)	10.2 (65)	0.08†	31
	%			%
12 - 16 July¶				
12 July	22.4	15.5	0.11	28
13 July	20.5	13.8	0.10†	29
14 July	20.9	13.2	0.12	35
15 July	18.8	11.8	0.05†	26
16 July	16.1 (72)	10.7 (69)	0.10†	30

† Significant at a 0.10 probability level.

‡ A 0.48-cm rainfall occurred during the afternoon of 21 June following data acquisition.

§ A 0.10-cm rainfall occurred during the afternoon of 28 June following data acquisition.

¶ A 0.03-cm rainfall occurred during the afternoon of 13 July following data acquisition.

Data in parentheses indicate percent of field capacity (100%) at dry-down termination.

Table 5.5. Influence of traffic on 10-cm evapotranspiration (ET) during dry-down periods (mobile unit).

Date	Treatment		F-test	CV
	Low Traffic	High Traffic		
14 - 16 June	cm			%
14 - 15 June	0.37	0.48	0.82	130
15 - 16 June	0.37	0.32	0.93	211
14 - 16 June (N)‡	0.74	0.78	0.84	38
19 - 20 June	cm			%
19 - 20 June (N)	0.36	0.33	0.91	99
21 - 23 June§	cm			%
21 - 22 June	0.38	0.34	0.91	140
23am - 23pm	0.42	0.27	0.27	50
21 - 23 June (N)	1.06	0.63	0.13	41
26 - 29 June¶	cm			%
26 - 27 June	0.55	0.52	0.91	45
28am - 28pm	-0.14	-0.14	0.98	-161
29am - 29pm	0.30	0.22	0.60	82
26 - 29 June (N)	0.98	0.89	0.81	55
12 - 16 July#	cm			%
12am - 12pm	0.29	0.14	0.19	71
13am -13pm	-0.05	-0.20	0.49	-231
14am - 14pm	-0.17	0.41	0.11	377
15am - 15pm	0.77	0.80	0.93	41
16am - 16pm	0.30	0.24	0.70	88
∑12 - 16 July (G)	1.15	1.37	0.54	39
12am - 16pm (N)	1.21	0.88	0.18	29

† Significant at a 0.10 probability level.

‡ (G) and (N) indicate estimated gross and net ET at dry-down termination, respectively.

§ A 0.48-cm rainfall occurred during the afternoon of 21 June following data acquisition.

¶ A 0.10-cm rainfall occurred during the afternoon of 28 June prior to pm data acquisition.

A 0.03-cm rainfall occurred during the afternoon of 13 July prior to pm data acquisition.

Table 5.6. Influence of traffic on 12-cm evapotranspiration (ET) during dry-down periods (hand-held unit).

Date	Treatment		F-test	CV
	Low Traffic	High Traffic		
14 - 16 June	cm			%
14am - 14pm	-0.11	0.45	0.24	352
14 - 15 June	-0.09	0.20	0.61	1368
15 - 16 June	1.28	0.49	0.01†	36
14 - 16 June (N)‡	1.19	0.69	0.27	62
19 - 20 June	cm			%
19am - 19pm	0.69	0.20	0.02†	52
20am - 20pm	0.75	0.41	0.38	86
19am - 20pm (N)	1.33	0.88	0.07†	26
21 - 23 June§	cm			%
21am - 21pm	0.50	0.08	0.26	164
22am - 22pm	0.93	0.61	0.41	66
23am - 23pm	0.50	0.37	0.54	68
∑21 - 23 June (G)	1.94	1.06	0.18	55
21am - 23pm (N)	1.72	0.96	0.14	48
26 - 29 June¶	cm			%
26am - 26pm	0.29	0.53	0.44	99
27am - 27pm	0.67	0.20	0.01†	23
28am - 28pm	-0.21	-0.10	0.57	-167
29am - 29pm	0.15	0.08	0.63	170
∑26 - 29 June (G)	0.90	0.71	0.68	77
26am - 29pm (N)	1.31	1.20	0.81	51
12 - 16 July#	cm			%
12am - 12pm	0.29	0.23	0.56	48
13am -13pm	-0.07	-0.05	0.84	-266
14am - 14pm	0.60	0.54	0.17	10
15am - 15pm	0.77	0.63	0.50	39
16am - 16pm	0.57	0.46	0.35	29
∑12 - 16 July (G)	2.16	1.82	0.06†	10
12am - 16pm (N)	1.22	1.01	0.42	30

† Significant at a 0.10 probability level.

‡ (G) and (N) indicate estimated gross and net ET at dry-down termination, respectively.

§ A 0.48-cm rainfall occurred during the afternoon of 21 June prior to pm data acquisition.

¶ A 0.10-cm rainfall occurred during the afternoon of 28 June prior to pm data acquisition.

A 0.03-cm rainfall occurred during the afternoon of 13 July prior to pm data acquisition.

Table 5.7. Influence of traffic on 20-cm evapotranspiration (ET) during dry-down periods (hand-held unit).

Date	Treatment		F-test	CV
	Low Traffic	High Traffic		
14 - 16 June	cm			%
14 - 15 June	1.24	1.15	0.82	46
15 - 16 June	0.89	0.64	0.38	48
14 - 16 June	2.13	1.79	0.42	28
19 - 20 June	cm			%
19 - 20 June	1.30	1.44	0.73	42
21 - 23 June‡	cm			%
21 - 22 June	0.13	0.20	0.81	262
22 - 23 June	0.99	0.98	0.98	51
21 - 23 June	1.12	1.33	0.61	46
26 - 29 June§	cm			%
26 - 27 June	0.79	0.14	0.20	138
27 - 28 June	0.79	0.78	0.98	63
28 - 29 June	0.33	0.20	0.66	147
26 - 29 June	1.91	1.12	0.08†	36
12 - 16 July¶	cm			%
12 - 13 July	0.38	0.34	0.73	45
13 - 14 July	-0.08	0.14	0.31	901
14 - 15 July	0.43	0.27	0.76	201
15 - 16 July	0.53	0.24	0.18	73
12 - 16 July	1.27	0.98	0.41	41

† Significant at a 0.10 probability level.

‡ A 0.48-cm rainfall occurred during the afternoon of 21 June following data acquisition.

§ A 0.10-cm rainfall occurred during the afternoon of 28 June following data acquisition.

¶ A 0.03-cm rainfall occurred during the afternoon of 13 July following data acquisition.

Table 5.8. Influence of traffic on normalized difference vegetative index (NDVI) during dry-down periods (mobile unit).

Date‡	Treatment		F-test	CV
	Low Traffic	High Traffic		
14 - 16 June				%
14 June	0.797	0.792	0.85	4
15 June	0.748	0.755	0.83	6
16 June	0.739	0.748	0.79	6
14 - 16 June	0.058	0.043	0.42	47
26 - 29 June§				%
26 June	0.868	0.870	0.81	1
27 June	0.847	0.847	0.98	2
28 June am	0.844	0.845	0.88	1
28 June pm	0.855	0.854	0.90	1
29 June am	0.851	0.852	0.94	2
29 June pm	0.832	0.834	0.86	1
26 - 29 June#	0.036	0.037	0.92	31
12 - 16 July¶				%
12 July am	0.881	0.869	0.16	1
12 July pm	0.864	0.852	0.08†	1
13 July am	0.867	0.856	0.22	1
13 July pm	0.870	0.859	0.16	1
14 July am	0.875	0.872	0.77	2
14 July pm	0.867	0.848	0.06†	1
15 July am	0.878	0.869	0.13	1
15 July pm	0.860	0.843	0.04†	1
16 July am	0.872	0.861	0.13	1
16 July pm	0.852	0.831	0.13	2
12am - 12pm#	0.018	0.018	1.00	26
13am - 13pm#	-0.004	-0.003	0.92	-181
14am - 14pm#	0.008	0.025	0.05†	62
15am - 15pm#	0.018	0.026	0.01†	15
16am - 16pm#	0.020	0.030	0.30	53
12am - 16pm#	0.029	0.038	0.49	54

† Significant at a 0.10 probability level.

‡ The mobile NDVI data were not recorded from 19 June to 23 June.

§ A 0.10-cm rainfall occurred during the afternoon of 28 June prior to pm data acquisition.

¶ A 0.03-cm rainfall occurred during the afternoon of 13 July prior to pm data acquisition.

NDVI change.

Table 5.9. Influence of traffic on canopy temperature during dry-down periods.

Date	Treatment		F-test	CV
	Low Traffic	High Traffic		
14 - 16 June	°C			%
14 June	29.3	30.1	0.44	5
15 June	29.4	29.4	0.97	6
16 June	25.6	26.0	0.78	7
19 - 20 June	°C			%
19 June	26.5	27.2	0.72	9
20 June	34.5	33.9	0.65	5
21 - 23 June‡	°C			%
21 - 22 June	30.4	30.9	0.73	7
22 - 23 June	26.6	26.2	0.85	12
21 - 23 June	30.8	32.6	0.06†	3
26 - 29 June§	°C			%
26 June	35.3	34.5	0.51	5
27 June	29.3	28.4	0.35	5
28 June	30.3	29.7	0.14	2
29 June	29.4	29.7	0.76	4
12 - 16 July¶	°C			%
12 July	26.9	26.6	0.57	3
13 July	22.4	23.2	0.03†	2
14 July	30.0	30.3	0.43	2
15 July	29.6	30.0	0.74	6
16 July	25.8	26.2	0.84	12

† Significant at a 0.10 probability level.

‡ A 0.48-cm rainfall occurred during the afternoon of 21 June following data acquisition.

§ A 0.10-cm rainfall occurred during the afternoon of 28 June following data acquisition.

¶ A 0.03-cm rainfall occurred during the afternoon of 13 July following data acquisition.

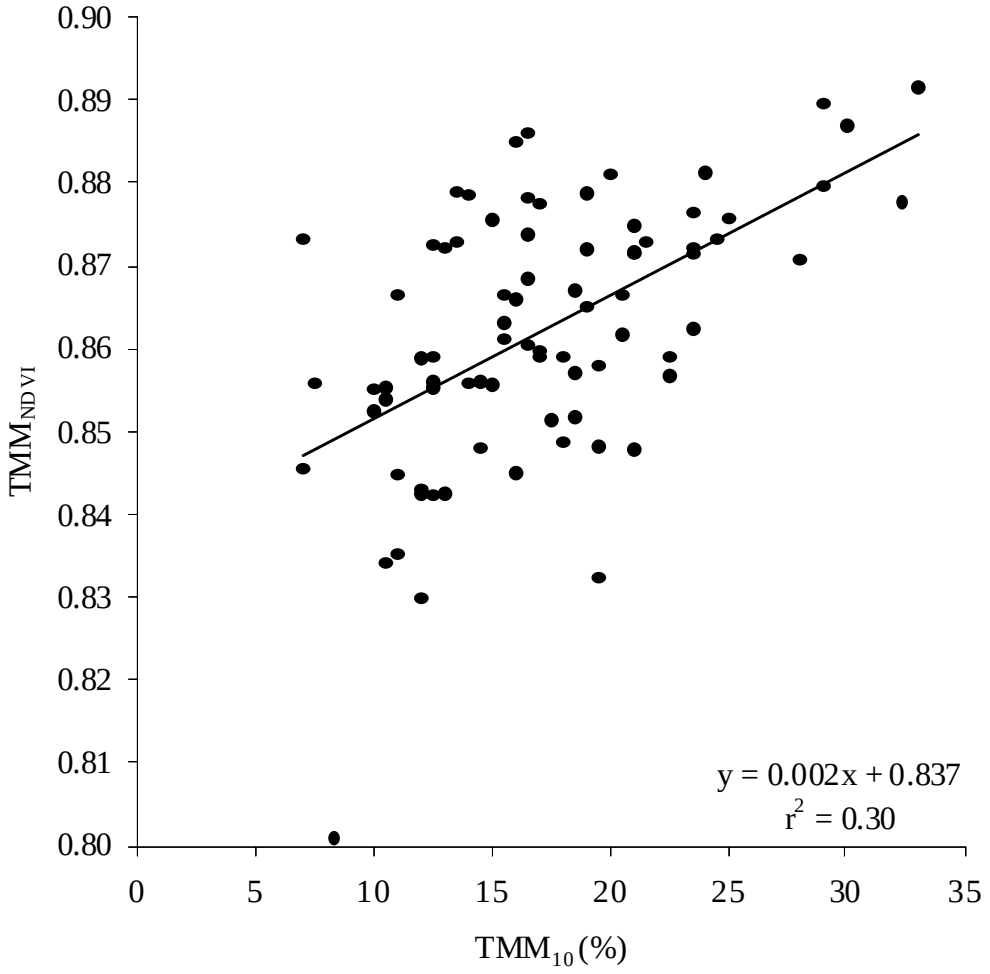

Figure 5.1. Linear relationship between TMM_{10} (mobile) volumetric water content (VWC) and TMM_{NDVI} (mobile) normalized difference vegetative index (NDVI) consisting of low and high traffic treatments and replications during the 12 to 16 July dry-down.

CHAPTER 6

CONCLUSIONS

An essential requirement for principles of precision agriculture (PA) to be applied to turfgrass situations and foster a parallel precision turfgrass management (PTM) philosophy is the ability to obtain site-specific information in a timely and detailed fashion. In PA the initial use of detailed spatial mapping is normally to define site-specific management units (SSMUs), which are within-field areas similar in crop performance because of similarities in soil and microclimate properties. The first experimental mobile platform unit developed for turfgrass situations to obtain spatial and temporal soil and plant data over large landscape areas was the Toro Mobile Multi-Sensor (TMM; patent pending) (The Toro Company, Bloomington, MN). The TMM is capable of rapid measurement of GPS referenced (Global Positioning System) soil volumetric water content (VWC) and penetrometer resistance in the surface 0- to 10-cm zone; the TMM also measures turfgrass performance by normalized difference vegetative index (NDVI). We used the TMM for a spatial and temporal mapping study on two golf course fairways in Naples, FL and for a series of three studies related to assessing microclimate effects on water relations, where the "microclimates" were topographic aspect, low light, and high traffic areas. In the microclimate studies we also used hand-held instruments typical of sensors available for monitoring small areas, as opposed to large scale mapping. The TMM VWC sampling scheme was a 2.5-m grid composed of 825-cm^3 samples. Conversely, NDVI was measured with a continuous 60- ± 10-cm field of view.

Spatial and temporal characterization of surface zone VWC and associated real-time NDVI responses offers the potential for several field applications that could improve water-use

efficiency. In Study 1 (Chapter 2), two field applications were investigated, the first being to define SSMUs within a landscape area based on spatial patterns of VWC at field capacity, where field capacity has been shown to be strongly related to the relatively stable soil properties of soil texture and organic matter content. Golf course fairways are a challenging landscape for defining SSMUs since they comprise much smaller and are often characterized by more complex contouring than traditional PA sites. Also, they may have single sprinkler head irrigation control that could allow irrigation alterations on a small scale basis. Thus, when defining SSMUs on complex turfgrass landscapes, identification of relatively small areas exhibiting very low or very high VWC is important to maximize water-use efficiency. The second field application investigated in Study 1 involved using dry-down responses of VWC and NDVI to provide a spatial and temporal understanding of water-use and drought stress, where water loss (evapotranspiration; ET) is influenced by both stable and variable soil and climatic factors over a landscape. Turfgrass sites offer easier access and mapping conditions relative to most traditional PA fields, thereby allowing for temporal mapping during a dry-down from field capacity. Mapping data from both of these field applications provide valuable information related to irrigation scheduling, especially for scheduling individual SSMUs based on their rate of dry-down to a selected trigger value of allowable water depletion (AWD) percentage (issues of where and when to irrigate) with field capacity considered as a 100% baseline (full point).

Choosing the appropriate classification scheme for mapping data is essential to properly define SSMUs. While some classifications relied on arbitrary divisions (manual, quantile, and 1/3 query), other divisions were specific to the data distribution (Jenk's natural breaks, standard deviation, histogram, and SD-Integrated). We selected the histogram method divisions considering agronomic information, which primarily focused on VWC ranges that suggested a

soil texture class and associated NDVI maps. The standard deviation method was very good for defining the lowest and highest VWC areas in a detailed, small scale manner. Since the standard deviation and histogram procedures provide a better basis for defining VWC extremes, with the standard deviation including a statistical measure of data dispersion and the histogram incorporating agronomic experience, we used both the standard deviation and histogram classification schemes to assist in defining SSMU boundaries with the combination method entitled "SD-Integrated".

The purpose of a SSMU is to define an area that is more similar than the whole field area. Standard deviation and CV comparisons reflected lower variability within SSMUs than across a whole fairway. The lower quarter distribution uniformity (DU_{lq}) is a common means of assessing irrigation water distribution uniformity based on placement of uniform grids of catch-cans, but this concept can be adapted to soil moisture uniformity using VWC data. The DU_{lq} within SSMUs indicated greater SSMU moisture uniformity at field capacity relative to the whole fairway, suggesting DU_{lq} based on VWC could be a beneficial component of irrigation scheduling. Modifications of existing irrigation systems or new system designs could be more efficient if SSMUs with high DU_{lq} are used as decision making tools. Furthermore, strategic placement of in-situ soil sensors could be based on SSMU locations and VWC thresholds used to trigger required irrigation events as needed in the SSMU.

Linear and quadratic correlation coefficients of VWC versus NDVI across entire fairways at field capacity were linear $r^2 = 0.27$ and 0.10 and quadratic $r^2 = 0.33$ and 0.15 for Fairways 10 and 13, respectively. At first view, a higher correlation might be anticipated, but the whole fairway areas include a wide range of soil conditions with associated differences in VWC, while the objective on the turf manager is to avoid visual differences in turf performance (i.e., NDVI).

Within SSMUs with the lowest average VWC at field capacity, linear $r^2 = 0.39$ and 0.17, while the moderate and high VWC SSMU correlations were weaker than for the whole fairway. The VWC data (point measurements) provide a smaller representation of the site compared to NDVI (continuous measurements), which could help to explain the correlation statistics.

Maps illustrating VWC and NDVI changes during dry-downs showed that corresponding areas of low, moderate, or high VWC and NDVI existing at the beginning of dry-downs maintained consistent locations and expanded by the end of dry-downs. Thus, changes during dry-downs confirmed that initial SSMU boundary delineation based on field capacity VWC and NDVI were appropriate over the whole dry-down period. Since each SSMU has a unique VWC at field capacity, the dry-down VWC patterns also indicated when a SSMU achieved an AWD of a 50% trigger value for irrigation. Aside from an NDVI increase from 12 to 13 July on both fairways, VWC and NDVI decreased daily. The statistical relationship between VWC and NDVI was associated with the highest correlation (quadratic $r^2 = 0.33$) occurring on 12 July, Fairway 10.

In addition to illustrating the potential use of spatial mapping for development of SSMUs and dry-down maps within SSMUs, our objective was to develop suggested protocols for data presentation and analysis that would be both science-based and practical for integration into a decision support system (DSS) approach. When presenting spatial VWC maps based on field capacity used for SSMU delineation, we would suggest the following protocol (using the example of a fairway):

- The histogram of each fairway should be presented with an indication of agronomic breaks. This information provides a visual display of data distribution and dispersion at the low and high end of VWC values.

- The histogram-based map should be presented with the class intervals selected reflecting the best agronomic consideration of the histogram. This map is likely to be less complicated than the standard deviation map for sites with relatively wide VWC ranges, because fewer classes are present and the classes are agronomic-based estimates of possible sites with similar soil texture and organic matter content (based on similar VWC values). No SSMU boundaries would be defined on this map.
- The SD-integrated map should then be displayed with class intervals based on standard deviation. The SSMU boundaries would be delineated on this map with consideration of the histogram map in order to obtain the least number of practical SSMUs. When first defining the SSMU boundaries, the lowest and highest VWC areas should be isolated. Then, the remaining area can be evaluated as to whether more than one additional SSMU area is necessary, with the histogram map providing the best guidance for this decision.
- Because our study only involved two fairway areas, we believe that further case studies where dry-down maps can be developed will provide the best insight as to whether the SD-Integrated or histogram classification method results in the most reasonable and science-based SSMUs. The SD-Integrated method was used as the standard in this study.
- Descriptive statistics and information on DU are suggested for the whole fairway and within each SSMU based on presentations for a DSS approach.

The effects of topography, light, and traffic microclimates on VWC, estimated evapotranspiration (ET) and NDVI were also investigated (Chapters 3, 4, and 5). A mobile platform (TMM) and hand-held instruments were used in these assessments. Comparisons

between mobile and hand-held VWC data yielded linear correlations of r^2 = 0.06 and 0.85 for the 14 to 16 June and 12 to 16 July dry-downs, respectively. These data, along with results of differing VWC after a rainfall at field capacity, support the assertion that residual salinity from irrigation water was present in the soil earlier in the study period. Different measurement depths (TMM: 10-cm; hand-held: 12-cm), collection of five hand-held readings per plot during the 12 to 16 July dry-down (as opposed to two during previous dry-downs), and sampling volume differences could also help explain correlation data. Of all slope treatments, the low, north, and west slopes exhibited greatest ET; the east and south facing slopes demonstrated lower water loss. These results occurred throughout all dry-downs and during the 12 to 16 July dry-down, which was the longest dry-down and was not influenced by salinity. Assessing VWC on a percent of field capacity basis at the end of dry-downs yielded the same treatment results. Using estimated ET by the soil water balance method did not lead to consistent results, but using VWC data to assess microclimates appeared to be valuable for determining a trigger AWD value; hand-held instrumentation could be useful when mobile methods are not available for this purpose.

Field capacity VWC was lower under morning shade and high traffic treatments compared to their respective full sunlight and low traffic controls. When ET was averaged over the dates when significant differences did occur, the morning shade plots exhibited an ET of 60% that of full sunlight conditions. High traffic plots exhibited an average of 59% ET compared to the low traffic plots on dates when significant traffic treatment differences were observed. No statistical differences in morning shade versus full sunlight occurred in terms of NDVI, possibly reflecting the low light resistance of seashore paspalum (*Paspalum vaginatum* Sw.). However, greater NDVI reduction and reduced ET resulted from high traffic; lower canopy biomass or leaf area index as indicated by NDVI could have influenced ET.

Mobile, rapid data collection and mapping of soil moisture and plant stress on golf courses provides the basis for addressing microclimate differences within landscapes by using the SSMU concept. In certain cases, hand-held data acquisition on a smaller scale can help determine AWD and aid in the development of DSS. This approach could be used in obvious microclimates such as low light, traffic, or topographic microclimates. Making management adjustments according to SSMU requirements promotes PTM, leading to healthier turf by more efficient use of management inputs.

APPENDIX

Table A-1. Rain events prior to dry-downs.

	cm		
Date	Fairway 10†	Fairway 13‡	Fairway 3§
10 June	3.05	3.05	3.05
11 June	1.50	1.50	1.50
12 June	0.86	0.86	0.86
13 June	2.01	2.01	2.01
14 June	- - - - - - - - - - - - Dry-Down Initiation - - - - - - - - - - - -		
16 June	0.64	0.64	0.64
17 June	5.87	5.87	5.87
18 June	0.81	0.81	0.81
19 June	- - - - - - - - - - - - Dry-Down Initiation - - - - - - - - - - - -		
20 June	0.94	0.91	0.97
21 June	- - - - - - - - - - - - Dry-Down Initiation - - - - - - - - - - - -		
23 June	0.18	0.43	0.23
24 June	0.53	0.53	0.53
25 June	6.65	5.94	6.30
26 June	- - - - - - - - - - - - Dry-Down Initiation - - - - - - - - - - - -		
6 July	0.81	0.74	0.69
7 July	1.57	1.83	1.73
8 July	0.00	0.00	0.20
9 July	0.69	0.86	0.83
10 July	0.03	0.03	0.03
11 July	1.09	1.02	1.14
12 July	- - - - - - - - - - - - Dry-Down Initiation - - - - - - - - - - - -		

† Rainfall measured by rain guage adjacent to Fairway 10.

‡ Rainfall measured by rain guage adjacent to Fairway 13.

§ Rainfall data averaged from all rain gauge measurements (6) distributed throughout the Old Collier Golf Course after 19 June 2006.

Table A-2. Treatment 10-cm electrical resistance (ER) and corresponding electrical conductivity (EC) determined via the four-wenner array configuration.

	Topography						Light		Traffic	
Date	North	South	East	West	Low	High	Full Sunlight	Morning Shade	Low	High
ER	ohm m^{-1}									
19 May	11.83	11.05	14.82	10.55	14.46	13.34	—	—	—	—
30 May	10.37	7.65	12.47	9.69	12.24	12.25	—	—	14.96	14.44
5 June	8.41	6.36	8.77	7.67	8.15	9.23	—	—	11.59	15.36
6 June	4.77	5.10	5.22	6.12	7.02	6.68	—	—	—	—
13 June‡	32.41	28.84	43.81	40.45	42.51	49.42	233.52	225.56	43.32	45.92
14 June	166.62	158.83	142.48	141.00	122.56	141.64	140.78	147.84	129.65	124.77
15 June	233.20	237.11	236.66	234.14	253.30	261.69	214.42	231.86	202.39	208.03
16 June	121.57	134.67	138.24	111.54	122.69	74.33	—	—	—	—
EC	dS m^{-1}									
19 May	5.29	5.66	4.22	5.93	4.33	4.69	—	—	—	—
30 May	6.04	8.18	5.02	6.46	5.11	5.11	—	—	4.18	4.34
5 June	7.44	9.85	7.14	8.16	7.69	6.78	—	—	5.40	4.08
6 June	13.12	12.28	12.00	10.23	8.92	9.37	—	—	—	—
13 June‡	1.93	2.17	1.43	1.55	1.47	1.27	0.27	0.28	1.45	1.36
14 June	0.38	0.39	0.44	0.44	0.51	0.44	0.44	0.42	0.48	0.50
15 June	0.27	0.26	0.26	0.27	0.25	0.24	0.29	0.27	0.31	0.30
16 June	0.51	0.46	0.45	0.56	0.51	0.84	—	—	—	—

† No data denoted by "—"

‡ Rainfalls totaling 7.42 cm occurred from 10 to 13 June.

Table A-3. Treatment particle size analysis, organic matter content, and slope for each microclimate study.

Microclimate Treatment	Sand†	Silt†	Clay†	Organic Matter‡	Slope§
Topography			%		
High	97ab	1	2	4.00	1.98d
North	96b	2	2	3.45	4.18bc
South	96ab	2	2	3.90	7.90a
East	97a	1	2	3.70	4.38b
West	97ab	1	2	3.88	6.05ab
Low	96ab	2	2	3.66	2.20cd
F-test¶	0.41	0.70	0.75	0.49	<0.01
CV	1	63	31	11	38
Light			%		
Full Sunlight	96	3	1	4.23a	3.23
Morning Shade	96	2	2	3.46b	4.10
F-test¶	0.75	0.37	0.14	0.07	0.70
CV	1	41	32	13	83
Traffic			%		
Low	97	1	2	3.65	2.60
High	96	2	2	3.18	1.78
F-test¶	0.37	0.54	0.80	0.27	0.64
CV	0	34	25	16	109

† Particle size analysis determined via hydrometer.

‡ Organic matter content determined via loss-on-ignition.

§ Slope determined via transit.

¶ F-test data are unit-less.

Table A-4. Study plot particle size analysis, organic matter, and plot slope for each microclimate study.

Microclimate Plot	Sand†	Silt†	Clay†	Organic Matter‡	Slope§
Topography			%		
10.1	97	2	1	4.09	7.8
10.2	96	3	1	4.02	6.7
10.3	97	2	1	3.73	2.5
10.4	96	3	1	3.55	3.3
10.5	96	3	1	4.68	2.1
10.6	97	2	1	4.02	2.1
10.7	97	0	3	3.64	5.0
10.8	96	3	1	4.51	7.5
10.9	96	1	3	3.89	8.3
10.10	96	1	3	3.60	8.8
10.11	96	1	3	3.25	2.9
10.12	96	3	1	3.22	4.6
10.13	96	3	2	3.16	1.9
10.14	97	1	2	3.37	5.6
13.15	97	1	2	4.12	5.8
13.16	96	1	2	3.88	0.0
13.17	97	1	2	4.22	1.3
13.18	98	0	2	4.02	0.0
13.19	97	0	2	3.54	6.3
13.20	96	1	2	3.83	5.4
13.21	96	2	2	3.62	5.4
13.22	97	2	1	3.70	3.8
13.23	98	0	2	3.69	7.1
13.24	97	1	2	2.95	2.5
Light			%		
3.1	95	4	1	3.27	2.7
3.2	96	3	1	3.54	0.8
3.3	95	3	1	4.94	9.2
3.4	96	3	1	3.71	3.3
3.5	96	2	2	3.31	5.6
3.6	97	0	3	3.54	4.8
3.7	96	3	1	3.83	0.4
3.8	96	3	1	4.60	2.5
Traffic			%		
13.1	97	2	1	3.76	0.6
13.2	97	1	2	3.09	0.0
13.3	97	2	1	3.23	0.0
13.4	97	1	2	4.49	0.8
13.5	96	1	2	2.52	4.0
13.6	96	1	2	3.57	3.3
13.7	95	2	2	3.34	2.5
13.8	97	1	2	3.30	6.3

† Particle size analysis determined by hydrometer.

‡ Organic matter content determined by loss-on-ignition.

§ Slope determined by transit.

Table A-5. Treatment and replication designation for microclimate study plots.

Microclimate Treatment	Study Plots Replication			
Topography	A	B	C	D
High (Control)	10.3	10.4	10.5	13.18
North Facing	10.11	10.12	13.21	13.22
South Facing	10.1	10.2	10.9	10.10
East Facing	10.6	13.15	13.23	13.24
West Facing	10.7	10.8	13.19	13.20
Low	13.13	13.14	13.16	13.17
Light	A	B	C	D
Full Sun	3.2	3.3	3.7	3.8
Morning Shade	3.1	3.4	3.5	3.6
Traffic	A	B	C	D
Low Traffic	13.3	13.4	13.6	13.8
High Traffic	13.1	13.2	13.5	13.7